TITAN EXPLORER

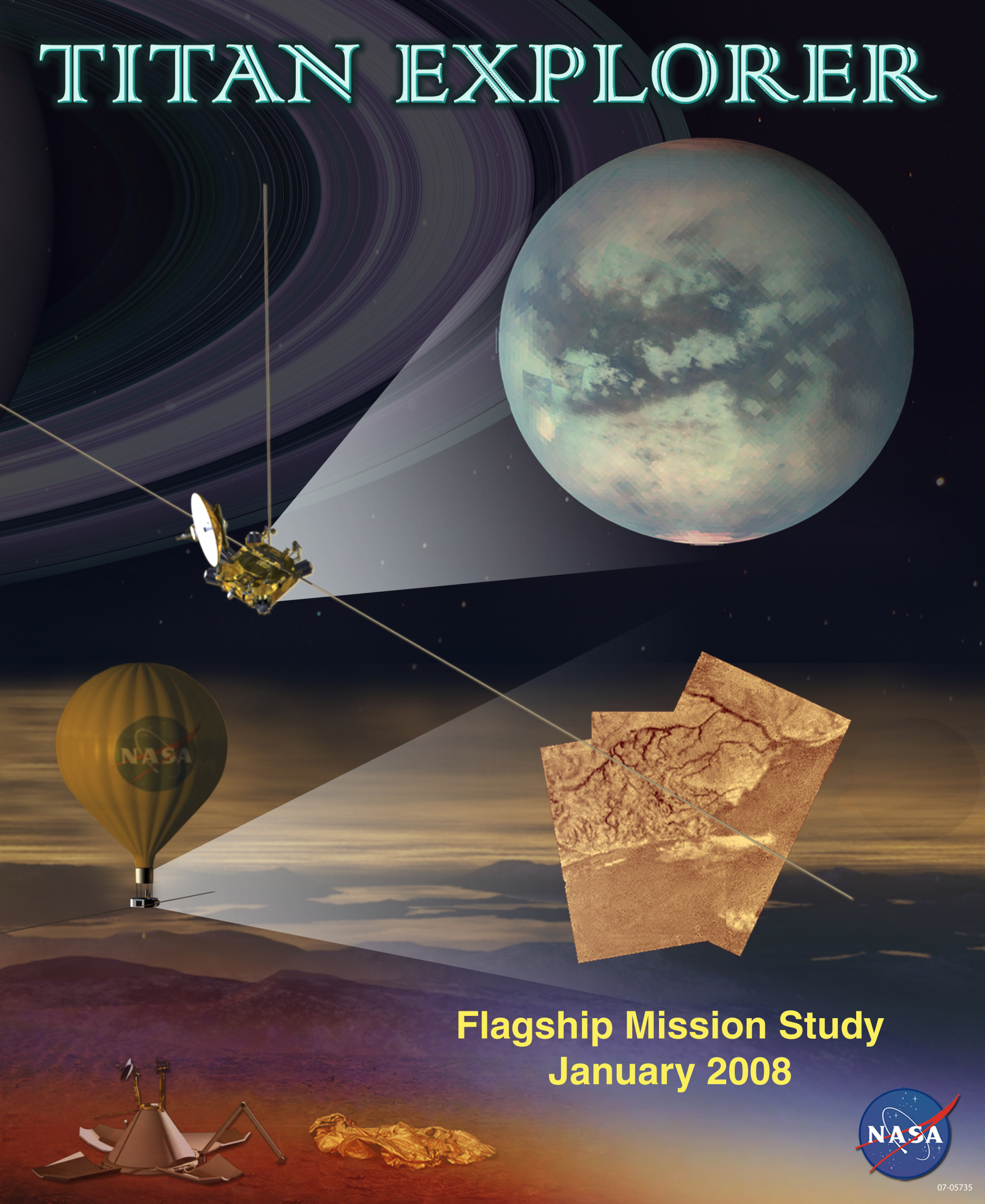

Flagship Mission Study
January 2008

NASA

07-05735

January 2008
Public Release Version

Titan Explorer Flagship Mission Study

Prepared for NASA's Planetary Science Division

By The Johns Hopkins University Applied Physics Laboratory

APL

Approved By:

James C. Leary
Study Lead, The Johns Hopkins University Applied Physics Laboratory

Robert D. Strain
Space Department Head, The Johns Hopkins University Applied Physics Laboratory

Ralph D. Lorenz
Science Definition Team Co-Chair, The Johns Hopkins University Applied Physics Laboratory

J. Hunter Waite
Science Definition Team Co-Chair, Southwest Research Institute

ACKNOWLEDGMENTS

The Johns Hopkins University would like to extend a special thank you to all of the team members and to NASA's Planetary Science Division for the opportunity to investigate this amazing mission concept.

The Titan Explorer Team

Science Definition Team

- Ralph Lorenz (APL, Study Scientist & co-chair)
- J. Hunter Waite (SwRI, co-chair)
- Rosaly Lopes (JPL)
- Scot Rafkin (SwRI)
- Devon Burr (SETI)
- F. Michael Flasar (NASA GSFC)
- Andrew Steele (CIW)
- Gerald Schubert (UCLA)
- Kevin Baines (JPL)
- Bill Kurth (U. Iowa)
- Jonathan Lunine (U. Arizona)
- Dale Cruikshank (NASA Ames)

JPL

- JPL Team Lead – K Reh
- Systems Engineering & Instruments – J Elliott
- Mission Concept/Architect – T Spilker
- Mission Design & Navigation – N Strange, J Sims, R Haw, Damon Landau, Peter Antreasian
- Aerial Vehicle Design – J Hall, J Jones
- Avionics – Jason Willis, T Hoffman
- Power – R Ewell
- Telecom – B Lovick
- Thermal – B Miyake
- MOS/GDS – G Welz
- Costing – E Jorgensen

NASA LaRC

- Atmospheric Flight Trajectory Simulation, Aerodynamics, G&C – J Prince, D Powell, E Queen

NASA ISPT

- TitanGRAM, Consulting – Michelle Munk (NASA LaRC)

Stanley Associates

- TitanGRAM, Cassini/Huygens Comparison – Carl G. (Jere) Justus (NASA MSFC)

APL

- Study Lead – JC Leary
- Systems Engineer – MK Lockwood
- Mission Design – JJ Guzman
- Propulsion – SS Bushman
- Avionics – P Eisenreich
- Power – G Dakermanji
- Mechanical Design – W Cheng, SR Vernon, DH Napolillo
- Software & Data Systems – DA Artis
- Communications – JR Bruzzi
- Thermal – CJ Ercol
- Guidance & Control – JW Hunt
- Mission Operations – RL Nelson
- Parts – JL Farnan
- I&T, Contamination, & Planetary Protection – SP Thibault
- Instruments – JD Boldt, WB Brinckerhoff
- Structural Analysis – DF Persons
- Costing – ME Jones, LS Wolfarth
- Mission Assurance – CK Kim
- Report Generation – MK Morris, DJ Dorsey, VM Grey, J Elbaz, D George

ILC Dover – Landing System Design

TABLE OF CONTENTS

LIST OF FOLDOUTS

LIST OF FIGURES AND TABLES

ACKNOWLEDGMENTS

The Johns Hopkins University would like to extend a special thank you to all of the team members and to NASA's Planetary Science Division for the opportunity to investigate this amazing mission concept.

The Titan Explorer Team

Science Definition Team

- Ralph Lorenz (APL, Study Scientist & co-chair)
- J. Hunter Waite (SwRI, co-chair)
- Rosaly Lopes (JPL)
- Scot Rafkin (SwRI)
- Devon Burr (SETI)
- F. Michael Flasar (NASA GSFC)
- Andrew Steele (CIW)
- Gerald Schubert (UCLA)
- Kevin Baines (JPL)
- Bill Kurth (U. Iowa)
- Jonathan Lunine (U. Arizona)
- Dale Cruikshank (NASA Ames)

JPL

- JPL Team Lead – K Reh
- Systems Engineering & Instruments – J Elliott
- Mission Concept/Architect – T Spilker
- Mission Design & Navigation – N Strange, J Sims, R Haw, Damon Landau, Peter Antreasian
- Aerial Vehicle Design – J Hall, J Jones
- Avionics – Jason Willis, T Hoffman
- Power – R Ewell
- Telecom – B Lovick
- Thermal – B Miyake
- MOS/GDS – G Welz
- Costing – E Jorgensen

NASA LaRC

- Atmospheric Flight Trajectory Simulation, Aerodynamics, G&C – J Prince, D Powell, E Queen

NASA ISPT

- TitanGRAM, Consulting – Michelle Munk (NASA LaRC)

Stanley Associates

- TitanGRAM, Cassini/Huygens Comparison – Carl G. (Jere) Justus (NASA MSFC)

APL

- Study Lead – JC Leary
- Systems Engineer – MK Lockwood
- Mission Design – JJ Guzman
- Propulsion – SS Bushman
- Avionics – P Eisenreich
- Power – G Dakermanji
- Mechanical Design – W Cheng, SR Vernon, DH Napolillo
- Software & Data Systems – DA Artis
- Communications – JR Bruzzi
- Thermal – CJ Ercol
- Guidance & Control – JW Hunt
- Mission Operations – RL Nelson
- Parts – JL Farnan
- I&T, Contamination, & Planetary Protection – SP Thibault
- Instruments – JD Boldt, WB Brinckerhoff
- Structural Analysis – DF Persons
- Costing – ME Jones, LS Wolfarth
- Mission Assurance – CK Kim
- Report Generation – MK Morris, DJ Dorsey, VM Grey, J Elbaz, D George

ILC Dover – Landing System Design

TABLE OF CONTENTS

LIST OF FOLDOUTS

LIST OF FIGURES AND TABLES

Fact Sheet

TITAN EXPLORER

Exploring Titan, an Earthlike Organic-Rich World ...

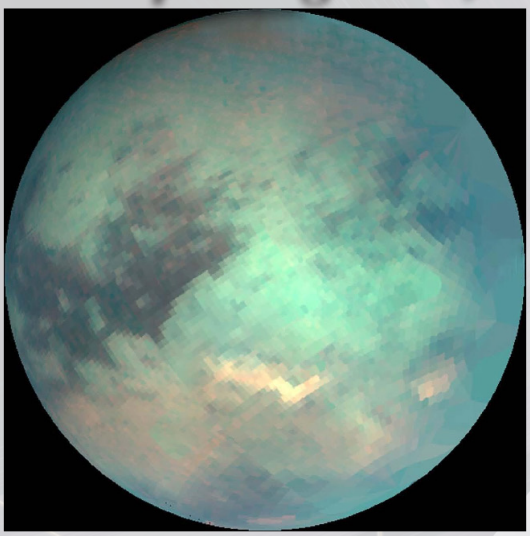

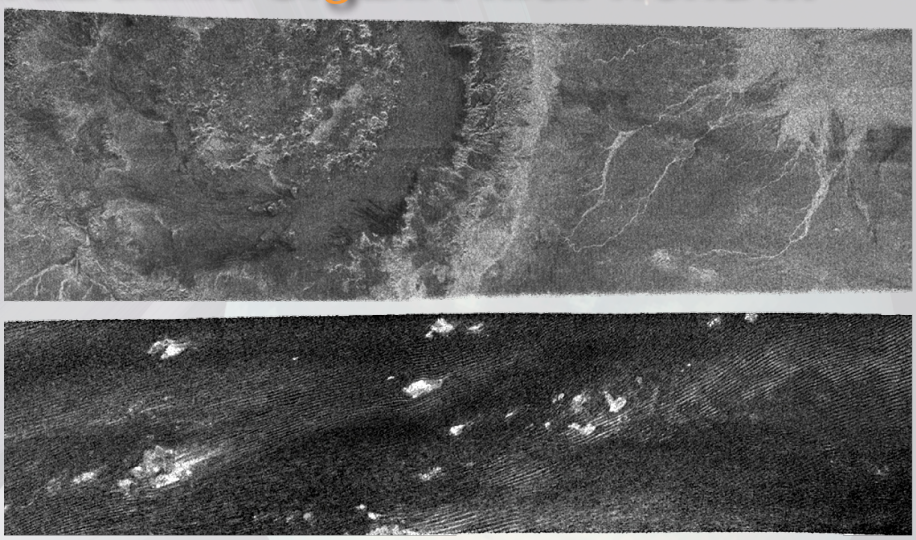

Titan System Science – The rich interactions at Titan among the surrounding space environment, the atmosphere, the surface, and the interior mirror processes on Earth. Titan is a dynamic world: clouds and rainfall change on hourly timescales. On ~16-day timescales, tides rise and fall in lakes of liquid hydrocarbons, drive winds in the atmosphere, and raise stresses deep in the interior. Year-to-year, seasonal changes are observed in atmospheric composition, aerosols, temperatures, and wind patterns. On geological timescales, atmospheric evolution occurs via escape, photochemical reactions, and cryovolcanism. Many analogs to Earth have been found. Titan's surface has been eroded by rivers, the precipitation may be torrential enough to cause flash floods, and the atmosphere exhibits a greenhouse effect and stratospheric anomalies analogous to Earth's ozone hole.

Titan and the Origins of Life – The inventory of complex organic material on Titan is remarkably rich. Synthesis of organics begins in the active ionosphere; it results in the thick haze lower in Titan's atmosphere, the surface accumulations of organic liquids and particles that form lakes in polar regions, and the vast expanses of dunes near the equator. Further processing by exposure for thousands of years to liquid water at sites of impacts and cryovolcanism should yield building blocks of life, such as pyrimidines and amino acids. Given such timescales and conditions, Titan holds possibilities for fundamentally new organic chemistry that cannot be reproduced in the laboratory on Earth.

Synergistic Science – Owing to its unique atmosphere, Titan engages a more extensive range of scientific disciplines than other icy satellites. It is an outstanding target for comparative planetology, both with other satellites and with the terrestrial planets. Titan's environment also enables uniquely affordable deployment of a wide array of instrumentation at the surface, in the atmosphere, and in orbit. Thus, the powerful complement of scientific tools necessary to understand such a complex system can actually be brought to bear. For example, in situ investigations such as seismic sensors and detailed chemical analyses support and inform an orbital survey of this diverse target. Combinations of techniques provide more robust constraints on mysteries such as Titan's interior structure and atmospheric circulation.

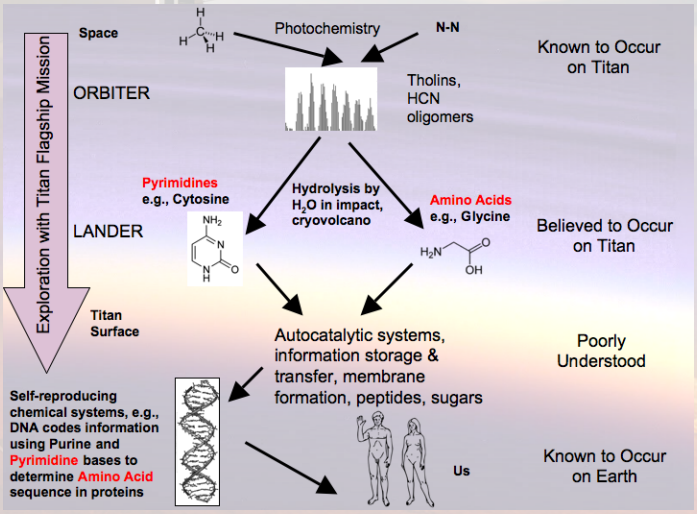

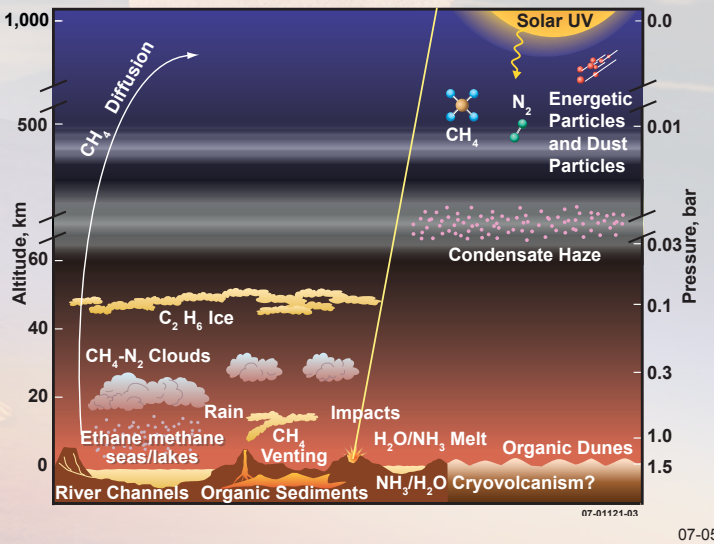

TITAN EXPLORER

Mission Overview

An Orbiter, Lander, and Balloon designed to provide synergistic science at multiple, complementary locations, arrive at Titan in 2028. The 4-year orbital mission returns orders of magnitude more data about Titan than Cassini – this mission will spend more time at Titan in its first 3 days in orbit than the nominal and extended Cassini missions – and at a complementary season for the 1-year in situ Lander and Aerial Vehicle (Balloon) mission elements are tremendously enhanced by data relay from the Orbiter. They provide enabling scientific context for remote sensing measurements.

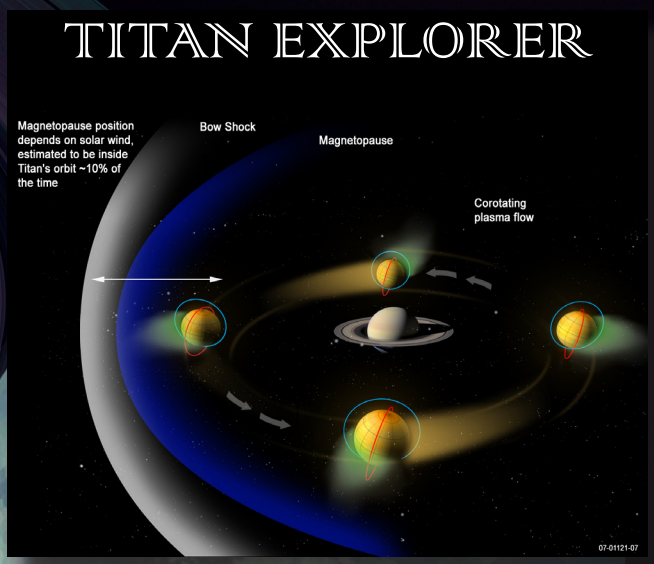

Mission Implementation

The three elements, Orbiter, Lander, and Balloon, are housed in individual aeroshells and are carried by a cruise stage launched by the Atlas V 551 in 2018 through Earth, Venus and two Earth flybys until separation begins ~1 month before Titan arrival in 2028. Four years of operation are planned for the Orbiter, including relaying communications for the two in situ elements in the first year and two "aerosampling" phases where the Orbiter passes through the upper atmosphere to perform in situ scientific analyses.

The Orbiter, carrying 12 instruments and supporting radio science investigations, provides global mapping, remote sensing observations, and in situ neutral atmospheric measurements, allowing significant science objectives to be addressed; the objectives are addressed in full when Orbiter measurements are augmented by those from the in situ elements. The Orbiter design utilizes aerocapture in Titan's atmosphere to save ~2 km/s of propulsive ΔV.

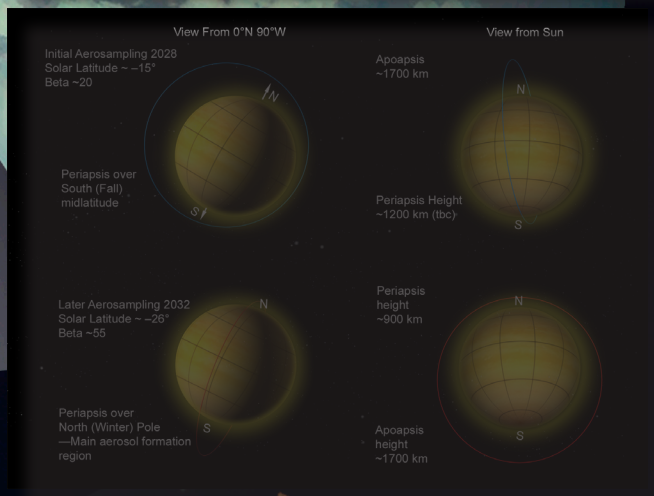

A direct-entry Lander, leveraging experience from Huygens and Mars missions, carries eight instruments and addresses the surface science objectives, in particular allowing seismic measurements and direct analysis of surface composition.

An Aerial Vehicle, a Montgolfière hot air balloon, addresses the remaining science objectives by passively circumnavigating Titan using zonal winds and making measurements with five instruments. The Balloon inflates during atmospheric entry and remains near an altitude of 10 km to bridge the science gap between the Orbiter and the Lander scales, notably providing widespread meter-scale imaging of the surface. Technology developments for aerocapture, balloon technologies, cryogenic applications, and landing systems are funded and scheduled for completion by the mission Preliminary Design Review.

	Mass* (kg)	Power* (W)	ΔV (m/s)	Science Data Volume**
Orbiter	1810	638	408	3.4 Tbits
Lander	897	255	0	5.5 Gbits
Aerial Vehicle	588	128	0	4.6 Gbits
Cruise Stage	1419	0	341	0

*Mass and power are allocations. Mass margin is 19.9%; contingency is 17.5%. Power margins are ≥26% for all modes.

**Science data volumes are current best estimates. Margin on downlink rate is 30%; margin on downlink time is ≥18% above shown volumes.

1: Executive Summary

1. EXECUTIVE SUMMARY

Titan, a complex, Earthlike system abundant with organics, should be the next scientific target in the outer Solar System. Titan shares features with both icy satellites and the terrestrial planets. It is subjected to tidal stresses, and its surface has been modified tectonically to form mountains and likely also by cryovolcanism, where liquid water and methane make their way to the surface from the interior. Titan has the largest concentration of organic material in the Solar System aside from Earth, and its active hydrological cycle is analogous to that of Earth, with methane replacing water. Titan's clouds, rain, flash floods, and greenhouse and anti-greenhouse effects may provide important lessons for Earth. Albeit with bizarrely different chemistry, Titan's landscape is remarkably Earthlike, featuring dunes, streambeds, and mountain ridges, as well as polar lakes filled with liquid hydrocarbons. The thick, largely nitrogen, Titanian atmosphere varies seasonally in temperature, dynamical behavior, and composition, including a winter polar structure analogous to Earth's ozone hole, and a mission launched in the 2015–2022 timeframe has a prime opportunity to measure a season complementary to that observed by Cassini. Although Titan is similar to Earth in many ways, its atmosphere is unique in the solar system in experiencing strong dynamical forcing by gravitational tides (a trait Titan may share with many extrasolar planets). Study of these scientific aspects maps well to NASA's scientific objectives as presented in the first Decadal Survey report, the 2006 Solar System Exploration Roadmap, the 2007 NASA Science Plan, and the 2006 Outer Planets Assessment Group Pathways Document. Titan, with low gravity and a thick atmosphere, is also uniquely accessible for in situ exploration, allowing a broader range of scientific tools to be affordably brought to bear on its exploration than other satellites. Therefore, Titan, a rich, diverse body offering extraordinary scientific return, is an excellent choice for the next Flagship mission.

Recent discoveries of the complex interactions of Titan's atmosphere with the surface, interior, and space environment demand focused and enduring observation on a range of temporal and spatial scales. A 4-year orbital mission will sample the diverse and dynamic conditions in the ionosphere where complex organic chemistry begins, observe seasonal changes in the atmosphere, and make global near-infrared and radar maps of the surface. This immersion in Ti-

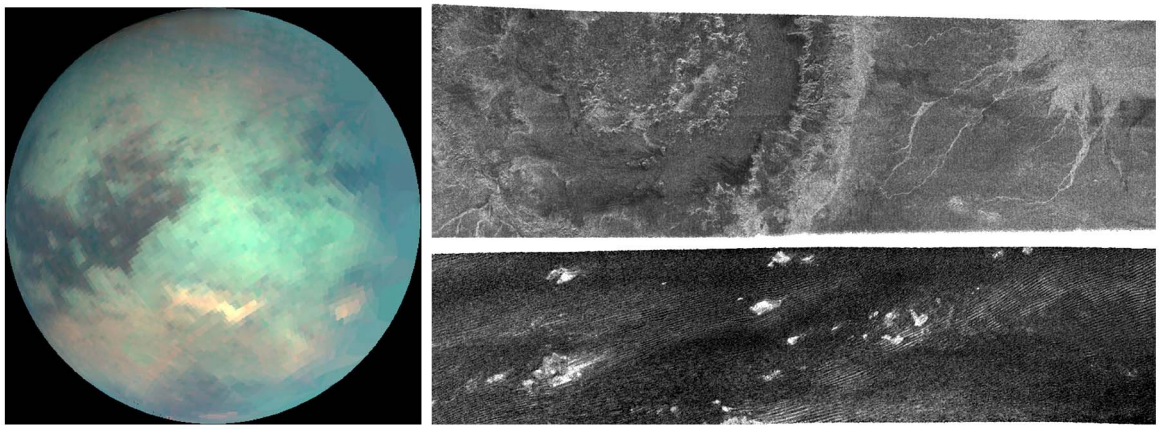

Titan contains a wealth of scientific investigations best explored at multiple scales. Left: Global-scale image of Titan in false color from Cassini VIMS images *(NASA/JPL/Space Science Institute; PIA02145)*. Right: Cassini RADAR image showing a 440-km impact structure and network of braided river channels (top); giant longitudinal sand dunes near the equator (bottom).

tan's environment provides 2–3 orders of magnitude increase in Titan science return over the Cassini mission. Known chemical processes on Titan's surface take key steps toward the synthesis of prebiotic molecules, but to assess how far these (and other as yet unknown reactions) have advanced requires in situ chemical analysis. Titan's thick atmosphere makes deploying a lander to perform such measurements vastly easier than at any other large icy satellite, and the rich inventory of complex hydrocarbons makes new insights inevitable. A lander also enables powerful techniques such as seismology to be applied to exploring Titan's interior structure. Understanding the forces that shape Titan's diverse landscape necessitates detailed investigation at a range of locations, a demanding requirement anywhere else, but something that is uniquely straightforward at Titan: a Montgolfiere hot-air balloon can circumnavigate Titan, exploring with high-resolution cameras and subsurface-probing radar. The combination of these mission elements (orbiter, lander, and balloon) is a powerful and unprecedented opportunity for synergistic investigations – synthesis of data from this arsenal of instrumentation is the pathway to understanding this profoundly complex body. Titan system science embraces geology, meteorology, chemistry, geophysics, space physics, hydrology, and a host of other disciplines, engaging a wider community than many other targets in the outer Solar System.

The Titan Explorer (TE) mission architecture, including separate Orbiter, Lander, and Balloon, encourages teaming and meets comprehensive science objectives. The multi-element architecture satisfies the multi-scale measurement requirements. Representative payloads were selected for each element to properly evaluate accommodation requirements, since instrument selection will be performed via the Announcement of Opportunity process after project start. An orbiter carrying 12 instruments and facilitating radio science provides global mapping, remote sensing observations, and in situ upper atmospheric measurements, allowing over half of the science objectives to be at least partially addressed (synergy with the in situ element measurements realizes the remaining objectives). The orbiter design utilizes aerocapture in Titan's atmosphere to save ~4 km/s of velocity change capability. A direct-entry lander, leveraging experience from Huygens and Mars missions, carries eight instruments and addresses more of the science objectives, in particular allowing seismic measurements and direct analysis of surface composition. An Aerial Vehicle – a Montgolfiere hot-air balloon – achieves the remaining science objectives by passively circumnavigating Titan using zonal winds and taking measurements

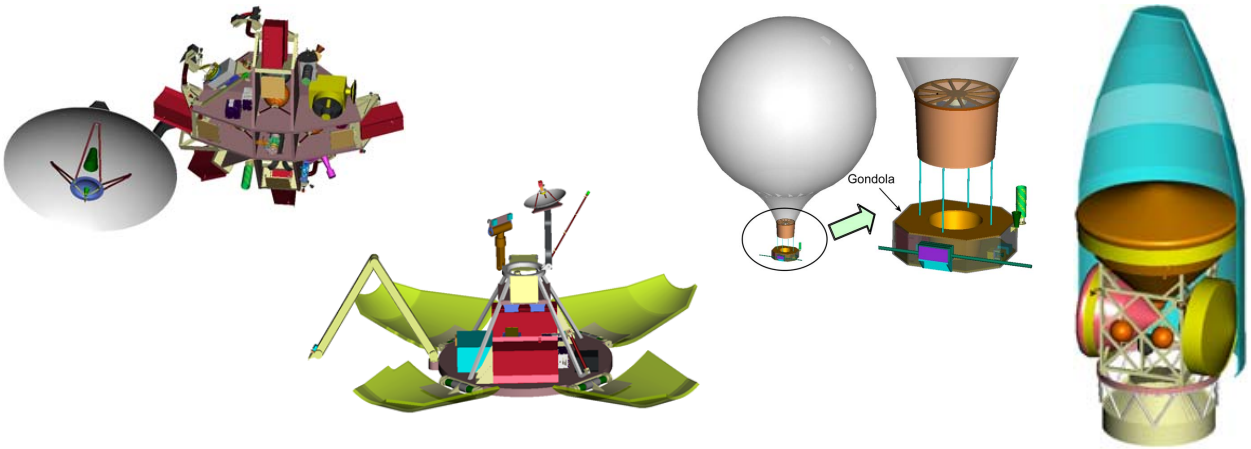

The TE architecture is flexible with (from the left) an Orbiter, Lander, and Balloon housed in individual aeroshells attached to a Cruise Stage arriving at Titan in 2028.

with five instruments. This Balloon inflates during entry and descent and remains near an altitude of 10 km to bridge the science gap between the orbiter and lander scales, notably providing widespread meter-scale imaging of the surface and subsurface radar sounding. A cruise stage mounts to the Atlas V 551 and carries all three elements housed in individual aeroshells from launch in 2018 through two Venus and two Earth flybys until separation begins ~1 month before arrival at Titan in 2028. Four years of operation are planned for the Orbiter, including communications relay for the two in situ elements, which operate during the first year, and two "aerosampling" phases where the orbiter passes through the upper atmosphere to perform its own in situ scientific analyses. The elements could also be launched separately, but to maximize the science return, the Orbiter should relay communications for other elements. Therefore, multiple individual elements can be developed by organizations providing the most benefit to NASA, engaging multiple centers and including international partners. Also, the in situ elements, especially the Balloon, provide an exceptional opportunity to engage the public with detailed scenes of interactions with and exploration of an alien, and yet familiar, landscape.

The conservative, robust mission architecture allows TE to have an acceptable level of risk for a Flagship mission. All technology developments (including aerocapture, balloon technology, cryogenic applications, and landing system) are fully funded and scheduled to be complete by mission Preliminary Design Review. Element design emphasizes leveraging past experience, and commonality lowers risk. All design margins satisfy both APL and JPL requirements. Since plutonium availability is a concern, the Advanced Stirling Radioisotope Generator (ASRG) is baselined as the power source for all elements, greatly reducing the plutonium requirements. (Other radioisotope power systems could be used, however.) The Earth flyby and National Environmental Policy Act (NEPA) launch approval strategies use past experience to provide conservative estimates. Planetary protection for Titan is Category II, but Huygens-based requirements are levied on the program to reduce the impact of potential future changes. Fully addressing the TE risk set in the budget and schedule reduces the chance of unforeseen complications disrupting the project plan.

TE schedule and financial options provide flexibility in an uncertain fiscal environment. The TE schedule is based on past successful flagship missions (e.g., Cassini and Galileo) and contains 5.5 months of reserve during the critical 4.5-year development period. Multiple launch opportunities allow further schedule flexibility (approximately one opportunity per year from 2015 to 2022). Financial options include international partnerships and a large set of descope options, ranging from individual instruments to full elements. The TE baseline mission is $4B (FY'07) to meet all science objectives and enables powerful synergistic science. A $2B (FY'07) Orbiter-only science floor option addresses over half of the science objectives but loses the in situ measurements and much of the detailed context for the remote sensing. Cost realism was obtained by performing the TE cost estimate using four different methodologies: two APL parametric estimates based on past missions and the NASA/Air Force Cost model (NAFCOM); a JPL parametric estimate using the JPL Outer Planet Mission Cost Model (OPMCM); and a "grassroots" estimate performed at the detailed task level by the study team. Therefore, the TE cost and schedule requirements are conservatively estimated and can be molded to fit within the resources available to the next Flagship mission.

2: Titan Science Goals and Objectives

2. TITAN SCIENCE GOALS AND OBJECTIVES

2.1 Introduction

Exploring an Earthlike Organic-Rich World

- Titan shares many features with other icy satellites but also with the terrestrial planets.
- Titan is the richest concentration of organic compounds known beyond the Earth's biosphere and thus offers a vital window into the origins of life in the universe.
- Titan's hydrological cycle with methane clouds and rain is analogous to the Earth's water cycle, but taken to extremes, with catastrophic downpours spaced by centuries-long droughts.
- Titan likely has an internal water–ammonia ocean.
- Titan's atmosphere shows dramatic seasonal variations in temperature, dynamics, and composition, together with a winter polar structure analogous to the Earth's ozone hole.
- Titan is a tidally stressed icy satellite with tectonically formed mountain chains, and it shows evidence of cryovolcanism.
- Titan's landscape is remarkably Earthlike, with dunes, streambeds, and presently liquid-filled lakes, as well as mountain ridges, karst-like depressions, and rare, eroded impact structures.
- Titan's atmosphere is unique in the solar system, but similar to many extrasolar planets in having strong dynamical forcing by gravitational tides.

Titan is an outstandingly rich scientific target. Much of this rich scientific interest can be captured in the theme "Exploring Titan – An Earthlike Organic-Rich World." Titan is Earthlike in both its hydrologically carved appearance and in its complex, highly coupled system from interior, to surface, to atmosphere, and through the magnetospheric interaction region that links it to the rest of the Saturn system. Titan therefore engages a wide range of scientific disciplines, many considered until now to be only "Earth sciences." Titan is rich in organics, not only in terms of its elemental inventory of carbon, but also in the wide array of forms and settings in which carbon appears, starting from the remarkably complex organic ionosphere to the lakes of liquid hydrocarbons at the poles and the seas of giant organic sand dunes that extend for thousands of kilometers across its equatorial region. Finally, Titan is a uniquely accessible body, easier to explore in situ than any other body in the outer solar system. Titan's thick atmosphere allows us to easily deliver instrumentation on a Lander and Balloon as well as on an Orbiter, and thus a wider range of scientific tools can be affordably applied to the investigation of Titan than of other icy satellite.

In this section, we first outline the Titan science background, noting a number of recent developments. We then lay out the formal science objectives determined by the Science Definition Team (SDT) and their relationship to previous studies, including the first (2003–2013) Solar System Decadal Survey and the 2006 Solar System Exploration Roadmap. These objectives are then tied to a representative payload (offered as an example only). The synergies between the three mission elements are noted, and the capabilities of the Orbiter relative to Cassini are explained. Orbit and mission design considerations are discussed, and payload details are given. Finally, some background on descope options, failure scenarios, and the methodology used to assess science contributions from the mission elements are presented.

2.1.1 Titan and Earth

It is surprising that in many ways the most Earthlike body in the solar system is not another planet, but Saturn's largest moon, Titan (Fig. 2-1). Indeed, if Titan orbited the Sun rather than Saturn, we would have no hesitation in calling it a planet in its own right. This strange new world is larger than the planet Mercury and has a thick nitrogen atmosphere laden with organic smog, which hid its surface from view until only recently. Far from the Sun, methane plays the active role on Titan that water plays on Earth, acting as a condensable greenhouse gas, forming clouds and rain, and pooling on the surface as lakes. Titan's icy surface is shaped not only by impact

craters and tectonics but also by volcanism in which the lava is liquid water spiked with ammonia ("cryovolcanism"), by rivers of liquid methane, and by tidally driven winds that sculpt drifts of aromatic organics into long linear dunes. This varied landscape, seascape, and weather make Titan uniquely like Earth.

The other dimension to Titan is its massive inventory of organic chemicals. The first step in understanding the role of organics in Titan's atmosphere was Kuiper's discovery of methane (CH_4) on Titan in 1944. Subsequent polarization measurements by Veverka and separately by Zellner, both in 1973, indicated the presence of a solid phase component in the atmosphere. These observations were the impetus for the laboratory experiments of Khare and Sagan (1973), which first suggested that methane photolysis could result in solid organic aerosols that Sagan referred to as "tholins."

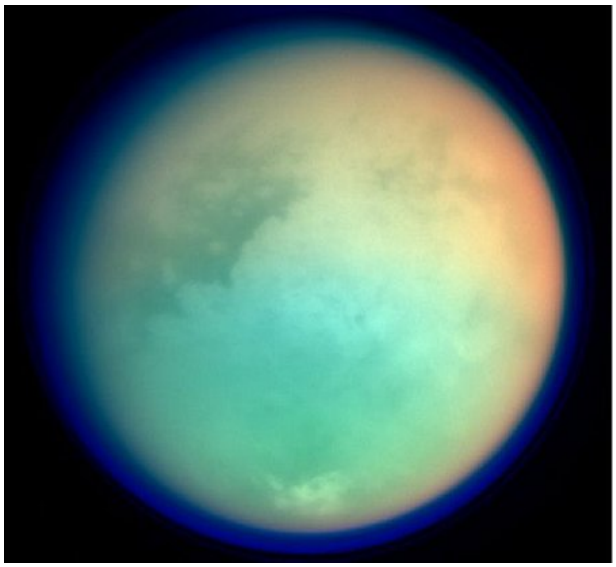

Figure 2-1. Titan in false color from Cassini ISS images *(NASA/JPL/Space Science Institute; PIA 06139).*

2.1.2 Titan's Atmosphere

When Voyager 1 flew past Titan in the early 1980s, it verified the presence of methane in a thick background atmosphere of nitrogen. Even more interesting was the detection of a host of more complex hydrocarbons and nitriles that resulted from the photolysis and energetic particle bombardment of the atmosphere. These hydrocarbons and nitriles form a thick organic haze that both scattered and absorbed visible and infrared (IR) photons and that was asymmetrically distributed in latitude, thereby playing an important role in determining the satellite's thermal structure and global dynamics. The laboratory studies carried out on the basis of the Voyager observations thus provided a tholin that was a good analog for the Titan haze. Based on this analog it could be concluded that the haze on Titan is composed of refractory organics that, once condensed, do not evaporate and are ultimately deposited on the surface with a net production rate of $\sim 10^{-14}$ g cm^{-2} s^{-1} (see review in McKay et al., 2001).

The Cassini-Huygens era of investigation has furthered understanding of Titan as the largest abiotic organic factory in the solar system. Mass spectrometry in the upper atmosphere showed that the process of aerosol formation appears to start more than 1000 km above the surface through a complex interplay of ion and neutral chemistry initiated by energetic photon and particle bombardment of the atmosphere (Waite et al., 2007). Measurements throughout the atmosphere, both remotely and in situ, have detected numerous hydrocarbon and nitrile gases, as well as a complex layering of organic aerosols that persists all the way down to the surface (Coustenis et al., 2007; Tomasko et al., 2005). Radar observations suggest that the ultimate fate of this aerosol may be the generation of expansive organic dunes that produce an equatorial belt around the surface. These sand dunes are remarkable in being exactly the same size and shape as linear (longitudinal) dunes on Earth (Lorenz et al., 2006), such as those found in the Namib and Saharan deserts. This type of dune forms in a fluctuating wind regime, which on Titan may be provided by the tides in the atmosphere due to Saturn's gravity acting over Titan's eccentric orbit (Fig. 2-2).

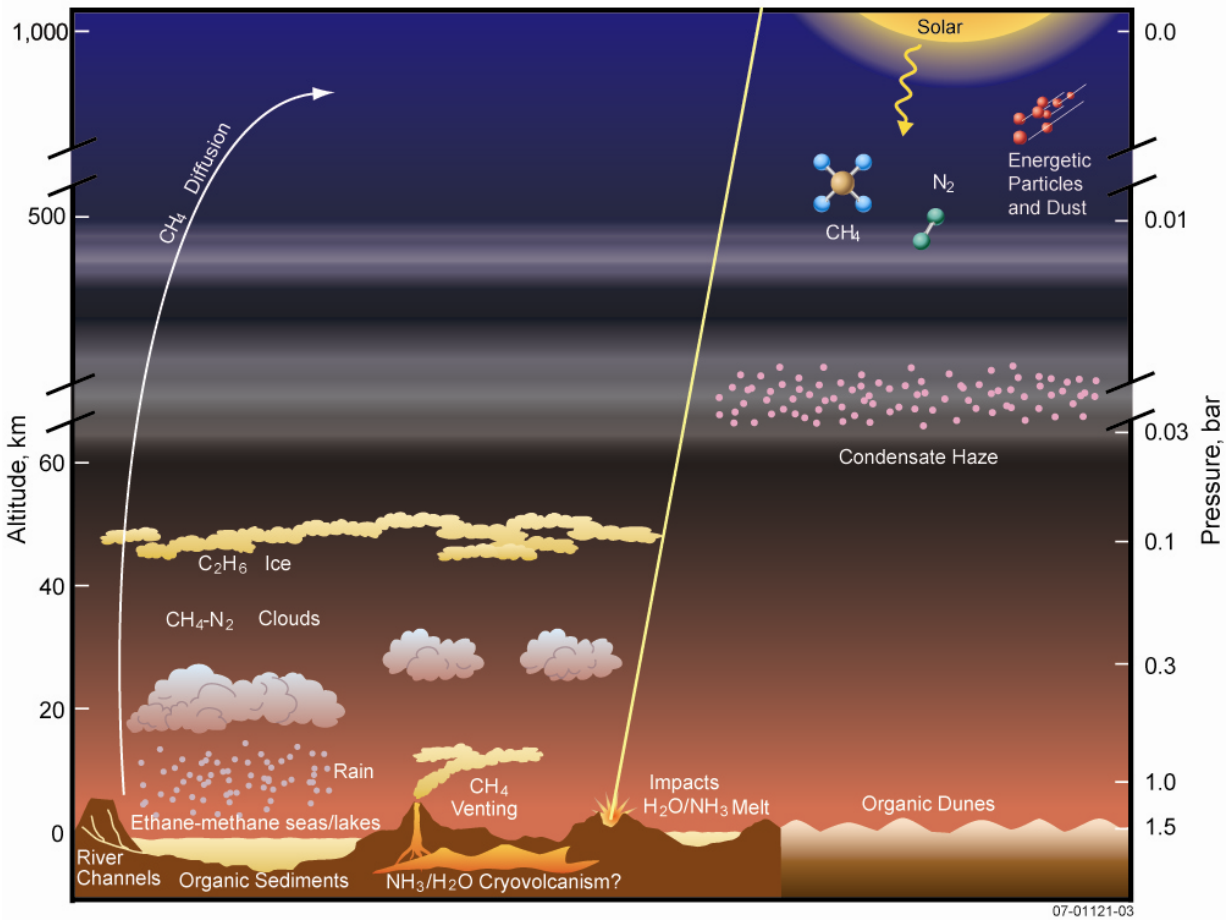

Figure 2-2. Processes on Titan. Material – most notably methane – cycles between the surface and atmosphere in a setting determined by long-term delivery from the interior and conversion to heavier organics by ultraviolet light and energetic particles.

Meteorologically, Titan is an outstanding body for comparative planetology. In some senses it resembles Venus (a slowly rotating body with a massive, optically thick atmosphere – conditions that lead to superrotating zonal winds). In other respects it may resemble Mars, in having a seasonal cycle forced by an appreciable obliquity (Titan 26°, Mars 25°) and having asymmetric seasons, since both orbits around the Sun are eccentric. Titan's southern summer (like that of Mars) is shorter but more intense than the corresponding season in the north. The seasonally changing solar forcing leads to an asymmetric hemisphere-to-hemisphere meridional ("Hadley") circulation, with only a transient epoch of Earthlike symmetric equator-to-pole Hadley circulation around equinox. Titan's thermally direct stratospheric meridional circulation transports organic gases and haze, leading to the seasonal north–south albedo asymmetry in the haze observed by Voyager. (The northern hemisphere, observed by Voyager at northern spring equinox in 1980, had more haze and was thus darker at blue wavelengths; this situation had reversed half a Titan year later when the Hubble Space Telescope [HST] re-observed Titan. Substantial changes in the haze structure are apparent even after only 1 or 2 years.)

The three most powerful atmospheric analogies for Titan, however, are those with the Earth. First, Titan's overall temperature structure is like that of Earth, with a troposphere warmed by a condensable greenhouse gas (methane on Titan, water on Earth), and is augmented by noncondensable greenhouse gases (hydrogen on Titan, methane and carbon dioxide on Earth). The fact

that the major greenhouse gas can condense – as with CO_2 on Mars and water on Earth – enables interesting climate feedbacks like the runaway greenhouse effect. The troposphere is topped by a stable stratosphere heated by absorption of sunlight (on Titan due to haze, on Earth due to ozone). This solar absorption by the haze is a powerful antigreenhouse effect on Titan, like the "nuclear-winter" or "impact-winter" scenarios described for Earth.

The second, and most obvious, analogy is the existence of a hydrological cycle involving methane clouds, rain, and at least transient rivers. While the possibility of such a cycle was predicted as soon as the proximity of Titan's surface conditions to the methane triple point had been noted in Voyager data, the first evidence of clouds emerged in spectroscopic data (Griffith et al., 1998) and in HST images (Lorenz and Mitton, 2002), both acquired in 1995. Subsequent observations showed clouds to be evolving on timescales of only hours, suggesting that precipitation may be occurring, and around the turn of the millennium large ground-based telescopes with adaptive optics systems showed massive variable cloud systems around Titan's south pole (where it was approaching midsummer). Cassini observations soon after its arrival in 2004 showed considerable detail on these clouds (although only a handful of different cloud systems have been observed on Cassini's sporadic flybys), and showed that the cloud tops ascended at velocities comparable with those predicted in models. These clouds, then, seem fully consistent with cumulus convection like that seen on Earth in desert summer.

From a thermodynamic viewpoint, the relative scarcity of clouds on Titan compared with Earth can be understood as a consequence of the efficient utilization of a much smaller thermal flux (Lorenz et al., 2005). The geographical distribution, however, is rather different. On Earth, rain clouds occur dominantly in the intertropical convergence zone, while on Titan models predict that they will track the subsolar latitude (e.g., Mitchell et al., 2006), although the details among models differ (e.g., Rannou et al., 2006). By analogy with Titan seen from 2000 to 2004, vigorous cloud activity is expected in the south polar region at the epoch of the Titan Explorer (TE) mission in 2028–2032.

Titan presents an interesting extrapolation of the Earth's hydrological cycle. The overall intensity of the cycle is weak: the available solar heating to evaporate surface moisture and drive the cycle is tiny and is not substantially compensated by the lower latent heat of methane compared with water. Thus, instead of the ~100 cm of annual rainfall observed on Earth, Titan must see on average only about 1 cm per (Earth) year (Lorenz, 2000a). However, Titan's thick atmosphere can hold a prodigious amount of moisture – equivalent to several meters of liquid. Therefore, were Titan to dump the moisture out of its atmosphere (which to a crude approximation, is what happens in violent rainstorms, as indicated in models of Titan rain clouds, e.g., Hueso and Sanchez-Lavega, [2006]), it would require ~1000 years to recharge the atmosphere with moisture. (The corresponding numbers for the present-day Earth are ~10 cm and a month.) A warmer atmosphere can hold more moisture, and it may see more intense storms separated by longer droughts, a pattern being discerned in the present epoch of global warming on Earth (Fig. 2-3).

Titan thus has a greenhouse hydrology taken to extremes. Although the broad characteristics of methane rain clouds can be reproduced in terrestrial models adapted to Titan, the resultant precipitation is crucially sensitive to parameters that are completely unknown and likely to be different between Earth and Titan, such as the droplet coalescence efficiency (e.g., Barth and Rafkin, 2007). Remote sensing (e.g., combined near-IR and radar observations) that can quantify the cloud ascent and the formation of precipitation will be key to resolving these issues. A further issue is that much precipitation may manifest itself as possible "rain without clouds" (e.g., Toon et al., 1988). Some indications from the Huygens probe (Tokano et al., 2006) point to driz-

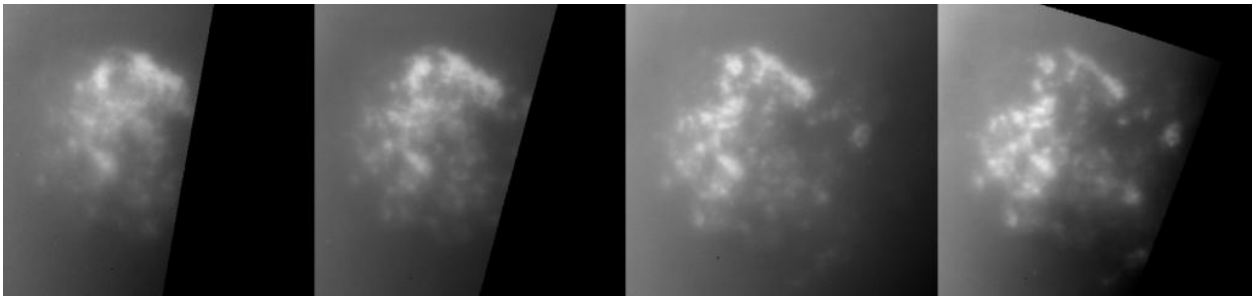

Figure 2-3. A sequence of Cassini near-IR images acquired by Cassini ISS (Porco et al., 2005) at arrival in 2004 showing evolving clouds over the south (summer) pole. The cloud system can be seen to evolve over timescales of just a few hours.

zle without optically thick cloud. Such subtle phenomena may be detectable by remote sensing, but in situ observations may be the only way to be sure.

Titan's clouds are not limited to convective cumulus. A pervasive, lingering cloud of ethane particles has been observed (Fig. 2-4) in the northern polar stratosphere in the present season (northern late winter), probably related to the downwelling of organic-rich air over the winter pole. Additionally, sporadic small cloud streaks have been noted at mid-latitudes with a possibly nonuniform longitudinal distribution. There is debate as to whether these cloud streaks are associated with the Hadley circulation and/or tides, or whether they are tied to surface features, either as orographic clouds or clouds triggered by surface venting of methane. Some support for a low-latitude methane supply has been noted in models (much as the Martian climate causes water to migrate to high latitudes), which point out that the low latitudes on Titan should progressively become methane-desiccated (e.g., Rannou et al., 2006) unless replenished by a surface source.

In this connection, the Science Definition Team – following the Titan Community Panel report to the Decadal Survey – strongly recommends that ground-based monitoring of Titan's seasonally varying weather is an important bridge between, and adjunct to, space missions.

A third analogy with the Earth relates to the polar stratosphere. Voyager observed Titan to have a UV-dark "polar hood," a dark haze cap over the winter pole (see Fig. 2-23 in Section 2.6.1.5). This cap was seen in high-phase-angle images to stand above the main haze deck and to connect with the detached haze layer. Circulation models (e.g., Rannou et al., 2006) can reproduce this behavior. These same latitudes are also known to have both the warmest and the coldest parts of the stratosphere, as well as enhancements by factors of ~100 in the abundance of certain nitrile gases. Evidently the upper atmospheric meridional flow converges at the pole and downwelling brings organic-rich air to lower levels. At low altitudes in this polar haze cap, low temperatures are found because the region is in winter shadow, and the rich supply of gas and haze provides efficient radiative cooling. In contrast, higher altitudes are illuminated, and also heated adiabatically by the descending air. Although it is connected to the detached haze at high altitude, the region is dynamically isolated by the circumpolar vortex. On Earth, the corresponding circumpolar winds isolate the winter stratosphere from the rest of the atmosphere; the catalytic surfaces of polar stratospheric clouds (PSCs) that form in the winter night cause the destruction of ozone, whose concentration becomes locally depleted, producing the ozone hole. On Titan, a complex cloud system (Fig. 2-4) may be triggered by the availability of condensation nuclei descending from the polar hood.

A rich set of chemical, radiative, and dynamical feedback mechanisms is associated with the evolution of the polar hood, with many analogies to the ozone hole on Earth. Cassini may ob-

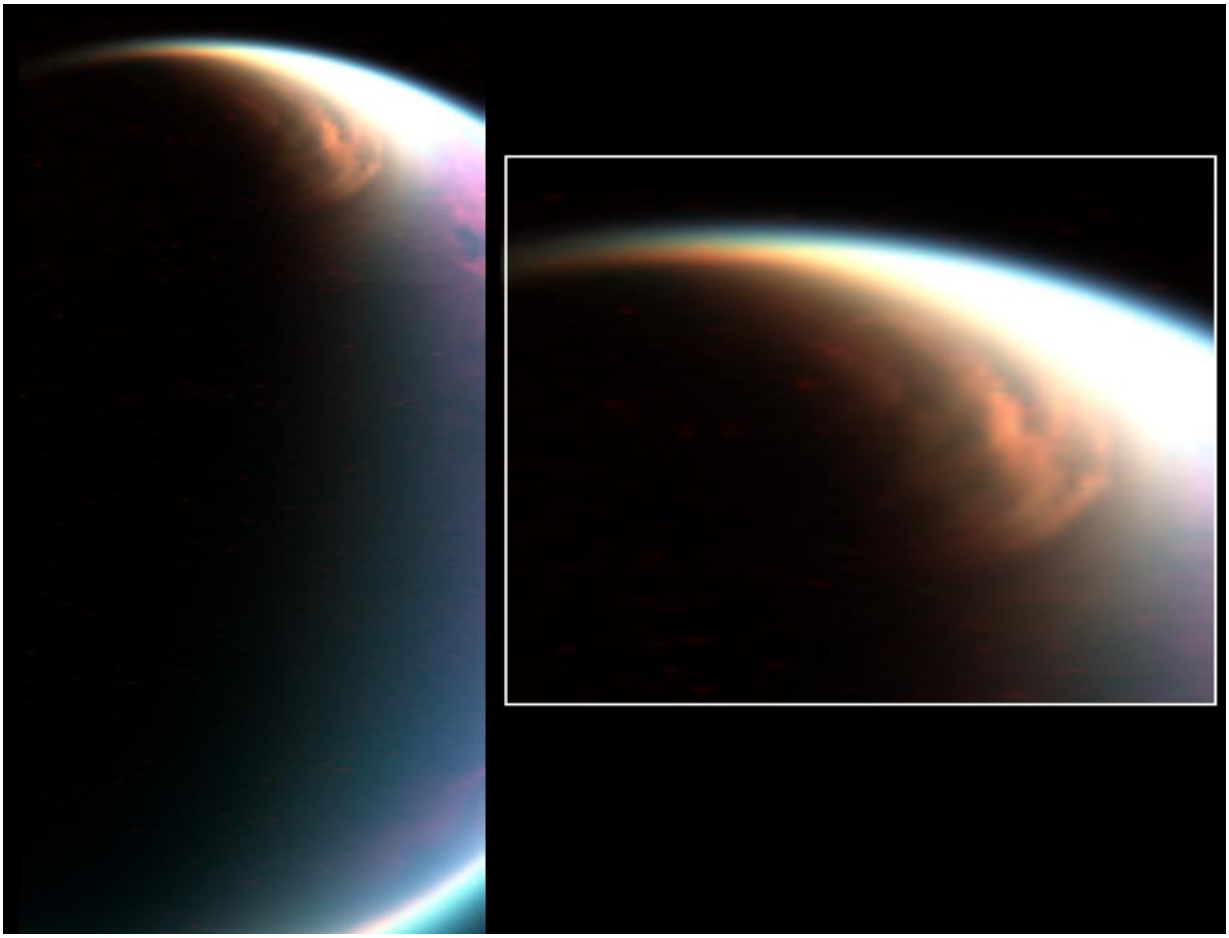

Figure 2-4. Cassini VIMS image showing a complex cloud, apparently of ethane, over Titan's north polar region in 2006, possibly connected with the polar hood at higher levels, and the hydrocarbon lakes on the polar surface *(NASA/JPL/University of Arizona).*

serve the early decay of the hood in the north, but a flagship will be able to observe the formation of a corresponding southern feature. HST observations of the decay of the south polar hood (Lorenz et al., 2005) at the same season (2002–2003) show that there are substantial year-to-year changes to observe. An important aspect of studies of these features with a follow-on mission is not only to observe the optical albedo (possible only in illuminated areas) but also to observe the coupled temperature, composition, haze, and wind fields, over the entire globe regardless of illumination, in order to disentangle the chain of cause and effect. The Titan Explorer Orbiter's suite of thermal IR and microwave instrumentation will be a powerful tool in this investigation.

A final, and perhaps unexpected, analogy may be between Titan and many extrasolar planets. Many of the known planets are close enough to their primary to be tidally locked and thus rotate synchronously. However, nonzero eccentricity (as for Titan) nonetheless may cause significant tidal effects. Walterscheid and Schubert (2007) have suggested that tidal forcing may be responsible both for the shear layer measured by Huygens Doppler tracking and for the distinct haze layers observed in Cassini images of Titan's atmosphere; see also Strobel (2006). Therefore, Titan may provide insight into models of the circulation and opacity structure of extrasolar planets.

2.1.3 Atmospheric Evolution and Magnetospheric Interaction

The evolution of Titan's atmosphere operates on two quite different timescales. The longest is the billion-year timescale commensurate with the origin and subsequent evolution of the overall system. This timescale is best studied by measuring the noble gas concentrations and their isotopic abundances, as well as the nitrogen and carbon stable isotope ratios. Cassini-Huygens provided important information in this regard. The abundance of the radioactively derived ^{40}Ar indicates that only a few percent of the total volatile inventory has been outgassed from the interior (Waite et al., 2005; Niemann et al., 2005). In contrast, the relatively low abundance of the primordial ^{36}Ar isotope suggests that nitrogen was not delivered during Titan's initial formation as molecular nitrogen, but more likely as ammonia that underwent subsequent chemical conversion into N_2 – the predominant constituent of Titan's present-day atmosphere. Furthermore, the enrichment of ^{15}N in N_2 to ^{14}N relative to an Earth reference suggests that, as at Mars, Titan has lost most of its nitrogen over the course of its evolution (Waite et al., 2005). This premise is substantiated by Cassini INMS measurements of isotopic separation in the upper atmosphere; by the escape of methane and hydrogen inferred from the altitude structure of these species in Titan's upper atmosphere (Yelle et al., 2006; and unpublished data analysis from Cassini INMS); and by the modeling of hydrodynamic escape processes. Measurement of the isotopic ratios of other noble gases such as those of neon, krypton, and xenon will provide important clues about the overall role of escape in the evolution of Titan's atmosphere, but such measurements must await new surface analysis techniques such as noble gas enrichment cells that will allow higher sensitivity than the Huygens GCMS (Niemann et al., 2005).

Escape processes can also be understood through in situ sampling of the plasma and energetic particle environment surrounding Titan and resulting from the interaction of Saturn's magnetospheric particles with the thick upper atmosphere (Fig. 2-5). Measurements by the Cassini CAPS Ion Mass Spectrometer (IMS) have shown the presence of Titan ionospheric species (e.g., nitrogen compounds) in the neighboring Saturn magnetosphere. These ions appear as isolated "lumps" or plumes in several of the Cassini Titan flybys. This material presumably is incorporated into the Kronian magnetosphere and may be lost down the magnetotail; it represents a pathway for energy and mass exchange between Titan and the rest of the Saturn system. The process by which these blobs or plumes are created and ejected from the Titan ionosphere, along with the role they play in the overall Titan evolution, is poorly understood. One puzzle in particular is where these plumes are created. Do they come directly from the ionosphere or are they "scraped" off by penetrating magnetospheric flows? The only data we have so far are from the Cassini spacecraft flybys of Titan about once per orbit, each at a different altitude, local time, longitude, and position in Saturn's magnetosphere.

This study that began during the Cassini-Huygens mission will benefit greatly from an orbital mission that samples the atmosphere near the exobase as proposed for the mapping phase of the TE mission. Here a complement of plasma, fields, and energetic particles experiments will be able to determine the three-dimensional structure of the sputtering interactions that leads to the heating and erosion of the upper atmosphere (De La Haye et al., 2007). By understanding the physics of these processes we will be able to extrapolate the escape rate back in time to appreciate their impact on the evolution of the Titan system, much in the same way that a future Mars aeronomy mission is expected to provide an understanding of Mars volatile escape history.

Understanding the history and present dynamics of the Titan atmosphere also requires understanding the mass and energy inputs. Although much of the energy that drives Titan's complex chemistry and dynamics comes from solar radiation, a substantial portion also comes from Ti-

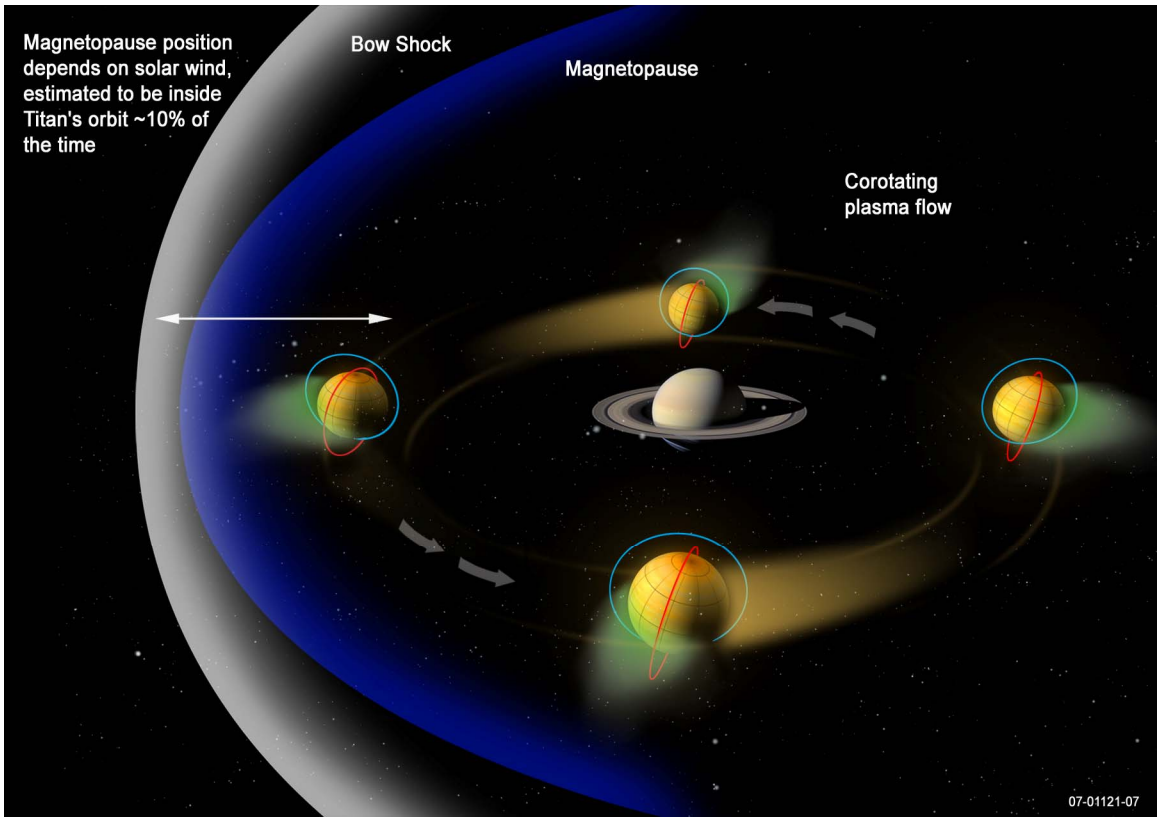

Figure 2-5. Schematic of the Titan interaction with the Saturnian magnetosphere. The TE mission orbits are shown as blue and red ellipses around Titan. Corotating plasma flow sweeps heavy ions (methane, nitrogen) along the orbit (yellow streak), while the electric field pulls light ions away radially (green streak). Normally Titan orbits inside the magnetopause, but sometimes solar wind pushes the magnetopause inside Titan's orbit.

tan's interaction with the Saturn magnetosphere. The electron spectrometer portion of the CAPS investigation has measured a substantial flux of energetic electrons from 0.1 to several kiloelectron volts on almost every flyby through the Titan atmosphere during the Cassini mission. This provides 10% to 20% of the energy that drives the complex organic chemistry in the upper atmosphere and ionosphere and maintains an appreciable nightside ionosphere despite the short chemical lifetime of many of these complex molecules (Cravens et al., 2004). The distribution of this energy input into the atmosphere is highly dependent on the magnetospheric interaction region to which a given parcel of atmosphere connects, which changes positions with respect to the solar input once per orbit of Titan around Saturn. Furthermore, Cassini has measured considerable temporal variation. Therefore, an orbital sampling mission such as the TE Orbiter, embedded in the magnetospheric interaction region, is an excellent way to determine this variability.

Another startling aspect of the energy input into the Titan upper atmosphere is the input of energetic ions as measured by the Cassini MIMI investigation (Mitchell, 2007). The energy of the observed protons ranges from several hundreds of electron volts to hundreds of kiloelectron volts and results in energy deposition from the exobase to altitudes as low as 500 km. This energy flux is highly variable and probably depends on orbital position. At times it appears to far exceed the solar x-ray and UV energy deposition at altitudes above 500 km (Ledvina, 2007). In addition, the lower-energy portion of this incident ion flux that deposits its energy and momentum near the exobase plays an important role in atmospheric escape and heating of the upper at-

mosphere through sputtering of the upper atmosphere (Johnson, 2007). Finally, it is worth noting that some of the incoming ions are not protons but oxygen ions derived from the Enceladus geysers and transported by Saturn's magnetosphere to Titan's orbit (Young, 2005). Although the flux is not extremely large, it may represent the only source of oxidized material in Titan's atmosphere above 500 km and may play an important role in the chemistry of negative ions and in the formation of carboxylic acids, aldehydes, and ketones in the upper atmosphere.

The second timescale of relevance at Titan is the timescale for the conversion of methane in the atmosphere irreversibly into higher-order organic/nitrile compounds that eventually end up deposited on Titan's surface. The irreversibility ties back to the escape of hydrogen from the system noted above, so that for every methane molecule photolyzed a molecular hydrogen molecule escapes. Given the present rate of photolysis and energetic particle–induced conversion processes, and given the size of the present atmospheric reservoir of methane, the atmospheric methane will be completely converted to higher-order organics on a ~10-million-year timescale if not replenished from the interior. Current escape rates for methane cut this timescale by a factor of 2. Evidence for the replenishment of methane from interior processes is found by observing the ^{12}C to ^{13}C ratio forming the methane of the upper atmosphere. The measured value is near that of the terrestrial reference, indicating that methane is resupplied and converted at a rate that prevents the buildup of the heavier isotope over time as is the case of nitrogen. The source of the resupply is a mystery that a future mission must address. Potential candidates include an evolving interior thermal history leading to episodic releases of methane over geological time, serpentization processes in the interior, and perhaps reprocessing of higher-order organics that have been buried by surface geological processes (see Atreya, 2006, for further discussion).

Regardless of the source, however, the methane/nitrogen conversion process that begins in Titan's upper atmosphere via ion neutral chemistry and leads to the creation of minor higher carbon and nitrile gases and their aerosol counterparts throughout the stratosphere is a story whose basic features have been revealed by Cassini-Huygens (Tomasko et al., 2007; Coustenis et al., 2007; Waite et al., 2007). It is a story that begs for a follow-up mission to sample an increased mass range and size distribution of particles at higher mass resolution and at many latitudes, altitudes, and positions within the magnetospheric interaction region in order to uncover the secrets of the most active abiotic organic factory in the solar system.

The most surprising aspect of the formation of the complex organics at 1000 km above the surface is the role that the ionosphere plays in the overall process. The chemistry of formation involves a complex coupling of neutral and ion chemistry and results in positive ions with masses over 1000 daltons (Da) and negative ions with masses exceeding 40,000 Da – larger than an insulin molecule (Waite et al., 2007). Cassini's measurements reveal a highly structured and variable ionosphere based on the ~32 close flybys to date. However, the Cassini measurements are in situ and occur at intervals of about 2 weeks or more, at varying altitudes, phase angles, and Titan orbital phase (or Saturn local time), all of which significantly affect electron density. At the lowest altitudes achieved by Cassini, just under 1000 km, it appears that the spacecraft has marginally detected the ionospheric peak, near 1000 km, although radio occultations seem to find the peak closer to 1200 km. The nature of this difference is not understood, but it may be a phase angle or temporal difference. In one as-yet unpublished flyby (T32) it appears that Titan was beyond Saturn's magnetopause, providing a first observation of Titan's ionosphere interacting with the shocked solar wind in Saturn's magnetosheath. All of this complexity and variability suggests that a future mission should be able to map the ionosphere over an extended altitude range and under a variety of orbital positions and conditions.

2.1.4 Titan's Geology

That the surface of Titan was largely hidden from Voyager's view precluded much thought on its landscape before the development of Cassini. The detection of rotational variability in Titan's radar and near-IR albedo in the early 1990s suggested that the surface was not homogenous, as might be expected from a uniform deposition of photochemical debris; something had to be making or keeping bright areas bright and dark areas dark. The variegated surface was revealed with near-IR images by HST in 1994, yielding the first maps (e.g., Smith et al., 1996). However, the poorly resolved patterns of bright and dark gave few clues to these areas' origin, and efforts to interpret the near-IR albedo in the few methane window regions in which the atmosphere is transparent did little more than suggest "dirty ice," with various compositions and amounts of dirt suggested.

The first Cassini data (e.g., Porco et al., 2005; Elachi et al., 2005; Sotin et al., 2005) showed that Titan has striking surface features on all scales, the result of a variety of geological processes. The pattern of bright–dark boundaries (Fig. 2-6) is reminiscent in places of terrestrial shorelines; a striking and as yet unexplained feature is that bright–dark contrasts are muted at midlatitudes.

One remarkable surprise is the relative paucity of impact craters, indicating a relatively young and active surface. Only a handful of impact structures have been named on Titan, ranging from 27 to 440 km in diameter, although some dozens of other likely candidates are identified. Most striking of these are the bright rings such as Guabanito, whose floors are covered in dark sediment (in some places visibly sculpted into dunes). It seems likely that a substantial population of impact structures is buried on Titan and could be revealed (as in the Martian low-

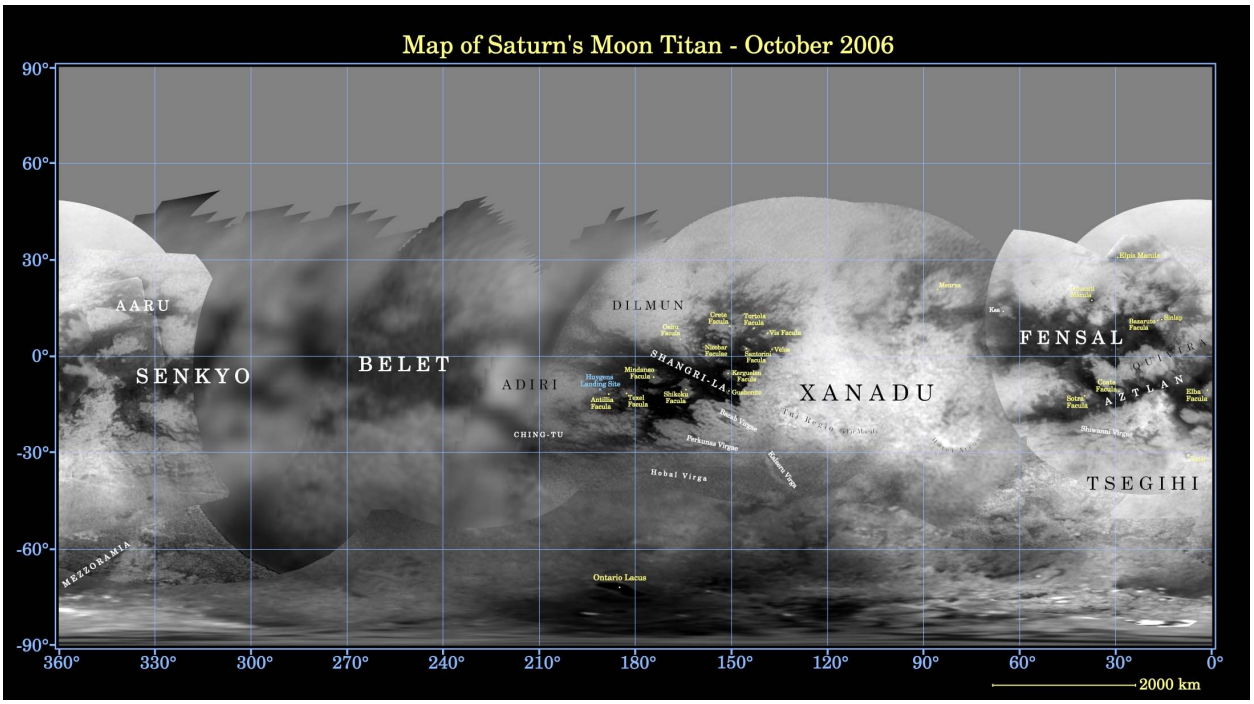

Figure 2-6. Map of Titan in the near-IR from Cassini ISS data. Note the large areas presently unimaged north of 40°N, and large tracts seen only at low resolution. The propensity for large bright–dark contrasts to be seen near the equator is real, however, not due to observational selection *(NASA/JPL/Space Science Institute).*

lands) by ground-penetrating radar on a future mission: the present inventory of impact structures, or even that expected by extrapolation into Cassini's extended mission, is too sparse to draw strong conclusions on issues such as leading:trailing asymmetry. Titan's craters appear morphologically different from those on other icy satellites, perhaps due to the role of the atmosphere or subsurface volatiles.

Fluvial modification of the surface was very evident at the Huygens landing site. Not only were steeply incised channels a few kilometers long and ~30 m across observed in the bright highland (which models of sediment transport suggest can be formed in methane rainstorms (Perron et al., 2006), but the knee-height vista from the probe after landing showed rounded cobbles characteristic of tumbling in a low-viscosity fluid.

Radar imagery has revealed channels on much larger scales than those seen by Huygens (Fig. 2-7). Radar-bright channels (probably cobbled streambeds like that at the Huygens landing site) have been observed at low and mid-latitudes (Lorenz et al., 2007a), while channels incised to depths of several hundred meters are seen elsewhere, and at high latitudes radar-dark, meandering channels are seen that suggest a lower-energy environment where deposition of fine-grained sediment occurs. Whether these larger channels and the large-scale flow features near the landing site (Soderblom et al., 2007a) would require a different climate regime to be formed remains to be determined – the flow of methane rivers in an unsaturated atmosphere on Titan is very analogous to the problem of ephemeral water flow on Mars; finding out whether the rivers dry out, freeze solid, or drain into an ephemeral sea will depend on presently unknown topographic and meteorological factors.

Aeolian activity on Titan has proven to be one of the major forces at work at low latitudes. Almost half the terrain within 30° of the equator is covered in dark (presumably organic-rich) streaks or dunes. In a few of the best-imaged regions, these prove to be dunes many tens of kilometers long and about 150 m high. Almost all appear to be linear (longitudinal) dunes, a type common in the Arabian, Sahara, and Namib deserts on Earth, but very rare on Mars: such dunes form typically in bidirectional wind regimes. A tidal wind origin has been proposed for Titan, but seasonal wind changes may play a role. It is assumed, but has not been shown, that these dunes are presently active.

Titan's tectonism is not well understood. A number of very-large-scale linear features are seen optically (Porco et al., 2005), notably the dark dune-filled basins Fensal and Atzlan (known collectively as the "H"). Smaller-scale "virgae" are also seen but are not understood. Radar imagery is not sufficiently widespread to evaluate tectonic patterns, although some linear mountain ranges (Radebaugh et al., 2007) have been detected, several forming a chevron pattern near the equator, and near-IR imagery by Cassini VIMS has also shown long ridges. An outstanding mystery is the nature of the large bright terrain Xanadu and its adjoining counterpart Tsegihi: these areas are distinct optically, and they have unusual radar properties. SAR imagery shows Xanadu to be extremely rugged, much like the Himalayas on Earth, although the mountain-forming process on Titan has not been robustly identified and may differ from place to place.

Cryovolcanism is a process of particular interest at Titan because of the known astrobiological potential of liquid water erupting onto photochemically produced organics (see Section 2.1.6). Radionucleides in Titan's interior, possibly augmented by tidal heating, can provide enough heat to drive a substantial resurfacing rate. Kinetically cryovolcanism is much easier in the Saturnian system, where ammonia can facilitate the rise of water through an ice crust. Ammonia not only depresses the freezing point of water by some 97 K but also lowers the density of the fluid, thus avoiding the negative buoyancy that likely inhibits cryovolcanism on the Galilean

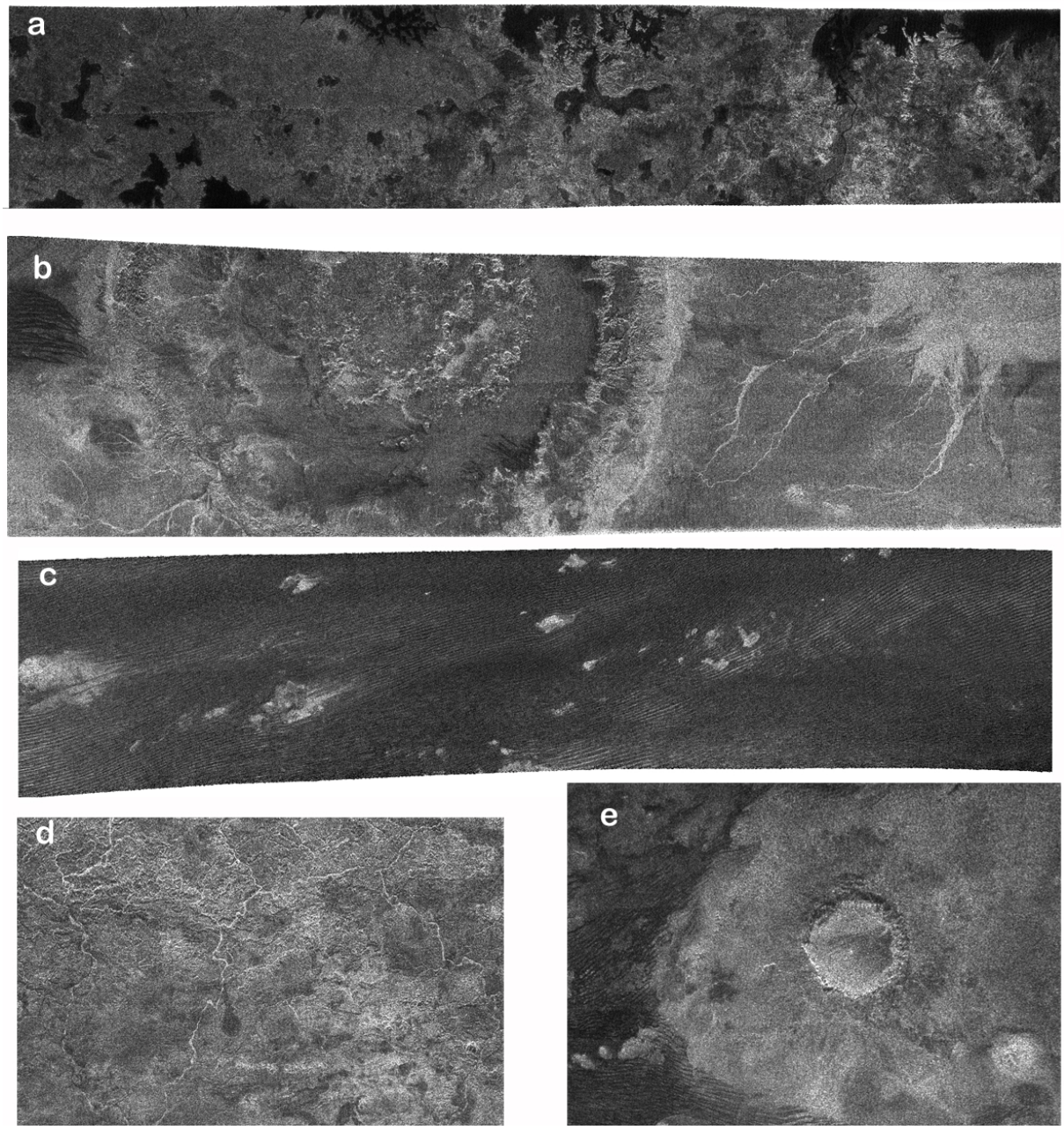

Figure 2-7. Montage of Cassini RADAR images showing the diversity of landforms on Titan's surface at a common scale. Location names are indicated in Fig. 2-6, and north is roughly upward. (a) Lakes near 80° North latitude, (b) the 440-km impact structure Menrva and network of braided river channels to the east, (c) giant linear sand dunes in the near equatorial region Belet, (d) dendritic river channel network in the western end of Xanadu, and (e) the 80-km impact crater Sinlap.

satellites. Several likely cryovolcanic structures have been identified in Cassini near-infrared (Sotin et al., 2005) and radar (Lopes et al., 2007) images (Fig. 2-8). Although evidence for active volcanism has not yet been widely convincing, there are apparent surface changes in Cassini data that require explanation (e.g., Nelson, 2007).

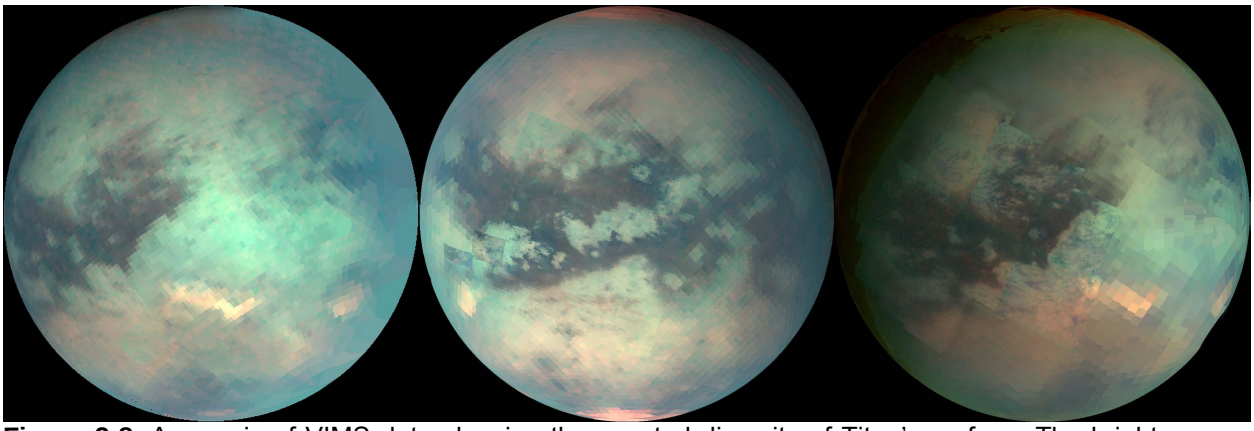

Figure 2-8. A mosaic of VIMS data showing the spectral diversity of Titan's surface. The bright orange areas, notably Tui Regio and inside Hotei Arcus, are particularly reflective at 5 μm, perhaps indicating CO_2-rich deposits that might be associated with cryovolcanism. In this mosaic, bright clouds are present around the south pole (*NASA/JPL, University of Arizona*).

An important Cassini finding needs to be underscored: at all spatial scales, there are structures seen in radar images that correlate with those in the near-IR, and there are structures that do not correlate at all. Radar and optical data thus tell us very complementary things about Titan's surface, and consequently a follow-on mission requires high-resolution global coverage by both techniques. At the near-IR, high-resolution coverage is particularly lacking from Cassini because of the short, rapid flybys. While the surface is spectrally diverse (e.g., Fig. 2-8) the identification of surface materials in the spectral windows Cassini is able to observe has proven challenging, making both in situ confirmation of composition and the extension to slightly longer wavelength in the Orbiter spectral map highly desirable.

2.1.4.1 Titan's Topography

Initial altimeter observations suggested that Titan may be rather flat (elevation changes of only a few tens of meters over hundreds of kilometers [Elachi et al., 2005]), but this impression has been overturned by new data. Mountain chains with heights >700 m have been measured (e.g., Radebaugh et al., 2007), and crater Sinlap is known to be 1300 m deep. As more data arrive, it is clear that Titan in fact has substantial topography (>1 km) on a variety of length scales. Cassini is not well equipped to generate a global topography dataset, and generating such data is a key goal for a follow-on mission, not only for geological studies such as impact crater relaxation but also as a boundary condition for atmospheric circulation models. Determining the topography is also essential for quantitative understanding of sediment transport processes, which have clearly played a major role in Titan's geological history, and particularly in combination with gravity data can constrain models of the lithosphere and interior. The revolution in Mars science permitted by the generation of a consistent, high-quality global topography dataset by the Mars Orbiter Laser Altimeter (MOLA) instrument can be mirrored by a Titan Orbiter radar altimeter.

2.1.5 Titan's Interior

Titan's overall density requires it to have roughly equal proportions of rock and ice. The extent of its differentiation (ice from rock, rock from metal) constrains temperatures in the early Saturnian nebula: Titan was almost certainly warm enough to allow differentiation into a rocky core with a water/ice envelope, but whether an iron or iron–sulfur core formed is not known.

Thermal evolution models suggest that Titan may have an ice crust between 50 and 150 km thick, lying atop a liquid water ocean a couple of hundred kilometers deep, with some amount (a

few to 30%, most likely ~10%) of ammonia dissolved in it, acting as an antifreeze. Beneath lies a layer of high-pressure ice (Fig. 2-9). The presence of ammonia, from which Titan's nitrogen atmosphere was presumably derived, distinguishes Titan's thermal evolution from that of Ganymede and Callisto.

A key piece of information, missing from Cassini results, is detection of the isotopic abundances of noble gases other than argon. In particular, the apparent loss of many atmospheres of nitrogen (implied by the nitrogen isotope ratio, but not in the carbon) may be reflected in isotopes of krypton or xenon, which were not detected by the Huygens GCMS. Another possibility, which lower detection limits could explore, is that some other removal process has operated on Titan (perhaps capture as guest molecules in methane clathrate or some other trap). Because Titan is an environment in which to grapple with such questions, investigation of Titan will support investigation of other aspects of solar system history.

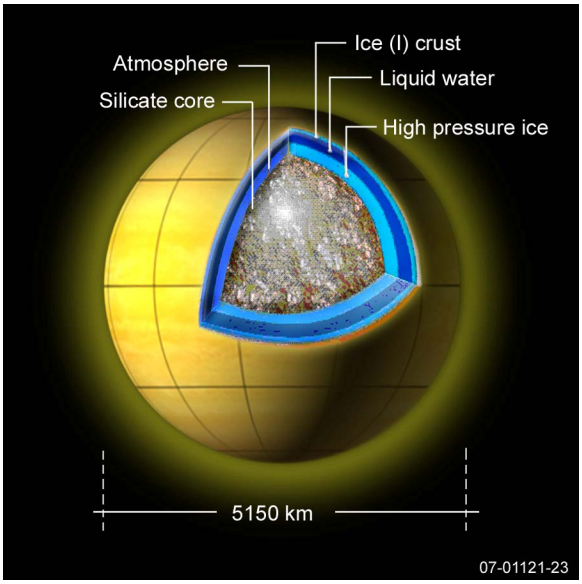

Figure 2-9. Putative internal structure of Titan. The amounts of ammonia and water in the internal liquid ocean, the thickness and strength of the ice crust, and the possibility of differentiation of the core into silicates plus iron are unknown *(PIA09171).*

Titan's interior has surely been affected by tidal evolution, since tidal dissipation with the present large (and unforced) eccentricity can be significant. A thermal evolution model by Tobie et al. (2005) suggests that Titan's ice crust was in fact as thin as Europa's (~15 km) for much of Titan's history, and only thickened to ~50 km in the last 500 million years or so (perhaps not coincidentally, the crater retention age determined by Porco et al., 2005, and Lorenz et al., 2007b).

Cassini will make gravity measurements on four flybys to determine the gravity coefficients J_2 and C_{22} near apoapsis and periapsis. These coefficients will change appreciably if the interior is fluid enough to respond to the changing tidal potential; it is expected that the tidal Love number k_2 can be determined with modest precision (~0.1), enough to discriminate between the internal ocean and no-ocean cases. A series of measurements by a Titan Orbiter is required to more quantitatively constrain the internal structure, measuring k_2 more precisely through the lag in tidal response and determining higher-order (up to 5 or 6) gravity coefficients. (Even after only a few days the tracking dataset for the Orbiter will surpass the Cassini data.) The gravity coefficients may shed light on whether continental-scale features on Titan such as Xanadu are associated with gravity anomalies. The geodetic combination of Orbiter tracking and precision surface ranging by altimeter has been shown at Mars to be very powerful: in addition to k_2 (which reflects the change in mass distribution), the surface height changes of several meters detectable by a radar altimeter can also constrain the h_2 Love number.

Titan's rotational dynamics are also a window into its interior. As on Earth, the rotation period of the surface can change over the course of a year as a result of changes in atmospheric angular momentum (see Section 2.6.3 on the Lander). On Titan these changes could be significant (altering the day length by some hundreds of seconds, leading to many tens of kilometers of displacements, depending on whether the crust is decoupled from the interior by an ocean or not). The pole position of Titan also has significance: gravitational torques should cause this to pre-

cess (in a Cassini state, the orbit normal and rotational pole precess together, with the obliquity between them dependent on the body's moment of inertia) with a period of around 600 years, perhaps a short enough timescale for differences between a Cassini determination and a follow-on mission to be noticeable. Radar imagery is particularly suited to rotation determination, although with adequate orbital position and attitude knowledge, near-IR sensing may work too. Precision tracking of a Lander, as with Pathfinder on Mars, brings another capability to bear.

We know more about the Earth interior from seismology than from any other technique. Although many seismic investigations are facilitated by networks of stations, even a single seismometer will answer many questions about Titan; tidal stresses on the moon will cause some excitation in addition to thermally driven seismicity, and the record will constrain the mechanical properties of the crust.

In addition to short-period seismic signals excited by earthquakes, we note in passing the surprising correlations recently observed at Earth between ionospheric disturbances and earthquakes (e.g., the ~40-km upward displacement of ionospheric boundaries by gravity waves during the Sumatra earthquake in December 2004 [Liu et al., 2006]). The combination of an Orbiter and Lander allows exploration of whether such correlations occur in an entirely different planetary setting.

Magnetometry is a proven tool in the investigation of planetary interiors. In particular, the field generated in an electrically conductive ocean by currents induced by a varying primary field has been used to infer an ocean on Europa. This technique can be applied to Titan, but is more of a challenge because of the much smaller magnetic stimulation by the near-polar Saturnian field and the shielding due to Titan's ionosphere. However, the combination of a magnetometer below the ionosphere (nominally on the Lander, although a magnetometer could instead be carried on a Balloon) allows the excitation and response to be separated.

Finally, a conductive water–ammonia ocean can act as the lower boundary of a waveguide cavity, with the ionosphere as the upper boundary. This cavity resonates, providing a set of harmonics (the Schumann resonances – on Earth with frequencies of ~8 Hz, 14 Hz, 22 Hz, etc.) in magnetic and electrical field measurements. An electric field sensor on the Huygens probe detected signals that might have been due to Schumann resonance (Simoes et al., 2007), but alternative explanations during the probe's dynamic descent, such as parachute oscillations, are possible. A more quiescent platform such as a Lander or Balloon will be a far more sensitive means of detecting any Schumann resonance.

The suite of tools made available by the combination of Orbiter and Lander (gravity, rotation, seismology, subsurface sounding, and magnetometry) offers a robust capability to probe Titan's interior, exposing not only an icy satellite interior in ways not possible at other satellites but also allowing an understanding of the particular role interior processes have had in shaping the atmosphere and surface of Titan.

2.1.6 Titan and the Origins of Life

While the chemical reactions that drive living things take place in liquid water, the reactions themselves are almost entirely between organic (i.e., carbon-bearing) compounds. The study of organic chemistry is an important, and arguably richer, adjunct to the pursuit of liquid water in the solar system. Titan's organic inventory is nothing short of massive – organic dunes cover some 20% of the planet, organic lakes and seas pockmark its polar regions, and the atmosphere itself displays a rich array of compounds even 1000 km above the surface.

In Titan's present, highly reducing atmosphere, photochemistry alone is something of an evolutionary dead end in that only hydrocarbons and nitriles (i.e., H, C, and N-bearing molecules)

are formed in any abundance. Oxygen-bearing compounds are generally too involatile to have a significant presence in Titan's atmosphere; water vapor and carbon dioxide have been detected in IR spectroscopy at part-per-billion levels, but probably derive from outside (like the traces of sodium and iron in the Earth's upper atmosphere) from the ablation products of meteoroids.

However, as noted by Thompson and Sagan (1992), tholins deposited on Titan's surface may be able to take the next evolutionary step by reacting with transient exposures of liquid water, namely, impact melt and cryovolcanism. Subsequent work has confirmed that such geological structures would indeed permit aqueous chemistry to occur for centuries or longer (e.g., O'Brien et al., 2005; Neish et al., 2006). Laboratory experiments have shown that the interaction of water with tholins can yield amino acids in substantial amounts – roughly 1% by mass (e.g., Khare et al., 1986; McDonald et al., 1994). Simpler nitriles have been detected in the gas phase on Titan (and indeed in the solid phase [Khanna, 2005]). These nitriles will be deposited as condensate on the surface and also can react to form astrobiologically interesting material in water. For example, Ferris et al. (1978) show that moderately concentrated HCN solutions can hydrolyze to form oligomers that in turn yield amino acids and pyrimidines. (Purines and pyrimidines – organic rings with some substitution of carbon atoms by nitrogen – form the bases that encode information in DNA in terrestrial living things; this information is used to determine the sequence of amino acids used to assemble into proteins.)

Laboratory work is needed to explore the temperature- and pH-dependence of the rates and yields of these reactions, although Titan reactions at a geological scale cannot be reproduced on Earth, at least not on conventional research timescales. Other factors (e.g., inorganic catalysts, or the pressure and concentration enhancements that can occur at a freezing front) may accelerate these reaction rates; for example, Takenaka et al. (1996) explored how freezing can accelerate by a factor of 100,000 the oxidation of nitrite by dissolved oxygen to form nitrate.

Specific geological sites such as the floors of impact features and the margins of cryovolcanic flows (Fig. 2-10) would of course be of particular interest for these investigations, but data at the scale of Cassini (or even an Orbiter) do not permit confident determination of the ease of landing or acquiring desired samples. However, the ample evidence of fluvial and aeolian transport on Titan suggests that sediments everywhere likely contain a component of eroded material from such structures.

Hodyss et al. (2004) recently noted that hydrolyzed tholins display a distinctive fluorescence under UV light (unhydrolyzed tholins do not), offering promise that such materials can be readily identified through proximity remote sensing before being sampled. For this reason, a dedicated UV illuminator is included on the sampling arm of the Lander to investigate whether such fluorescent materials are present in some or all of the surface material (UV light is scattered over too short a distance in Titan's dense atmosphere to be useful from kilometer distances).

Titan, an organic paradise, is certain to tell us much about the chemical evolution that may lead to life (Fig. 2-11). An important question is whether the synthesis pathways from atmospheric photochemistry via photolysis lead to a different assemblage of prebiotic material than those that occur on comets and meteorites; e.g., low-carbon ("Triton") tholin hydrolysis yields appreciable amounts of the amino acid leucine, which is not found in meteorites. An important additional consideration is whether the stereochemical preference for life to use left-handed enantiomers is a result of mere chance, or whether prebiotic synthesis yields non-racemic abundances of these stereoisomers.

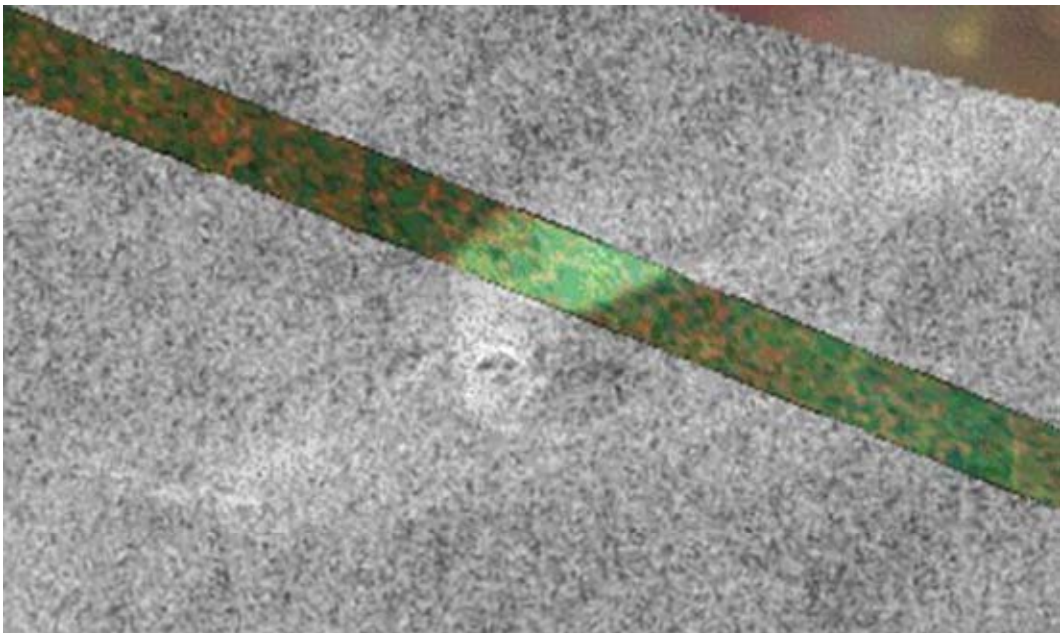

Figure 2-10. Circular feature about 7 km across with emergent flow identified as a likely cryovolcanic feature in Cassini radar image (Lopes et al., 2007). The near-IR spectrum of the flow (color band from Cassini VIMS data) shows the flow to be compositionally distinct from the surrounds. Note that very few high-resolution overlaps of Cassini near-IR and radar data like this exist at present *(PIA09036).*

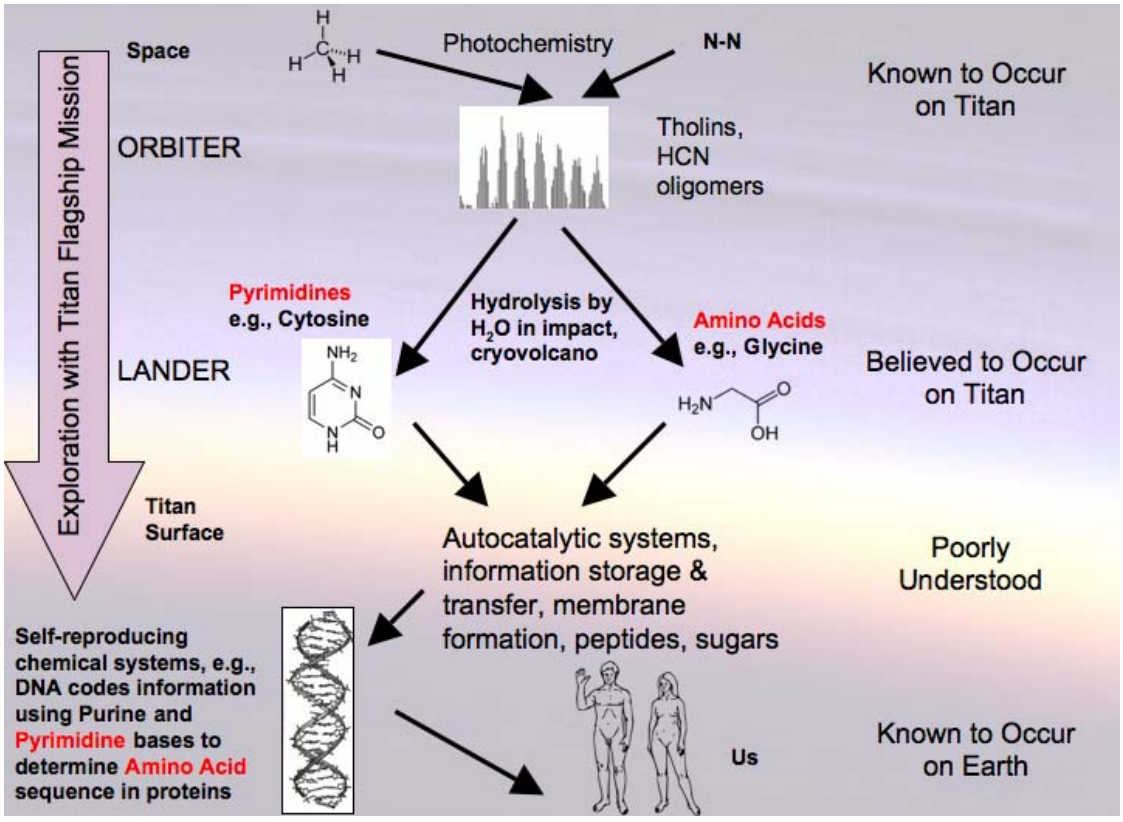

Figure 2-11. Relationship of materials and processes known and suspected to occur on Titan to the Orbiter and Lander measurements to be made by the TE mission and to the origins of life.

Titan is highly complementary with Mars in origins of life questions, in that Mars is an oxygen- and water-rich body, with little, if any, organic carbon, while Titan is an organic-rich body with little available oxygen. Europa is at least water-rich, but its formation history likely prevented the incorporation of much carbon. A significant geophysical difference with Europa is that on Titan the liquid water is not presently in contact with a silicate core (presently, the Titan core is isolated from the ocean by a layer of a high-pressure ice phase, although in the past there would have been intimate mixing of silicates with liquid).

Like the surfaces of Mars and Europa, the surface of Titan appears an unlikely location for extant life. However, it has been noted (Fortes, 2000) that Titan's internal water ocean might support life that had been introduced there previously. McKay and Smith (2005) noted that Titan's surface has photochemically derived sources of free energy that could support life, albeit cryogenic life-not-as-we-know-it using liquid hydrocarbons as solvents. Stoker et al. (1994) observed that terrestrial bacteria can in fact derive their energy and carbon needs by "eating" tholin. In this sense, a methane-rich atmosphere could act as a "poor-planet's photosynthesis," providing a means to capture the free energy from UV light and make it available for metabolic reactions.

The extent to which present-day Titan resembles the prebiotic Earth is not clear, since the oxidation state of the early Earth is not well determined. Certainly the present Titan is more reduced than was Earth, but formation of organic haze may nonetheless have taken place. Trainer et al. (2006) show that organic haze forms under UV illumination as long as the carbon:oxygen ratio is above about 0.6, and methane photolysis would have provided a richer organic feedstock than the delivery of organics from meteorites. In addition to the prebiotic synthesis role, haze on the early Earth may have been significant in the radiative balance (acting as an antigreenhouse agent) and in particular in providing UV opacity, which may have protected nascent biota in the absence of an ozone shield. Thus, while the analogy of Titan to the early Earth is sometimes overstated, insights clearly can be gained from studying Titan. Furthermore the universe may contain more Titan-like than Earth-like planets, whose habitability Titan may usefully inform.

The Limits of Organic Life in Planetary Environments (National Research Council, 2007) recently recommended reexamining the order or priority for future NASA missions in light of discoveries at Titan. This report highlights the preceding discussion relating to the "known" or at least suspected set of processes on Titan that may contribute to life as we understand it, with water as solvent, but also underscores a wider range of possibilities that cannot be rejected completely (informally, "weird life"), for example, based on chemistry in the hydrocarbon lakes. One of the most striking scenarios is the possible formation of solvents such as formamide in the interaction region between water–ammonia and nonpolar organics. Formamide as a solvent is more conducive to the formation and long-term survival of nucleotides than is water. In fact, formamide can form the amino acid adenine when trace quantities of hydrogen cyanide are present. Such processes would also be enabled by the ability of methane/ethane solvents in the lake layer above the interface to provide a rich chemical environment for evolution of bipolymers that would be impossible to obtain with water as the predominant solvent; by the ability of the ammonia–water mixture to supply trace minerals or trace compounds such as phosphor or arsenic; and by the rich heteroatomic nature of the seed organics formed by dissociation of nitrogen and methane in the upper atmosphere of Titan.

A separate aspect of living processes, quite distinct from the metabolic perspective, is informational and theoretical: can information be encoded and duplicated in the various organic chemical systems on Titan? Are there autocatalytic reactions that might, for example, give an isolated lake its own molecular fingerprint, or do all lakes have the same "genome" ?

Such possibilities help to build a tantalizing case for the astrobiological surface mission of the Titan Explorer multi-element architecture. These questions cannot be addressed from orbit. They also suggest that the methane lakes and seas should not be neglected as regions of interest for surface exploration, although transport processes may make traces of various environments accessible all over Titan. Furthermore, such an exploration scenario suggests that some basic chemical studies in Earth-based laboratories be initiated to examine the plausibility of these speculative suggestions.

2.2 Titan Science Objectives Development

With such a scientifically rich target body, the formality of establishing science objectives almost seems irrelevant; almost any measurement in such an interesting environment is likely to yield enormous scientific return. Evaluation of mission options, however, requires a formal statement of prioritized objectives against which the bewildering array of mission and payload options can be measured. The science objectives were determined by a NASA-appointed Titan Flagship Study Science Definition Team (SDT) drawn from community volunteers:

Ralph Lorenz (APL, Study Scientist and co-chair)	
J. Hunter Waite (SwRI, co-chair)	Aeronomy, Chemistry
Rosaly Lopes (JPL)	Geology (especially volcanism)
Scot Rafkin (SwRI)	Meteorology
Devon Burr (SETI)	Geology (especially fluvial)
F. Michael Flasar (NASA GSFC)	Atmospheric dynamics, Thermal IR
Andrew Steele (CIW)	Astrobiology, In Situ Chemistry
Gerald Schubert (UCLA)	Geophysics, Atmospheric dynamics
Kevin Baines (JPL)	Atmospheres, Near-IR Spectroscopy
Bill Kurth (U. Iowa)	Magnetosphere, Radio methods
Jonathan Lunine (U. Arizona)	Surface/atmosphere, Origins
Dale Cruikshank (NASA Ames)	Organics, Ices, Near-IR Spectroscopy

The SDT conducted activities from late January until August 2007, with three meetings, weekly telecons, and much electronic communication. The SDT formulated the objectives after review of the following documents:

- *New Frontiers in the Solar System: An Integrated Exploration Strategy* (Decadal Survey Report, 2003–2013) (National Research Council, 2003)
- *Titan,* first Decadal Survey Titan Community White Paper (Lorenz et al., 2002a)
- *Solar System Exploration,* the Solar System Roadmap (NASA, 2006)
- *Scientific Goals and Pathways for Exploration of the Outer Solar System* (Outer Planets Assessment Group [OPAG], 2006)
- *Titan Working Group Presentations* (OPAG, 2005)
- *Titan Prebiotic Explorer (TiPEx) Mission Study Final Report* (Reh et al., 2007b)
- *Titan Orbiter Aerorover Mission (TOAM)* (GSFC 2005–2006)
- JPL and Langley Titan Vision Studies (JPL, 2005; LaRC, 2005)
- *Titan and Enceladus $1B Mission Feasibility Study Report* (Reh et al., 2007a)

The adopted objectives mirror the two aspects of the mission theme "Exploring Titan, an Earthlike Organic-Rich World." The objectives of a Flagship-class mission are broader than those of several prior ad hoc mission studies (TiPEx, Visions, TOAM), which tended to empha-

size the surface chemistry/astrobiology aspects that Cassini could not address. A new understanding of Titan's remarkable diversity brings exploration of the variations in surface and atmosphere, and the coupling of interior-surface-atmosphere-space to the fore, while retaining the interest in prebiotic chemistry and in the geophysical/geochemical aspects of icy satellite surfaces and interiors.

The two nominally equal objectives each have four investigations, listed in priority order.

Exploring an Earthlike Organic-Rich World

OBJECTIVE 1: Titan: An Evolving Earthlike System

- How does Titan function as a system? How do we explain the similarities and differences among Titan, Earth, and other solar system bodies? To what extent are these controlled by the conditions of Titan's formation and to what extent by the complex interplay of ongoing processes of geodynamics, geology, hydrology, meteorology, and aeronomy in the Titan system?

OBJECTIVE 2: Titan's Organic Inventory: A Path to Prebiological Molecules

- What are the processes responsible for the complexity of Titan's organic chemistry in the atmosphere, within its lakes, on its surface, and in its subsurface water ocean? How far has this chemical evolution progressed over time? How does this inventory differ from known abiotic organic material in meteorites and biological material on Earth?

- **Investigation 1.1**
  - Determine the composition and transport of volatiles and condensates in the atmosphere and at the surface, including hydrocarbons and nitriles, on both regional and global scales, in order to understand the hydrocarbon cycle. Determine the climatological and meteorological variations of temperature, clouds, and winds.
- **Investigation 1.2**
  - Characterize and assess the relative importance today and throughout time of Titan's geologic, marine, and geomorphologic processes, e.g., cryovolcanic, aeolian, tectonic, fluvial, hydraulic, impact, and erosion.
- **Investigation 1.3**
  - Determine the role of the interaction of Titan's upper atmosphere and ionosphere with Saturn's magnetosphere in determining the evolution and climatology of Titan's atmosphere, especially the loss of materials and as a source of free energy and heat for driving the chemistry and dynamics. Determine the chemical pathways by which the nascent tholin formation takes place in the upper atmosphere.
- **Investigation 1.4**
  - Determine the state of internal differentiation. Understand the heat sources and thermal evolution of Titan. Determine if Titan has a metallic core and an intrinsic magnetic field. Determine the extent and origin (tidal vs. tectonic) of Titan's geodynamic activity.
- **Investigation 2.1**
  - Determine the chemical pathways leading to formation of complex organics at all altitudes in the Titan atmosphere and their modification and deposition on the surface with particular emphasis on ascertaining the extent of organic chemical evolution on Titan.
- **Investigation 2.2**
  - Determine geochemical constraints on bulk composition, the delivery of nitrogen and methane to the surface, and exchange of surface materials with the interior over geologic time.

- **Investigation 2.3**
  - Determine where chemical modification of organics on the surface may have occurred, in particular, possible hydrolysis of tholins by transient liquid water into pyrimidines, amino acids, e.g., via impact melt or cryovolcanic deposits.
- **Investigation 2.4**
  - Determine the depth of any subsurface liquid water ocean, its thickness and electrical conductivity, and the lateral variations in thickness and rigidity of the overlying icy crust.

The objectives and investigations are related to the goals in the Solar System Roadmap and the first Decadal Survey as shown in Fig. 2-12. The objectives, investigations, and the measurement goals that support each investigation are mapped onto various instruments of a representative payload in the strawman payload in Foldout 2-1.

<table>
<tr><th>2003–2013 Solar System Exploration (First Decadal Survey)</th><th>2006 Solar System Exploration Roadmap and 2007 NASA Science Plan</th><th>Titan Flagship Objectives</th></tr>
<tr><td rowspan="2">Learn how the Sun's retinue of planets originated and evolved.</td><td rowspan="2">How did the Sun's family of planets and minor bodies originate?</td><td>Obj. 2 Inv. 2: Determine geochemical constraints on bulk composition.</td></tr>
<tr><td rowspan="2">Obj. 1 Inv. 4: Determine differentiation and thermal evolution.</td></tr>
<tr><td rowspan="2">Discover how the basic laws of physics and chemistry, acting over aeons, can lead to the diverse phenomena observed in complex systems such as planets.</td><td rowspan="5">How did the solar system evolve to its current diverse state?</td><td>Obj. 2 Inv. 4: Determine depth, thickness of any subsurface ocean.</td></tr>
<tr><td>Obj. 1 Inv. 2: Geologic, marine processes, etc.</td></tr>
<tr><td rowspan="2">Understand how physical and chemical processes determine the main characteristics of the planets, and their environments, thereby illuminating the workings of the Earth.</td><td>Obj. 1 Inv. 1: Determine composition and transport of volatiles.</td></tr>
<tr><td>Obj. 1 Inv. 3 Determine interaction of atmosphere with Saturn magnetosphere.</td></tr>
<tr><td rowspan="3">Determine how life developed in the solar system, where it may have existed, whether extant life forms exist beyond Earth, and in what ways life modifies planetary environments.</td><td rowspan="2">What are the characteristics of the solar system that led to the origin of life?</td><td rowspan="2">Obj. 2 Inv. 1: Determine chemical pathways of complex organic formation.</td></tr>
<tr><td rowspan="2">How did life begin and evolve on Earth, and has it evolved elsewhere in the solar system?</td></tr>
<tr><td rowspan="2">Obj. 2 Inv. 3: Determine chemical modification of organics to prebiotic molecules.</td></tr>
<tr><td>Explore the terrestrial space environment to discover what potential hazards to the Earth's biosphere may exist.</td><td>What are the hazards and resources in the solar system environment that will affect the extension of human presence in space?</td></tr>
</table>

Figure 2-12. The Titan Explorer objectives and investigations are related to the Solar System Roadmap and the first Decadal Survey.

FOLDOUT 2-1: Traceability Matrix. The instruments of the TE Orbiter, Lander, and Balloon implement the mission objectives, which flow from the Solar System Roadmap and the first Decedal Survey.

				Orbiter														Lander								Balloon							
Objective	Investigation	Measurement	New Objective/Investigation	Radar Altimeter	SAR capability	Subsurface Sounding Radar	Orbiter Radio (Tracking & Occultations)	Orbiter Magnetometer	Orbiter Microwave Spectrometer	Ion and Neutral Mass Spectrometer	Orbiter Thermal IR	Orbiter UV Spectrometer	Plasma Package	Langmuir Probe	Energetic Neutral Particles	1-Micron Camera	Spectral Mapper	Lander Precision Tracking	Lander Seismometer	Lander Magnetometer	Descent Imager/ Radiometer	Lander Meteorology Package	Lander Spectrometer	Lander Camera & Microscope Camera	Lander Chemical Analyzer	Balloon TDL Spectrometer & Nephelometer	Balloon Imager	Balloon Subsurface Radar Sounder	Balloon Downlooking Spectrometer	Balloon Met Package	Balloon Tracking/ Navigation and Altimetry	Atmospheric Optics Monitor
OBJECTIVE 1: Titan: An Earthlike System. How does Titan function as a system? How do we explain the similarities and differences between Titan and other solar system bodies in the context of the complex interplay of the geology, hydrology, meteorology, and aeronomy present in the Titan system?	Determine the composition and transport of volatiles and condensates in the atmosphere and at the surface, including hydrocarbons and nitriles, on both regional and global scales, in order to understand the hydrocarbon cycle. Determine the climatological and meteorological variations of temperature, clouds and winds.	Determine composition of surface volatile inventory (minerals)	1.1														■							■								
		Global distribution of condensates	1.1													■	■															
		Deterrmine volatile distribution in atmosphere	1.1						■		■	■					■								■	■						
		Obtain vertical temperature soundings	1.1				■																									
		Direct measurement of zonal winds	1.1						■								■	■	■				■									
		Determine mean meridional circulation via tracers	1.1						■	■	■	■					■	■													■	
		Measure profiles of organic gas abundance	1.1						■	■	■	■																				
		Measure time-series meteorology	1.1																			■								■	■	
		Determine clouds at all altitudes: distribution, morphology, etc.	1.1	■					■		■						■	■														
		Measure surface temperature distribution	1.1																													
		Measure deposition of sunlight as fn(altitude)	1.1									■																				
		Measure optical properties of aerosol particles	1.1								■	■					■	■				■										■
		Measure number density and size of aerosol	1.1							■	■	■					■	■				■				■						■
		Measure the abundance of radiocarbon in surface materials	1.1																						■							
	Characterize and assess the relative importance today and throughout time of Titan's geologic, marine and geomorphologic processes, e.g., cryovolcanic, aeolian, tectonic, fluvial, hydraulic, impact and erosion.	Detect morphological indicators of exchange (vents, etc.)	1.2		■												■	■									■					
		Map global topography (1km/10m)	1.2	■																												
		Measure dynamic lake topography (10km/1m)	1.2	■	■												■	■									■					
		Measure regional topography (100m/1m)	1.2																									■			■	
		Regional morphology (1m)	1.2																								■					
		Global morphology and texture (100m)	1.2		■													■									■					
		Global near-IR albedo (100m)	1.2																													
		Regional variations of reflectance spectrum (10m)	1.2																								■					
		Local-scale morphology (0.1-0.01m)	1.2																					■			■					
		Regional subsurface structure (10km/100m)	1.2			■																										
		Regional subsurface structure (1km/10m)	1.2																									■				
		Measure topography boundary (100km/100m)	1.2	■	■	■																										
	Determine the interaction of Titan's upper atmosphere with Saturn's magnetosphere and the evolution of Titan's atmosphere, loss of materials, source of free energy and heat. Determine the chemical pathways of tholin formation.	Measure vector magnetic field	1.3					■													■											
		Measure high-energy magnetospheric electrons	1.3										■																			
		Measure thermal electron density and temperature	1.3			■	■						■	■																		
		Mesure ion velocity distribution in the ionosphere	1.3							■			■																			
		Measure high-molecular mass ion composition	1.3							■			■																			
		Measure high-molecular mass neutral composition	1.3							■																						
		Measure escape flux of superthermal neutrals	1.3							■																						
		Detect high-energy neutrals and ions from interactions	1.3												■																	
		Measure flux and energy of cosmic rays	1.3																													
	Determine internal differentiation, thermal evolution of Titan. Determine if Titan has a metal core and an intrinsic magnetic field, extent and origin of geodynamic activity.	Measure rotation parameters (pole position)	1.4		■													■	■													
		Local subsurface seismic structure	1.4																■													
		Low-order gravity field (N=6)	1.4				■																									
		Low-order topography (polar/equatorial radii)	1.4	■		■																										
		Vector magnetic field around Titan	1.4					■													■											
		Detect presence of seismic activity (tidal and tectonic)	1.4																■													
OBJECTIVE 2: Titan's Organic Inventory - A Path to Prebiological Molecules. What is the complexity of Titan's organic chemistry in the atmosphere, within its lakes, on its surface, and in its putative subsurface water ocean and how does this inventory differ from known abiotic organic material in meteorites and therefore contribute to our understanding of the origin of life in the solar system?	Determine the chemical pathways leading to formation of complex organics at all altitudes in the Titan atmosphere and their modification and deposition on the surface with particular emphasis on ascertaining the extent of organic chemical evolution on Titan.	Determine CHONPS elemental composition of surface	2.1																						■							
		Determine surface composition of complex organics	2.1																						■							
		Characterize physical state of organics	2.1																					■								
		Measure isotope ratios of C,N,O of surface organics	2.1																						■							
		Measure chirality of organic compounds	2.1																						■							
		Measure chemical abundance of gases in atmosphere	2.1						■	■	■	■													■	■						
		Measure chemical composition of particulates	2.1								■														■							
		Measure sources of free energy	2.1									■	■																			
		Measure atmospheric thermal structure with latitude	2.1				■		■		■																					
	Determine geochemical constraints on bulk composition, the delivery of nitrogen and methane and exchange of surface materials with the interior	Measure noble gases and isotopes (esp Kr, Xe)	2.2																						■							
		Detect ammonia in surface material	2.2															■												■		
		carbon, nitrogen isotopes in surface/atmosphere reservoirs	2.2						■		■														■	■						
		Measure D/H in surface material	2.2																						■							
		Composition of gases released from vents, etc.	2.2						■															■	■	■				■		
	Determine chemical modification of organics on surface, e.g., hydrolysis via impact melt.	Determine CHONPS composition of modified deposits	2.3																						■							
		Determine composition of complex organics in special sites	2.3																						■							
		Identify potential chemical modification sites from mapping	2.3		■													■												■		
	Determine the depth of any subsurface liquid water ocean, its thickness and electrical conductivity and the lateral variations in thickness and rigidity of the overlying icy crust.	Measure induced magnetic field	2.4					■													■											
		Detect seismic reflections within crust	2.4																■													
		Measure normal seismic modes	2.4																■													
		Detect subsurface radar reflections	2.4			■																						■				
		Measure libration and variations in rotation period	2.4		■														■													
		Regional scale topography (~20 km) (flexure)	2.4	■		■																										
		Measure changes in gravity field (k_2)	2.4				■																									
		Measure orbital changes in topography (h_2)	2.4	■																												

2.3 Titan Explorer Capabilities

2.3.1 Inter-Platform Synergy

There is substantial (and, in the outer solar system, unprecedented) synergy between the three platforms on this mission. The synergy between in situ measurements and orbital data is so pervasive in the Earth sciences that it is often forgotten: satellite measurements have not displaced the need for networks of meteorological stations and the daily release of hundreds of balloons. The formation of the Antarctic ozone hole escaped notice from satellite measurements until observations from the ground in 1985 determined a dramatic drop in ozone concentration and prompted a re-examination of the satellite data, and it was in situ measurements that confirmed the mechanism of ozone destruction. At Mars, it was known from orbit that Meridiani displayed the spectral signature of haematite, but only in situ observations gave the startling insight that this signature was due not to outcrops but to "blueberry" particles littering the surface.

At Titan, for example, consider the determination of Titan's crustal properties and internal ocean. While analysis of long time-series of Orbiter magnetometer data alone might permit the isolation of an induced magnetic field from an internal water-rich ocean beneath Titan's surface from the varying Saturn field, this separation becomes much easier with simultaneous measurements from the Lander (a Lander–Orbiter combination of measurements that has not been performed since Apollo). Analysis of these data may constrain some combination of the depth, thickness, and conductivity of the ocean, into which some further insight might be gained by studying Schumann resonances by measurements on the Lander or Balloon. Similarly, the response of Titan's crust to the changing gravitational tidal potential measured by Orbiter precision altimetry and gravity field (essentially measuring how deformable the crust is, i.e., a combination of its thickness and strength) becomes much more interpretable with the inclusion of seismic measurements from the Lander, which provide insight into the mechanisms and scale of crustal deformations, as well as perhaps a direct measurement of its thickness. Lander precision tracking and radar imaging from orbit constrain variations in the Titan's length of day, which are a measure of the crustal response to torques (i.e., its moment of inertia – thickness and density).

In studying Titan's geology and sedimentology in particular, Balloon imagery and high-resolution subsurface sounding will be key in investigating the contacts between various geological units to establish superposition relationships, such as the depth profile and boulder size distribution at, for example, alluvial fans. Meanwhile, the radar and near-IR imaging from orbit will lay out geological units on the global scale, together with the topography that drives much of the transport. Lander data will characterize the sediment itself (e.g., parameters such as grain rounding measured with a microscope camera will constrain how the sand was formed and transported). Together these data form a powerful picture of how Titan's landscape has evolved.

As another example, the long-term variation of the position of the Balloon provides enormously powerful integral constraint on tropospheric winds (i.e., even Hadley motions of millimeters per second can add up to substantial displacements after days or weeks), while Lander meteorology measurements at a single location yield a time series isolating diurnal (tidal), seasonal, and stochastic variations. Large-scale seasonal changes in the bulk tropospheric zonal motion averaged over the entire planet will manifest themselves in changes in the length of day, which can be monitored by radar imaging and by precision tracking of the Lander. These datasets on the tropospheric winds can be augmented by cloud-tracking from the Orbiter. Then, stratospheric winds can be determined at some altitudes directly by microwave spectroscopy, and indirectly by thermal IR and microwave temperature measurements and the thermal wind equa-

tion. Stratospheric meridional motions can be inferred from tracers such as haze and nitrile species. All these datasets can be combined into an integrated picture via Global Circulation Models (GCMs).

It can be seen from these examples that many individual measurements combine several unknowns, which can only be robustly teased apart by combining multiple datasets.

We have not attempted to quantify these synergies, but even this short set of examples demonstrates that the science value of the mission elements in combination is vastly superior to that of the individual elements or a subset thereof in isolation. These rich synergies ensure that the archived datasets from the mission will be an enduring contribution to a wide range of planetary (and Earth) sciences.

2.3.2 Orbiter Capabilities Compared with Cassini

Clearly, the Cassini-Huygens mission continues to dramatically advance understanding of Titan. Exciting though these developments are, the Titan Explorer mission offers several orders of magnitude advance upon Cassini. This section quantitatively compares the capabilities of both the nominal and planned extended mission of Cassini with the capabilities of TE.

The most obvious advantage is immersion in the Titan environment. Cassini is in orbit around Saturn, a body that is 1.2 million km away from Titan (three times farther than the Moon is from the Earth). Most of Cassini's Titan exploration is on fleeting (and intensely choreographed) encounters. Taking 4 Titan radii (10,000 km range) as a threshold for close investigation, Cassini's total observing time is very short. Even combining the 44 flybys in the nominal Cassini mission with the 26 planned in an extended mission yields a total time of less than 72 hours. In other words, in the first 3 days of a TE mission, an Orbiter will spend more time close to Titan than Cassini will have spent in its 6 years at Saturn. The 3 to 4 years of operation at Titan will therefore represent about a three hundredfold time increase in Titan immersion. (For certain measurements, the enhancement is even greater due to the addition of a year of measurements from the Lander and Balloon.)

This prolonged immersion permits a systematic and complete survey of what Cassini has shown to be a highly variable and diverse system. Whereas Cassini's Titan mapping is piecemeal (perhaps 35% of the surface will be mapped by radar at resolutions of 300–1500 m, and altimetry is recovered only in short scattered swaths), the Flagship will attain 100% coverage at 100-m resolution, and obtain a complete topography dataset plus a regional imagery survey from the Balloon attaining ~1-m resolution.

Fig. 2-13 lists TE Orbiter returns that are directly comparable to Cassini's. The TE mission provides 2 or 3 orders of magnitude improvement. (Note that the enhancement in Titan data volume over Cassini is about one and a half orders of magnitude: Cassini spends about 8 hours downlinking the ~3 Gbits of data from each flyby during which it spends 1 hour closer than 10,000 km. The total return, ignoring some distant monitoring, is therefore ~200 Gbits over the ~72 flybys, over 6 years.) Depending on the efficiency of utilization of DSN time, a 4-year Titan Orbiter with 8 h/day at 100 kbps can return ~4200 Gbits.

Similarly, the more advanced instrumentation proposed for TE makes measurements that Cassini was simply not equipped to make. In some cases this is simply a feature of knowing from Cassini measurements that there are new puzzles to solve (such as the formation of remarkably complex organics at high altitude on Titan); in others the reason is that much Cassini instrumentation was designed as a "Swiss Army Knife," able to tackle various scientific problems throughout the Saturnian system. TE's focus on Titan allows its instrumentation to be more efficiently designed, scalpel-like, for Titan specifically.

Measurement	Cassini Nominal Mission (through July 2008)	Cassini Extended Mission (2008–2010)	TE Mission
Radar surface mapping	~25% coverage at 300 m–1 km SAR resolution. Few % at 1–2 km Global coverage at 20+ km resolution (Magellan ~100% at 100 m)	~35% coverage by high-resolution SAR, ~10% lower-res (1–2 km) (~30 Gbits)	100% at 100 m
Near-IR surface mapping	<1% coverage at better than 2 km/pixel Near-global coverage at 10–20 km Spectral Resolution $\lambda/\Delta\lambda$~200	Few % at 2 km/pixel? (~80 Gbits)	90%+ at 100 m (depending on season)
Interior structure	J_2, C_{22}	Tidal Love number k_2 to ±0.1 (interior ocean ~0.2; without ~0.0)	Coefficients to order 5 or 6 Robust k_2, h_2
Topography	~10,000 km of altimetry tracks, ~20 km footprint, 50-m resolution (MOLA ~ 20 million km, 200-m footprint, 1-m resolution)	~15,000 km (3 Gbits?)	~5,000,000 km at 20 m or better (plus lake tides to 1.5 m)
Troposphere	~8 radio occultation profiles	~12 radio occultation profiles	Microwave soundings plus ~ several hundred occultations
Stratosphere	~8 radio occultations. ~4 solar and stellar occultations Few hundred (?) hours of mid/far IR spectral observation (yielding composition maps, etc.)	~12 radio occultations, ~15 solar and stellar occultations Few more hundred hours IR	Microwave, mid/far IR, stellar and radio occultations
Ionosphere	~30 profiles. Some neutrals-only. Total ~100 min ram-pointed 950 < 2500 km	~50 profiles. ~150 min	Hundreds of deep samplings. >3 years below 2500 km
Magnetic field	~40 magnetic field observations above the ionosphere – one or two perhaps below peak	~ 70 observations as left 1 low observation likely to be below ion peak	~5000 orbits, hundreds below ion peak
Total time within 10,000 km	~40 hours	~ 60 hours	~3–4 years (~30,000 hours)

Figure 2-13. Comparison of Cassini Titan measurements with those of the TE Orbiter.

Finally, the architecture of TE permits altogether new kinds of science beyond those possible with Cassini. For example, the long-term monitoring of seismic and meteorological activity enabled by the Lander will provide enduring in situ science products of a sort not seen anywhere in the solar system since Viking and Apollo.

2.4 Mission Factors

2.4.1 Timeframe

The SDT considered science desires along with practicalities regarding the TE mission epoch and duration. The two most relevant timescales are the Titan year (which is the same as Saturn's orbital period around the Sun, 29.5 Earth years) and the Titan day (its orbital period around Saturn, 15.945 Earth days).

Although observing 2 Titan years would be desirable (by analogy with Mars missions), to establish the full annual cycle and identify interannual variability, 2 Titan years exceeds both the demonstrated lifetime of any space system and the productive longevity of scientists. However, observations with HST and other astronomical facilities show that Titan's atmosphere displays significant seasonal change over periods of 2 Earth years. An Orbiter mission duration of half a Titan season (i.e., ~3.5 Earth years) will certainly show profound changes, and is commensurate with the feasible longevity of a spacecraft and its power supply.

The SDT considered the most favorable epoch for a mission – notably, whether a solsticial or equinoctial mission might be more interesting. In fact, no strong preference was found; both sets of seasons are equally interesting, given available data. Key features of solsticial Titan are (1) the final decay of the UV-dark polar hood and the strong circumpolar winds in the summer hemisphere, (2) the formation of the corresponding winter polar structure linked to a detached haze layer, (3) corresponding latitudinal variations in several organic gas abundances such as HCN, and (4) tropospheric convective clouds of methane around the summer pole. At equinox, a corresponding set of phenomena is observed: (1) emergence of the winter polar hood into sunlight and the onset of its destabilization, (2) maximum interhemispheric haze asymmetry, (3) probable low-latitude cumulus clouds and rainfall, and (4) formation of a temporarily symmetric Hadley circulation with upwelling near the equator and downwelling near both poles. Since all these features appear to represent a continuum of linked processes, all seasons are of interest.

The seasons are presently assumed to be broadly symmetric, although as with Mars, the eccentricity of the body's orbit around the Sun causes the southern summer to be shorter and more intense than its northern counterpart. Whether surface changes occur is not yet known (although Cassini has revealed some indications of optical surface changes, together with theoretical arguments for seasonal changes via polar evaporation and deposition of liquid methane). It seems likely that surface changes may occur at least at the summer pole, if the large convective cumulus clouds there (such as those observed at the south in 2000–2004) are associated with rainfall and thus fluvial erosion.

Although no strong preference for season was determined, the epoch anticipated for the present mission (determined by the launch epoch and the feasible range of trip times) is complementary to Cassini (Fig. 2-14). Cassini's nominal and extended missions (2004–2008 and 2008–

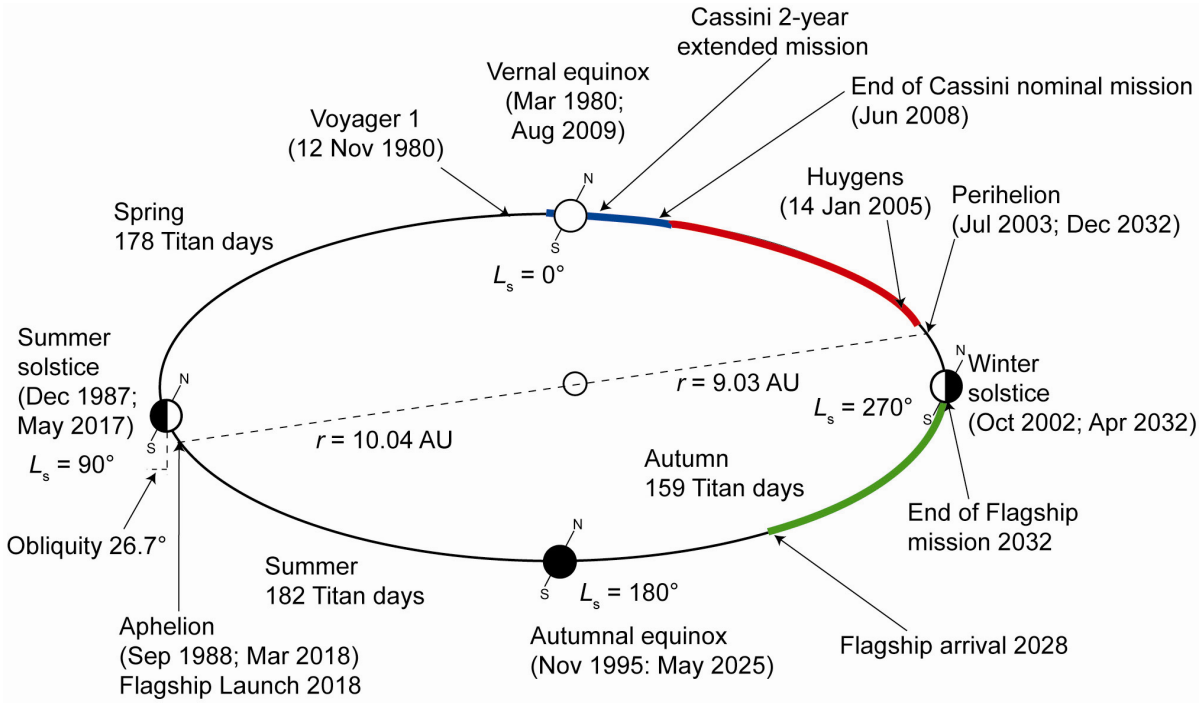

Figure 2-14. Seasons on Titan. TE arrives between equinox (2025) and northern winter solstice (2032) (i.e., same season as 1995–2002, thus complementary to the season presently observed by Cassini).

2010) follow Titan through late southern summer (southern summer solstice was in 2002, with perihelion in 2003), across the northern spring equinox in 2009, and into the first part of northern spring. The TE launch in 2018, with a 9–10 year trip, sees Titan arrival in 2027–2028, with operations through ~2032. Thus, TE will observe buildup to summer solstice, the part of the seasonal cycle most complementary to Cassini.

Titan's diurnal period of ~16 days also defines a key set of variable phenomena. Not only does the illumination of Titan change, but the magnetospheric setting for Titan (and thus the intensity and orientation of various energy sources driving activity and chemistry in the ionosphere) changes. Furthermore, Titan's orbit is appreciably eccentric (e = 0.029), and thus the tidal stresses change by some 10% throughout 1 day, leading to likely variation of seismic activity on this timescale. Uniquely in the solar system, Titan's near-surface winds may be dominated by a tidal component, and meteorological records on the surface should extend over at least two tidal periods.

In fact, any platform (Lander, Balloon, etc.) able to survive more than one orbital period on Titan is likely to be able to survive many. The science return from these platforms is likely to be downlink-limited, and so mission duration translates directly into science value. A nominal value of a year is therefore assumed as a reasonable science requirement (further study will reconcile data volumes with telemetry capability).

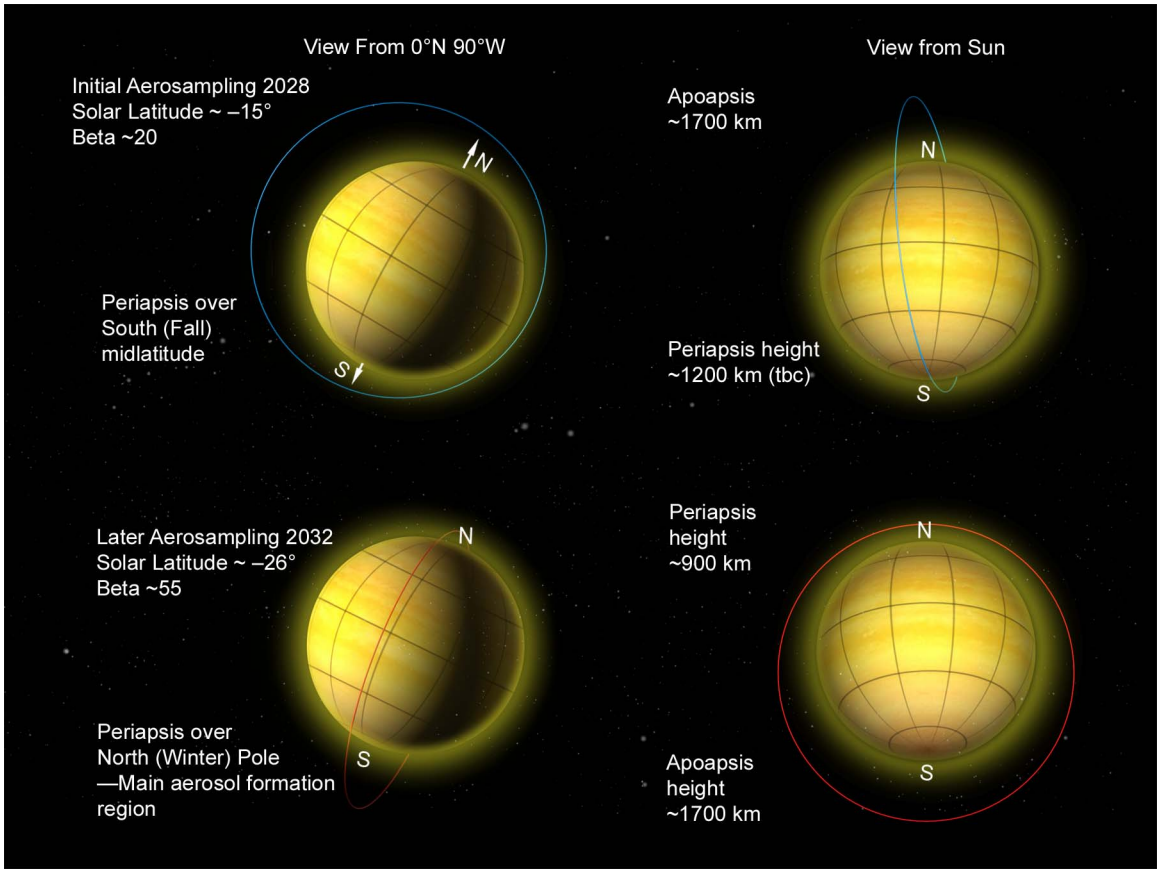

Figure 2-15. Orbit geometry showing sampling of diverse regions. Upper panels show near-noon-midnight aerosampling orbit immediately after arrival. Orbit is then circularized to the apoapsis shown of 1700 km. Orbit precesses during main 3-year mission to become close to dawn–dusk, and periapsis is lowered for deeper aerosampling at end.

To sample a large range of ionospheric conditions, a range of orbit geometries is desired (Fig. 2-15). The Saturn perturbation to the orbit is useful here (and increases for lower inclinations), but a high inclination is desired to accomplish polar mapping, gravity measurements, and high-latitude occultations. An 85° orbit was judged a good compromise. A circular orbit is desired for mapping, although lower periapses are of interest for ionospheric chemistry and other in situ goals. A deep aerosampling phase towards the end of mission addresses much of this intent, and is supplemented by a "gentle" aerosampling at the beginning, exploiting the arrival orbit conditions immediately after aerocapture.

2.4.2 Landing Site Selection

As evidenced by Mars lander experience, determining the landing site for a surface vehicle is a prolonged exercise with many factors to be considered, demanding the latest information. By the time of this decision for TE, more information will be at hand from Cassini (a comparable situation with Viking and Pathfinder); thus, we attempted only proof of the existence of a viable landing site.

Since the equatorial dune fields are the largest area with contiguous surface properties, and the presence of sand dunes suggests boulder hazards should be rare, the regions Belet, Senkyo, Shangri-La, and Fensal-Aztlan suggest themselves as potential landing sites, with Belet the largest area (~1800 km across E–W, ~900 km wide N–S) of which a 200-km swath has good Cassini data so far (~400 m/pixel radar imaging). Since the belt of longitudinal dunes implies transport of materials over long distances, dune sand should contain small amounts of material from many processes on Titan – not only the presumed organic deposition making the sand, but also at least traces of ice bedrock, impact ejecta, etc. Thus, the dunes are an attractive target for surface chemistry goals. Sand is also favorable for sample acquisition and seismometer deployment. As with all regolith targets, some acoustic attenuation may occur in sand, but the seismic signals of most interest are those at low frequency, which are not strongly damped in sand (recall that oil exploration seismic work is done in sandy deserts all the time, and Apollo seismometers functioned well on regolith).

Other potential target areas of interest could be fluvial outwash areas (much like the Huygens landing site), where a selection of materials may have been deposited by rivers – a reasoning much like the rationale for selection of the Mars Pathfinder landing site. Clearly, however, such a choice embraces boulder and gully hazards, as well as the potential for methane-wet as well as dry surface materials.

Of particular interest for some investigations are cryovolcanic deposits and the edge of impact melt sheets, where tholin hydrolysis may be expected to have occurred. These areas also are likely to be rather rough and variable on short length scales.

Polar seas and lakebeds make another contiguous and flat target, although they obviously demand a specific approach to landing and surface operations that cannot easily be generalized to all of Titan. Polar sites have the advantage of Orbiter overflights on every, or nearly every, orbit. Summer polar sites also have continuous sunlight and large duty cycle of direct-to-Earth communication availability.

Crudely from radar backscatter, one might infer a typical 5% upper limit on boulder coverage for the dune areas, although one might realistically expect considerably less. A simple radarclinometric analysis indicates average slopes of 6° or less in the areas where the largest dunes are resolved in data so far, although examination of terrestrial analogs shows that local slopes up to the angle of repose (~30°) can be encountered, with shallower slopes between.

Thus we baseline the Belet dune field as a landing site, but conservatively include scraping capability on the robot arm in case hard ice targets are found. A self-righting ability on the Lander appears prudent in view of the large slopes that can appear on dunes. The low impact velocity and the addition of airbags to the Lander is somewhat conservative. Further Cassini data, and more detailed analysis, may make it possible to delete the airbags for selected landing sites such as Belet or to retain them for consideration of more aggressive scientific targets.

Note that a tradeoff exists between the size of the landing ellipse and the descent duration: a larger parachute would offer a longer ground track and descent duration, and a lower impact velocity, at the expense of larger uncertainty in touchdown location. We have shown, however, that at least one viable and attractive descent/landing site combination is identified even in present data.

2.4.3 Balloon Deployment Location

The primary drift of a balloon, like that of the Huygens probe, is expected to be toward the East. Although the nominal 10-km altitude is close to the zero-wind altitude measured by Huygens, examination of wind models and Huygens data suggests that adjusting the float altitude between 6 and 10 km should permit a zonal wind to be found of the order of 1 m/s – enough to circumnavigate twice during 1 year of operation. A periodic meridional component to winds due to tidal effects (Tokano and Neubauer, 2002) may be confirmed by the Balloon during early operations: such tidal winds may be deterministic to exploit predictively if targets of specific interest are identified close to the Balloon latitude.

Nominally, a low-latitude deployment is anticipated to avoid proximity to strong convective clouds and to provide a long ground track. An alternative scenario (which might be particularly attractive if a change in the budget or partnering assumptions in this study were invoked to permit two Balloons) would be to deploy a Balloon near the summer pole. This location would permit detailed inspection of lakes (in continuous daylight), perhaps allowing observation of tides and wind-driven waves, as well as exciting proximity to summer rainstorms.

2.5 Operations/Mission

Given the overall power and downlink limitations on outer solar system missions, data return overall obviously correlates with mission duration. A number of scientific goals require temporal or geographic extent, for example, the desire to map the surface topography. Surface topography mapping requires, with a 20-km footprint spacing at the equator, $2575 \times 2\,\pi/20$ km, or some 808 perfectly spaced orbit ground tracks. If radar mapping for this phase is conducted only on the nightside, this in turn means 808 orbits, or about 160 days. (The perfect spacing is easy to attain, by minor adjustments to the orbital period). In general, these science goals are decoupled; there is no need to map the seasonally varying atmospheric composition at the exact same time as the surface topography is determined. The Orbiter mission is therefore split into "campaigns" to achieve the various objectives. Only a preliminary layout of these campaigns has been conducted

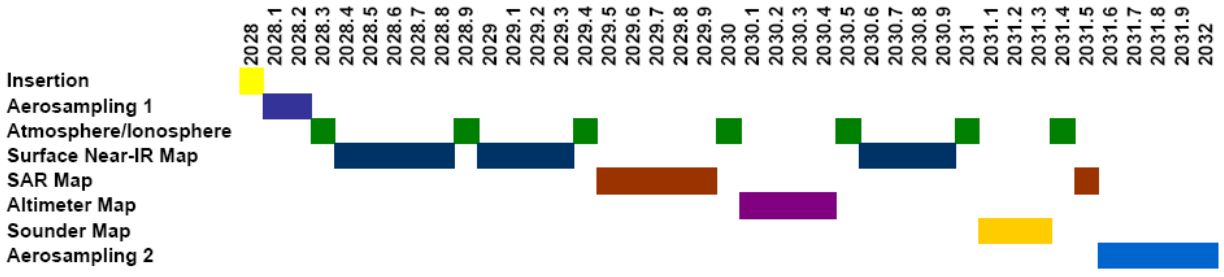

Figure 2-16. The TE Orbiter science measurement campaigns meet all science objectives.

so far (Fig. 2-16). Optimization of such a plan will be subject to much discussion in a further study. However, it is clear that this strategy permits an efficient attainment of the mission goals. The decoupling of these goals permits a subset of the payload to be operated at one time and thus permits power-sharing. (And in any case there is not enough feasible bandwidth to downlink data from the whole payload at the same time.)

More generally, the seasonal variation occurring on Titan during the multi-year mission will require repeats of a number of campaigns, notably the atmosphere campaign (gas composition, haze, temperatures, and winds) at widely spaced intervals. Similarly, the precession of the orbit plane changes the geometry of various factors. (The precession of the plane is intimately linked with the orbital inclination; however, there is little freedom in orbital inclination, since a near-polar orbit is required for global altimetry coverage and for occultations and aerosampling at high latitudes.)

For example, the beginning of the mission, with beta = 20º (see Section 4), permits polar occultations (both radio occultations for ionospheric structure and stratospheric/tropospheric temperatures and solar occultations to be measured by the UV spectrometer for upper atmospheric temperatures, composition, and haze). Successive occultations are not likely to differ significantly one from another, so a campaign of occultation measurements could be short – perhaps 16 days at most. However, repeating such measurements would be desirable after an interval of perhaps 6 months, by which time the orbit plane will have precessed to move the occultation points to lower latitudes.

Similarly, spectral mapping of the surface in the near-IR requires good illumination (no shadows) and thus should be conducted near the beginning of the mission, with beta low. A second mapping phase (with lower priority) might be usefully conducted later in the mission with higher beta. The surface spectroscopic information will not be as useful, but the data will be quite useful in exploring the phase function of surface materials and scattering/absorption in the atmosphere, as well as high-resolution topography information via shadowing, stereo, and photoclinometry in the more transparent windows.

A key science goal of the mission is to measure in situ the chemistry of the upper atmosphere. Cassini has shown that benzene (molecular weight 78) is abundant even at 1000 km and increases rapidly with depth (see Fig. 2-33, Section 2.6.3.4) There are also less direct indications of much heavier molecular weight compounds such as anthracene. Direct sampling via extended-mass-range mass spectroscopy and possibly other techniques at altitudes as low as possible is desired (900 km being an initial estimate of feasible altitudes). This requires a maneuver out of the circular mapping orbit (or requires that the Saturn orbit perturbation evolve the orbit to bring the periapsis down).

In the present plan, a "gentle" aerosampling phase will be performed soon after arrival, probing down to an altitude yet to be determined (perhaps 1000–1200 km) for some weeks in order to exploit the arrival orbit conditions. Then after other mission goals (surface mapping, etc.) are attained, a more aggressive aerosampling campaign to lower altitudes (e.g., progressive steps down to 900 km) will be invoked.

The details of each campaign (near-IR mapping, radar, atmospheres, aerosampling, and likely others) will be the subject of further work.

2.6 Payload

This section describes a strawman payload for the three mission elements that addresses the science goals described in Section 2.2. ***These instruments are given as a demonstration of what is possible; they do not constitute the only instrument set that can address the science goals.***

Instruments might well be proposed that address the goals by other techniques than those assumed here, or that combine some of the functions shown. The following strawman payload is an existence proof only. The eventual payloads that fly will be determined by measurement performance of the proposed instruments, their technological readiness, flight experience, etc.: we show here that existing instruments and some modest updates can meet all the science objectives. We explore some of the payload alternatives in a later section. We further acknowledge that an eventual payload set may include fewer instruments than we have outlined.

2.6.1 Orbiter Payload

The payload for the Orbiter is briefly described in Fig. 2-17. More detail on each instrument is then provided in the following paragraphs.

2.6.1.1 Radar Altimeter

A key requirement to understanding Titan as a system is a uniform high-precision global topographic dataset. As well as a direct constraint on lithospheric deformation, crater relaxation, etc., as on other icy satellites, such data are essential as the lower boundary condition on Titan's global circulation and for understanding transport and erosive processes (e.g., rivers, aeolian transport). Cassini generates only very limited altimetry coverage (a couple of long ~3000-km altimetry tracks and a couple of dozen ~400-km tracks, all with altimetric resolution of 50 m and beam-limited footprint size of 20–50 km) plus some indirect topographical measurements. In this respect, the post-Cassini topographic knowledge of Titan resembles that of Mars prior to the sur-

Representative Instrument	Mass (kg)	Power (W)	Description
Radar Altimeter/SAR	20	170 (SAR) 44 Altim	X-band global topography mapping. Global SAR mapping at 100 m/pixel. Precision altimetry mode has 20-cm resolution.
Subsurface Radar/Ionosphere Sounder	15	60	1–5.5 MHz topside Ionosphere sounding. Global mapping of subsurface reflectors with <150-m depth resolution.
Spectral Mapper	25	37	1-6 μm global mapping at 100 m/pixel in 256 channels. Adjustable spectral editing for surface/atmosphere studies.
Visible/1-Micron Imager	3	7	7° field of view (FOV), 12 filters from the near-UV to 1040 nm. Surface mapping, cloud monitoring, and haze structure.
Ion/Neutral Mass Spectrometer	25	38	Upper atmospheric in situ analysis of gases and aerosol precursors – M/ΔM ~ 10,000 for masses up to 10,000 Da. Focus instrument for aerosampling down to 900 km.
Plasma Package	6	10	Measures ion and electron fluxes at few eV to few keV. ΔM/M~10.
Energetic Particle Instrument	6	9	Magnetospheric particle fluxes, ~10 keV to > MeV. Three heads each with 120° × 12° FOV.
Magnetometer	1	2	Interaction of field with ionosphere: internal and induced field.
Langmuir Probe	1	2	Swept voltage/current probe. In situ electron density and temperature, ion speed constraint – including during aerosampling.
Thermal IR Spectrometer	35	20	Organic gas abundance and temperature mapping 30–500 km, aerosols. Passively cooled Fourier spectrometer, 17–1000 μm.
UV Spectrometer	5	4	Upper atmosphere (450–1400 km) gas and haze profiling by occultation over 500–1870 Å.
Microwave Spectrometer	30	80	Direct winds from Doppler and temperature mapping down to surface; CO and nitrile profiles. Heterodyne spectrometer with scanned mirror (0.2, 0.8, 1.3,1.7, 2.6 mm channels).
Orbiter Radio Science	(system)	(system)	Lower stratosphere and troposphere temperature profile. Gravity field.

Figure 2-17. Suggested Titan Orbiter science payload.

vey by MGS-MOLA. There were radii determined from Viking radio occultations, together with a couple of altimeter profiles from the Viking landers and indirect data such as channel directions, shadow height and depth measurements, and photoclinometry, but it was the MGS-MOLA generation of a homogenous, controlled dataset that revolutionized Mars studies.

The data at hand for Titan show a very diverse topography (Fig. 2-18). Although some areas such as sand seas are very flat (<50 m relief) on large scales (~200 km), patches and ridges of mountains over 1 km high have been identified in radar and near-IR images, and the crater Sinlap (80-km diameter) is known to have a floor depth of 1300 m. The sand dunes themselves have spacings of up to 3–4 km and heights of up to 150 m. Lakes of hydrocarbons, of course, will be flat. (One, but only one, altimeter observation of a lake is planned in the Cassini extended mission.)

As on Earth, the altimetric and horizontal resolution requirements for land and ocean topography are very different. A 20-km circular footprint can be achieved with the 3-m high-gain an-

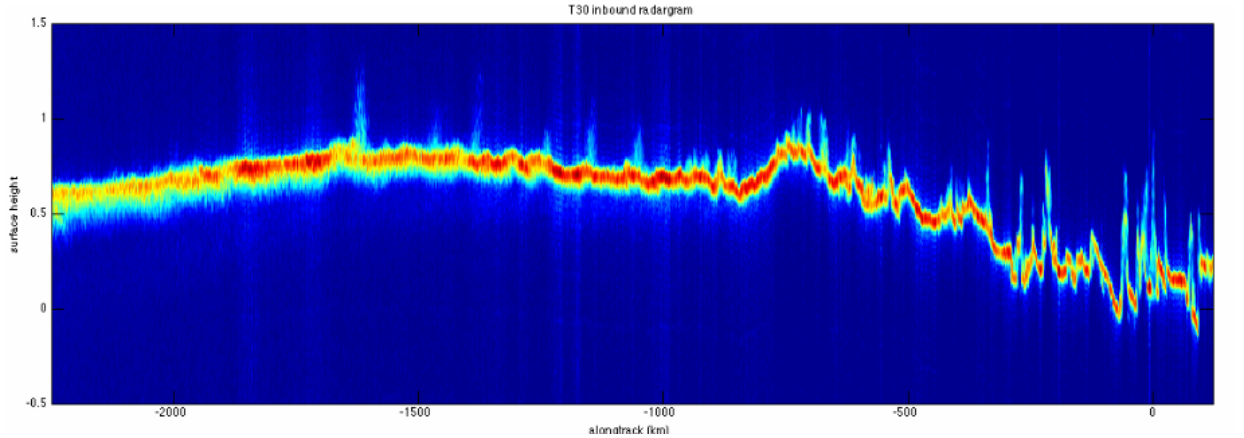

Figure 2-18. The longest topographic profile (T30, ~2500 km – most profiles are only ~300 km long) from Cassini, running roughly from the equator (left) to the northern polar areas (right). Note the gentle slopes with occasional ~200-m ridges, then a steeper fall towards the polar lake lands which are interspersed with sharp ~700-m mountains. Echo strength (represented by color) conveys information on small-scale roughness *(Preliminary unpublished data, courtesy of Cassini RADAR team).*

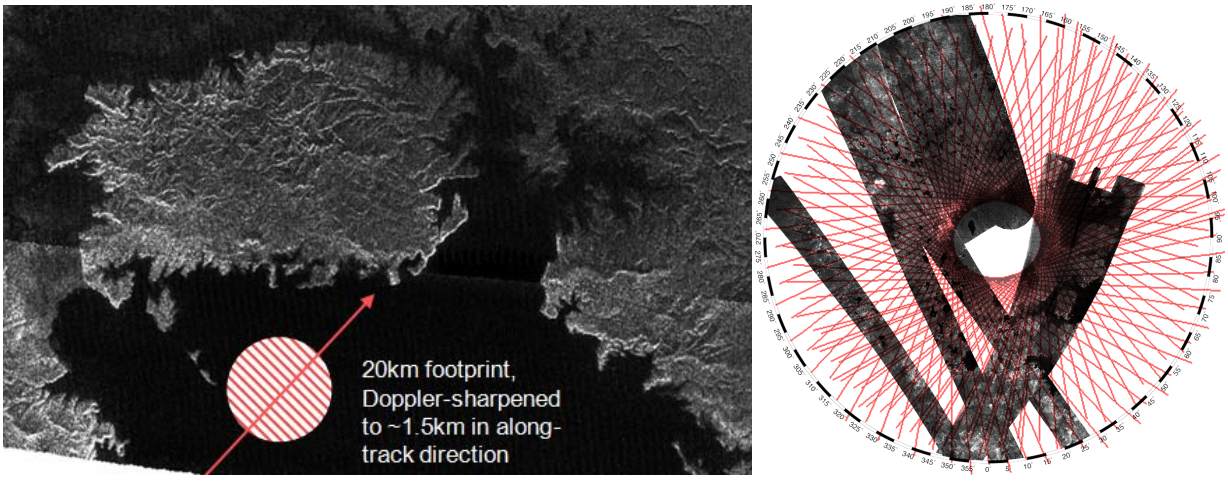

Figure 2-19. The 20-km footprint (sharpened along-track to 1.5 km) resolves key features such as dunes and lakes (left). Ground tracks have many crossovers at high latitude to permit good global control and to detect tidal effects in the lakes found around the pole (right). Shown are 20 days' worth of ground tracks; the full topography campaign will yield a topography sampling eight times denser than shown here.

tenna (HGA) at X-band. Doppler sharpening considerably improves the along-track resolution to 1.5 km. This resolution is ample (see Fig. 2-19) to obtain many independent footprints across the several hundred kilometer wide bodies of liquid at high latitudes; in addition, the along-track resolution of 1.5 km will be enough to resolve individual sand dunes near the equator (where the along-track direction is orthogonal to the long axis of the dunes).

The Titan ionosphere does not have a high enough electron column density to degrade altimetry; a modest correction may be needed for the thick neutral atmosphere, but this correction is essentially uniform across Titan. With 20-km track spacing, about 800 ground tracks are needed to span Titan's equator. Assuming only one track per orbit (e.g., half of each orbit is spent downlinking data), 800 orbits or approximately 160 days are required.

The 85° orbit inclination obviously does not cross the pole: as with Mars Global Surveyor, this gap in the global dataset can be filled by some dedicated off-nadir (and therefore degraded) measurements. However, the inclination selected allows many repeat ground tracks over high-latitude regions, providing opportunities to observe the lakes (between the pole and 70° latitude) at different times in the tidal cycle and permitting precision orbit determination and topography correlation between orbits.

In principle, backscatter from methane hail or raindrops can be detected in altimeter measurements. An experiment with Cassini achieved a better than –55 dB backscatter threshold with a few kilometer altitude resolution (Lorenz et al., 2007c). This threshold would be exceeded by factors of many thousand in methane rainstorms, which are expected in the southern polar region in the late 2020s. Optimizing the ability of the radar to make such measurements will be the subject of future study.

The representative Titan altimeter/SAR is based on the delay-Doppler technique developed and demonstrated by JHU/APL for the NASA Instrument Incubator Program (IIP). This technique applies synthetic aperture principles to altimetry and realizes several significant advantages in precision, along-track spatial resolution, and power consumption. The altimeter/SAR uses the Orbiter HGA with a dedicated traveling wave tube amplifier (TWTA) and a compact, flexible FPGA-based control and waveform processing unit. Various operating modes are possible depending on available spacecraft power and telemetry bandwidth. Low-precision altimetry mode with high noise equivalent backscatter sensitivity ($\sigma^o < -30$ dB) provides ~1 m height precision with 14-km cross-track width and 2-km along-track spatial resolution. Average power in this mode is ~38 W and peak power is ~53 W, with 3 kbps telemetry bandwidth. High-precision altimetry mode with good back-scatter ($\sigma^o < -26$ dB) provides ~20-cm height precision with 5.2-km cross-track width and 0.3-km along-track spatial resolution. Average power in this mode is ~42 W and peak power is ~44 W, with 24 kbps telemetry bandwidth.

2.6.1.2 Synthetic Aperture Radar

The radar altimeter instrument can be used for synthetic aperture radar (SAR) imaging (much as the multimode Cassini RADAR is used in both ways) by applying different signals, processing, and pointing. SAR operation is described separately, although the same altimeter hardware is used. The HGA is pointed ~24° off-nadir to achieve the desired incidence angle at the surface.

Many features on Titan that are visible at 350-m resolution (the best achieved by Cassini, at the closest, usually central, part of the SAR swaths) are invisible or indistinct at the 1 to 2 km resolution obtained at longer ranges. For example, the glints from up-range edges of sand dunes are visible only at the higher resolution (allowing dune height measurement by radarclinometry), and many fluvial channels are visible only at the smaller scales. Thus, even where the Titan Orbiter obtains repeat coverage of the ~35% coverage from Cassini, new insights will emerge from

the higher-resolution TE data. It should also be noted that the X-band radar wavelength is roughly double that of the 2-cm Ku-band, and so the combination of Cassini and TE radar data will provide new information, constraining particle size and roughness scales.

With radarclinometry from the SAR and photoclinometry from near-IR spectral mapping, both in principle at pixel-scale resolution (100 m), local slopes can be generated from those respective instruments on the Orbiter, but only in areas where the respective reflectance functions are uniform. Tying together these local slopes (and the topographic profile developed by the Balloon) will require an independent controlled dataset from Orbiter ranging measurements: even a sparsely sampled altimetry dataset would be valuable in order to provide a reference shape onto which to lay additional datasets. In this connection, we note that the subsurface radar/ionosphere sounder should generate a dataset of surface returns (i.e., topography of the highest point in the beam footprint) with a height resolution of ~200 m.

For a pixel spacing of 175 × 175 m (350 m resolution), a swath width of 30 km and $\sigma^\circ < -25$ dB, altimeter/SAR average power is ~30 W and peak power is 220 W, with 49 kbps telemetry bandwidth. For a pixel spacing of 100 × 100 m (200 m resolution), a swath width of 27 km, and $\sigma^\circ < -22$ dB, altimeter/SAR average power is ~38 W and peak power is 220 W, with 85 kbps telemetry bandwidth. The flexibility of the Titan altimeter/SAR and careful operational planning will be used to balance the Orbiter resources with science measurement requirements.

2.6.1.3 Subsurface Radar/Ionosphere Sounder

A subsurface radar and ionosphere sounder fulfils several scientific functions. The long-wavelength radar sounding permits deep penetration into Titan's interior. In addition to the possibility of detecting near-surface water-ice interfaces (e.g., where cryomagma is within a few kilometers of the surface), this instrument will reveal, for example, impact structures buried under the sand dunes that cover some 20% of Titan's surface, and can profile the depth of hydrocarbon lakes.

In addition, the same instrument operated in an ionosphere sounding mode will give topside ionospheric profiles down to the ionospheric peak. This capability is important given the diversity of ionospheric conditions at Titan: the Langmuir probe records conditions locally (i.e., typically only at the orbital altitude of 1700 km, well above the peak) and radio occultations will be available only for a restricted range of latitudes and times.

This instrument is patterned after the successful MARSIS instrument on board ESA's Mars Express (see Figs. 2-20 and 2-21). MARSIS is a multifrequency, synthetic-aperture, orbital sounding radar that operates in four frequency bands between 1.3 and 5.5 MHz, with a 1-MHz instantaneous bandwidth providing a free-space range resolution of ~150 m. Horizontal resolution is typically 10 to 30 km cross-track, Doppler-sharpened along-track to 5 to 10 km. Peak

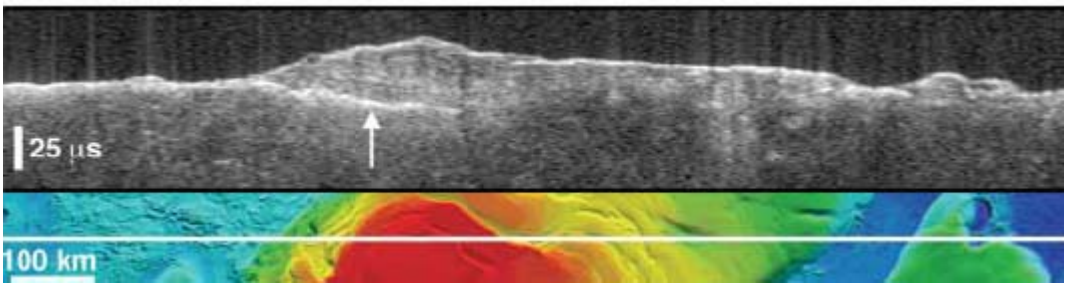

Figure 2-20. MARSIS radargram of the south polar layered deposit (SPLD) and ground track over MOLA topography, showing strong subsurface contrast at the base of the SPLD (from Plaut et al., 2007).

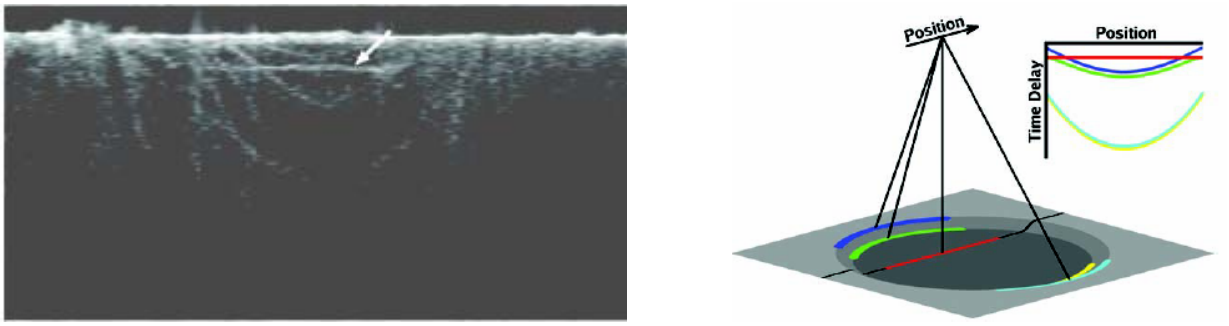

Figure 2-21. 4-MHz subsurface returns from Chryse Planitia in the flat northern plains of Mars (from Picardi et al., 2005), where subsurface radar has found many buried impact structures. The low crater count and the vast sand dunes suggest similar discoveries await at Titan.

transmitted power out of the 40-m dipole antenna is ~10 W. Coherent azimuth sums are performed onboard on ~100 pulses per second with a resulting signal-to-noise ratio for a typical Mars surface of 30 to 50 dB at the operating altitude range of 250 to 800 km. Operation of a comparable instrument will suffer a ~6 dB loss owing to the higher operating altitude of 1700 km, and the horizontal footprint will be larger by a factor of ~2. However, given that targets of interest for subsurface sounding (such as the low-latitude sedimentary basins, or the polar hydrocarbon seas) have horizontal extents of hundreds of km, a ~50 km resolution is adequate.

At an assumed circular orbital altitude of 1700 km, the local ionospheric density is of order 1 cm^{-3} and the associated plasma frequency 10 kHz. Titan's ionospheric peak, based on Cassini in situ measurements, is at about 1000 km with a density of order 3000 cm^{-3} and a plasma frequency of order 500 kHz. Hence, the ideal sounding range would be from 10 kHz to 1 MHz.

The strawman system employs two 20-m antennas forming a 40-m dipole oriented perpendicular to both the ram and nadir axis. The antenna consists of simple conducting wires supported by a 3.8-cm diameter fiberglass tube that is folded and compressed into a compact box prior to deployment. For Titan, the MARSIS antenna is mounted on the Orbiter top-side deck and is self-deployed upon release by pyro mechanisms. The radar operates from 1.3 to 5.5 MHz for surface and subsurface sounding with bands centered at 1.8, 3.0, 4.0, and 5.0 MHz. In the active ionospheric sounding mode MARSIS steps through 160 frequencies from 0.1 to 5.5 MHz. It might be desirable to extend the frequency range down to 10 kHz. Such an instrument could, with little increase in resources, use a passive mode to detect plasma waves, such as the upper hybrid resonance frequency band, as was successfully done with the Cassini RPWS. The passive measurement would then provide an alternate means of determining the in situ electron density.

Although a shorter-wavelength instrument like SHARAD on Mars Reconnaissance Orbiter can achieve better depth resolution and use shorter antennas, the availability of short-wavelength sounding from the Balloon, plus the ionospheric science from a long-wavelength instrument, made a MARSIS-type sounder more appropriate for the Titan Orbiter.

Note that the MARSIS instrument includes a monopole antenna in the nadir direction: due to RF interference from other spacecraft systems, this antenna has not been used extensively (Safaeinilli, 2007). However, in principle the monopole can substantially improve clutter rejection by measuring the clutter alone to allow its subtraction from the dipole signal of (subsurface + clutter) and may be implemented more effectively on a Titan Orbiter. It is therefore included in the spacecraft payload accommodation layout, although of course the MARSIS experience shows that impressive results may be obtained without it.

The deployment of the long dipole antenna is deferred until after the first aerosampling campaign, nominally a couple of months after arrival, but later in the mission if a capability to jettison the antennas is included. Pending further study (and in situ measurements during the mission) the jetisson may be performed just prior to the second, main, aerosampling phase of the mission (or late during this phase, depending on the depth profile adopted).

2.6.1.4 Spectral Mapper

Along with topography, high-resolution spectral mapping of Titan's diverse surface will be a major gap in knowledge after Cassini. Cassini's VIMS instrument is expected to cover only a few percent of Titan's surface at kilometer-or-better resolution, even after the extended mission. Thus a prime element in the Orbiter payload is a spectral mapper. In essence this instrument addresses two main goals: high-resolution near-IR imaging (essentially acting as a 2-µm camera) and spectroscopy of the surface. The concept described here is only one representative option of many instrument possibilities that address these goals.

Cassini VIMS data already point to four distinct spectral units on Titan (with a fifth surface type, hydrocarbon lakes, indicated in radar data but not yet well measured in the near-IR). These units are "bright," characteristic of Xanadu and other generally bright terrains; "brown" materials that are associated with sand dunes; "blue" material that appears at the edge of bright terrain, perhaps due to fluvial erosion; and anomalously "5-µm bright spots," notably Tui Regio and the area bounded by Hotei Arcus. These 5-µm bright regions may be associated with recent cryovolcanic constructs. Although many large regions on Titan have not been spectrally mapped at all, these results already show the spectral diversity of Titan's surface. Other spectral end-members will likely appear as a dedicated Orbiter mission improves the spatial resolution and coverage by orders of magnitude.

An important augmentation beyond Cassini is that the TE spectral mapper should cover the 5- to 6-µm wavelength range. This spectral region (in a methane window, thus the atmosphere is quite transparent) is highly diagnostic of several organic compounds expected on Titan's surface (Fig. 2-22).

A representative heritage instrument is the Compact Reconnaissance Imaging Spectrometer for Mars (CRISM) on the Mars Reconnaissance Orbiter. While CRISM uses two detectors to cover a spectral range of 400 nm to 4.0 µm, the Titan spectral mapper is assumed to use a single detector, likely an HgCdTe array, covering a spectral range of 1.0 to 6.0 µm. Assuming the CRISM design, the spectral mapper generates a full spectrum of 256 channels, providing ~20 nm resolution, which can be selectively windowed such that only wavelengths of interest are output to conserve telemetry bandwidth. Spatial binning and a variable frame rate relative to a fixed ground track rate are used to vary spatial resolution for global mapping and high-resolution targeted imaging. Ideally passive cooling can be used to eliminate the

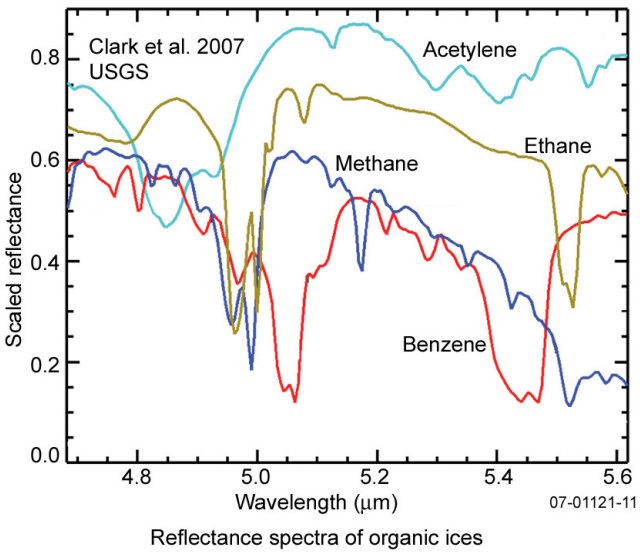

Figure 2-22. Reflectance spectra of several compounds known to be abundant on Titan: the 5- to 6-µm spectral window is particularly rich in discriminating features.

complexity and lifetime limitations of active cryocoolers, and the spectral mapper is mounted on the cold side of the Titan Orbiter to facilitate such passive cooling. For flexibility in operations, the spectral mapper (like CRISM) is articulated.

2.6.1.5 Visible/1-Micron Imager

While the opacity of Titan's haze at short wavelengths impedes visible imaging of the surface, the phase function of the aerosols is strongly forward peaked, so some surface information is conveyed even at visible wavelengths (e.g., Xanadu can be picked out with a contrast of a few per cent in Voyager images [Richardson et al., 2005]). At 940 nm, a window between methane absorption bands, surface features down to ~1 km in scale can be readily seen in Cassini images (Porco et al., 2005); see also the map of Fig. 2-6.

Imaging also reveals many atmospheric features, such as the detached haze (see Fig. 2-23), observed at a different altitude in 2004 from what Voyager had measured in 1980, and the rich layered structure of the polar hood. Tropospheric clouds are also readily studied with such an instrument, with filters at different depths in methane bands allowing cloud-top height to be measured.

This instrument is anticipated for large-scale monitoring of tropospheric clouds and the detached haze, for example, and for support imaging to document other observations. A CCD camera may also offer a useful capability for optical navigation and imaging of other targets in the Saturnian system.

A representative heritage instrument is the Mercury Dual Imaging System (MDIS) developed by JHU/APL for MESSENGER. MDIS contains a pair of co-boresighted 1-megapixel CCD cameras: the Narrow Angle Camera (NAC) having a 1.5° FOV and the Wide Angle Camera (WAC) having a 10.5° FOV. The WAC includes a 12-position multi-spectral filter wheel providing color imaging over the spectral response of the CCD detector (395 to 1040 nm). Ten spectral filters are defined to cover wavelengths diagnostic of different surface compositions, while a medium-band filter and a panchromatic filter are included to support short exposure times and optical navigation, respectively. Filter selection for Titan will be tailored to a variety of science goals including global surface mapping, cloud top height, and haze studies, with UV, 940 nm, and various depths in methane bands being obvious choices. For the Titan Orbiter a single imager with filter wheel is assumed, resulting in significant simplification from MDIS. From a 1700 km mapping orbit a 1-megapixel camera with a 7° FOV produces 100-m pixels. Higher

Figure 2-23. Cassini ISS image (in the near-UV) showing the detached haze and exotic layered structure of the winter polar hood presently over the north pole.

resolution can be achieved either through narrowing of the field of view, which impacts global mapping, or through use of a CCD with higher pixel count, which impacts telemetry bandwidth. An attractive option would be the use of a higher pixel count CCD with region of interest readout to support high-resolution imaging and with spatial pixel binning, a feature included in MDIS, to support lower-resolution global mapping.

The Titan visible/1-micron imager is assumed to be mounted on a pivot platform to allow flexibility in pointing, since both limb and nadir observations are anticipated during several of the different measurement campaigns. This arrangement also permits some flexibility in imaging other targets in the Saturnian system.

2.6.1.6 Ion/Neutral Mass Spectrometer

The Cassini Ion Neutral Mass Spectrometer (INMS) was based on a quadrupole mass spectrometer with dual ion sources for neutral measurements: a closed source to detect inert neutrals at high sensitivity and an open source to detect reactive neutrals (Fig. 2-24). The open source with the filament turned off also seconded as an ion mass spectrometer. Due to the relatively low sensitivity of the neutral ion source and the unexpected importance of ions in the chemistry of the upper atmosphere most operations were performed with the open source in an ion measurement configuration with the ion source filament turned off. Such a multiple inlet system approach proved extremely useful and should be repeated on a future INMS.

Cassini INMS performed extremely well over its limited mass range of 100 Da. However, the

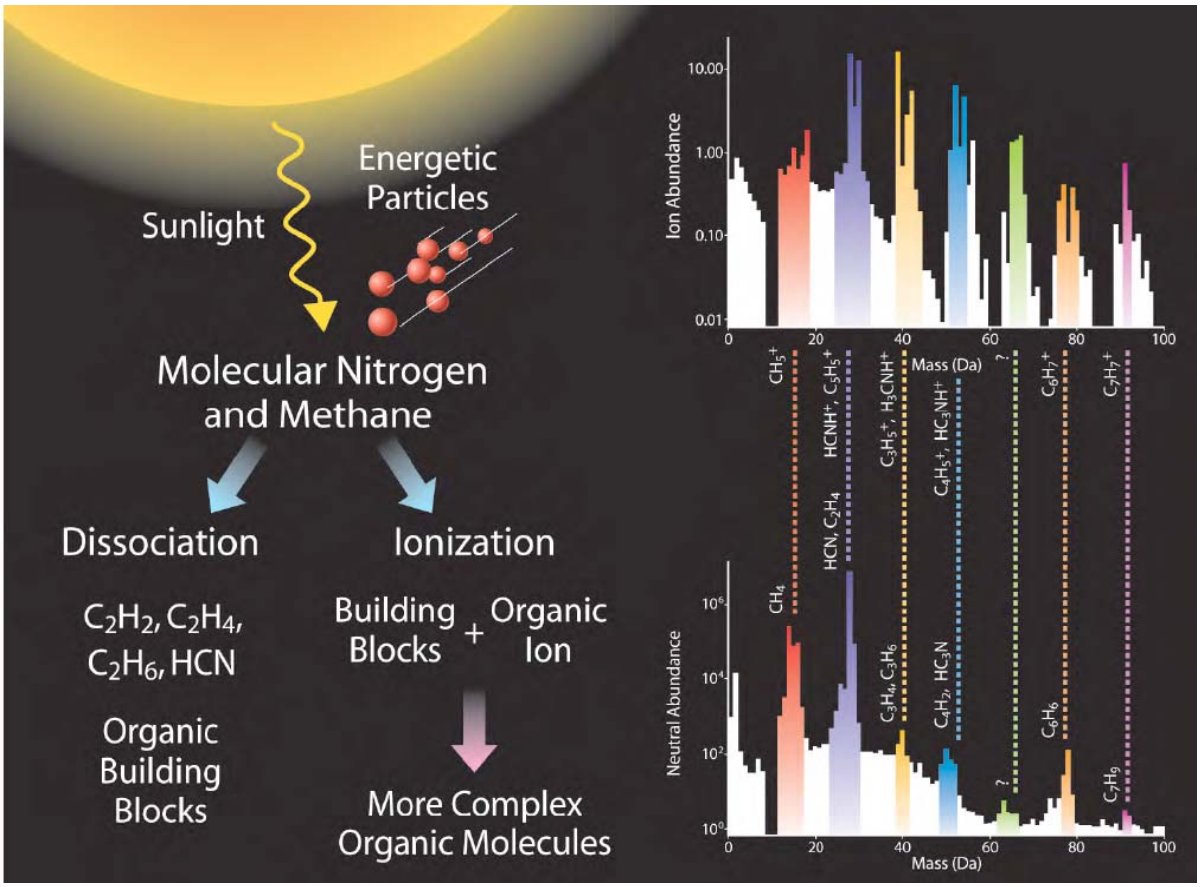

Figure 2-24. Ion (upper) and neutral (lower) species detected by the Cassini INMS. Many of these species vary in abundance by an order of magnitude over height differences of only 50 km (after Waite et al., 2007).

complexity of Titan's atmosphere indicated by the CAPS large positive and negative ion measurements suggests that a future mission will need a mass range of 10,000 Da for neutral species and both positive and negative ions. Furthermore, some combination of an aerosol/dust collector might be considered as an additional inlet system for the mass spectrometer to determine the composition of the nascent aerosols seen by Cassini at these altitudes. And if we are to understand the complex chemistry, the mass resolution of unity over the whole mass range is a necessity, implying a mass resolution ($M/\Delta M$) of 10,000 in contrast with the Cassini INMS resolution of 100. Furthermore, this increased mass resolution in the lower portion of the mass range will provide an important capability of separating overlapping (at resolution 100) mass species such as HCN from C_2H_4 (seen only as a dissociative ion fragment at masses below 28 Da due to the interference with the dominant gas N_2).

Another important attribute of the Titan INMS is a dynamic range of at least 8 orders of magnitude. This range is needed to provide an altitude coverage from 1700 down to below 900 km and to be able to detect important minor species at part-per-billion levels. Although Cassini INMS carried this specification, the problems of background that occur at high source pressures in quadrupole mass spectrometers made measurements over the full range impossible below 1100 km. This shortcoming should be rectified on a future mission to take full advantage of the expected complex organic chemistry during the lowest altitudes of the aerosampling mission. In all cases the Titan INMS must point in the spacecraft ram direction to make effective measurements. Based on these specifications, the Rosetta ROSINA Reflectron Time-of-Flight (TOF) Mass Spectrometer was selected as a representative instrument that has a mass resolution and range close to what is needed. However, the increased dynamic range at high ram pressures and the need to measure negative ions and small aerosols suggest that significant modification would be needed for the Titan INMS.

2.6.1.7 Plasma Package

The plasma package is used to measure the low-energy electrons (<2 keV) and ions (<10 keV) that rain down onto Titan's atmosphere, providing a mass influx of hydrogen and oxygen and a robust momentum source due to the plasma interaction speed of over 50 km s^{-1} that leads to energy deposition and sputtering removal of Titan's atmosphere.

In a 1700-km circular orbit, on a 3-axis stabilized spacecraft, two ion sensors are proposed. They need only modest ion mass resolution (e.g., $M/\Delta M$ around 10), covering a few dozen electron volts to a few dozen kiloelectron volts and with ~20° angular resolution. Two sensors, using deflectors, will give full coverage on a 3-axis spacecraft independent of orientation. In addition, one electron sensor would also be included in the package. The designs would be based on the Deep Space 1 PEPE instrument, which incorporated an electron electrostatic analyzer and an ion electron electrostatic analyzer coupled to a reflectron TOF mass determination system.

2.6.1.8 Energetic Particle Instrument

The most important energetic particle measurement that can be made is the energy deposition in the upper atmosphere as a function of altitude. Cassini MIMI results at Titan indicate that energetic electrons (>20 keV) deposit most of their energy around 1000 km altitude, whereas energetic ions deposit the bulk of their energy somewhere in the 500- to 1000-km altitude level. The latter is of considerable interest; therefore it would be nice to dip to about 700 km, if possible. However, at all dipping altitudes interest in knowing the particle fluxes will be considerable.

The ion fluxes are of great interest because of their altitude deposition profile. Although their total energy input to the atmosphere is smaller than that for UV most of the time, they are the dominant source of particle energy in the 800- to 1000-km altitude range, a region where much

interesting, complex chemistry is occurring that is dependent on the ion energy input precisely in that altitude range. The peak energy input seems to be around 100 keV particle energy, falling slowly with energy to either side of that value.

Aerosampling is important to measure the absorption vs. altitude profile. However, the measurements during the 1700-km mapping phase would also be of primary importance and value, as they indicate what the energy input is as a function of time and orbital position.

The instrument to be used for this measurement of the energetic ions and electrons is based on the JUNO Energetic Particle Detector Instrument (JEDI) in development at JHU/APL for the JUNO mission. JEDI consists of three identical sensor heads with 120° × 12° fields of view arrayed to cover phase space on a nonspinning 3-axis stabilized spacecraft. Each JEDI head uses a mixture of time-of-flight, pulse height, and energy measurements to classify protons from 10 to 3000 keV, electrons from 20 to 1000 keV, alphas from 50 to 3000 keV, O/S from 50 to 16000 keV, and CNO/sulfur from 90 to 16000 keV. For Titan, three JEDI sensors are currently arrayed on the top deck of the Orbiter as for JUNO, although subsequent analysis of measurement requirements may result in fewer sensors needed to cover the phase space. For this mission, at least one of the instrument heads should have a fan aperture that can look from near zenith to near nadir and follow the particle extinction curve as a function of the atmospheric line of sight path.

2.6.1.9 Orbiter Magnetometer

The Orbiter magnetometer contributes to the understanding of the interaction of Titan with its magnetospheric environment. Even though the Saturnian field is not appreciably inclined to the Titan orbit normal, the applied field varies during Titan's eccentric orbit, and the field is draped over the Titan atmosphere by the co-rotating plasma flow. An additional dynamic factor is the solar wind, which can push the Saturnian magnetopause inside Titan's orbit, allowing Titan into the magnetosheath, where conditions are very different. These changing conditions may in turn stimulate an induced response from a possible conductive internal ocean on Titan. The long mission duration allows a large body of data to be built up at different times and conditions to probe these dynamic effects. The second aerosampling phase of the mission gets beneath the peak of Titan's ionosphere, allowing better insight into any induced or permanent internal fields. Such observations can be powerfully combined with those from a magnetometer on a Lander.

A representative instrument is the MESSENGER MAG instrument developed jointly by NASA Goddard Spaceflight Center and JHU/APL. The MESSENGER MAG is a 3-axis ring-core fluxgate magnetometer with 40-Hz sampling and selectable sampling, averaging, and readout rate. The operational range is ±1024 nT with 0.03 nT resolution. The Titan MAG probe will be deployed on a two-element boom extended along the anti-ram axis of the Orbiter with length comparable to the 3.8-m boom used on MESSENGER. A small electronics box at the base of the boom consumes less than 2 W and together with the probe weighs less than 1 kg.

2.6.1.10 Langmuir Probe

A Langmuir probe on the Orbiter provides, with minimal resources, a very reliable in situ measurement of electron density and temperature as well as some ion diagnostics, given either a measured or modeled composition. Further, this instrument does not rely on the long antennas required by the ionospheric sounder, and hence would be available for orbits in which the periapsis dips well below 1000 km. A Langmuir probe measures current as a function of the voltage applied to the probe to determine the number density of electrons and their temperature in the positive (electron collecting) portion of the current–voltage sweep. In fact, detailed modeling of the sweep can distinguish between photoelectrons and ionospheric electrons and can provide in-

formation on the spacecraft potential (important for the interpretation of plasma measurements by a plasma instrument) and even UV input, also important to the interpretation of the ionosphere. In the negative (ion collecting) portion of the current–voltage curve, some information on the ion speed (a combination of thermal motion and bulk motion) is available, provided there is some information on the characteristic mass of the ions, available either from other onboard measurements or from models.

The Langmuir probe, much like that flying on Cassini, would likely be operated in a mode with periodic voltage sweeps, on the order of once per second, with rapid (tens of milliseconds) fixed-voltage current measurements in between to provide high-resolution density measurements between the sweeps. The basic measurements are electron density and temperature, ion speed (or temperature), UV flux (modeled), and spacecraft potential.

2.6.1.11 Orbiter Thermal IR Spectrometer

Many space-based thermal IR spectrometers have been Fourier-transform spectrometers, which have an extensive heritage on Earth-based satellites, at Mars, and orbiting or flying by the outer planets. The strength of this type of instrument lies in the versatility that its broad spectral range and medium-to-high spectral resolution afford. Thermal-IR spectra of Titan can be inverted to obtain the spatial distribution in the stratosphere and mesosphere of organic gases – hydrocarbons (CH_4, C_2H_2, C_2H_4, C_2H_6, C_3H_4, C_3H_8, C_4H_2, . . .) and nitriles (HCN, HC_3N, C_2N_2, . . .) – and of oxygen compounds (CO, CO_2, H_2O). They can also probe the distribution of condensates, seen at high latitudes in winter and early spring, as well as aerosol hazes. Atmospheric temperatures can be retrieved from 300 to 0.003 mbar (30- to 500-km altitude). Mean zonal winds can be derived from the thermal-wind equation, provided they are specified at some level independently (see the cross section, Fig. 2-25, for an example depicting the stratosphere and mesosphere). The ability to map all these quantities simultaneously is significant because several – temperatures, winds, several of the organic gases, and condensates and hazes – vary on seasonal and perhaps mulit-year timescales. In an Orbiter mission, the IR spectrometer would heavily use limb-viewing geometry to achieve the best vertical resolution, but nadir viewing would also be used to generate quick maps.

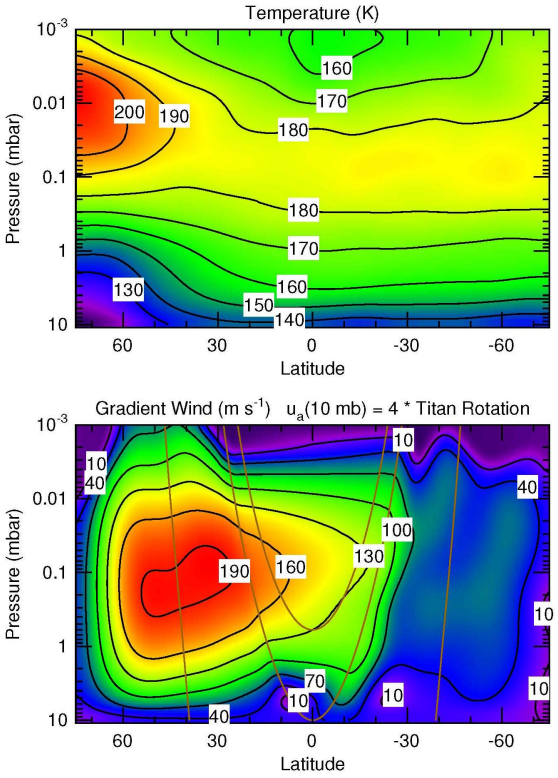

Figure 2-25. Meridional cross section of temperatures (upper panel) and zonal winds (bottom panel), assuming an atmospheric rotation rate at 10 mbar equal to four times that of the surface (after Achterberg et al., 2007).

A representative heritage instrument is the Composite Infrared Spectrometer (CIRS) on Cassini. CIRS consists of a 50.8-cm Cassegrain telescope and three interferometers. The far-IR interferometer covers a spectral range of 17 to 1000 μm (600 to 10 cm^{-1}) using thermopile detectors and has a 4.3 milliradian field of view. The mid-IR interferometer covers a spectral range of 7 to

17 μm (1400 to 600 cm^{-1}) using a pair of 1 × 10 pixel HgCdTe detector arrays with 0.27-milliradian pixels. A reference interferometer provides timing correlation to the scan mechanism. Changing the length of the scans allows the spectral resolution to be set between 0.5 and 15.5 cm^{-1}. CIRS employs passive cooling via a 40-cm radiator to space to achieve a cold-finger temperature of ~80 K for the mid-infrared detectors. For the Titan Explorer, improved far-IR detector and beam splitter technology will likely reduce the size of a CIRS-like instrument, but significant passive cooling and radiator requirements remain. With interferometric instruments of this sort, particular attention will need to be paid to vibration induced by moving elements such as reaction wheels or the Stirling converters in the ASRG power sources. The cold side of the Titan Orbiter is reserved for the IR spectrometer and the spectral mapper. The IR spectrometer is body-mounted to the Orbiter and is used during the atmospheric and ionospheric science campaigns. During these campaigns the Orbiter will perform roll maneuvers for atmospheric and ionospheric scanning.

2.6.1.12 Orbiter UV Spectrometer

Cassini UV occultations have yielded profiles of nitrogen and methane in the upper atmosphere. Analysis (Shemansky et al., 2005) of one stellar occultation so far has indicated abundances at a range of altitudes from ~450 to ~1400 km for the following species: CH_4, C_2H_2, C_2H_4, C_2H_6, C_4H_2, and HCN. Although the robustness of these retrievals has been called into question given the large CH_4 optical depth, the modest resource requirements and the good complementarity in species coverage of this instrument with the microwave spectrometer and complementarity of altitude range with the thermal IR spectrometer led to its retention in the strawman payload. Whether significant science could be gained from observations by this instrument in emission was not determined: attention focused on occultation measurements.

A representative heritage instrument is the Alice instrument on New Horizons. Alice is designed to perform spectroscopic measurements of planetary atmospheres at extreme and far-UV wavelengths between 520 and 1870 Å, a similar range to that observed by Cassini's UVIS, and includes both a 40 × 40 mm aperture for air-glow measurements and a reduced 1-mm-diameter aperture with 2° × 2° FOV for solar occultation measurements. (Note, however, that a near-UV capability was originally also proposed for Cassini but was not flown. The scientific potential of near-UV measurements may merit reassessment, given what is now known about Titan.) A toroidal holographic diffraction grating is employed with light dispersed onto a microchannel plate (MCP) detector assembly with double delay-line readout scheme. The MCP detector uses side-by-side solar-blind photocathodes: potassium bromide (KBr) to cover the wavelength range from 520 to 1180 Å, and cesium iodide (CsI) to cover the range from 1250 to 1870 Å. A gap between the detectors was designed to attenuate bright solar H I Ly-alpha emissions at 1216 Å, reducing the risk of detector saturation. Alice has two detector data collections modes: image histogram mode and pixel list mode, with the later employed for solar occultation measurements. In pixel list mode, individual events are collected sequentially in instrument memory at rates exceeding 50 kHz, with periodic insertion of time tags to allow time binning of events at up to 256 Hz. The output telemetry rate in this mode is scene dependent and is limited to a maximum of ~400 kbps. The UV spectrometer is body-mounted to the Titan Orbiter, which will perform Sun tracking maneuvers during the dedicated solar occultation campaign.

2.6.1.13 Orbiter Microwave Spectrometer

Like the thermal-IR spectrometer, the microwave instrument would observe both in limb- and nadir-viewing geometries. The extremely high spectral resolution of the microwave hetero-

dyne spectrometer permits it to resolve individual lines and provides a high signal-to-noise ratio for detecting trace species within its wavelength channels. However, it can measure only a few species, since its wavelength channels must be chosen to select specific sets of lines. Examples to date include:

- 115, 177, 230 GHz (2.6, 1.7, 1.3 mm): CO, HCN (MSAR, proposed for Cassini)
- 320 to 360 GHz (0.8 to 0.9 mm): includes CO, ^{13}CO, $C^{18}O$, HCN, HC_3N, H_2O, HDO – technology well established (French MAMBO Mars proposal; also recent developments at LERMA in France)
- 1000 to 1300 GHz (0.2 to 0.3 mm): includes CH_4, NH_3 in addition to all others – developments under way (LERMA)

The ability of the microwave spectrometer to resolve individual lines enables it to measure stratospheric and mesospheric winds directly, via the Doppler shift (in the troposphere, pressure broadening vitiates this technique). Doppler measurement of Titan's winds from Earth-based observations has already been achieved, albeit at very low spatial resolution (Fig. 2-26).

Using lines of CO and pressure-induced absorption from the N_2 "continuum," the MAMBO-class instrument could be used to retrieve temperatures over a range similar to the thermal IR spectrometer. However, the increasing transparency of Titan's atmosphere to N_2 absorption at longer wavelengths should permit the retrieval of temperatures closer to the surface with a microwave instrument having channels longward of 1 mm, at least in the nadir-viewing mode.

The Titan microwave spectrometer provides detailed analysis of atmospheric composition (many different molecules with permanent dipole moments, with detection sensitivity of parts per billion or less, depending on integration time); atmospheric temperature vs. pressure vs. altitude; and direct measurement of (Doppler) winds. It is based on the Submillimeter Investigation of Geothermal Networks and Life (SIGNAL) design developed at JPL for the MARVEL Mars Scout mission. This instrument represents a compact design package derived from numerous terrestrial, solar system (MIRO), and astronomical remote sensing instruments (see layout, Fig. 2-27). The optical bench carrying the primary reflector and turntable is externally mounted on the anti-ram side of the Orbiter to facilitate cross-track scanning. The primary reflector's center position is in the nadir direction, with a scan range of ±90° to provide horizon-to-horizon coverage. The synthesizer, spectrometer, and electronics boxes are shown together, but may be remotely mounted inside the spacecraft bus. Use of the Orbiter as a roll platform during the atmospheric

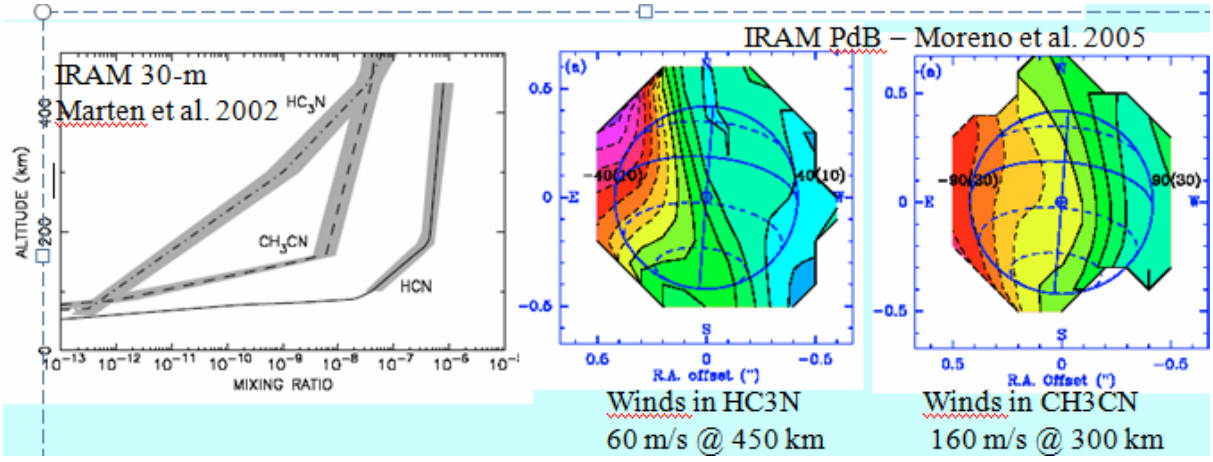

Figure 2-26. Vertical profiles of nitrile species and Titan zonal winds measured from Earth by millimeter-wave observations. Corresponding measurements made from orbit will have a resolution more comparable with the Cassini thermal-IR maps – see Fig. 2-25 *(compilation figure by E. Lellouch, 2007).*

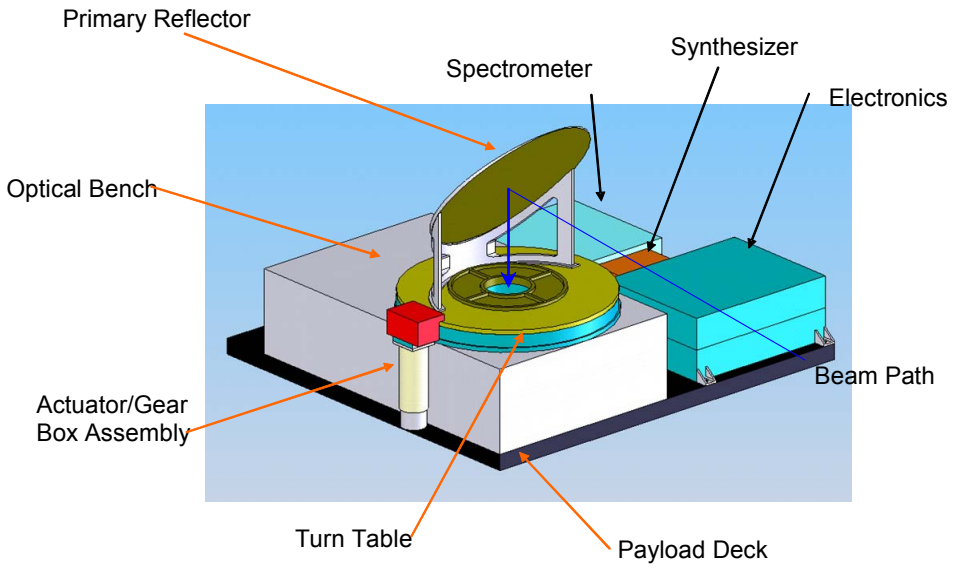

Figure 2-27. Microwave spectrometer layout.

science campaign may eliminate the need for the instrument scan capability, simplifying instrument design.

A simple radiometer channel would give information on Titan's surface temperatures and emissivity (or indeed, opacity due to clouds or rain) at marginally better spatial resolution than Cassini.

2.6.1.14 Orbiter Radio Science

As on Cassini, there is formidable science to be obtained from radio science. As with many of the Orbiter investigations, the ~2 orders of magnitude enhancement in observation opportunities vastly improves the science capability. The polar orbit will permit a much more secure determination of tidal changes in Titan's gravity field, which will be determined up to order ~6 via tracking.

Radio occultation science will be performed at intervals through the mission, yielding at all phases path-integrated ionospheric electron density profiles, and during the early half of the mission (while beta is below 45º) stratospheric and tropospheric temperature profiles at a range of latitudes (Fig. 2-28).

The radio system hardware, including an ultrastable oscillator (USO), is described in Section 4. Note that the radio science capability also is enhanced by synergy with the altimeter, and the potential for precision ranging to the Lander, and possible propagation radio science with the Balloon and Lander.

2.6.2 Aerial Vehicle (Balloon) Payload Overview

Even a minimal Balloon payload can yield impressive scientific results (for example, the ~6.9-kg balloon gondolas of the VEGA balloons to Venus, e.g., Blamont et al., 1986). However, the coarse quantization of the available power sources for this mission makes it logical to carry a sizeable instrument payload, although if a small (~10-W) RTG were available, a very small helium balloon carrying perhaps only a camera, meteorology package, and radio beacon would be an attractive option.

The **representative** Aerial Vehicle science payload described here directly addresses the measurement objectives requiring a mobile platform at several kilometers altitude, and contrib-

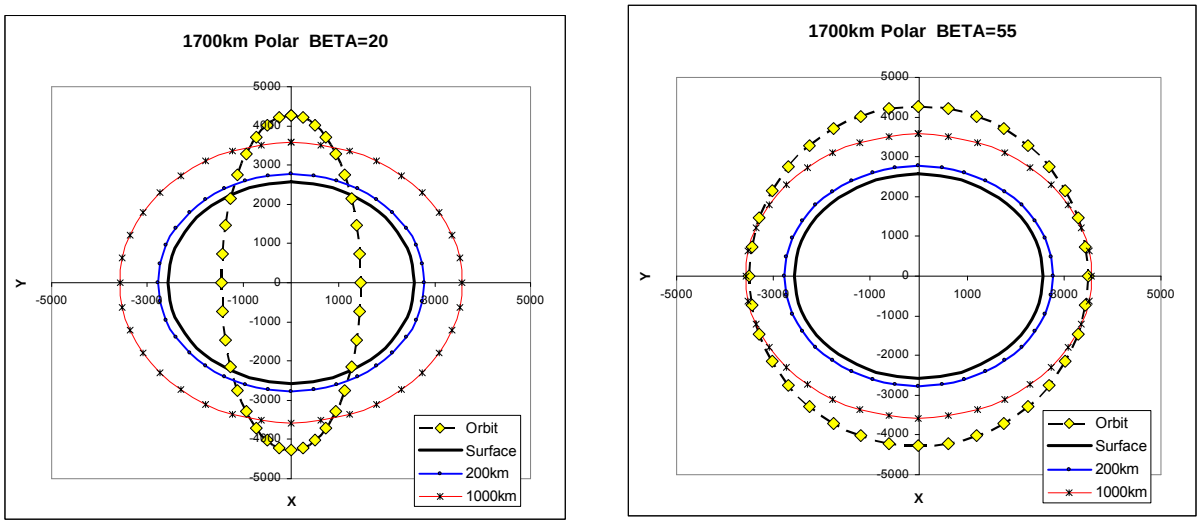

Figure 2-28. Schematic of occultation geometry. At the beginning of mission, occultations down to the surface occur at latitudes of around 70°. The occultation points progressively move equatorward until after ~1 year the occultations no longer intersect the surface but are tangent at various levels in the atmosphere. See also Fig. 2-15.

utes to achieving global and surface science goals by providing measurements linking data at orbital and lander scales. As discussed in Section 2.10, other payloads or packaging options exist. Fig. 2-29 lists the Aerial Vehicle representative instruments and key characteristics. Details of each investigation, including science goals addressed, measurement objectives, allocated resources, and accommodation and operations particulars are provided in following subsections.

2.6.2.1 Balloon Visible Imager

The prime function of the Balloon camera is high-resolution geomorphological studies, although side-looking images also provide meteorological observations, and imagery also permits wind measurements from platform motion (as for the visible Descent Imager/Spectral Radiometer DISR on the Huygens probe [Tomasko et al., 2005]).

Comparison of imagery with orbital datasets (including, initially, Cassini data) for navigation

Representative Instrument	Mass (kg)	Power (W)	Description
Balloon Visible Imager	2	10	Pair of visible 1 Mpixel, ~60° FOV cameras pointed nadir and horizon.
Balloon Meteorology Package	3	4 (peak)	Point temperature, pressure, relative wind speed. Acoustic signatures. Includes inertial measurement unit (IMU) TBD atmospheric electricity.
Balloon NIR Spectrometer/ Atmospheric Optics Monitor	7	15 (peak)	Downward looking NIR (1 to 6 μm) point spectrometer; up-looking FOVs for atmospheric studies. solar aureole; Sun sensor.
Tunable Laser Spectrometer (incl. Nephelometer)	4	40 (peak)	Abundances (to ppbv) and isotope ratios (to per-mil precision) of targeted species; characterization of cloud structure and microphysics.
Balloon Subsurface Sounder	9	15 (peak)	Dual frequency (50, 250 MHz) sounding with compact antenna (3 m) 1.5-m depth resolution for sedimentology.
Balloon Radio Science	(system)	(system)	USO permits precision tracking from orbit and ground. Winds.

Figure 2-29. Suggested Titan Aerial Vehicle science payload.

is not envisaged onboard but could be performed by scientists (and, indeed, the public, since Balloon imagery in particular is likely to have substantial outreach appeal) on the ground. However, onboard image differencing to determine displacements across the ground and thus wind motions would be implemented (e.g., the Descent Image Motion Estimation System [DIMES] used to measure sideways motion on MER just prior to landing shows that such measurements can be straightforwardly implemented on aerial vehicles). Rather than telemetering substantially similar images, only the difference vector need be transmitted.

Two wide-angle imaging heads are anticipated here: one pointing to nadir, the other pointing sideways. The nadir imager clearly performs a mapping function, and has a nominal resolution of 7 to 10 m (although resolutions 50× higher could be attained if the altitude were dropped towards the end of mission). In addition to outreach and geomorphological studies, these data will be essential for assessing the viability of landing sites for potential future missions. The side-looking imager would see somewhat above as well as below the horizon (Fig. 2-30). Control of the Balloon azimuth is not expected, although the attitude will be monitored.

A representative heritage instrument is the Mars Descent Imager (MARDI) for Mars Polar Lander, Phoenix, and MSL. Two cameras, each with a 60° FOV are deployed below and/or to the side of the gondola, with a small overlap in ground coverage. In the nominal geometry, one camera is pointed toward nadir and the other at an angle just under 60° off nadir, providing maximal nadir ground resolution as well as significant down-range coverage in a selected direction. Nadir resolution is 7.5 m/pixel at 6-km altitude. The total allocated visible imager mass is 2 kg. A frame rate of one image per 1000 s conservatively provides complete ground coverage with some overlap at 10 km altitude and 2 m s^{-1} drift. Each returned image pair is ~200 kB, compressed.

Extensive onboard data selection anticipated to make optimum use of the limited bandwidth (autonomous identification of "interesting" images via entropy measurement, Fourier analysis, or more elaborate image classification). Similarly, optical odometry (differencing images to obtain a displacement vector) will be performed onboard. In general nadir images may be mosaicked onboard to eliminate overlaps, although some overlaps will be sought, e.g., for stereo analyses, change detection, or phase function studies.

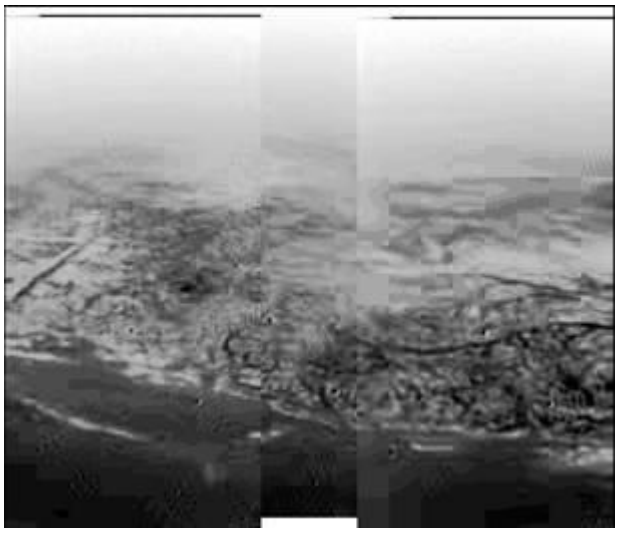

Figure 2-30. Montage of three highly compressed images of Titan's surface by the Huygens probe DISR instrument, from a nominal float altitude of 10 km. Pixel scale is 20 m; for the Titan Balloon, the pixel scale would be better by a factor of ~3, compression artifacts would be far less severe, and images would be ~50 times bigger in terms of number of pixels.

2.6.2.2 Balloon Meteorology Package

A simple atmospheric structure/meteorology (MET) package is included in the Balloon payload. A pressure sensor will give an indication of altitude; combined with a dedicated altimeter, synoptic pressure changes can be independently recovered. A temperature sensor and an anemometer are mounted on a small mast away from the body of the gondola, although it is recognized that during ascents at least, sensor results may be influenced by waste heat from the Balloon.

Measurements by the VEGA balloons at Venus (e.g., Sagdeev et al., 1986) show that even though a balloon might be thought of as a Lagrangian particle moving along with its local air mass, substantial winds relative to the Balloon can be detected. The high-frequency turbulent components are of particular interest, and thus a 3-axis ultrasonic anemometer is anticipated.

An inertial measurement unit (IMU) is included providing an important supplement to the episodic opportunities for radio navigation and will be valuable in evaluating Balloon response to winds or buoyancy changes.

Possible augmentations to the Titan Balloon MET package might include a microphone. A separate capability to measure methane humidity and cloud opacity would be appropriate were the tunable diode laser spectrometer/nephelometer to be deleted. Finally, some atmospheric electricity measurements (electric field, relaxation probe, detection of Schumann resonances) could be contemplated.

The Titan Balloon MET package provides atmospheric science data, including ambient temperature, atmospheric pressure, and wind speed and direction. Temperature and pressure sensors are based on Phoenix MET instrument. Sensors will be placed along the gondola perimeter to be isolated from interference. An acoustic anemometer (AA) and an IMU, if present for navigation, are included for wind vectors. Low-rate continuous measurements of the *p, T,* attitude ($\Delta\Theta$, $\Delta\phi$), and relative velocity (Δv) provide vehicle baselines for review or direct polling at high rate for characterizing density or other types of atmospheric gradients. The point microphone is used to characterize the acoustic environment of the vehicle, such as weather-related phenomena. The total mass allocation is 3 kg (including the AA, IMU, and microphone). The average power required by the package is 2 W, with a peak of 4 W.

2.6.2.3 Balloon Near-IR Spectrometer

The near-IR spectrometer/atmospheric optics monitor (NIRS/AOM) provides near-IR point spectroscopy of surface targets and atmosphere and measures atmospheric particle distributions. This instrument will obtain spectra in the 1- to 6-μm region of a spot immediately below the Balloon (attitude data and context images would be acquired simultaneously and time-tagged). We recognize that spectral imaging is desirable, but it is unlikely that adequate downlink bandwidth can be provided. Since the goal is to obtain "ground truth" end-member spectra, a point spectrometer is adequate. A number of separate upward-looking fields-of-view via lenses and fiber-optic light guide would be incorporated for atmospheric measurements to quantify haze scattering and absorption at different solar times and from different altitudes.

Note that while the nominal Balloon altitude of 8–10 km gets the instrument well beneath the bulk of the atmospheric haze opacity, almost the entire methane column remains below the vehicle, and thus large chunks of the surface spectrum remain windowed out. To obtain useful surface data in the wings of the methane bands will require observations from altitudes of ~200 m or less, which would be attempted only toward the end of the nominal Balloon mission, when atmospheric winds and Balloon responsivity to control inputs are fully understood.

A representative heritage instrument is the Descent Imager/Spectral Radiometer (DISR) on Cassini/Huygens. It incorporated up- and down-looking IR spectrometers with a wavelength range of 1 to 2.5 μm, a solar aureole camera, and Sun sensors, as well as down- and side-looking imaging. For the NIRS/AOM instrument on a Balloon, we extend the detector capability to 6 μm, employ a narrower FOV and a larger aperture for down-looking spectra. The imaging function is accomplished by a separate imager. Several wide-FOV Sun sensors arrayed on the gondola perimeter permit tracking and attitude inputs for navigation and image correlation. The total mass allocation for NIRS/AOM is 7 kg. The average operating power is 10 W.

2.6.2.4 Balloon Tunable Diode Laser Spectrometer/Nephelometer

The tunable diode laser (TDL) spectrometer/nephelometer requires a small mirror assembly cantilevered from the side of the gondola. This mirror, together with a facing mirror, acts as a multipath Herriott cell across which a small number of laser beams are bounced. These TDLs are swept across a narrow wavelength range, yielding a gas absorption spectrum with very high spectral resolution, sufficient to resolve separate lines for different gas isotopes. Similar instruments have been flown on Mars Polar Lander (e.g., May et al., 2001) and on stratospheric balloon and aircraft flights, and a TDL subsystem is included in the SAM instrument on MSL. Mounting of separate detectors and possibly additional light sources to measure light at various scattering angles provides a nephelometry function to determine the number density, refractive index, size. and possibly the shape of haze particles.

Operation in Titan's cold lower troposphere means the lasers need no cryocoolers (in fact, modest electrical heating is needed). Each laser sweeps a modest wavelength and targets a small set of molecular lines. A candidate laser suite would be able to measure, with part-per-billion sensitivity (Webster et al., 1990), carbon and hydrogen isotopes in methane, and isotopes of elements in hydrogen cyanide (CO, CO_2 C_2H_2, C_2H_4, C_2N_2, and HC_3N) are also readily feasible.

Representative heritage for this instrument is based on the developments of Huygens/PIRLS and MSL/SAM-TLS. The TLS multi-pass (Herriott) cell lies open to the ambient atmosphere outside a side of the gondola. A dedicated laser source for detection and characterization of aerosol particles and clouds is included for nephelometry. The total mass allocation is 4 kg. The average operating power is 20 W, with a 40 W peak power. The data rate is 10 kb per measurement per channel over a 10-s integration time, with low duty cycle.

2.6.2.5 Balloon Subsurface Sounder

The subsurface radar sounder takes advantage of the low-altitude platform to provide high-resolution regional characterization of the subsurface structure of Titan, as well as altimetry data for the vehicle (Fig. 2-31). Representative heritage is a modification of the MRO Shallow Subsurface Radar (SHARAD) developed by the Italian Space Agency. A 3-m tip-to-tip antenna system is baselined for the Aerial Vehicle, following the design for the JPL TiPEx study (Safaenili, Jordan, and Im, unpublished, 2006). The subsurface radar operates in two bands: 40–60 MHz for depths up to 3 km with depth resolution of 5 m, and 200–300 MHz for depths up to 400 m with depth resolution of 1.5 m. The high-frequency band is used for altimetry. The antenna deploys from the side of the gondola (1.5 m in each direction). Mass and power allocations are 9 kg and 15 W, respectively.

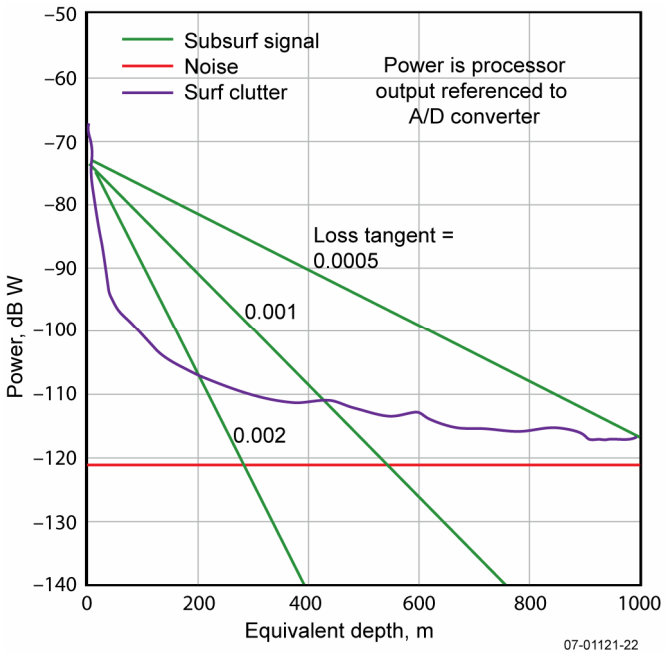

Figure 2-31. 250-MHz sounding performance from a 10-km altitude. The depth penetration of the 50-MHz channel is about 5× better, but has poorer range resolution. Performance improves at lower altitudes for both channels *(courtesy of E. Im, R. Jordan, & A. Safaenili).*

Since the drift rate of the Balloon is neither large nor predictable with precision, nor is the Balloon's azimuthal pointing with respect to the drift controlled, Doppler sharpening is not available to the Balloon sounder. However, the geometric footprint of the system is rather small.

Any altimetric function for Balloon altitude monitoring (and possibly altitude control experiments later in the mission) would be likely be provided by a dedicated microwave radar or laser altimeter, although it is recognized that the short-wavelength channel of this sounder in particular could be used for altitude monitoring.

(*Note:* In principle, longer-wavelength radar sounding is quite possible from the Balloon, allowing bottomside ionospheric sounding, which would strongly complement topside Orbiter sounding, occultation, and in situ measurements. Long-wavelength sounding offers greater penetration depth at the expense of vertical resolution, but operation requires long antennas, which might cause deployment/gust response concerns [the volume or mass accommodation of a stowed 10-m antenna is not expected to be problematic]. The efficiency and beamshape performance of long antennas integrated as wires or tapes into the inflated Balloon envelope itself were not explored, but creative solutions might be developed in these or other directions. Because the particular added value of a Balloon-borne instrument was considered to be the good horizontal and depth resolution, short-wavelength sounder was defined in the strawman payload.)

2.6.2.6 Balloon Radio Science

The timing of communications with the Orbiter provides an indication of the latitude (principally via the time in an orbit where peak elevation, and thus zero Doppler shift, occurs) and the longitude (principally via which orbit sees the peak elevation, together with the steepness of the Doppler curve, which determines the distance of the Balloon from the Orbiter ground track, much like the JHU/APL-developed U.S. Navy TRANSIT system, a precursor to GPS). In addition to this position information, the refraction of the radio signal may allow recovery of some atmospheric structure information, as if each communication session were half a radio occultation.

As with Huygens and Galileo, transmission (even an unmodulated carrier) from the Balloon could be detected at Earth with radio telescopes, and thus precision Doppler measurements and Very Long Baseline Interferometry (VLBI) techniques may be employed to determine the Balloon position. Via the latter technique, even eavesdropping on the unoptimized S-band Huygens-Cassini radio link, radio astronomers were able to determine a position history for the Huygens probe using the VLBI technique with a precision approaching 1 km (Pogrobenko et al., 2004; Gurvits et al., 2007). Even some 19 years before the Huygens success, VLBI was successfully employed to track the VEGA balloons in the Venus atmosphere (e.g., Preston, 1986).

As with Huygens, short-term variations in signal strength (e.g., Dzierma et al., 2007) and Doppler shift (Folkner et al., 2006) allow measurement of the Balloon attitude motion and thus its response to turbulent air motions (e.g., gravity waves or shear associated with topography). Thus, some measurements of interest may be obtained even without the Orbiter's contribution.

If by design or otherwise there should be much RF energy radiated downwards, it may be possible (especially over very smooth terrain) to detect the reflected radio signal, either by the Orbiter as it sets on the Balloon's horizon, or even by monitoring from the Earth under similar geometry. The direct radio signal may constructively and destructively interfere with the reflected radio signal to produce a fading pattern (multipath) that is diagnostic of the surface reflectivity function and thus its roughness – in essence a bistatic radar experiment for free. These effects were observed during the late descent of the Pioneer Venus probes (Croft, 1980) between

the Viking landers and orbiters (Tang et al., 1977) and on the Huygens probe signal from Titan's surface measured by Cassini (Perez-Ayucar et al., 2006).

2.6.3 Lander Payload Overview

The **representative** Lander science payload directly addresses the measurement objectives requiring a surface element on Titan, and it contributes to achieving regional and global science goals by providing ground truth for measurements from the Orbiter and/or Aerial Vehicle. Fig. 2-32 lists the Lander representative instruments and key characteristics. Details of each investigation, including science goals addressed, measurement objectives, allocated resources, and accommodation and operations particulars, are provided in following subsections.

2.6.3.1 Seismometer

Our knowledge of the interior structure of Earth is owed to seismic measurements more than to any other investigations (e.g., Lognonne, 2005). The comparative ease with which instrumentation can be placed on Titan's surface, in comparison with other satellites, makes this mission an important opportunity to compare Titan with the Moon and with Mars, where a long-lived lander network with seismometers may be emplaced in the coming couple of decades.

Although some marsquakes were detected by the seismometer on Viking 2, in general that instrument's performance was compromised by poor placement (on the upper part of the lander, making it sensitive to wind vibration; the Viking 1 seismometer failed to uncage). Apart from the thousands of seismometers on Earth, we have seismic data in hand only from the Apollo seismic experiments on the Moon, which were instrumental in our understanding of the deep structure of

Representative Instrument	Mass (kg)	Power (W)	Description
Seismometer	2.8	3	Broadband seismic measurement – teleseismic events from tidal excitation, possible detection of normal modes.
Lander Meteorology Package	2	2	Temperature, pressure, wind speed + direction. Observes winds $\Delta u < 0.1$ m/s, $\Delta T < 0.1$ K, $\Delta P < 0.1$ mb. Methane humidity, (microphone for saltation, etc., atmospheric electricity TBD).
Robotic Arm	10	20 (peak) 5 typical	Sample acquisition; surface mechanical properties. Deploys seismometer and magnetometer. Pointing of microscopic imager and UV illuminator. Extends to 2.3 m.
Lander Chemical Analyzer	30	100 (peak) 40 typical	Molecular and isotopic analysis of surface samples and atmosphere using pyrolysis, GC-GC-MS, HPLC, TDL and other techniques. Radiocarbon and noble gas.
Microscopic Imager	1	2	High resolution close-up imaging of surface materials (≤30 μm/pixel) LED illuminator array.
Lander Point Spectrometer	5	6 (peak)	NIR (1 to 6 μm) point spectroscopy of surface and atmosphere, 256 channels, with 0.3 mrad FOV. Supported by Lander illumination.
Lander Panoramic Imager	4	5 (peak)	NUV-NIR 1 Mpixel, ~17° FOV distance imaging; 300 to 1100 nm with multiple filters. Geomorphology, sampling support, atmospheric optics. Detection of fluorescence with UV illuminator.
Descent Imager	2	10	Visible 1 Mpixel, ~60° FOV; deployed to beyond heat shield.
Lander Magnetometer	2.5	4	Fluxgate magnetometer to detect induced field from internal water ocean. Range ± 1024 nT, 0.03 nT resolution; deployed.
Student Experiment	2	n/a	Example: miniature airplane launched vertically from Lander; obtains regional imagery and boundary layer over ~1 hour flight.
Lander Radio Science	(System)	(System)	X-band USO facilitates precision tracking for rotation state and pseudo-occultation experiments.

Figure 2-32. Suggested Titan Lander science payload.

the Moon (e.g., a velocity discontinuity at 550 km depth is interpreted as the base of the magma ocean; see review by Wieczorek et al. [2006]) and of the its megaregolith.

The size of Titan's rock core requires the removal of 5 to 10 mW m^{-2} of geothermal heat, only a factor of ~10 less than the heat flow driving the Earth's tectonics. If seismicity driven by endogenic heat occurs on any icy satellite, it likely occurs on Titan. However, Titan is subjected to larger tidal stresses than is the Moon (e.g., Mitri et al. [2006] calculate a tidal flexing amplitude of 4 m and a stress of nearly 9×10^4 Pa) where much seismic activity occurs on an orbital cycle. Kovach and Chyba (2001) have considered how seismic measurements might be used to detect a subsurface ocean on an icy satellite (see also Lee et al. [2003] for a discussion of natural sound sources). Panning et al. (2006) and Cammarano (2006) have considered the seismic structure of icy satellites: of note is that the normal modes of the crust have periods of hours.

Some seismic questions, such as the determination of the core radius, require several (4+) seismometers on the surface. However, as noted by Panning et al. (2006) for Europa, if the deep interior is decoupled from the crust by an internal ocean, such investigations may be impossible in any case. A single seismic station offers substantial insights by itself and as a precursor to evaluating the worth of larger networks at Titan and elsewhere.

A representative heritage instrument is the Netlander Very Broad Band Seismometer (Lognonne et al. [2000], now being improved as the SEIS experiment under development for ExoMars), although in some respects performance for Titan can be expected to improve, since the thermal environment at Titan is much less dynamic. This type of instrument has a demonstrated capability to detect teleseismic events (period tens of seconds) and should permit the detection of submillihertz normal modes. As with the Lander magnetometer, the seismometer will be deployed to the surface by the robotic arm during the initial phase of surface operations. Small spikes on one side of the unit provide the option of enhanced, arm-actuated coupling to the surface in case of a sandy or loose regolith material. Operation from the stowed position will be possible if arm difficulties arise, albeit with higher noise levels. A shielded umbilical to the Lander provides power and data transfer. The mass allocation is 2.3 kg total (2.8 kg with umbilical). The seismometer average operating power is 3 W. A compressed dataset of a few megabits per day is anticipated.

2.6.3.2 Lander Meteorology Package

Time-series meteorology from a landed station will constrain many aspects of Titan's meteorology. In addition, simple meteorology measurements can fulfill a valuable outreach function.

Apart from a handful of brief measurements on Russian Venus probes and Huygens, only Viking and Pathfinder to date featured successful landed meteorology. Data from these instruments (e.g., Schofield et al., 1997) allowed the identification of slope winds, dust devils and dust storms, tidal modes, and the annual pressure cycle. Establishing the variability of meteorological parameters, even at a single site and single season, is an important constraint on engineering models for future missions.

Titan's surface is not expected to undergo significant diurnal temperature changes (perhaps ~1 to 2 K) since the sunlight is so weak and the thermal inertia of the atmosphere so large. However, quantifying the amount of diurnal variation is important to understanding boundary layer exchange in particular. Several temperature sensors are mounted along the mast of the Lander meteorology package (MET) to profile the layer, ideally supplemented with a temperature sensor on the sampling arm to allow temperatures of the actual surface to be determined. Short-term fluctuations in temperature serve in estimating turbulence.

On the other hand, a substantial diurnal pressure signal (~1 mbar) is expected owing to the gravitational tide in the atmosphere. (Whether there are likely to be higher-order modes in the pressure field has not yet been evaluated.) This pressure bulge drives the tidal wind field, which in turn is likely modified by regional and local topography. Wind speeds of only ~1 m/s are expected. These small changes imply sensitive instrumentation, with pressure, temperature, and windspeed resolutions of better than 0.1 mbar, 0.1 K, and 0.1 m/s, respectively.

Methane humidity, a key meteorological variable for Titan, can be estimated from the speed-of-sound measurements, e.g., from an ultrasonic anemometer. (The speed of sound can be recovered independently from chemical analyzer and spectroscopic measurements as well.)

The MET package is expected to include a simple microphone, much like that flown on Mars Polar Lander. In addition to the outreach value and utility as an engineering diagnostic (e.g., to hear arm sampling operations or the takeoff of an unmanned aerial vehicle [UAV]), such a sensor may act as a backup wind monitor and could separately detect the acoustic signature of saltation in the sand grains expected at the landing site. An additional possibility might be an atmospheric electricity experiment to study diurnal variations in electric fields, to study triboelectric effects in saltation, or to pick up Schumann resonances.

Representative heritage instrumentation includes the Phoenix MET package (not including lidar). Sensors are arrayed on a dedicated meteorology mast deployed (from the ring truss) to a canted angle, to maximize sensor separation from the Lander structure. An additional temperature sensor is included on a miniature probe mounted at the end of the robotic arm. The sensor mass allocation (excluding the mast) is 2 kg. The average operational power required is 2 W. The uncompressed data return with fast sampling for detailed studies could be about 40 Mb/day, but a routine compressed report could be 1 Mb/day.

2.6.3.3 Robotic Arm

The robotic arm is a critical enabling element of the Titan Lander. The arm is a central part of the system that obtains and delivers solid samples for chemical analysis. It positions the microscopic imager close to surface targets of interest and may be used to point UV or other illumination at targets of interest for observation by the camera or spectrometer. It also deploys the magnetometer and the seismometer. The representative heritage system is the Robotic Arm (RA) developed for Phoenix. The Titan robotic arm is a foldable, multi-segment system mounted at the edge of the Lander deck. It can extend up to 2.3 m and rotate through a 270° angle to reach maximal surface area (~8 m^2) on Titan. The end of the arm supports a sample acquisition system comprising a scoop and a cutting tool. The microscopic imager is located near the end as well, just behind the "wrist" joint. Autonomous, precision motion-to-target is obtained using iterative workspace modeling, via Lander panoramic and microscopic imager data, during a stepwise approach. The magnetometer and seismometer are deployed by the robotic arm to surface positions up to about a meter from the Lander. Each is a shielded sensor module connected to the Lander via umbilical and released from a clamped position on the robotic arm. The total mass allocation for the robotic arm (including sampling tools but not instruments) is 10 kg. It consumes approximately 5 W average and 10 W when moving its main joints. Peak power of 20 W is required when cutting and scooping.

2.6.3.4 Lander Chemical Analyzer

Since the surface chemical composition is of such importance in the prioritized objectives, and is only usefully addressed by an in situ investigation, the study team devoted significant time to the Lander chemistry package. A variety of techniques are possible, and several are combined in the proposed package.

Cassini-Huygens firmly established the presence of complex hydrocarbons and nitriles in both the gaseous components of the atmosphere and in the atmospheric aerosols (Waite et al., 2007; Coustenis et al., 2007; Tomasko et al., 2007). Strong inferences have been also been put forward that this material is deposited on the surface of Titan, eventually forming extensive organic dunes in an equatorial belt (Lorenz et al., 2006). Furthermore, the Huygens GCMS obtained evidence of a volatile organic-laden surface material near the Huygens' landing site (Niemann et al., 2005). However, Huygens was not designed to thoroughly characterize the rich range of organics likely to be found in surface materials. This characterization must await a Lander mission to the surface that is properly equipped for a range of analytical chemistry analyses that can characterize the aerosol deposits and their evolved counterparts resulting from transient aqueous chemistry or other geochemical processes.

The laboratory-derived analog to the Titan aerosols "tholin" has been analyzed by a host of techniques in terrestrial laboratories – most notably IR spectroscopy (e.g., Imanaka et al., 2004) and pyrolysis gas chromatography mass spectrometry (GCMS) (e.g., McGuigan et al., 2006). One of the difficulties with tholin analysis is that its non-volatile nature makes it virtually impossible to dissolve in simple organic solvents (McGuigan et al., 2006). Thus, pyrolysis appears to be the easiest method to produce volatile substructures that can be analyzed by standard techniques such as GCMS or enhanced separation techniques such as GS × GC MS. Such studies show a range of derived volatiles that number in the thousands (see Fig. 2-33), clearly indicating the vast organic complexity of laboratory tholins and, by inference, Titan aerosols.

There are difficulties with volatile release through pyrolysis and subsequent analysis with GCMS, however. The first is the quantitative reproducibility of such techniques for analytical purposes and the concern that the pyrolysis process itself at 600°C can lead to the formation of new compounds not found in the original structure (e.g., McGuigan et al., 2006). Ways around this shortcoming may include more aggressive front-end wet chemistry, such as derivatization or the use or acids to cleave the macromolecule into its functional monomers. Laser ablation represents another alternative (Ganesan et al., 2007). In spite of these shortcomings, present analyses indicate that pyrolysis GCMS should be a basic analytical chemistry tool for a future Titan Lander, consistent with the choice of the core analysis tool of the MSL's chemical analyzer, SAM.

Other means of chemical analysis must be used in tandem to provide a comprehensive analysis of the materials. The measured existence of adsorbed volatiles in the surface material seen by the Huygens GCMS (Niemann et al., 2005) suggests that thermal desorbtion of volatiles and processing either directly by MS or perhaps by a tunable diode laser absorption technique are necessary to prevent the saturation of the sensitive parts-per-million to parts-per-trillion range of the GC × GC MS. These techniques may also be important in the determination of the stable isotopic abundances of the organic materials. In fact, isotopic analysis of both the bulk volatile organics and the minor species released by pyrolysis gas chromatography through effluent cutting followed by an isotopic conversion oven are essential elements of the analysis to gather information on the origin and evolution of the organic materials that compose the surface organics.

The desire to understand the extent of organic chemical evolution in the Titan environment suggests that alternative analysis pathways less destructive of the original material should also be considered. One such technique used to analyze complex proteins in terrestrial laboratories is high-pressure liquid chromatography followed by electrospray ionization and finally high-mass-resolution mass spectrometry. Advanced development and testing must prove the space applications of these more advanced techniques before a flight version could be considered.

Alternatives to understanding the extent of carbon complexity include targeted chemical analyzer techniques such as the amino acid analyzer of Skelley et al. (2006). The difficulty with these approaches is that some chemical pathway (or a series of pathways) must be determined prior to development, making it difficult to outwit the boundless complexity offered by nature.

One other element of the chemical analyzer is the analysis of atmospheric volatiles and aerosols. Perhaps most importantly is the inclusion of a noble gas enrichment cell to enable the isotopic and elemental analysis of higher-mass noble gases such as krypton and xenon, which were below the threshold of detection of the Huygens GCMS (Niemann et al., 2005). Measurements of the abundances and isotopic ratios of the noble gases are crucial to understanding the evolution of the Titan system. Furthermore, analyzing the variability of the stable isotopes of carbon and nitrogen in various gases near the surface may prove useful in understanding outgassing from the interior. Finally, in situ analysis of precipitating aerosols, although difficult, will help provide an understanding of the important chemical link in the process of atmospheric formation and subsequent surface modification.

In summary, a sophisticated and well equipped chemical analyzer onboard a Lander is key to understanding the role of complex organics as an element of the Titan system. A schematic of such an analyzer is shown in Fig. 2-34.

The Lander chemical analyzer (CA) package will provide molecular and isotopic analysis of geologic and atmospheric samples. Solid samples are delivered by the arm from the scoop into

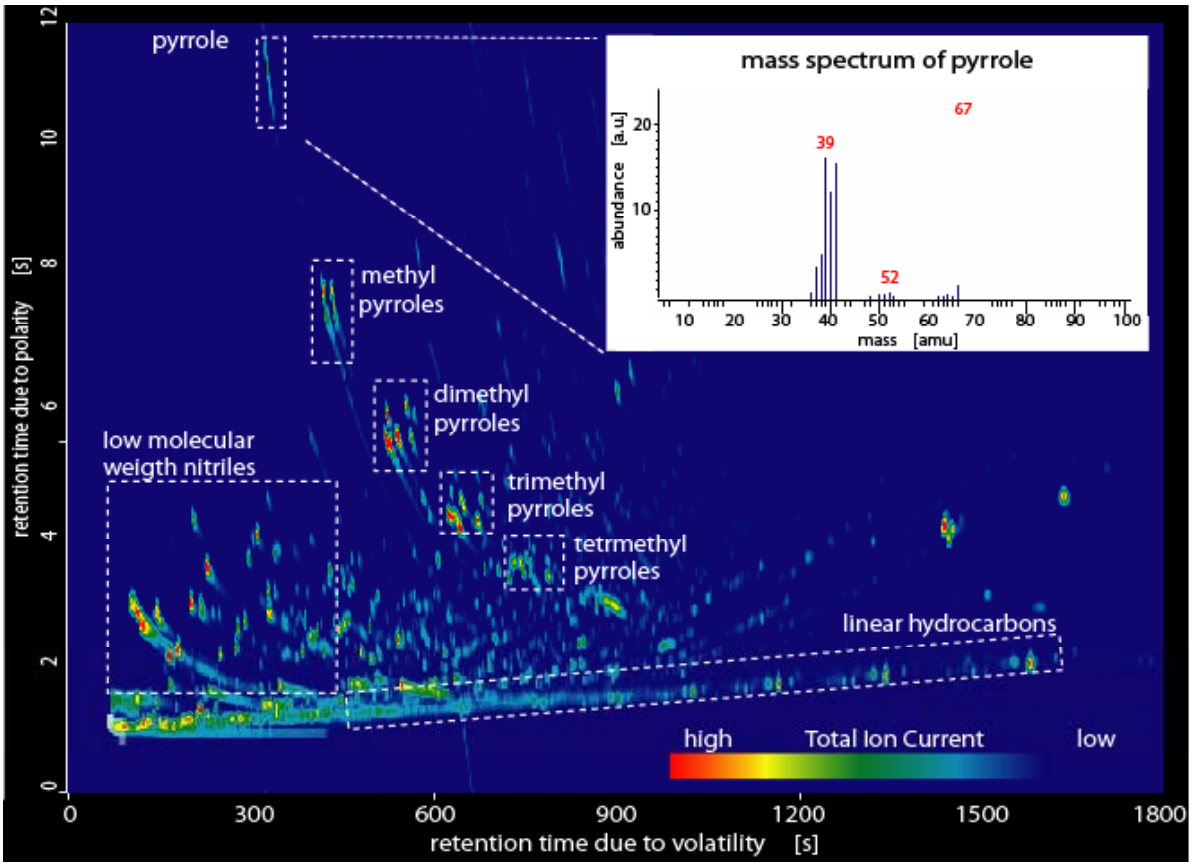

Figure 2-33. Chromatogram of tholins using gas chromatography (GC × GC) time-of-flight mass spectrometry (TOFMS). The complexity of Titan surface chemical products can be disentangled with such techniques (McGuigan et al., 2007).

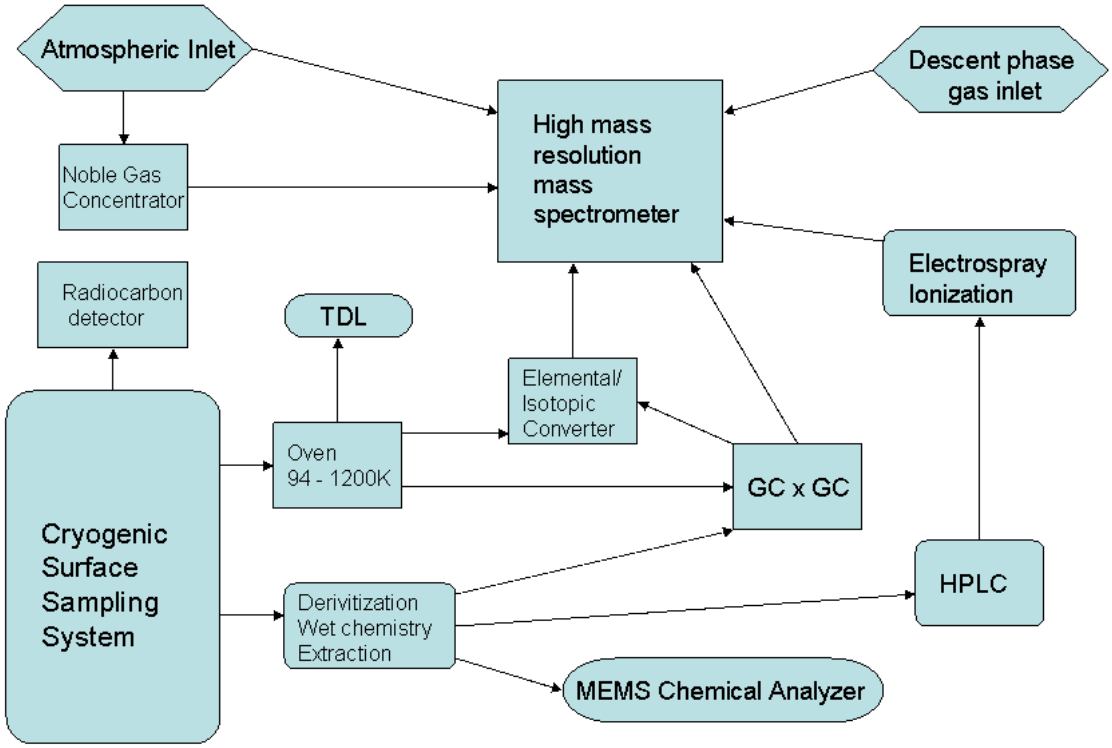

Figure 2-34. Schematic of the elements of a comprehensive Titan surface chemical analysis package.

the inlet of the sample processing subsystem. Depending on the particle size distribution and nature of the sample (fines, pebbles, ice cuttings, etc.) the sample is optionally crushed and/or size sorted to obtain optimal processed sample for chemical analysis. The CA includes more than one type of analytical technique, and more than one type of sample metering and loading approach may be selected for delivered sample. The required volume of sample is delivered to a specific sample holder for a given CA technique, as appropriate. Depending on the sample type and the measurement objectives, multiple aliquots of processed sample may be loaded in sequence. Excess sample is discarded, perhaps as simply as by ejecting sample powder into a waste cell of the CA. Atmospheric samples are obtained through valved inlet ports on the side of the analyzer, away from any contaminating Lander outgassing sources.

A representative heritage instrument for part of the Titan chemical analyzer is the SAM suite under development for MSL. SAM combines an advanced pyrolysis GCMS with a tunable laser spectrometer (TLS), and incorporates complex gas processing, sample preparation and handling, and control subsystems to enable a wide variety of organic and inorganic analyses of Mars samples. The Titan CA similarly baselines mass spectrometry and tunable laser spectroscopy, but strongly emphasizes distinct capabilities optimized for in situ analysis at Titan. The required measurement capabilities may be summarized as follows:

1. Broad, comprehensive inventory of organic compounds in all samples, with
   a. Molecular weight range to at least 10,000 Da
   b. Sensitivity to a wide range of volatility (nonvolatile, semi-volatile, volatile)
   c. Sensitivity to polar and non-polar compounds
   d. Ability to resolve isobaric/isomeric forms of major components

   e. Species list includes alkanes and alkenes through C35, polyaromatic hydrocarbons and heterocyclics through C/N of 60, nitriles and amides, alcohols, aldehydes, ketones, and carboxylic acids up to 10,000 Da, etc.
2. Atmospheric noble gas abundances and major isotope ratios
   a. Neon, argon, krypton, xenon
   b. Isotope ratio precisions <1%
3. Compound-specific isotope ratios in solid and atmospheric samples
   a. $\delta^{13}C$ in methane, carbon dioxide, and key organics of 0.1 per mil
   b. $\delta^{15}N$ in ammonia, dinitrogen, and key amides and nitriles of 1 per mil
   c. $\delta^{18}O$ in H_2O, CO_2 and key aldehydes, alcohols, ketones, and carboxylic acids of 1 per mil
4. Abundances of key inorganic species in solid and atmospheric samples
   a. NH_3
   b. CO
   c. CO_2, H_2O, N_2, etc., evolved from rock and ice samples
   d. Ammonia and water and their isotopic ratios top the priority list

Pyrolysis GCMS

The core analytical capability of the CA is pyrolysis GCMS. This technique requires samples in particulate form (<1 mm) to be loaded into a small, hermetically sealed and thermally isolated pyrolysis cell, where they are controllably heated to high temperatures, driving out volatile chemicals. The baseline number of individual CA pyrolysis cells is 12. Volatilized molecules are swept up with an inert gas such as He, and transferred to the GCMS via the gas processing subsystem. The maximum pyrolysis temperature requirement is 800°C, with a desired maximum of 1200°C. Some semi-volatile compounds that do not evolve readily with such direct heating are analyzed with a modified protocol, wherein the sample is delivered to a cell pre-loaded with a liquid chemical derivatization agent. During a short reaction period under modest heating, the derivatization agent bonds to these compounds, thereby increasing their volatility significantly. The derivatization protocol is reserved for a very limited number of samples (2 to 3 cells) for high-priority follow-up analyses.

GC × GC MS

Gas chromatography is an analytical technique that is particularly useful for separating complex organic mixtures. A capillary column 0.1 to 0.3 mm is coated with a stationary phase that is chemically selective to some characteristic of the organic molecule, such as volatility. This differential chemical reactivity results in a temporal and spatial separation as the molecules move through the capillary column. A separation by volatility usually involves a temperature ramping of the coated column as well. If a second column is coupled to the first through a thermal modulator that can be cycled from a cryotrap to column ambient every few seconds, then the resolution of the separation goes up by a product of the first and the second column, providing much greater separation in complex organic mixtures such as those we anticipate at Titan. The second column is coated with a polar phase to separate the molecules by their polarity. This is particularly useful for heteroorganics, such as amides, nitriles, alcohols, ketones, etc. An example of this separation for a laboratory tholin was shown in Fig. 2-33.

Isotopic Determination

Isotopic ratios in many inorganic and organic molecules are best determined by high-temperature reactions with oxidants. For example, carbon isotopic ratios of organics are gener-

ally determined by reacting them in an oven with dioxygen to form carbon dioxide. This elemental conversion process can be performed on the bulk mixture for an average isotopic value or on individual organics by using pressure diversion from the GC × GC effluent to an oven for specific compounds. This isotopic analysis is generally a repeat analysis of a given sample, so that separation times can be determined prior to pressure heartcutting of the mixture.

Non-Pyrolysis Sampling for MS

A separate, non-pyrolysis technique for complementary chemical analysis is baselined. Previous work on Titan tholin analogs indicates that while powerful for GCMS, pyrolysis alone may not give a complete picture of the chemical composition due to heat-induced chemical alteration of the non-volatile heteropolymer matrix during the temperature ramp. A non-pyrolysis technique can provide a more pristine analysis of this matrix, as well as data that facilitate interpretation of pyrolysis GCMS spectra, particularly of fragment ions. Some complex, high-molecular-weight oligomeric compounds that do not readily pass through a gas chomatograph would benefit from an alternative sampling approach. Two examples of such analytical protocols, which have been used to analyze tholins, are mentioned here:

1. *LE-ESI-MS:* A liquid-based chemical extraction (LE) system, including solvent-based analyte extraction from sample powder, and micro-capillary electrophoresis (μCE) and/or high-performance liquid chromatography (HPLC), is used to concentrate, separate, and transfer key molecular species in solution. These are ionized directly from the liquid phase with electrospray ionization (ESI), which forms singly or multiply charged ions of large parent molecules for MS analysis, including amino acids/peptides, carboxylic acids/lipids, purines, pyrimidines, and other compounds of biochemical interest. Limits of detection for certain compounds can be extremely low (parts per trillion by weight) when the protocol is properly calibrated.
2. *LDI-MS:* A pulsed laser desorption/ionization (LDI) system obtains gas phase ions directly from the surface of a solid sample in vacuo. In this case a thin layer of the sample is positioned at the inlet of the mass spectrometer. If a TOF-MS is used, the short laser pulse serves as the ion "zero time" for determining flight times (and thereby ion mass-to-charge [*m/z*] ratios). LDI is strongly biased to the analysis of non-volatile compounds, such as polycyclic aromatic hydrocarbons, macromolecular carbonaceous material, and polymers: high *m/z* "parent" ions can survive without being quantitatively fragmented in desorption. LDI has been used to study the distribution of molecular weights in the polymeric phase of Titan tholins.

Tunable Laser Spectroscopy

A particularly sensitive means of measuring isotope ratios in certain species is tunable laser spectroscopy. In particular, the carbon and hydrogen isotopes in methane and isotopes of elements in hydrogen cyanide (CO, CO_2 C_2H_2, C_2H_4, C_2N_2, and HC_3N) can be measured, not only in the atmosphere (a measurement repeated at other locations by the TLS instrument on the Balloon) but also in the pyrolysis products of surface material. On the Lander instrument a small multi-pass cell with aligned mirrors provides the optical path for the diode laser suite.

Radiocarbon Detection

The interaction of galactic cosmic rays (GCRs) with nitrogen atoms in Titan's atmosphere has the same effect as on Earth, the production of radioactive carbon-14 (Lorenz et al., 2002). This material is likely incorporated into the haze as it descends, and with a half-life of ~7000 years offers a means of determining whether surface material is "fresh": fresh haze material is

expected to have an activity of thousands of decays per gram per minute. A simple beta-detector can perform this measurement.

The mass allocated for the chemical analyzer is 30 kg, as broken out in Fig. 2-35. The allocation for a non-pyrolysis sampling method is included as a range (1 to 2 kg) but only one such method is accounted for.

The average operating power is 40 W; peak power is 100 W. Maximum integrated energy for a complete pyrolysis GCMS experiment on a bulk sample is expected to be 200 W-h. The data volume, uncompressed, will be 100 Mb/sample.

Subsystem	Mass Allocation (kg)
Sample Processing (inlet, crusher, size sort/discard, meter)	3
Sample Handling (sample cells, derivatization, holding fixtures/plates, motion, radiation detector for radiocarbon measurement)	2
Gas Processing (valves, lines, tanks, pumps, scrubbers, getters, traps, gauges)	3
2D Gas Chromatograph	
Mass Spectrometer (ionizer/s, ion optics, housing, detectors)	2 to 3
Tunable Laser Spectrometer	2
a. Liquid Extraction (valves, reservoirs, lines, manifolds, holding fixtures, ESI)	1 to 2
b. Laser Desorption (stage, load lock, laser, optical focusing)	1 to 2
Mechanical (structure)	5
Electrical (power, control, data)	7
Thermal (heaters, coolers)	2
Total	(28 to 31)

Figure 2-35. Mass allocation for the chemical analyzer, 30 kg, includes a range (1 to 2 kg) for a single non-pyrolysis sampling method.

2.6.3.5 Cryogenic Surface Sampling and Processing System

The cryogenic surface sampling and processing system acquires, handles, and delivers solid samples for chemical analysis. The sampling subsystem is formally a part of the robotic arm, and the processing subsystem is formally part of the chemical analyzer. The primary sampling tool is a scoop at the end of the arm. For simplicity, it has a static shape similar to the Viking or Phoenix scoop, positioned by the arm so that the acquired sample remains in the scoop under Titan gravity (the opening faces up). Local articulation of the scoop is single-axis (pitch hinge), with other motions (yaw, roll, translation) provided by arm service.

The volume of the scoop may be comparable to the heritage scoops. The scoop should securely capture and hold several cubic centimeters of sample, throughout its delivery motion. Although most measurement techniques only require a small volume of sample per analysis (1 cm^3 at most; many require far less), extra sample delivery capability is robust to a range of implementation options.

The prime samples to be collected are unconsolidated fines up to small (about a centimeter diameter), intact pebbles, and rocks (which may be icy). The simple scoop does not discriminate among them; directed sampling is controlled only by arm/scoop motion. The scoop also incorporates a rock and ice cutting device, such as a rasp (used on Phoenix), to obtain particulate samples from ground ice, bedrock outcrops, or large boulders. Cutting speed is kept relatively low to avoid imparting excess heat to the samples, which could cause volatile sublimation. A particulate sample obtained with the tool is driven ballistically into the scoop. Some scraping may also be possible with the scoop blade, appropriately machined, using the arm motion. Digging/trenching is possible, with the strength limit to be determined.

The processing subsystem receives samples from the scoop, optionally crushes and/or size-sorts them to obtain the desired particulate size fractions, and then delivers processed sample to the chemical analyzer. In addition to providing a homogeneous analysis, crushing and sorting enable the analysis of millimeter-to-centimeter-scale loose rock or ice samples obtained by the scoop that are too small to be amenable to the arm cutting tool. The crusher requirements may be

simpler than those originally levied on MSL. The Titan chemical analyzer may require particles only smaller than ~1 mm in diameter, rather than the 150 μm required by the CheMin instrument on MSL. Considering the additional likelihood at Titan of ice-bearing samples (which can sublimate volatiles with extended mechanical processing), an appropriate strawman device may be an attrition mill, which crushes the sample directly between churning platens. An example of such a device is the recently developed Mechanized Sample Handler (MeSH). Large particles remaining after one mill cycle can be separated with subsequent sieving or other aperture stop methods. The challenges for this processing system will be limiting thermal effects on the samples and coupling the required sample into the chemical analyzer.

2.6.3.6 Microscopic Imager

The microscopic imager acquires very high spatial resolution visible images of surface materials within reach of the robotic arm, as well as samples collected by the acquisition tools and any calibration targets on the Lander. A representative heritage instrument is the Microscopic Imager (MI) developed for MER. Optional additional capabilities such as variable working distance and z-stacking are represented by the Mars Hand Lens Imager (MAHLI) in development for MSL. The Titan microscopic imager is mounted near the end of the robotic arm for precision placement at a working distance of ~3 cm and has a set of light-emitting diode (LED) illuminators, including UV for fluorescence imaging. A single 1-Mpixel array detector provides a resolution of approximately 30 μm/pixel over a ~3 × 3 cm FOV. The allocated mass is 1 kg total. The imager consumes a maximum of 2 W during image acquisition and transfer.

2.6.3.7 Lander Spectrometer

The Lander spectrometer is intended to have wavelength range and resolution that are nominally equivalent to those of the Balloon and Orbiter instruments. It is a point spectrometer boresighted with the Lander panoramic imager (much like MiniTES and Pancam on Spirit and Opportunity). It has two significant advantages: it samples spots down to a few centimeters across, a resolution of ~10^4 higher than that of the Orbiter, and thus it is more likely to isolate spectral end-members and, rather more important, much more of the spectrum is available for analysis, by virtue of observing through a very short column of atmosphere. Using a lamp, the Lander will fill in some of the spectral gaps that cannot be seen from orbit. In addition, observations of the sky with the Lander spectrometer will help characterize the atmospheric effects on surface spectra, facilitating the recovery of surface spectra from orbital data.

A final advantage is that illumination conditions can be explored easily with the Lander, both by observing the same spots at different times of day and by using dedicated local illumination (a lamp and/or LEDs) perhaps mounted on the robotic arm. In addition to providing this spectral ground truth for comparison with Orbiter/Balloon datasets, the Lander spectrometer will be used to characterize material prior to ingestion into the chemical analyzer. Thus, the Lander as a whole acts as a spectroscopy calibration laboratory.

The point spectrometer provides narrow FOV ("point") spectroscopy over the wavelength range 1 to 6 μm. The spectral range is divided into 256 channels, providing ~20-nm resolution. Accommodation of the point spectrometer is similar to that of the Mini-Thermal Emission Spectrometer (Mini-TES) on MER. Light is collected with a 0.3 mrad FOV inlet in the scan platform of the Lander mast. A periscope mirror arrangement directs the light down the hollow interior of the mast into the spectrometer unit located within the Lander body. Representative heritage for the point spectrometer includes elements of existing point spectrometers such as SIR on SMART-1 (1 to 2.4 μm) and MiniTES (5 to 29 μm), possibly with detector advances from Mars-

orbiting imaging spectrometers such as OMEGA and CRISM. The selected filter set is TBD. The total mass allocation for the instrument is 5 kg. Average operating power is 3 W, and peak power is 6 W. Near-IR images are built up by scanning the rotation/tilt platform at an appropriate sampling interval. The data volume of a nominal panorama is ~76 Mb, uncompressed. Particular surface features of interest may be targeted individually.

2.6.3.8 Lander Panoramic Imager

The Lander panoramic imager (camera) provides several functions; analogies with imagers on Pathfinder, Viking, and MER will be familiar. A primary function is to support surface sampling and provide context for spectroscopy measurements. Additionally, the small-scale geomorphology of the landing site will be characterized (e.g., sediments, wind ripples, and so on).

The panoramic imager will be able to perform atmospheric optics measurements by imaging the solar aureole. (It may also be possible to detect other astronomical targets at night – not least the crescent limb of Saturn – and several Saturnian satellites are brighter at Titan than Venus seen from Earth.) Soil mechanics experiments are possible by inspecting the walls of trenches, the angle of repose of piles of sediment, etc. Witness plates or photometric targets may be observed at regular intervals to determine if aerosols are sedimenting out of the atmosphere. Such a target could be patterned on the Planetary Society's sundial target on the MER rovers. Although large amounts of meteoric metals are not expected at Titan, a permanent magnet experiment would be an easy way to detect the presence of at least some inorganic material in sediments. The use of blue- and UV-filters, while not expected to see anything under Titan illumination, may be used in combination with a UV-illuminator (nominally mounted on the sampling arm) to search for fluorescence characteristics of hydrolyzed tholins (Hodyss et al., 2004).

A representative heritage instrument is the Pancam developed for MER. As with Pancam, the Lander panoramic imager is deployed at the top of a vertical mast on a scan platform. Full 360° azimuth rotation and 90° polar tilt are provided. This imager comprises a stereo camera pair (each with a 1 Mpixel array detector) with multiple (~8) color filters allocated among the two cameras, indexed with a wheel mechanism. Sensitivity ranges from near UV (~300 nm) to near IR (~1100 nm). The field of view of ~17° translates to 0.3 mrad per pixel (e.g., 3 mm/pixel at 10-m distance). Solar illumination is assumed for primary imaging, while an array of bright LEDs is included for specific tasks, such as blue albedo measurement and UV fluorescence. The allocated mass for the panoramic imager is 4 kg including, the LED array. The average operating power is 2 W, with a peak power utilization of 5 W. The imager system will be capable of operating in thumbnails or full-image mode. It will be capable of obtaining panoramic images, as well as targeting specific geologic features of interest.

2.6.3.9 Descent Imager

Because the horizon as seen from the Lander may be nearby, a broader view of the terrain around the landing site is desired during dayside descent. This broader view permits location of the landing site in orbital maps and also offers a higher-resolution geomorphological view of the site. From higher altitudes of 10 km or more, the descent imager will yield data comparable with that from the Balloon imager. But since (unlike Huygens) operation and transmission after landing is assured, descent imagery would be obtained to within a few meters of the ground, providing a nested image dataset spanning 2 to 3 orders of magnitude of scale.

A representative heritage instrument is the Mars Descent Imager (MARDI) developed for Mars Polar Lander, Phoenix, and MSL. The Titan descent imager uses a 1024 × 1024 (1 Mpixel) detector. At the start of its descent operations, an arm deploys it to a position beyond the edge of the heat shield. This arrangement avoids the need for optical penetration of the heat shield. The

relatively slow descent of the Lander, compared with Mars EDL, permits the descent imager to acquire a significant number of nested images with increasing spatial resolution as the landing approaches. With the arm mechanism, the allocated mass is ~2 kg. Peak operating power during active imaging is 10 W. As with other cameras in the payload, images are available in compressed and/or thumbnail formats for rapid uplink as well as in raw, uncompressed format.

2.6.3.10 Lander Magnetometer

Significant permanent magnetic fields are not expected near the Titan surface (unlike Mars, for example), since the crust is likely to be organics and ice. A modest remnant field may exist in a rock or rock-iron core, and an internal dynamo field cannot be ruled out but appears unlikely, given the constraints from Cassini. Of particular interest, however, is the effect of the changing Saturn field at Titan's surface, and the possible induced response of a conductive water ocean in the interior. Such changes at Titan will be small – a few nanoteslas – since the Saturn field is not substantially inclined to Titan's orbit. However, the changing radial distance to Saturn and possible excursions into the magnetosheath offer two sources of external modulation of the field sensed at the surface. Another factor, which may lead to at least faster, if not larger, effects, is the "gating" of the Saturn field by Titan's ionospheric conditions.

Stability of the instrument against zero shift and bias changes is the key to meeting the science goal. Magnetic cleanliness of the Lander is less important, since its fields are either permanent or are very short-term events correlated with motor actuations such as tracking the HGA or performing sampling. The changes of interest are principally on hour to day timescales associated with orbital and ionospheric modulation of the applied Saturn field.

The Lander magnetometer characterizes any intrinsic magnetic field that Titan may retain at its surface (global or local). The sensor is assumed to be of the same type, a fluxgate magnetometer with a range of ±1024 nT and 0.03-nT resolution, as on the Orbiter (following MESSENGER MAG heritage). The Lander magnetometer, however, is deployed by the robotic arm as a standalone surface module (i.e., no boom). The baseline deployment is a single-time event at a position selected during the initial imaging phase. The capability to pick up and reposition the module using a suitably modified arm-based grasping device is a possible enhancement; measurement of the field at more than one point allows the contribution of the Lander to any magnetic field to be cancelled. Should emplacement be impossible, operation from the stowed position is still possible and may not suffer significantly, given the excitation timescales discussed above. A shielded umbilical between sensor and Lander provides a power and data link. The insulated sensor module also includes heater elements to meet survival and operational temperature requirements. The mass allocation for the magnetometer is 2 kg (2.5 kg including umbilical). The average operating power is 4 W.

2.6.3.11 Lander Radio Science

The regular communications sessions with the Lander provide opportunities for radio occultation experiments, recovering the refractivity profiles (and thus the temperature structure) over a range of azimuths around the Lander location. While not sampling a large range of latitudes, these data provide, over the duration of the mission, a strongly complementary dataset to the Orbiter radio occultation measurements and microwave and thermal-IR measurements.

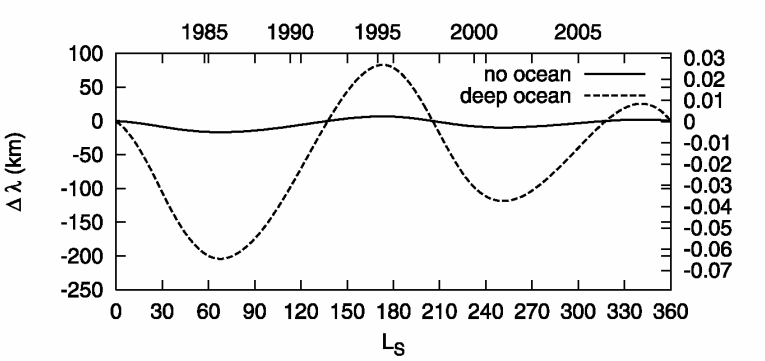

Figure 2-36. Simulated offset in the position of a point on Titan's equator relative to an assumed synchronous rotation (Tokano and Neubauer, 2005). Over a 1-year mission a change in position of tens of kilometers is likely and provides a test of Titan's moment of inertia, which is highly sensitive to whether the ice crust is decoupled from the interior by an internal water–ammonia ocean. The shift, furthermore, is a test of changes in the angular momentum budget of the atmosphere.

Additionally, precision measurement of the Doppler shift recorded by the Orbiter (or vice versa) allows the determination of the position of the Lander. Corresponding measurements were made on Mars with Pathfinder (Folkner et al., 1997), allowing, even during that short mission, determination of the polar precession (implying the existence of a dense core) and change in rotation rate associated with mass redistribution between atmosphere and polar caps. Global Circulation Model (GCM) simulations it have shown (Tokano and Neubauer, 2005) that Titan's massive atmosphere can have dramatic seasonal exchange of momentum with the surface, leading to changes in its length of day, which in turn can lead to displacement of surface features (or a lander) from their expected position by several kilometers per year (Fig. 2-36). Considerable work has been done on evaluating the potential geophysical results, such as core nutation and polar wander that can be derived by precision lander location measurements from Orbiter Doppler at Mars (e.g., Yseboodt et al., 2003; Duron et al., 2003). We expect comparable insights at Titan but have not yet been able to explore the possibilities quantitatively.

2.6.3.12 Outreach Experiment – UAV

It would be remiss not to at least mention the possibility of in situ "subvehicles" on the Titan Lander, as an analog of the Microrover Flight Experiment (MFEX, subsequently named Sojourner) on Mars Pathfinder. Following the successful development of a student experiment on New Horizons, we suggest the possibility of devoting some of the project outreach budget to one or more in situ packages (which could be determined by competitive selection); as a strawman example we consider a small UAV. International partnering is another option.

UAVs of 1 to 3 kg carrying video and/or thermal cameras are now routinely used by armed forces for reconnaissance and perimeter security, e.g., at airfields. Systems like Dragon Eye (of which the USMC operates some 3000) are hand-launched and battery powered, have an endurance of 60 min and a range of 10 km. Teleoperation or GPS guidance is used, and video is streamed directly to the control station. Such a concept could be applied to Titan, where the low gravity and dense air greatly enhance the performance of aircraft; with no changes to the airframe or propeller, a terrestrial UAV could fly with 35× less power on Titan than on Earth. Realistically, a more compact design would be employed to match flight power with the dissipation required to stay warm. The wingspan of a 1-kg airplane need be only ~20 cm: payload could be as simple as a down- or side-looking camera and rudimentary meteorology sensors. The vehicle could be programmed to ascend vertically from the Lander (attaining thrust:weight > 1 on Titan is easy) and follow a preset circular or spiral ground track using dead-reckoning or inertial guidance; Lander beacon or Sun sensing could also provide a heading reference. Data could be

streamed by radio link to the Lander for a 1-hour operating life, with the Lander performing subsequent data compression, selection, and transmission to Earth.

In principle, much of the science of which the UAV is capable is already attained in part by the descent imager; the attainment of the science goals is not therefore contingent upon successful UAV operation. Scientifically, such a vehicle could augment the science return by following up on regions of interest identified in descent imaging, by searching for surface changes, or by providing stereo perspective or additional spectral channels. Boundary layer meteorology studies would be an additional opportunity. As a public relations tool, the possibility of aerial images showing the Lander itself on Titan's surface would be formidable. Launch of the UAV could be deferred until late in the Lander mission, to minimize any potential risk of collision with the Lander. This would also provide a mid-term public-relations boost some time after the excitement of Titan arrival.

A fixed-wing UAV is offered only as an example. The Titan environment permits many possibilities for in situ subvehicles that could be deployed from the Lander or the Balloon: microrovers, drop-zondes, subsurface moles, or even rotorcraft are possible. Design for the Titan environment offers an educational challenge, yet is tractable and testable with modest resources (e.g., a tent and lots of liquid nitrogen). We have not advanced a design here nor linked the UAV to any formal science objective, but retain a mass allocation on the Lander (notionally 2 kg; 1 kg for vehicle, plus a generous 1 kg for attach interface/radio) and a data allocation of some 0.3 Gbits. The system would likely use its own primary batteries except perhaps for pre-release warm-up, so no power allocation is made.

2.7 Science Return

2.7.1 Lander Data Return

A strawman allocation of the Lander science data is given in Fig. 2-37. A UHF data link permits transmission of 3 kbps of science data during communication windows, adding up to 700 minutes per 8 days and yielding a total data return of 5.4 Gbits over 1 year. (This is roughly equivalent to the data returned in ~2 months of downlink from MER Spirit or Opportunity, or almost three times the 2.3 Gbits returned from Mars Pathfinder, which lasted 3 months [see Golombek et al., 1999]). The Titan Lander payload is more elaborate, and operates for longer, but improvements in data handling will leverage this data volume. The continuous and robust

Instrument	Datasets (e.g., panoramas)	Images/ Spectra/ Channels	Pixels/ Samples	Bits	Compress Factor	Gbit/ Dataset	Total	Comment
Panoramic Imager	8	96	1.00×10^6	12	5	0.230	1.843	4p, 1 mrad FOV, 8 filters
Point Spectrometer	20000	1	1.00×10^3	12	1	0.000	0.240	
Microscopic Imager	80	3	1.00×10^6	8	5	0.005	0.384	3 colors
Chemical Analyzer	40	1	7.20×10^6	8	3	0.019	0.768	e.g., 7200 s GC run x 1000 Da
Seismometer	365	4	8.64×10^4	8	3	0.001	0.336	
Magnetometer	365	3	8.64×10^4	8	5	0.000	0.151	
MET Package	365	5	8.64×10^4	8	3	0.001	0.420	
UAV Survey	1	200	1.00×10^6	8	5	0.320	0.320	
Descent Imager	1	200	1.00×10^6	8	5	0.320	0.320	
EDL Dataset	1	12	7.20×10^4	8	1	0.007	0.007	2 h EDL 12 sensors @ 10 Hz
Specials	20	20	1.00×10^6	8	5	0.032	0.640	e.g., sample support imaging
TOTAL							**5.430**	**Gbit**

Figure 2-37. Strawman allocation of the Lander science data.

power source permits data compression and selection to operate as a background task during the long intervals between communication sessions.

As with the Mars missions, imaging is the principal user of bandwidth, followed by the surface composition and long-term geophysical/meteorological measurements that are main science objectives. Only modest data compression ratios have been assumed in the above, although the panoramic imager return is somewhat austere. Tracking the Orbiter with the pointable X-band HGA, however, provides a six-fold enhancement of the science bandwidth, which would permit in particular a considerably higher image science return than the budget of Fig. 2-37, which already suffices to meet the science objectives.

2.7.2 Balloon Data Return

A strawman allocation of the Balloon science data is given in Fig. 2-38. By virtue of being mobile, the Balloon's ability to acquire novel information far exceeds its ability to relay that information to the Orbiter. Extensive effort will be devoted to onboard data selection and compression. The majority of downlink is devoted to imaging, with the major other users being the near-IR spectrometer, subsurface radar sounder and MET package.

2.7.3 Data Return in Case of Orbiter Failure

The failure of the principal element in a mission is not something any Flagship likes to contemplate. However, it should be pointed out that while the data volume will be vastly reduced, significant science return may be possible from the in situ elements of the mission direct-to-Earth in the absence of an Orbiter relay. These scenarios have not been evaluated in detail, but note the robustness of the architecture.

VLBI tracking of the Huygens probe S-band signal has yielded a trajectory with a precision of ~1 km; rather higher precision could be attained for X-band transmission from the Balloon. (Note that solar wind dispersion precludes UHF from contributing usefully to VLBI tracking.) The Lander could be similarly tracked during descent. Measurement of Balloon position over weeks and months would provide a powerful constraint on the wind field.

The provision of an HGA on the Lander, as well as augmenting the data return from the surface, allows modest direct-to-Earth communication. Pointing knowledge could be achieved by a combination of camera imagery (to determine the obvious position of the Sun; Earth is in the ecliptic plane always within 6° of the Sun as seen from Titan) and scanning of the HGA to locate a beacon transmission from Earth. Once pointed, data rates of 200 to 300 bps – a factor of several higher than the highly successful Galileo mission – are possible to a 70-m DSN dish. Al-

Instrument	Datasets	Images/ Spectra/ Channels	Pixels/ Samples	Bits	Comp Factor	Gbit/ dataset	Total	Comment
Balloon Imager	365	8	1.00×10^6	8	10	0.007	2.336	8 images/day, with clever selection
Near-IR Spectrometer	40000	1	1.00×10^3	12	2	0.000	0.240	
Subsurface Sounder	20000	3	1.00×10^3	8	2	0.000	0.240	Assumes heavy onboard binning
TDL/Nephelometer	365	24	4.00×10^3	8	3	0.001	0.090	4000 spectral points, twice/h
MET Package	365	6	8.64×10^4	8	5	0.001	0.305	1/s
Navigation	365	4	8.64×10^4	8	10	0.001	0.102	IMU, image attitude solutions, etc.
Altimeter	365	1	8.64×10^4	8	5	0.000	0.050	
EDL Dataset	1	12	7.20×10^4	8	1	0.007	0.007	2-h EDL 12 sensors @ 10 Hz
TOTAL							**3.37**	**Gbit**

Figure 2-38. Strawman allocation of the Balloon science data.

though a detailed data volume budget has not been determined for this contingency scenario, it seems likely that the majority of the key objectives of the Lander mission (and thus 10% to 20% of the total science return of the overall mission) could still be recovered.

2.8 Mission Architecture and Rational Descopes

At the mission element level, the scientific priorities discussed in Section 2.2 (and also Section 2.9, where further mapping of the science objectives is described) are quite clear. An evaluation that proved robust to variations in the weighting applied to investigation and measurement priorities indicates that when considered in isolation (ignoring possible synergies), 60% to 65% of the mission goals are achieved by the Orbiter only. Orbiter only, therefore, is defined as the floor mission architecture. The Lander was a clear second, in providing 20% to 25% of the total science value, while the Balloon addresses 15% to 20% of the goals.

The descope pathway at the mission element level is straightforward:

- First, substitution of a second Lander for the Balloon results in some modest savings, and while failing to meet some measurement goals, provides for an augmented and robust surface science return: simultaneous seismic and meteorological measurements from different locations on the surface are powerful in combination. Furthermore, knowing that Titan's surface is compositionally diverse from Cassini near-IR data, the opportunity to obtain the in situ chemical data to understand what these different materials really are is an important one. Of course, this two-Lander option loses the attractive high-resolution surface imaging, meteorological information, and subsurface sounding over a range of terrains that only the Balloon can effectively perform.
- Second, an Orbiter + Lander mission yields substantial savings and simplification, while preserving >80% of the baseline science return. Consideration might be given to trading impact speed and landing site dispersion against a longer descent, to obtain some descent measurements that might substitute in part for those made from the Balloon.
- Finally, an Orbiter-only mission, while disappointing in that it would fail to capitalize on this most affordable opportunity to perform in situ science in the outer solar system, will nonetheless achieve a formidable return in a variety of scientific fields.

The broad range of thematic and physical targets, and the range of scales of investigation, mean that a comprehensive payload encompasses some overlap, providing scientific robustness as well as some modest technical redundancy. While there is some robustness of meeting objectives to payload descopes or failures, the payload is not *a priori* redundant. For example, while the subsurface radar/ionosphere sounder can provide a global topography dataset that could be applied to some scientific problems (e.g., large-scale meteorological effects, sediment transport in rivers, etc.) it cannot substitute entirely for the corresponding product generated by the radar altimeter, which is of higher spatial resolution and much higher precision, and can address a range of other questions (such as tidal variation in surface heights, evaporation of surface liquids, topography of dune forms, etc.). Similarly, abundances of several stratospheric molecules are measured by the thermal-IR spectrometer and are also measured by the microwave spectrometer or in some other cases by the UV spectrometer. However, these instruments sample different altitude ranges (with overlap), and each provides different ancillary results (e.g., condensate species for the IR spectrometer, Doppler winds for the microwave spectrometer, high-altitude haze opacity for the UV spectrometer, etc.). Thus, these instruments are fundamentally complementary. Together they form a synergistic core capability for Orbiter atmospheric sounding. For example, the former does not have the spectral resolution to directly measure wind vectors from Doppler

shifts, while the latter tracks few hydrocarbons (except for CH_4, few have emission features at millimeter and sub-millimeter wavelengths), and it cannot spectroscopically identify condensates or aerosol characteristics, because their features are too broad.

A prioritized list of instrument-level descopes has not been attempted since the choices might be different depending on whether cost, mass, power, or some other factor is driving the descope, and to what extent proposed and selected instruments actually resemble the strawman possibilities outlined as examples in this report. Furthermore, the overlap and complementarity between instruments on different platforms makes it difficult to discuss descopes in isolation. The "breakpoints" at which a progressive descoping might move from simplifying one or several instruments to deleting one altogether, and from curtailing mission duration or deleting instruments to deleting architectural elements, have similarly not been determined.

In terms of Balloon or Lander architecture, it may be noted that the designs discussed in this study are strongly constrained by the available radioisotope power sources (RPSs). For both electrical and thermal reasons, any in situ measurement platform at Titan that functions for more than a few hours can be practicably powered only by an RPS. The study guidelines assume only a 100-W-class RPS. Were smaller (1 to 20 W) power sources available, some interesting possibilities for smaller in situ vehicles such as distributed weather/seismic stations (i.e., micro-landers without large instrument complements) or small helium balloons could be envisioned.

The architecture presented here addresses the science goals robustly and conservatively and is directed toward implementation for 2018 launch. Other concepts in prior studies without the challenge of a specific launch period have considered, for example, more ambitious aerial vehicles with propulsion and surface sampling systems. Such vehicles ("aerobots") would offer the scientifically attractive capability of sampling multiple locations, considerably enhancing the achievement of objectives 2.1 and 2.3, but by omitting seismological study, for example, would fare more poorly at objectives 1.4 and 2.4. The overall science change over the baseline is therefore small, but having a separate vehicle and Lander, as in the baseline architecture, requires less technology development and entails less risk than an aerobot.

2.9 Science Objective Mapping to Instruments and Architecture

Assigning relative priority to science disciplines, or the instruments that address them, is a notoriously difficult problem in planetary science. The breadth of scientific topics engaged at Titan make assign relative priority particularly challenging, and the SDT emphasizes that proper understanding of Titan requires study as a system. However, early review of this study emphasized the need to make an evaluation of the various elements of the mission so that potential descope pathways have a clear scientific rationale. Foldout 2-2 captures the SDT assessment of the scientific priority of the various investigations and measurements, together with an estimate of how well each instrument in the suggested payload might address them. This information was given in a reduced form in Foldout 2-1; here further details are exposed to explain the priority order of the various platforms.

The SDT ranked in priority order *(R)* the four investigations under each of the two equal objectives, the score *X* being then 1/*R*. The cognizant members of the SDT in each subject area then estimated two parameters, with discussion and concurrence of the rest of the SDT. First, for each measurement objective, its relative importance was assigned a number from 9 to 1 (no duplicate scores allowed) in contributing to its investigation. This score was then normalized *(Y)* to the total of the measurements for that investigation. Second, an estimate of the degree *(Z)* to which the nominal mission (1 year Lander/Balloon, 4 years Orbiter, with parameters as understood by the SDT at its third meeting) would be fulfilled.

A score *(S)* for each instrument (and platform) was determined by the following formula $S = X^p Y^q Z^r$ where *p, q,* and *r* are weighting exponents. These exponents allow exploration of the sensitivity of the final scores to the various subjective parameters. It is recognized that a different SDT composition might estimate different values for any of these parameters, although the concurrence of the SDT suggests no gross biases were present. It is impossible to estimate to what extent the architecture of the measurements/investigations/objectives can affect the result; normalization of the measurement scores per investigation should at least prevent the number of such measurements being a major factor.

The first exponent, *p*, determines how important the ranked investigations should be. This exponent should have a low value: for $p = 0$, the ranked investigations have no priority, for $p = 1$ a rather severe ordering is implied (i.e., the second investigation being half as important as the first). A nominal value of 0.25 was adopted.

The second exponent, *q*, has a similar effect to determine how important the relative importance of measurements within an investigation might be, but (since measurements had scores ranked from 9 downwards rather than 1 upwards) a stronger value of the exponent was more appropriate. A nominal value of 0.5 was adopted.

The third exponent, *r*, assesses the significance of the extent to which an instrument or campaign addresses a specific measurement goal – an estimate of the completeness and/or definitiveness of a result. If the exponent is 1, then the final score linearly depends on this estimate (which may reflect completeness of spatial coverage, for example), while if the exponent is zero, then any instrument which makes any contribution is judged to have the same relative importance. Although a nominal value of unity is assumed, lowering the value of the exponent reflects the potential for measurements to have a higher significance than expected, which is often the case in exploration science.

The resultant scores for each instrument (and platform) are obtained by summing the scores for all measurement goals for it. These were then divided by the sum of all scores and multiplied by 100 to derive a percentage total.

The point of this exercise is not to defend any particular formulation of a metric, but rather to provide an example of one and show that in fact the results in aggregate are rather robust to the values chosen for the weights. The adoption of exponents allows the sensitivity of the results to the various (subjective) parameters to be explored conveniently. As an example, by setting exponents to zero, the information obtained from numerical parameters is discarded, such that any nonzero completeness entry in the table becomes of equal significance, and the resultant scores are in effect "counting checkmarks." No claim is made here that such an approach – often adopted – is more or less appropriate than the scores for the nominal exponents above, but the exponent approach separates the capture of scientific opinion from the weighting applied to it and its final presentation.

Note that this approach was guided by experience in the "Billion Dollar Box" (Reh et al., 2007a), which underscored that regardless of final presentation adopted (e.g., "XX," "XXXX," etc., or "RED," "YELLOW," "GREEN") the capturing of scientific opinion on relative importance of measurements, or effectiveness of given instruments, must be done with enough fidelity that the data provide a useful discrimination between options. For example, in that exercise, four metrics were added together, and the metrics were captured with three levels. However, because the metrics were being applied to derive final scores to rank some 20-plus options, summing such coarsely determined values in fact led to several options having equal scores. Retroactively applying adjustments to provide discrimination between such "ties" is inelegant and threatens the

integrity of the process. Scales of 1 to 9 (i.e., 3 to 4 bits of resolution) are a good compromise between ease of generation and required fidelity.

At an individual instrument level, the results will be sensitive to the specific choices of priority or completeness parameter (often obtained after less than a person-minute's deliberation) and blind adoption of the resultant scores as the sole decision metric for descope options is not recommended without further scrutiny (of course, the same could probably be said of any single metric, however generated). However, at the platform level there are enough combined parameters that the results are insensitive to small numbers of changed parameters, and insensitive to the adopted weighting exponents. Thus, the SDT is comfortable with justifying the platform-level priority of Orbiter-Lander-Balloon.

With the nominal exponent set (0.25,0.5,1), the scores for Orbiter, Lander, and Balloon are 63, 22, and 14, respectively. In other words, the majority of the science return is from the Orbiter, and is roughly three times the science return from the Lander. The Lander is roughly 50% more potent in addressing the stated science objectives than is the Balloon, although it is emphasized that all three elements provide significant science return. It may be observed that the relative costs of the various elements are not wildly different from the relative science values. It is acknowledged, however, that the scoring methodology does not take into account the added synergistic value of independent measurements. Although the costs of the various elements add roughly linearly (incremental elements have a smaller individual cost due to amortization of component developments, etc., but add a total systems complexity cost, the net result being approximately linear), the scientific returns, in contrast, are super-linear.

We may explore the sensitivity of this ranking by adjusting the weighting exponents. Consider a "highly focused mission," where the relative priorities determined by the SDT are afforded considerable significance, with the first investigation per objective being twice as important as the second, and similarly high weight applied to relative measurement contributions. Adopting the exponent set (1,1,1) yields the scores 63:24:14 (rounding errors mean these sum to 101) – barely different from the adopted exponent set.

The other end-member approach is to essentially discount the quantitative estimates of the SDT, and to assume all objectives are of equal weight and that any contribution to a given measurement is important. Here the exponent set (0,0,0) can be used, and the resultant scores are 61:21:19. This is interesting for two reasons: First, that the priority order remains consistent – Orbiter, Lander, Balloon; second, that the discrimination between the Lander and Balloon is barely significant, reflecting that both platforms address different science goals. Since no relative priority among goals is factored in due to the zero exponents, the resultant scores for the two platforms are similar.

It is acknowledged here that the metric above is somewhat subjective. However, no "objective" metric actually exists. In any case, evaluating descope or enhancement options requires consideration of the gain (by mass savings, cost savings, etc.) as well as the change in science. Architectural elements might be included or altered for nonscientific reasons such as technology demonstration or international partnering. These are beyond the scope of the present discussion. However, insofar as the SDT was charged with providing guidance on the relative scientific importance of various elements, that has been captured in the spreadsheet (Foldout 2-2).

FOLDOUT 2-2: The SDT's assessment and mapping of scientific priorities from science objectives to instruments and mission architecture.

Sensitivity parameters to explore sensitivity of results to science team subjective assessments			
	Investigation Exponent q (score = 100 * (1/RANK)^q	0.25	Says how important investigation ranking is. q=1 means a lot - Inv2 only half score of inv1 ; q=0.5 means inv2 is 71% of Inv1, etc.
	Measurement Exponent r (score = Investig score * (Priority/Total Priority)^r	0.50	Says how important measurement priority within investigation is
	Completeness Exponent s (score = measurement score* completeness^s	1.00	Says how much it matters a job is only part done. Suggest leave as s=1 since completeness estimation took that into account. S=0 says that any contribution is great

										Orbiter																Lander									Balloon						
Objective	Investigation	Measurement	New Objective/Investigation	RANK	Investigation Points	Measurement Points	Investigation Priority (9=high)	Measurement Duplicated between Investigations		Radar Altimeter	SAR Capability	Subsurface Sounding Radar	Orbiter Radio (Tracking & Occultations)	Orbiter Magnetometer	Orbiter Microwave Spectrometer	Ion and Neutral Mass Spectrometer	Orbiter Thermal IR	Orbiter UV Spectrometer	Plasma Package	Langmuir Probe	Energetic Neutral Particles	1-Micron Camera	Spectral Mapper	Lander Precision Tracking	Lander Seismometer	Lander Magnetometer	Descent Imager / Radiometer	Lander Meteorology Package	Lander Spectrometer	Lander Camera & Microscope Camera	Lander Chemical Analyzer	Balloon TDL Spectrometer & Nephelometer	Balloon Imager	Balloon Subsurface Radar Sounder	Balloon Downlooking Spectrometer	Balloon MET Package	Balloon Tracking / Navigation and Altimetry	Atmospheric Optics Monitor
Resultant scores		**Platform Total %**								**63.2**																**22.5**							**14.3**						
		Instrument Total %								**4.7**	**3.6**	**3.45**	**4.73**	**2.51**	**7.05**	**6.26**	**9.57**	**4.33**	**3.12**	**0.79**	**0.65**	**2.82**	**9.66**	**1.27**	**2.53**	**1.14**	**1.16**	**1.04**	**0.13**	**1.52**	**13.7**	**3.11**	**1.71**	**1.15**	**3.14**	**0.62**	**3.17**	**1.4**
		Platform Total Score								1910.5																679.6							432.1						
		Instrument SCORE (Mirrored from Bottom)								141	109	104	143	75.8	213	189	289	131	94.2	24	19.6	85.1	292	38.5	76.4	34.3	35	31.5	3.82	46	414	93.9	51.7	34.8	94.9	18.7	95.9	42.3
OBJECTIVE 1: Titan: An Earthlike System How does Titan function as a system? How do we explain the similarities and differences between Titan and other solar system bodies in the context of the complex interplay of the geology, hydrology, meteorology, and aeronomy present in the Titan system?	Determine the composition and transport of volatiles and condensates in the atmosphere and at the surface, including hydrocarbons and nitriles, on both regional and global scales, in order to understand the hydrocarbon cycle. Determine the climatological and meteorological variations of temperature, clouds, and winds.	Determine composition of surface volatile inventory (minerals)	1.1	1	100	35.1	9																0.8							0.9				0.8			
		Global distribution of condensates	1.1	1	100	33.1	8										0.6	0.1					0.3	0.7														
		Deterrmine volatile distribution in atmosphere	1.1	1	100	31.0	7								0.4	0.6	0.8	0.4					0.3								0.3	0.7						
		Obtain vertical temperature soundings	1.1	1	100	35.1	9						1.0		0.7		0.9																						
		Direct measurement of zonal winds	1.1	1	100	20.3	3								0.9								0.2	0.2	0.1			0.4								0.8		
		Determine mean meridional circulation via tracers	1.1	1	100	33.1	8								0.5	0.6	0.8	0.3					0.3	0.3												0.8		
		Measure profiles of organic gas abundance	1.1	1	100	31.0	7								0.4	1.0	1.0	0.7																				
		Measure time-series meteorology	1.1	1	100	23.4	4																					1.0							0.8	0.6	
		Determine clouds at all altitudes : distribution, morphology, etc.	1.1	1	100	28.7	6			0.3					0.1		0.8						0.7	0.9														
		Measure surface temperature distribution	1.1	1	100	11.7	1								0.9		0.8																					
		Measure deposition of sunlight as fn(altitude)	1.1	1	100	20.3	3											0.7										0.3									0.4
		Measure optical properties of aerosol particles	1.1	1	100	26.2	5										0.5	0.6					0.4	0.8				0.6				0.5					0.8
		Measure number density and size of aerosol	1.1	1	100	16.6	2									0.5	0.7	0.7					0.4	0.8				0.8				0.5					0.8
		Measure the abundance of radiocarbon in surface materials	1.1	1	100	11.7	1																								1.0						
	Characterize and assess the relative importance today and throughout time of Titan's geologic, marine, and geomorphologic processes, e.g., cryovolcanic, aeolian, tectonic, fluvial, hydraulic, impact, and erosion.	Detect morphological indicators of exchange (vents, etc.)	1.2	2	84.1	24.1	5				0.9												0.8	1.0								0.6						
		Map global topography (1km/10m)	1.2	2	84.1	28.5	7			0.9																												
		Measure dynamic lake topography (10km/1m)	1.2	2	84.1	24.1	5			0.8	0.7												0.2	0.7								0.1						
		Measure regional topography (100m/1m)	1.2	2	84.1	24.1	5																											0.2		1.0	
		Regional morphology (1m)	1.2	2	84.1	26.4	6																									1.0					
		Global morphology and texture (100m)	1.2	2	84.1	32.3	9				1.0												0.8									0.1						
		Global near-IR albedo (100m)	1.2	2	84.1	30.5	8																1.0									0.1			0.1			
		Regional variations of reflectance spectrum (10m)	1.2	2	84.1	26.4	6																												1.0		
		Local-scale morphology (0.1-0.01m)	1.2	2	84.1	21.5	4																							1.0		0.1					
		Regional subsurface structure (10km/100m)	1.2	2	84.1	18.6	3					0.8																										
		Regional subsurface structure (1km/10m)	1.2	2	84.1	10.8	1																											1.0			
		Measure topography boundary (100km/100m)	1.2	2	84.1	15.2	2			1.0	0.2	0.8																										
	Determine the interaction of Titan's upper atmosphere with Saturn's magnetosphere and the evolution of Titan's atmosphere, loss of materials, source of free energy, and heat. Determine the chemical pathways of tholin formation.	Measure vector magnetic field	1.3	3	76	27.7	6	a					1.0															0.2										
		Measure high-energy magnetospheric electrons	1.3	3	76	25.3	5												0.5																			
		Measure thermal electron density and temperature	1.3	3	76	30.0	7					0.7	0.3						0.6	0.8																		
		Mesure ion velocity distribution in the ionosphere	1.3	3	76	16.0	2										0.3		0.8																			
		Measure high-molecular mass ion composition	1.3	3	76	32.0	8										0.7		0.7																			
		Measure high-molecular mass neutral composition	1.3	3	76	34.0	9										1.0																					
		Measure escape flux of superthermal neutrals	1.3	3	76	22.7	4										1.0																					
		Detect high-energy neutrals and ions from interactions	1.3	3	76	19.6	3															1.0																
		Measure flux and energy of cosmic rays	1.3	3	76	11.3	1																															
	Determine internal differentiation, thermal evolution of Titan. Determine if Titan has a metal core and an intrinsic magnetic field, extent and origin of geodynamic activity.	Measure rotation parameters (pole position)	1.4	4	70.7	23.6	4				0.9												0.2	1.0														
		Local subsurface seismic structure	1.4	4	70.7	16.7	2																											0.8					
		Low-Order Gravity Field (N=6)	1.4	4	70.7	35.4	9						1.0																									
		Low-Order Topography (polar/equatorial radii)	1.4	4	70.7	33.3	8			1.0		0.9																										
		Vector magnetic field around Titan	1.4	4	70.7	31.2	7	a						1.0																					0.2			
		Detect presence of seismic activity (tidal and tectonic)	1.4	4	70.7	28.9	6																											0.8					
OBJECTIVE 2: Titan's Organic Inventory - A Path to Prebiological Molecules What is the complexity of Titan's organic chemistry in the atmosphere, within its lakes, on its surface, and in its putative subsurface water ocean and how does this inventory differ from known abiotic organic material in meteorites and therefore contribute to our understanding of the origin of life in the solar system?	Determine the chemical pathways leading to formation of complex organics at all altitudes in the Titan atmosphere and their modification and deposition on the surface with particular emphasis on ascertaining the extent of organic chemical evolution on Titan.	Determine CHONPS elemental composition of surface	2.1	1	100	34.6	6																								1.0						
		Determine surface composition of complex organics	2.1	1	100	42.4	9																								1.0						
		Characterize physical state of organics	2.1	1	100	24.5	3																							1.0							
		Measure isotope ratios of C,N,O of surface organics	2.1	1	100	40.0	8																								1.0						
		Measure chirality of organic compounds	2.1	1	100	20.0	2																								1.0						
		Measure chemical abundance of gases in atmosphere	2.1	1	100	34.6	6								0.3	0.8	0.7	0.4													0.6	0.3					
		Measure chemical composition of particulates	2.1	1	100	37.4	7										0.2														0.4	0.1					
		Measure sources of free energy	2.1	1	100	28.3	4											1.0	1.0																			
		Measure atmospheric thermal structure with latitude	2.1	1	100	31.6	5						1.0		1.0		1.0																					
	Determine geochemical constraints on bulk composition, the delivery of nitrogen and methane, and exchange of surface materials with the interior.	Measure noble gases and isotopes (esp Kr, Xe)	2.2	2	84.1	43.3	9																								1.0						
		Detect ammonia in surface material	2.2	2	84.1	40.8	8																0.5								0.7				0.5		
		carbon, nitrogen isotopes in surface/atmosphere reservoirs	2.2	2	84.1	35.3	6								1.0		1.0														0.7	0.5					
		Measure D/H in surface material	2.2	2	84.1	28.8	4																								0.8						
		Composition of gases released from vents, etc.	2.2	2	84.1	38.2	7								1.0															0.1	0.2	0.5		0.1			
	Determine chemical modification of organics on surface, e.g., hydrolysis via impact melt.	Determine CHONPS composition of modified deposits	2.3	3	76	41.0	7																								0.7						
		Determine composition of complex organics in special sites	2.3	3	76	46.5	9																								0.7						
		Identify potential chemical modification sites from mapping	2.3	3	76	43.9	8				0.1												0.8												0.3		
	Determine the depth of any subsurface liquid water ocean, its thickness and electrical conductivity, and the lateral variations in thickness and rigidity of the overlying icy crust.	Measure induced magnetic field	2.4	4	70.7	28.2	7							0.6														0.8									
		Detect seismic reflections within crust	2.4	4	70.7	23.8	5																						0.8								
		Measure normal seismic modes	2.4	4	70.7	26.1	6	b																					0.8								
		Detect subsurface radar reflections	2.4	4	70.7	21.3	4					0.8																							0.9			
		Measure libration and variations in rotation period	2.4	4	70.7	18.5	3				0.5																		0.7								
		Regional scale topography (~20km) (flexure)	2.4	4	70.7	15.1	2			1.0		0.6																									1.0	
		Measure changes in gravity field (k_2)	2.4	4	70.7	32.0	9						1.0																									
		Measure orbital changes in topography (h_2)	2.4	4	70.7	30.2	8			0.8																												

These numbers represent the extent 'Z' to which each measurement goal (row) is attained in the nominal mission by the relevant instrument (column), as determined by SDT

The Investigation priority determined by members of the SDT determines 'Y') the points per measurement goal that contribute to the total for that investigation (normalized by the total number of measurements in that investigation)

SDT determined rank R of the four investigations within each objective. A score is calculated as X=100/(R^p)

(Working area of spreadsheet for summing scores not shown)

Scores are calculated as described in the text as S=X*(Y^q)*(Z^r). Scores in each column are summed to determine the overall contribution of each instrument/element and the resultant percentage in the upper rows.

For simplicity, these contribution estimates are reduced to black boxes in Foldout 2-1

2.10 Payload Options

This section notes some of the discussion by the SDT and others on various techniques or capabilities for several of the payloads.

For example, two principal functions are desired for spectral mapping of the surface of Titan from orbit. In broad terms, the first desired function is high-resolution mapping of surface albedo, nominally in the 2-μm window (which has the most favorable combination of solar illumination and atmospheric transparency) but also perhaps at 1.1, 1.3, 1.6, 3, and 5 μm, and the second is the spectral identification of surface materials and measurement of cloud-top heights, requiring higher spectral resolution, perhaps tolerably with lower spatial resolution. One could envision a dedicated point or line spectrometer for the second function, with a filtered imager for the first. Or one might consider extending the short-wavelength capability of the thermal-IR spectrometer down to 5 μm. We have suggested a CRISM-type instrument, able to obtain high-resolution maps, that extends upwards in wavelength to 6 μm, but this is only one of several possibilities.

A corresponding situation exists on the Balloon, where we have outlined a down-looking point spectrometer which also performs atmospheric optics measurements, and a separate set of imagers. Options exist to combine these functions.

Similarly, the TDL instrument on the Balloon performs the primary function of measuring variation with time/position/altitude of specifically the most variable compounds, and this instrument can measure these compounds without any consumables or pumps. Other techniques, such as a mass spectrometer or GCMS, may be able to address these same goals and others as well, especially if equipped with an aerosol sampler and pyrolyzer. Commonality or complementarity with the Lander chemical analyzer may be a factor, as would longevity. Similarly, if the importance of cloud particle properties were emphasized over composition, a dedicated nephelometer might feature a more elaborate arrangement of scattering sources and detectors but without the TDL wavelength scanning. Even more speculatively, nephelometry or TDL spectrometry functions might be integrated with some sort of lidar instrument able to remotely measure haze density, surface reflectivity, and altitude. A considerable option space exists for integrating various measurement functions on the Balloon.

It may be that an Orbiter lidar system can generate topographic data with comparable horizontal or vertical resolution to the Orbiter radar altimeter we have proposed; however, at 1 μm and shorter, where previous space-based lidars have operated, the haze opacity on Titan is significant. Furthermore, a Titan Orbiter must operate at altitudes almost 10 times higher than those for Mars, so even if lasers were available at long enough wavelengths to minimize haze effects, the optics required for a narrow footprint and adequate signal-to-noise ratio are likely to be large. For the strawman payload the SDT considered a radar altimeter only but did not exclude the possibility that a lidar could be made to work. The team noted that a lidar, or indeed a Ka-band precipitation radar/altimeter, could perform interesting observations of Titan's haze and cloud.

3: Mission Architecture Assessment

3. MISSION ARCHITECTURE ASSESSMENT

The Titan Explorer (TE) Flagship Mission Study consisted of two phases, as shown in Fig. 3-1. During Phase I, discussed here, mission architectures were identified, evaluated, and narrowed down to a single architecture. Further analysis of the selected architecture was completed in Phase II, as described in Section 4.

Titan is a rich, diverse scientific target requiring a broadly scoped architecture addressing as many scientific objectives as possible within the programmatic boundaries.

- TE architecture is selected based on the science objectives, technical feasibility, minimum risk, and cost.
- Three elements best address the multi-scale science: Orbiter, Lander, and Balloon.
- Architecture maximizes flexibility while minimizing risk within the Flagship mission cost range.

3.1 Architectural Identification and Evaluation Process

As the Science Definition Team (SDT) progressed in defining the TE science objectives, it was clear that a multi-scale, multi-element architecture would best meet those objectives. The architecture tree, as shown in Fig. 3-2, was developed to identify candidate architectural elements for evaluation by the SDT and the engineering team. Based on initial cost estimates, including those completed in the Titan and Enceladus $1B Feasibility Study Report (Reh et al., 2007a), the TE study team estimated that two lower-level "boxes" on the architecture tree could constitute the flagship architecture. For example, an "Aerocapture" orbiter and a "Small Bal-

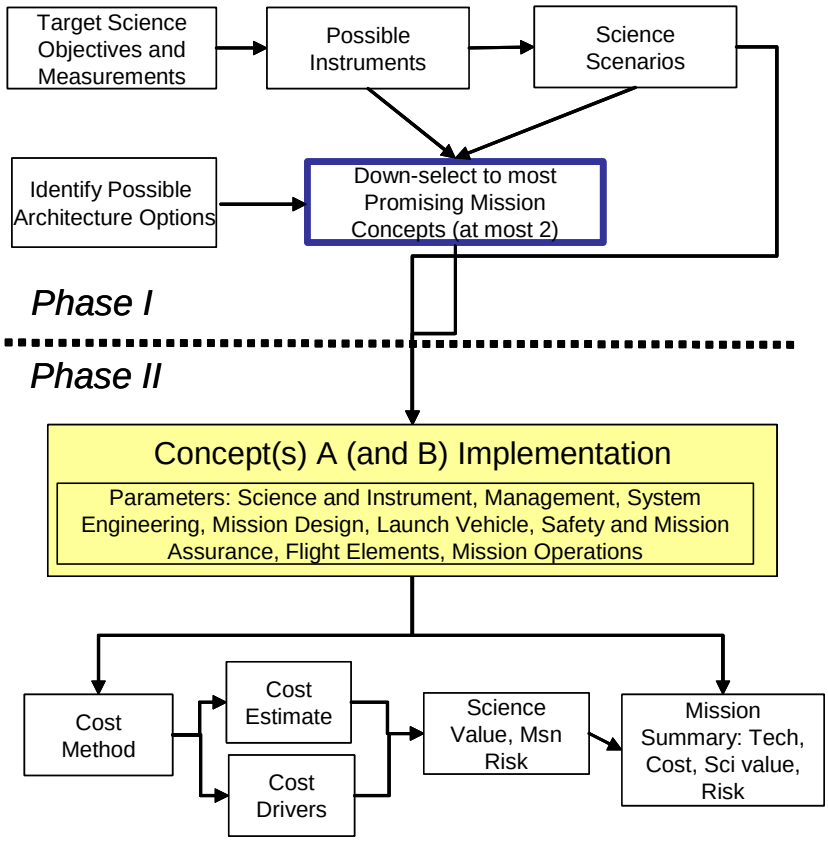

Figure 3-1. The structured approach used in Phase I for architecture definition resulted in a robust mission set for detailed analysis in Phase II.

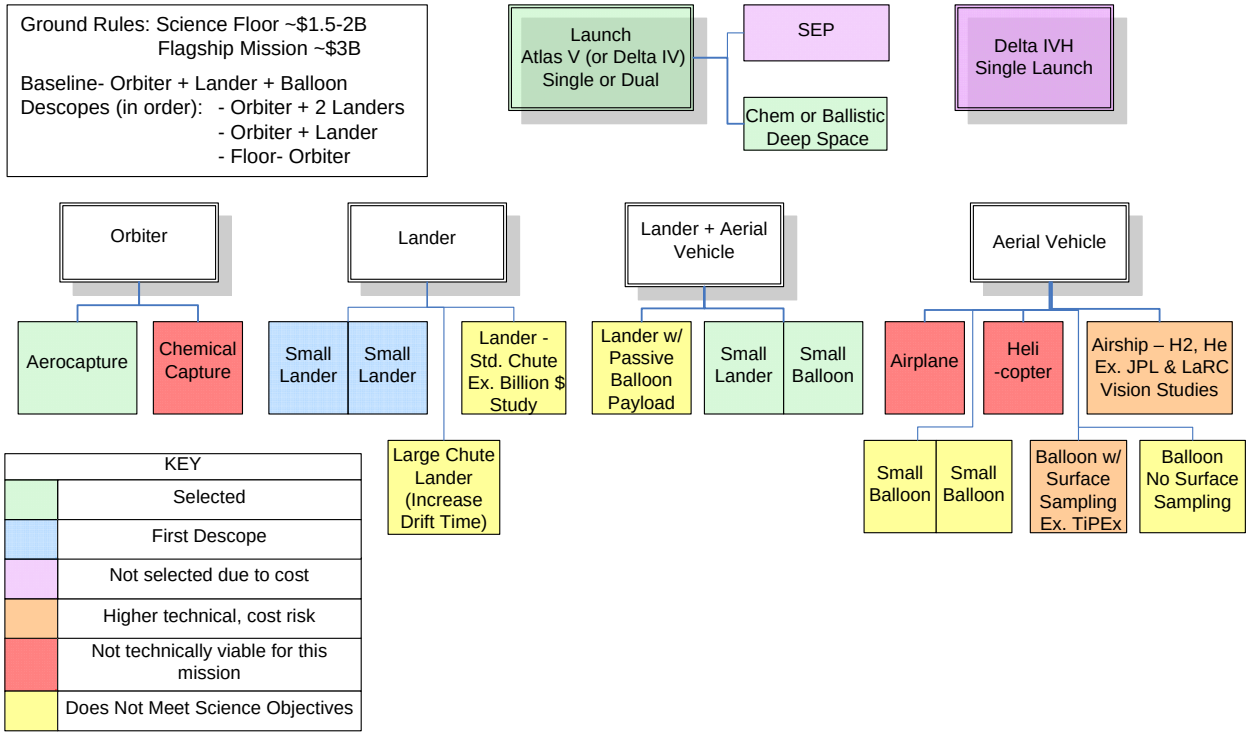

Figure 3-2. Science objectives, technical viability and risk, and cost were criteria used to select the TE baseline architecture.

loon/Small Balloon" could be selected as a baseline, with descope options if later cost estimates exceeded the $3B soft cap.

Architectures were evaluated as follows.

- Science: Architectural elements that did not meet the science objectives were eliminated.
- Technical Viability and Risk: Architectural elements that were not technically viable were eliminated. Elements that were viewed as carrying high technical risk and associated high cost risk were eliminated.
- Deep-space propulsion options were considered and selected to meet science requirements and to minimize mission cost and risk.
- Launch vehicles and launch stack configurations were considered and selected for cost, technical viability, and risk.
- Preliminary cost estimates were completed prior to final architecture selection.

3.2 Architecture Evaluation

3.2.1 Science Objectives

The TE science objectives, as described in detail in Section 2, included measurements that would require an Orbiter at Titan. In addition, surface measurements would be required, which therefore eliminated "Aerial Vehicles" (shown in yellow in Fig. 3-2) that did not provide access to the surface. The science objectives also specified measurements requiring an extended low-altitude (~10 km) atmospheric flight. These objectives led to elimination of elements under "Lander" and "Lander + Aerial Vehicle" (also shown in yellow in Fig. 3-2) that did not provide the extended atmospheric flight as part of the baseline architecture.

3.2.2 Technical Viability and Risk

While the science objectives were being formulated and architectural elements evaluated for science, the engineering team evaluated each element for technical viability and risk for TE.

- **Aerocapture vs. chemical capture:** Previous studies, including the NASA In-Space Propulsion Technology program–sponsored *2002 Titan Aerocapture Systems Analysis Team (ASAT) Study* (Lockwood et al, 2006), concluded that aerocapture is feasible at Titan and is enabling or strongly enhancing for a Titan mission that includes a Titan Orbiter, depending on mission requirements (i.e., launch mass required). For the TE mission aerocapture is enabling. Aerocapture was selected for TE and is discussed further in Section 4.6.5.
- **Airship (helium or hydrogen gas):** This concept, studied independently by NASA LaRC in the Vision Studies (Levine and Wright, 2005) and by JPL (Hall et al, 2006), required extensive technology development (materials development, manufacture and test processes, autonomy, surface sampling). The concept is susceptible to small holes in the airship material that risk operational lifetime. This susceptibility to small holes makes the manufacturing and test processes complex. Operations require extensive autonomy rules to accommodate powered flight with altitude and directional control outside of Earth and Orbiter view. In addition, the surface science is dependent on the success of both aerial vehicle technology development and surface sampling technology development.
- **Balloon with surface sampling:** This concept, proposed in the JPL TiPEx study (Reh et al., 2007b), utilizes a Montgolfiere-type hot air balloon with surface sampling. The Montgolfiere balloon is significantly more tolerant of small holes in the balloon and thus more robust than the helium or hydrogen gas airships. The Montgolfiere balloon utilizes heated ambient atmosphere to provide buoyancy, just like hot air balloons at Earth. Technology development for the Montgolfiere balloon, which includes validation of buoyancy and inflation (described further in Section 4.13.2), is significantly lower in risk than technology development for the airships. The coupling of the Montgolfiere balloon with surface science, however, makes the surface science dependent on the success of both the balloon technology development and the surface sampling technology development. In addition, directional control of the Montgolfiere balloon would be required to ensure that the balloon could overfly and hold at a location that could be sampled. Due to the high priority of the surface measurements for the TE mission and the increased risk resulting both from additional balloon technology development to support surface sampling and from surface sampling technology development, this concept was eliminated.
- **Airplane and helicopter:** The airplane was evaluated by NASA LaRC, as part of the NASA LaRC Vision Study mentioned above, and was eliminated in favor of the airship. Because of the high atmospheric density at Titan, the airplane either requires high power beyond near-term technology or high lift-to-drag ratios resulting in challenges for packaging inside aeroshells, or both. The helicopter, studied by Lorenz (2000b) and by the NASA LaRC Vision Study, required significant advancement in propulsion technology. The Vision Study concluded that it may be possible to overcome the challenges for the airplane and helicopter, but that other aerial vehicles require less technology development and provide adequate capability.

- **Two small landers, or one small lander and one small balloon:**
  - *Small lander:* A small lander was viewed as more on the scale of the Mars Exploration Rover mission than the Mars Science Laboratory mission to keep TE within the cost target. The ability of the lander to meet the science objectives, be technically feasible, and fit within the cost target depended in part on the Titan terrain selected. The dune regions offered a scientifically interesting site as well as a relatively benign landing terrain. The dune regions, located along the Titan equator, are characterized by large regions (several 1000 km) with few hazards based on Cassini radar data (although coarse) and analogies to Earth terrain, with a surface similar to sand, and maximum slopes at the angle of repose of approximately 30°. The team believes that a lander can be designed for landing in this terrain, recognizing that some terrain uncertainty exists.
  - *Small balloon:* The balloon was viewed as a Montgolfiere-type balloon with altitude control, but no horizontal direction control and no surface sampling. (This balloon is referred to in this report as either a Balloon or an Aerial Vehicle. The term "Aerial Vehicle" is used in Section 4 to define the whole element – the balloon itself plus the gondola, differentiating it from the balloon subsystem.) The team believes that a balloon can be developed with acceptable risk for the TE mission.

The most promising architectures were therefore an Orbiter plus a Lander and a Balloon, or an Orbiter plus two Landers. The Orbiter plus Lander and Balloon architecture met the baseline science objectives and was identified as the leading architecture. To minimize cost, all three elements would need to be packaged on a single launch vehicle. The engineering team assessed the feasibility as described in Section 3.2.6 below.

3.2.3 Deep Space Propulsion

Solar electric propulsion (SEP) and ballistic trajectories augmented by chemical propulsion were evaluated. The mission designs of interest for the Titan flagship study were those with launch opportunities every 1 to 2 years to provide flexibility for programmatic changes. Based on previous studies, including results of the Titan and Enceladus $1B Feasibility Study Report (Reh et al, 2007a), the mass that can be delivered to Titan with a chemical propulsion system or ballistic trajectory is equal to, and in some cases greater than, the mass that can be delivered with an SEP system. In addition, further analysis of the Titan and Enceladus $1B study results showed that total mission costs for SEP are ~$100M greater than total mission costs with chemical propulsion systems. The cost comparison includes the flight system, operations, reserves, project management, systems engineering, mission assurance, and integration and test. SEP systems also are not as mature as chemical propulsion systems, leading to potential additional cost risk. However, SEP provides 3- to 4-year shorter trip times to Titan compared with a chemical or ballistic trajectory. The trade becomes an additional $100M, and potential additional risk vs. a 3- to 4-year increased trip time. The on-orbit science duration requirement and the 14 year radioisotope power source (RPS) lifetime qualification constraint are the drivers for trip time. From the TE SDT, 3 to 4 years of on-orbit science was deemed acceptable. Thus, a 10- to 11-year cruise can be accommodated within the RPS qualification constraint, which provided a wide range of acceptable ballistic trajectory options augmented with chemical propulsion. Ballistic-type trajectories augmented by chemical propulsion were selected for TE.

3.2.4 Launch Vehicle

Because of the significant cost difference between the largest Atlas V/Delta IV and the Delta IVH, the TE mission was planned for the Atlas V 551 or smaller.

3.2.5 Launch Date and Trajectory Selection

An extensive launch opportunity search in the 2015–2022 timeframe, as defined by the study guidelines, was completed for ballistic trajectories to Titan. Ballistic trajectories were defined to exploit gravity assists both to lower the launch energy requirements and to maximize the mass delivered to Titan. In addition, trajectories were defined with trip times less than 10–11 years and that provided entry speeds for the Orbiter, Lander, and Aerial Vehicle < ~7 km/s. Chemical propulsion systems are used with these trajectories for trajectory correction maneuvers (TCMs) and deep space maneuvers (DSMs) to maximize the delivered mass to Titan over the required 21-day launch period.

Launch opportunities with similar launch mass capability were found every 1–2 years, as described further in Section 6. Of these, a 2018 Venus-Venus-Earth-Earth trajectory was selected as the baseline both to provide a launch mass capability repeatable every 1–2 years and to provide robust schedule margins for technology development (see Foldout 4-9 and Section 4.13). Earlier launch dates, while possible, would require a compressed technology development schedule. Details of the 2018 trajectory selected are included in Section 4.3.

Trajectories offering higher mass capability but that were not available every 1–2 years were not selected. Jupiter gravity assist trajectories were among those eliminated because of the phasing of their availability windows with respect to the specified launch timeframe. Jupiter/Saturn alignment, required for Jupiter gravity assist maneuvers to Saturn, occurs only 2–3 out of every ~19 years. There is some variability about this 19-year period as it translates to launch date frequency on the basis of the inner planet gravity assist design, launch energy, etc. Although the Jupiter gravity assist trajectories were not selected as the baseline, Section 6 provides data for reference on the highest-mass Jupiter gravity assist option, and the Jupiter gravity assist option offering the shortest trip time, both in the 2015–2022 timeframe.

3.2.6 Launch Stack Configuration

A mass assessment was made for launching three elements plus a cruise stage on a single Atlas V 551 based on the launch mass capability and trajectory selection discussed in the preceding section. Assumptions were made for the element payloads and corresponding accommodations based on previous studies, given that the payload had not been defined yet for TE. With these assumptions, results showed that the mass would be feasible.

Launch stack configurations were evaluated to determine packaging and load path feasibility of simultaneously launching three elements, each within an aeroshell. Fig. 3-3 shows the configuration types considered – an axial stack configuration proposed in the ASAT and TiPEx studies and a Cassini/Huygens-like configuration with placeholders shown for Orbiter, Lander, and Balloon. The Cassini/Huygens-like configuration was judged to be feasible for the three-element architecture and was selected for the TE mission. The advantages over the axial stack configuration are that the design coupling between the elements is low, with the majority of the interfaces to the cruise stage structure only; separation of each element is independent of the successful separation of the other elements; and no penetrations are required in any of the heatshields.

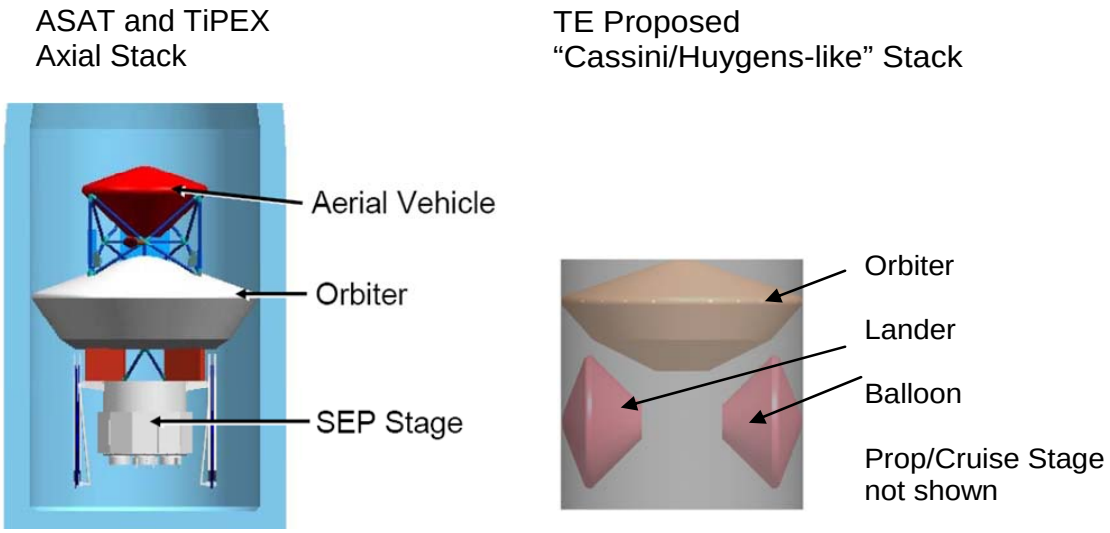

Figure 3-3. Cassini/Huygens-like launch stack configuration was selected for the TE mission.

3.3 Initial Cost Analysis

Two independent parametric cost analyses were performed to determine the mission cost relative to the $3B "soft" cost cap. JPL's analysis utilized their Outer Planets Cost Model and APL's analysis scaled costs from recent missions, primarily New Horizons. The models agreed well up to a three-element architecture. Both estimates fell in the $3B-$3.5B range with acceptable levels of uncertainty, leading the team to accept the three-element architecture (Orbiter, Lander, and Balloon).

3.4 Selection

On the basis of the science objectives, technical feasibility and risk, and cost, the baseline architecture was recommended as an Orbiter (aerocapture), Lander, and Balloon launched on an Atlas V 551 in 2018 with a ballistic trajectory augmented with chemical propulsion. The architecture, including descopes and science floor, is defined as follows.

- Baseline Mission: Orbiter + Lander + Aerial Vehicle
- Descopes in order:
  - Orbiter + 2 Landers
  - Orbiter + Lander
  - Science Floor: Orbiter

3.5 Initial Risk Analysis

Once the technical and cost feasibility for the mission were determined, a risk analysis was performed to outline the areas that the study should focus on to reduce the risk of moving forward with a mission to Titan. The detailed risk analysis can be found in Section 4. For the initial architecture definition, the only high risks were associated with the key technologies that need to be demonstrated: aerocapture, balloons, and cryogenic applications in the Titan environment (e.g., sampling mechanisms). All technology demonstrations were scoped and included in the cost estimate, lowering them to moderate risks.

4: Mission Concept Implementation

4. MISSION IMPLEMENTATION

Titan Explorer (TE) provides world-class science return at multiple scales utilizing simple interfaces and flight-proven designs wherever possible. TE is developed with proven processes incorporating lessons learned from many past missions.

The TE mission implementation maximizes science return while minimizing risk.

- The TE team members – APL, JPL, NASA LaRC, NASA ARC, and ILC Dover – have successfully built and flown many space missions, including New Horizons, MESSENGER, MSX, Cassini, and MER. Knowledge gained and lessons learned are incorporated into TE.
- Multi-scale architecture allows complementary vehicles to provide greater science than each element alone.
- Multi-vehicle architecture facilitates multi-organizational development, including international contributions.
- Robust descope methodology provides programmatic flexibility.

4.1 Mission Architecture Overview

TE science objectives drive the need for a multi-scale architecture. To this end, a three-vehicle architecture has been defined containing an Orbiter, Lander, and Aerial Vehicle (see discussion of architecture selection, Section 3).

4.2 Science Investigation

4.2.1 Science Payload

The science investigation and payload are described in Section 2. The science instruments described are representative; actual instruments will be selected through a process defined by NASA Headquarters. Payload accommodations are described in Sections 4.6.4, 4.7.4, and 4.8.4 for the Orbiter, Lander, and Aerial Vehicle, respectively.

4.2.2 Titan Explorer Draft Level I and Additional Driving Requirements

The draft Level 1 TE requirements are:

- Total mission cost should be within an approximately $3B (FY07) soft cost cap. The cost for all required technology shall be included within the project cost.
- Science floor mission should fit within a small flagship-class cost of $1.5–2B.
- Architecture definition:
  - Baseline Mission: Orbiter + Lander + Aerial Vehicle
  - Descopes in order:
    - Orbiter + 2 Landers
    - Orbiter + Lander
    - Science floor: Orbiter
- Science floor mission should be contributed by NASA only.
- TE mission shall provide option for international vehicle and/or instrument contributions at a later date (ground rules preclude international contribution in this study).
- Launch window shall be 2015–2022.
- Planetary protection requirements shall be met.

Additional key driving requirements include:

- Science instrument accommodation
- Robust margins, including JPL design principles of 43% above current best estimate (CBE) for total of contingency and margin
- 14-year radioisotope power source (RPS) qualification life
- All three vehicles (Orbiter, Lander, Aerial Vehicle) require atmospheric entry in the hypersonic continuum regime

4.2.3 Key Features

Key features and benefits of the TE mission are listed in Fig. 4-1.

4.3 Mission Design and Navigation

Key driving requirements for the mission design and navigation, flowed down from or in addition to those in Section 4.2.2, include:

Cruise

- Launch opportunities every 1–2 years
- Launch on Atlas V 551
- Launch period 21 days
- 3–4 year on-orbit science phase
- Trip time < 10–11 years
- Maximized mass to Titan
- TE will meet a 1×10^{-6} probability of Earth entry over the period from launch to launch + 100 years (Note the baseline mission includes Earth flyby distances greater than the Cassini Earth flyby distance of 1171 km. Trajectories for backup launch dates must be evaluated. Flyby distance is a derived requirement and must be evaluated in context with the overall mission design and flight system, which is recommended for future work in Section 4.12.1)
- Titan relative approach velocity less than ~7 km/s
- Approach sequence to facilitate critical event coverage for aerocapture, entry, descent, and landing (EDL), and entry, descent, and deployment (EDD)

Navigation

- Navigated Orbiter aerocapture entry flight path angle dispersions ≤0.93° 3-σ
- Navigated Lander entry flight path angle dispersions to enable 3-σ landing footprint within Belet dune region.

Feature	Benefit
Chemical propulsion trajectory	Lowest cost – saves $100M compared with solar electric propulsion (SEP); high mass delivery.
Launch opportunity every 1–2 years	Robust to programmatic changes in schedule.
Aerocapture	Enables TE science requirements to be met.
3 vehicles, instrument accommodations met on each	Complementary science for each vehicle provides total science greater than the sum of individual vehicles.
Individual vehicles and/or instruments	Readily facilitates participation of multiple organizations; provides multiple descope options.
Maximum use of Advanced Stirling Radioisotope Generators (ASRGs), minimal use of Multi-Mission Radioisotope Thermoelectric Generator (MMRTGs)	Reduces nuclear power source requirements; Lower heat output and lower mass and higher power compared to MMRTG
70-m equivalent Ka-band Deep Space Network (DSN) capability per study guidelines	Minimizes onboard requirements (high-gain antenna [HGA] size, comm power); Minimizes DSN time for same science; meets guideline
8 h/day DSN nominal track	Does not overstress DSN resources, meets guideline
Orbiter provides relay for Lander, Aerial Vehicle	Maximizes data downlink from in situ vehicles, provides critical event EDL, EDD coverage

Figure 4-1. Titan Explorer features provide multiple benefits.

Orbit

- Near-polar, circular orbit for global Titan science
- Circular orbit to facilitate science mapping campaigns
- Orbit altitude to minimize station keeping ΔV
- Solar beta angle < 45° for at least 1 year for spectral mapping
- Precessing orbit to provide latitude variability for radio occultation measurements
- Aerosampling to 800–900 km with maximum latitude, time of day, seasonal coverage within constraints of other science objectives and mission constraints

The TE mission design represents a robust result of an extensive launch opportunity search in the 2015–2022 timeframe defined by the study guidelines. Both chemical propulsion/ballistic and solar electric propulsion (SEP) options were examined with a downselection to chemical propulsion as described in Section 3. The chemical propulsion options analyzed start with a ballistic trajectory that exploits multiple flybys to both lower the launch energy requirements and to maximize the mass delivered to Titan while meeting entry speed requirements for the Orbiter, Lander, and Aerial Vehicle. The ballistic options analyzed require a chemical propulsion system to perform both trajectory correction maneuvers (TCMs) and deep space maneuvers (DSMs). The DSMs provide launch periods of at least 21 days while maximizing delivered mass to Titan.

The TE mission also employs three other innovative features that exploit the Titan environment. The first is the use of the atmosphere for aerocapture of the Orbiter, as described in Section 3 and in Section 4.6.5. The second is the use of the Saturn perturbation in conjunction with the Sun's motion to tailor the rate of change of the orbit plane-to-Sun geometry. This enables occultation and atmospheric science as a function of local true solar times. The third innovation is aerosampling. The aerosampling approach uses the combined atmospheric drag at periapsis altitudes (800–1200 km) and the Saturn perturbation effect to minimize the ΔV required for the aerosampling phases, as discussed further in Section 4.3.5.1.

4.3.1 Launch Requirements

The baseline TE mission is launched from Cape Canaveral, FL, on an Atlas 551 in September 2018. All three vehicles (Orbiter, Lander, and Aerial Vehicle) are integrated to the TE Cruise Stage and Adapter and launched together on a single launch vehicle. The selected mission design, developed by JPL, is a Venus-Venus-Earth-Earth (VVEE) trajectory design with a DSM allocation providing a 27-day launch period. The 27-day launch period opens Sept. 4, 2018, and closes Sept. 30, 2018, as shown in Fig. 4-2. Each trajectory arrives at Titan on Jan. 2, 2028, after a 9.3-year flight time, with effectively identical arrival geometries.

The vehicle stack (Orbiter, Lander, Aerial Vehicle, Cruise Stage, Adapter) is designed to a launch mass allocation of 4870 kg and a DSM allocation of 120 m/s. (Mass allocations for each of the vehicles in the vehicle stack are shown later, in Foldout 4-3C.) As shown in Fig. 4-3, for the required 21-day launch period closing on Sept. 24, 2018, the minimum launch capability is 5030 kg with a 120 m/s maximum DSM, providing 160 kg of launch capability above the launch mass allocation. Of the 160 kg available, 50–60 kg is allocated to accommodate declinations of launch asymptote (DLAs) up to −36°, resulting in 100 kg of unallocated mass margin. Alternative interplanetary trajectories with greater or equal Saturn delivery-mass capability, in comparison with the TE baseline, are available every 1–2 years in the 2015–2022 timeframe, as discussed in Section 6.

4.3.2 Cruise Trajectory

The cruise trajectory utilizes a VVEE flyby sequence to arrive at the Saturn/Titan system. (See Foldout 4-1A.) The gravitational assist flyby distances and times of flight are shown in Fig. 4-3. The ΔV budget for the mission cruise is shown in Foldout 4-1C.

Launch Date	Launch C_3 (km^2/s^2)	Launch DLA (deg)	Launch Mass (kg)	DSM (m/s)
9/4	12.1	–36	5100	120
9/5	12.0	–36	5110	120
9/6	12.0	–35	5110	120
9/7	11.9	–36	5120	120
9/8	11.8	–35	5130	120
9/9	11.8	–35	5130	120
9/10	11.8	–35	5130	120
9/11	11.7	–35	5140	120
9/12	11.7	–35	5140	120
9/13	11.7	–35	5140	120
9/14	11.7	–35	5140	120
9/15	11.7	–35	5140	120
9/16	11.8	–35	5130	120
9/17	11.8	–35	5130	120
9/18	11.9	–35	5120	120
9/19	12.2	–35	5095	120
9/20	12.2	–35	5095	120
9/21	12.3	–35	5085	120
9/22	12.5	–34	5065	120
9/23	12.7	–34	5045	120
9/24	12.9	–34	5030*	115
9/25	13.2	–34	5000	115
9/26	13.4	–34	4985	110
9/27	13.7	–34	4955	110
9/28	14.0	–34	4930	105
9/29	14.4	–33	4895	105
9/30	14.7	–33	4870	100

*21-day window launch mass capability.

Figure 4-2. The 27-day September 2018 launch period exceeds APL and JPL project practices.

Launch Date	Flyby Altitudes (km) V1, V2, E1, E2	Time of Flight for Each Flyby (years)
9/4	4408, 200, 3909, 4025	0.45, 1.59, 1.73, 5.73
9/5	4406, 200, 3909, 4025	0.44, 1.59, 1.73, 5.73
9/6	4405, 200, 3909, 4025	0.44, 1.58, 1.72, 5.72
9/7	4406, 200, 3909, 4025	0.44, 1.58, 1.72, 5.72
9/8	4407, 200, 3909, 4025	0.44, 1.58, 1.72, 5.72
9/9	4409, 200, 3909, 4025	0.43, 1.57, 1.71, 5.71
9/10	4417, 200, 3909, 4025	0.43, 1.57, 1.71, 5.71
9/11	4424, 200, 3909, 4025	0.43, 1.57, 1.71, 5.71
9/12	4408, 1056, 3818, 4010	0.42, 1.56, 1.71, 5.71
9/13	4440, 200, 3910, 4025	0.42, 1.56, 1.70, 5.70
9/14	4450, 200, 3910, 4025	0.42, 1.56, 1.70, 5.70
9/15	4461, 200, 3910, 4025	0.42, 1.56, 1.70, 5.70
9/16	4472, 200, 3910, 4025	0.42, 1.56, 1.70, 5.70
9/17	4408, 200, 3909, 4025	0.45, 1.59, 1.73, 5.73
9/18	4406, 200, 3909, 4025	0.44, 1.59, 1.73, 5.73
9/19	4405, 200, 3909, 4025	0.44, 1.58, 1.72, 5.72
9/20	4406, 200, 3909, 4025	0.44, 1.58, 1.72, 5.72
9/21	4407, 200, 3909, 4025	0.44, 1.58, 1.72, 5.72
9/22	4409, 200, 3909, 4025	0.43, 1.57, 1.71, 5.71
9/23	4417, 200, 3909, 4025	0.43, 1.57, 1.71, 5.71
9/24	4424, 200, 3909, 4025	0.43, 1.57, 1.71, 5.71
9/25	4408, 1056, 3818, 4010	0.42, 1.56, 1.71, 5.71
9/26	4440, 200, 3910, 4025	0.42, 1.56, 1.70, 5.70
9/27	4450, 200, 3910, 4025	0.42, 1.56, 1.70, 5.70
9/28	4461, 200, 3910, 4025	0.42, 1.56, 1.70, 5.70
9/29	4472, 200, 3910, 4025	0.42, 1.56, 1.70, 5.70
9/30	4408, 200, 3909, 4025	0.45, 1.59, 1.73, 5.73

Figure 4-3. TE flyby distances and times of flight are low risk.

FOLDOUT 4-1: Mission Design 1

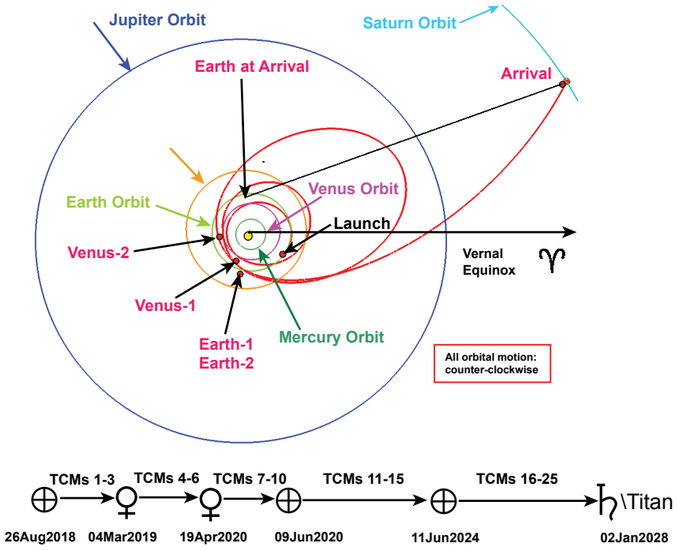

(A) 9.3-year ballistic cruise delivers maximum mass to Titan with launch opportunities every 1-2 years.

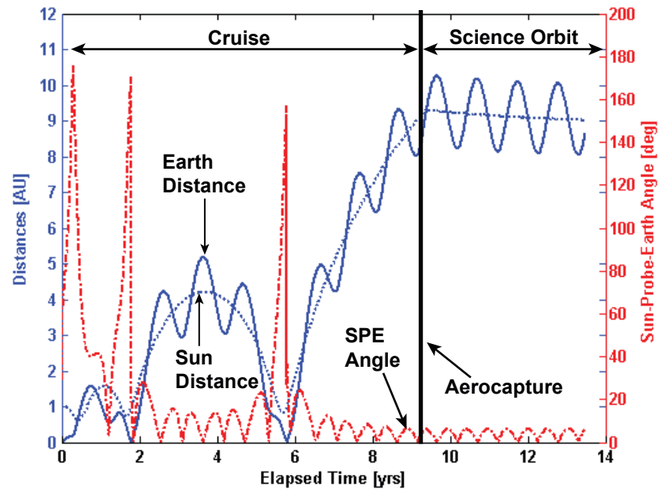

(B) TE flight system designed for range of Earth and Sun distances and SPE angles.

Maneuver/Event	ΔV (m/s)
Launch Injection Correction	30
Earth Flyby Biasing	50
Deep Space Maneuver	120
Other Cruise Statistical	20
Aerial Vehicle Targeting Maneuver	10
Orbiter Entry Targeting Maneuver	45
Targeting Maneuver Cleanups	5
Maneuver Delay Reserve	30
TOTAL (CBE)	310
Margin	31
TOTAL with Margin	341

(C) ΔV budget accounts for maximum ΔV required across 27-day launch period and includes robust margin for all maneuvers.

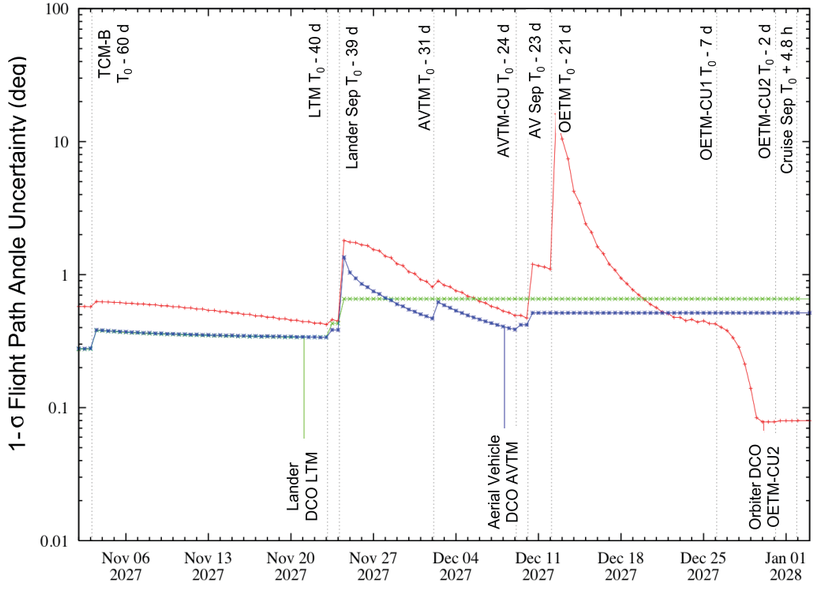

(D) Navigation delivery enables robust aerocapture with significant margin, and delivery to Belet dune region with landing footprint well within targeted terrain.

Earth-S/C Range	3 AU		10.4 AU	
Link	Cruise Stage DTE (X-Band MGA)	Cruise Stage DTE (X-Band HGA)	Cruise Stage DTE (X-Band MGA)	Cruise Stage DTE (X-Band HGA)
Gnd Antenna	70 m Equiv.	70 m Equiv.	70 m Equiv.	70 m Equiv.
Gnd RF Power	20 kW	20 kW	20 kW	20 kW
Gnd Coding	None	None	None	None
Orb. Antenna	Fanbeam MGA (12 dBi @ +/-45 ˚)	0.5m HGA (30.3 dBi @ 8.4)	Fanbeam MGA (15 dBi @ peak)	0.5m HGA (30.3 dBi @ 8.4)
Orb. RF Power	35 W	35 W	35 W	35 W
Orb. Coding	Rate 1/6 Turbo	Rate 1/6 Turbo	Rate 1/6 Turbo	Rate 1/6 Turbo
Uplink Data Rate	**100 bps** (20˚ EL)	**5 kbps** (20˚ EL)	**15 bps** (20˚ EL)	**400 bps** (20˚ EL)
Downlink Data Rate	**100 bps** (20˚ EL)	**12 kbps** (20˚ EL)	**10 bps** (20˚ EL)	**1 kbps** (20˚ EL)

- All DTE links assume 3dB S/C passive loss
- Downlink margin is 3dB to FER=10-4, Uplink margin is 6dB to BER=10-6

(E) Communication system is designed to accommodate the full range of Earth–spacecraft distances throughout cruise.

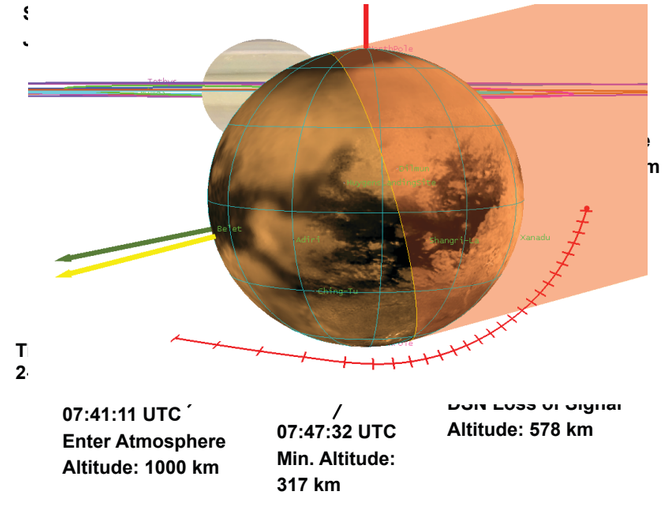

(F) Orbiter is within view of Earth 54% of Titan aerocapture and during all of the active guidance phase, including the minimum altitude.

07-01121-14

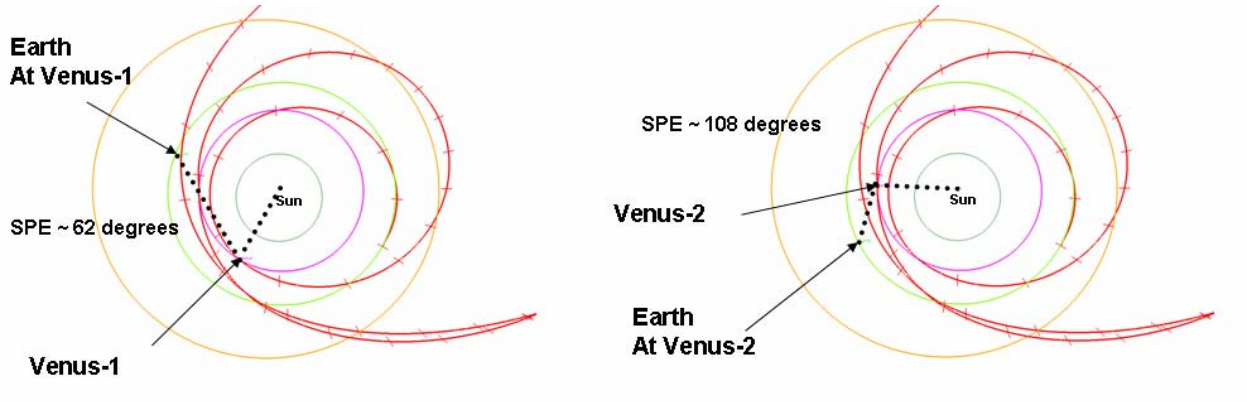

Figure 4-4. Venus Flyby Geometry: 30-day time ticks.

The two Venus flyby geometries allow tracking of the spacecraft by the DSN. Fig. 4-4 shows the Sun-Probe-Earth (SPE) angles for the two encounters, approximately 62° and 108°.

4.3.3 Titan Approach

Detailed event sequences near approach are provided in Foldout 4-1D. A simplified version highlighting the timing of vehicle separations from the Cruise Stage and atmospheric entry are included in Fig. 4-5.

4.3.4 Navigation

To verify that the three vehicles can be delivered with sufficient accuracy, a covariance study was conducted by JPL to assess the navigation uncertainties. Fig. 4-6 lists the assumptions for this analysis, intended to be reasonable but somewhat conservative. In this study, the principle sources of error (in decreasing significance) were found to be separation ΔV uncertainty, release time from entry (for Lander and Aerial Vehicle), targeting maneuver execution errors (for the Orbiter and Aerial Vehicle), and the radiotracking schedule.

Fig. 4-7 lists the entry flight path angle uncertainties at the 1700-km interface altitude for each vehicle. Foldout 4-1D shows the 1-σ uncertainty as a function of the tracking data and sources of error. The 3-σ errors for the Lander and the Aerial Vehicle in Fig. 4-7 compare favorably to the Huygens uncertainty of 2.4º 3-σ. The TE Orbiter results also compare favorably to

Titan Approach Sequence of Events
Lander separates (w/ radiator system) from Orbiter/Cruise Stage 39 days prior to Orbiter entry.
Aerial Vehicle separates (w/ radiator system) from Orbiter/Cruise Stage 23 days prior to Orbiter entry.
Titan arrival: 2 Jan 2028
Lander, Aerial Vehicle separate from radiator systems 10 min. prior to entry interfaces.
Lander enters 4 h 50 min prior to Orbiter separation from cruise stage.
Aerial Vehicle enters 3 h 50 min prior to Orbiter separation from Cruise Stage.
Lander and Aerial Vehicle complete EDL and EDD.
Orbiter/Cruise Stage provides EDL, EDD critical event coverage.
Orbiter separates from Cruise Stage 10 min. prior to Orbiter entry.
Orbiter completes aerocapture.
Orbiter completes aeroshell separation.
Orbiter completes periapsis raise maneuver.
Orbiter begins aerosampling phase.

Figure 4-5. Titan approach sequence provides required navigation accuracy and schedule margin.

Radiometric 2-way X-band Doppler and range • 3 passes/week up to 150 days before entry • 1 pass/day from 150 days before to 70 days before entry • 3 passes/day from 70 days before entry to entry
No optical navigation
No very long baseline interferometry (VLBI)
Separation ΔV error from Cassini/Huygens, scaled to mass ratios of vehicles
De-tumble ΔV error 50 mm/s spherical
2% ΔV error on deterministic maneuvers
5 mm/s spherical error on statistical maneuvers
Saturn & Titan ephemeris errors mapped from current Cassini estimates to 2028 and scaled by 10
Stochastic accelerations (8-h batches, spherical white noise, scaled to vehicle mass)
Consider errors: media, station location, ut1 and polar motion errors

Figure 4-6. TE navigation modeling assumptions are conservative.

	1-σ Errors	3-σ Errors
Lander	0.66º	1.98º
Aerial Vehicle	0.52º	1.56º
Orbiter	0.08º	0.24º

Figure 4-7. Entry flight path angle uncertainty (1700-km interface) meets aerocapture and landing requirements.

the 0.93º 3-σ results for the orbiter from the 2002 NASA Titan Aerocapture Systems Analysis Team (ASAT) study (Lockwood et al., 2006), meeting the TE mission requirements.

Monte Carlo simulations using the above navigated delivery errors for the Orbiter aerocapture and Lander EDL (Sections 4.6.5 and 4.7.5.3) show successful aerocapture and successful landing in the Belet region. Note that changing the order of the Lander and Aerial Vehicle separations would further reduce the Lander's entry flight path angle uncertainty and footprint.

4.3.5 Science Orbit

4.3.5.1 Aerosampling Orbit Design

The Titan aerosampling design, developed by NASA LaRC, is composed of two phases with the 3.3-year circular orbit design separating the phases. Aerosampling Phase 1 begins immediately after the Orbiter aerocapture and propulsive cleanup into a 1650 × 1170-km elliptical orbit. The Orbiter periapsis precesses from lower southern latitudes towards the equator, as shown in Section 4.6, Foldout 4-5C, achieving periapsis densities within 0.2 and 0.8 kg/km^3. Periapsis altitudes of 1000 to 1200 km are sampled during Phase 1, allowing for a broad spectrum of scientific analyses of these atmospheric levels. Because the orbit orientation relative to Saturn results in a naturally increasing apoapsis altitude, Phase I is designed to begin aerosampling at 1650 km in apoapsis altitude such that a 1700-km apoapsis, required for the circular orbit phase, is achieved in ~60 days with no propulsive maneuver for apoapsis correction. In 60 days, when the apoapsis altitude has reached 1700 km, a 63 m/s propulsive maneuver is made at apoapsis to raise periapsis to 1700 km, circularizing the orbit.

After the circular orbit phase, a second aerosampling phase begins, sampling northern latitudes not studied during Phase 1. Phase 2 lasts 177 days and requires two periapsis raise propulsive maneuvers during the aerosampling phase with a total of 45 m/s to extend the latitude coverage. During Phase 2, 40° of northern latitudes are sampled as shown in Foldout 4-5C. The maximum den-

sity is ~5 kg/km^3. The maximum aeroheating on the spacecraft is 1.5×10^{-3} W/cm^2, and the maximum dynamic pressure is 7.5×10^{-3} N/m^2, ~2 orders of magnitude less than that for the Mars Reconnaissance Orbiter (MRO) aerobraking mission.

4.3.5.2 Circular Orbit Design

The nominal circular orbit science phase has a duration of 3.3 years. During this period, the selected science orbit evolves under the dynamical environment of the Titan–Saturn system while meeting all science requirements. The NASA Cassini mission flybys have helped to characterize Titan's gravity field. (A degree 2 and order 2 field is used in this study. [Tortora et al., 2006]) Like the Earth's Moon, Titan orbits in synchronous motion, with a rotational and orbit period of ~15.95 days. Orbits in the vicinity of Titan have a strong third-body perturbation from Saturn. As a result, at altitudes that avoid atmospheric drag, Saturn is the dominant perturbation. In this analysis a conservative altitude of 1700 km is used to minimize station-keeping ΔV on the basis of an orbit analysis with TitanGRAM (Justus and Duvall, 2003) completed during the 2002 Titan ASAT study (Lockwood et al., 2006). As further analyses are completed and TitanGRAM further refined with Cassini data, an option to reduce the orbital altitude without an increase in station-keeping ΔV may be available.

As shown in Fig. 4-8, as inclination increases from 0° to 90°, the orbital lifetimes decrease (for small values of eccentricity). Although low-inclination orbits reduce station keeping, the requirement for global observations to include the interesting Titan poles precludes their use.

Another effect of the Saturn perturbation is to cause a westward precession of the orbit plane (ascending node precession), which affects the rate of change of the solar beta angle. (The solar beta angle is defined as the signed angle of the vector to the Sun relative to the orbital plane, as illustrated in Foldout 4-2B. The signed angle is positive when the vector to the Sun is in the di-

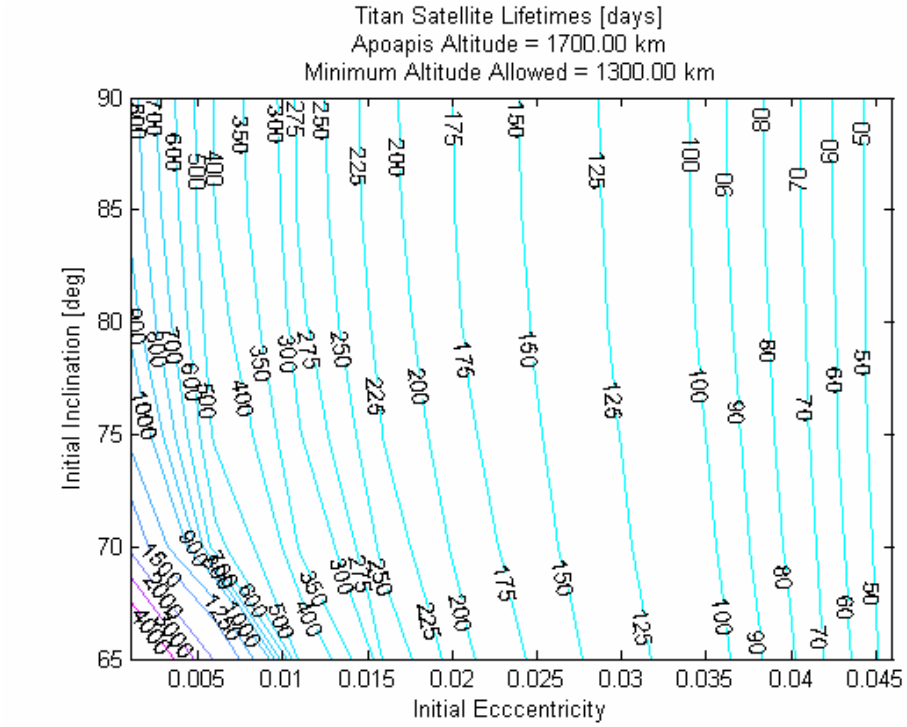

Figure 4-8. Lifetime computations result in reasonable station-keeping requirements.

rection of the orbit normal.) Solar beta rates for different inclinations are displayed in Fig. 4-9, and the angle history for the nominal mission is shown in Foldout 4-2B.[1] To understand the solar beta angle evolution note that (1) the orbit has an 85° inclination, (2) Titan is in orbit close to Saturn's equatorial plane, and (3) Saturn's equator is inclined ~26.73° relative to its orbital plane. In addition to considering the orbit plane orientation desired for science, careful selection of the initial orbit plane orientation is needed to avoid high entry speeds for the Orbiter, Lander, and Aerial Vehicle. Frozen (fixed periapsis location, fixed eccentricity) elliptical orbits have been found at Titan. However, these elliptical frozen orbits have very high apoapsis altitudes and are not favorable for the TE mission science.

The nominal science orbit balances orbit maintenance complexity and science requirements. To minimize and avoid drag effects, the altitude is maintained at 1700 km. For global coverage that includes the poles, and to enable orbit precession, the orbit inclination is selected at 85° relative to the Titan equator. To provide a stable altitude-rate platform for radar/altimeter science, the orbit is selected as near-circular. Station keeping is performed every 100 days. Without station keeping, the Orbiter will enter the Titan atmosphere in about 800–900 days. The orbit selection is summarized in Foldout 4-2A. The ΔV budget for the Orbiter is shown in Foldout 4-2H.

4.3.5.3 Relay Geometry

The Orbiter-to-Lander link is available twice during Titan's 15.95-day rotational period. At a 1700-km altitude, periods of Orbiter–Lander contact occur when the orbit plane-to-Lander longitude angle is less than about 40° with a 20° elevation constraint (e.g., a dune obstruction). The contact period lasts ~3 days and is followed by 5 days of blackout, as shown in Foldout 4-2E.

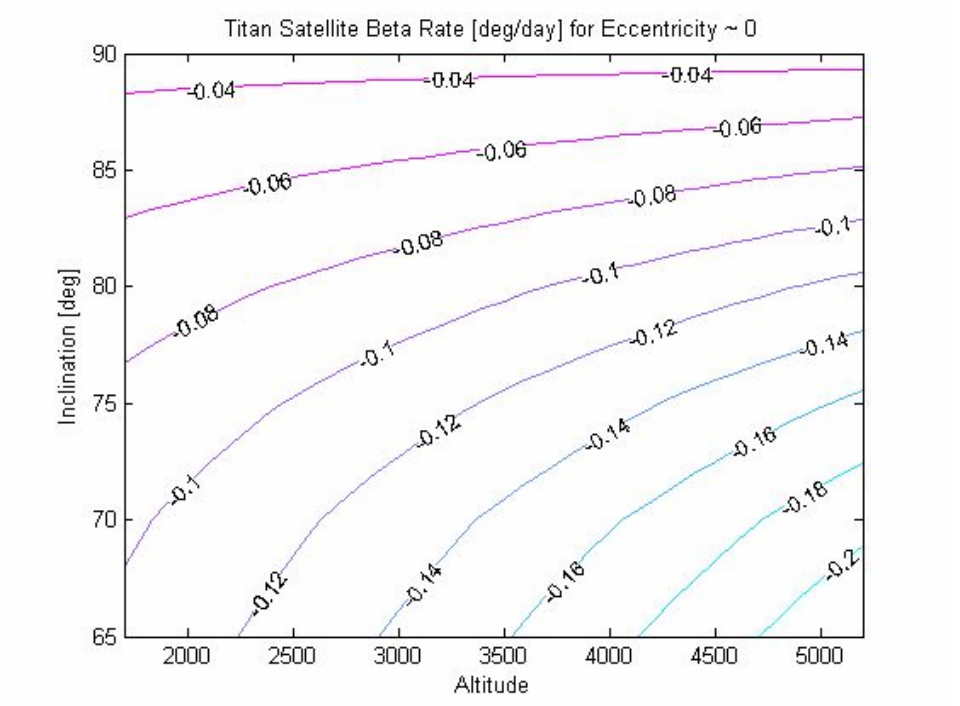

Figure 4-9. Solar beta angle rates.

[1] The Saturn non-spherical gravity field has a small effect on the beta angle evolution, but preliminary propagations using a Saturn field of degree 6 and order 0 show small differences (on the order of 10^{-3}°/day).

FOLDOUT 4-2: Mission Design 2

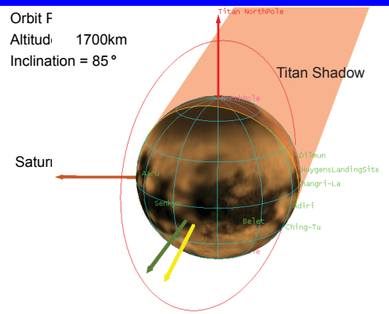

(A) Titan orbit provides global coverage.

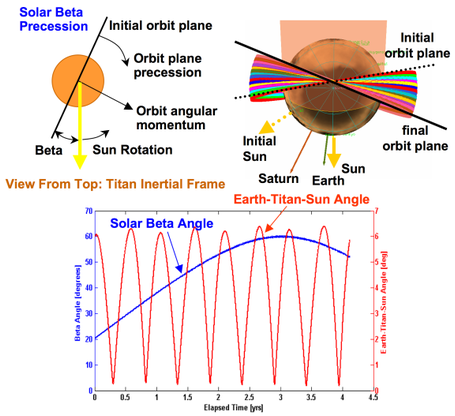

(B) Titan orbit initial beta provides lighting for spectral mapping, and beta precession enables multi-latitude occultation data.

Link	Orbiter DTE Ka-Band	Orbiter DTE X-Band	Orbiter DTE X-Band (Em. Mode)
Earth-S/C Range	10.4 AU	10.4 AU	10.4 AU
Gnd Antenna	70 m Equiv.	70 m Equiv.	70 m Equiv.
Gnd RF Power	N/A	20 kW	20 kW
Gnd Coding	N/A	None	None
Orb. Antenna	3m HGA (57.5 dBi @ 32)	3m HGA (45.8 dBi @ 8.4)	MGA Horn (17 dBi @ 8.4)
Orb. RF Power	35 W	35 W	35 W
Orb. Coding	Rate 1/6 Turbo	Rate 1/6 Turbo	Rate 1/6 Turbo
Uplink Data Rate	N/A	**15 kbps** (20° EL)	**20 bps** (6° EL)
Downlink Data Rate	**140 kbps** (20° EL) 237 kbps @8AU	**35 kbps** (20° EL)	**10 bps** (6° EL)

- All DTE links assume 3dB S/C passive loss
- Downlink margin is 3dB to FER=10-4, Uplink margin is 6dB to BER=10-6
- Ka-Band link calc. to 34m BWG for nom. weather (CD=0.9, 30mph wind), scaled to 70m by (702/342)
- 3m HGA pointing 0.05, using a monopulse tracking receiver (-0.7dB ptg. loss at Ka-Band)

(C) Orbiter communication system design provides a mission average science data downlink of >100 kbps CBE (>159 kbps with margin included).

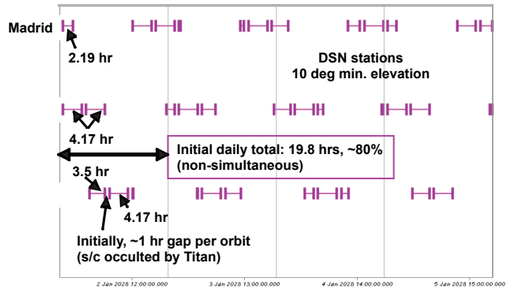

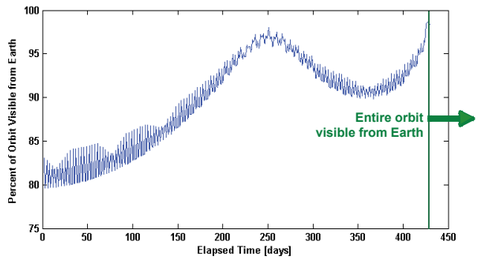

(D) Downlink is possible for >80% of DSN contact time.

Lander-to-Orbiter Access Times
- 20° minimum elevation at lander
- ~ 5 day blackout every 8 days, as Titan rotates under orbiter
- ~33% longer access time for aerial vehicle to orbiter

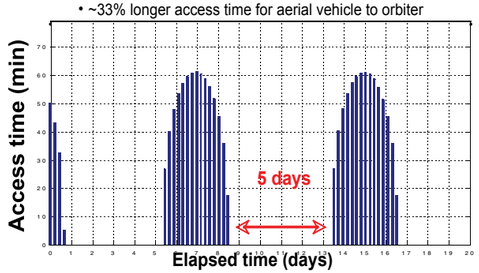

(E) Lander designed to relay Lander science to Orbiter during 3-day access times every 8 days.

Link	Lander Relay UHF	Lander Relay X-Band (0.5m HGA to LGA)	Lander Relay X-Band (LGA to 3m HGA)	Lander DTE X-Band (0.5m to 70m)
Orb. (or Gnd) Antenna	>+0 dBi	Hemi LGA (4 dBi at 35deg)	3m HGA (44.5 dBi)	70 m Equiv.
Orb. (or Gnd) RF Power	8.5 W	N/A	N/A	20 kW
Orb. (or Gnd) Coding	Rate ½ Conv.	N/A	N/A	None
Lander Antenna	Hemi (-3 dBi at edge)	0.5m HGA (30.3 dBi)	Hemi (0 dBi at 70deg)	0.5m HGA (30.3 dBi @ 8.4)
Lander RF Power	8.5 W	15 W	15 W	15 W
Lander Coding	Rate ½ Conv.	Rate ½ Conv.	Rate ½ Conv.	Rate 1/6 Turbo
Forward Data Rate	**2 kbps (5° EL) 4 kbps (20° EL) >8 kbps (90° EL)**	N/A	N/A	**500 bps (20° EL)**
Return Data Rate	**2 kbps (5° EL) 4 kbps (20° EL) >8 kbps (90° EL)**	**32 kbps (20° EL) >128 kbps (90° EL)**	**512 kbps (20° EL)**	**250 bps (20° EL Gnd) (62.5 bps w/Conv.)**

(F) Lander communication system provides several relay options to the Orbiter and a backup direct-to-Earth capability.

Link	AV Relay UHF	AV DTE X-Band (MGA to 70m)
Orb. (or Gnd) Antenna	>+0 dBi	70m Equiv.
Orb. (or Gnd) RF Power	8.5 W	20 kW
Orb. (or Gnd) Coding	Rate 1/2 Conv.	None
AV Antenna	Hemi (-3 dBi at edge)	MGA (16.5 dBi)
AV RF Power	5.5 W	5.5 W
AV Coding	Rate 1/2Conv.	N/A
Forward Data Rate	**2 kbps (5° EL) 4 kbps (20° EL) >8 kbps (90° EL)**	**Carrier Only**
Return Data Rate	**1-2 kbps (5° EL) 2-4 kbps (20° EL) >4-8 kbps (90° EL)**	**Carrier Only**

(G) Aerial Vehicle communication system is simple and meets the science downlink requirements via relay to the Orbiter.

Maneuver/Event	ΔV [m/s]
Aerocapture ACS	20.0
Aeroshell Separation	
3-σ Periapsis Raise & Apoapsis Correction to First Aerosampling Phase (1170km x 1650km)	120.0
Phase I Aerosampling, Circularization	63.0
Science Orbit Stationkeeping (wheel desat) 4yr	17.0
Periapsis Lower to 900x1700km	79.0
Phase II Aerosampling	45.0
Margin (includes 10% on all ΔV plus 30m/sec for potential aerosampling uncertainties)	64.4
TOTAL	408.4

(H) Orbiter ΔV budget includes 3-σ aerocapture ΔV and robust margins on all maneuvers.

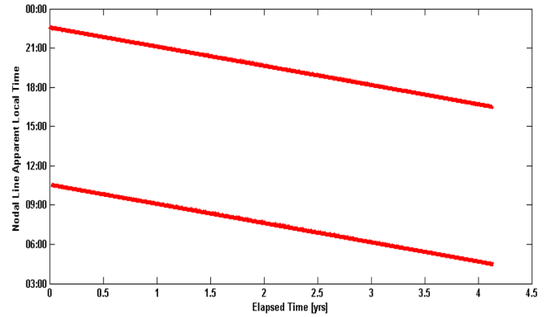

(I) Orbit design provides changes in local true solar time meeting science requirements.

Feature	Attribute	Benefit
Launch Period	27-day launch period	High probability of launch
Launch Site	Cape Canaveral	Launch infrastructure in place
Launch Vehicle	Atlas 551	Atlas V family, New Horizons launch vehicle (team familiar with rocket)
Launch Energy (C_3)	< 15 km^2/s^2	Great mass performance
Declination of Launch Asymptote (DLA)	> -36 deg	Well within Cape range limits
Gravitational Assists	Venus, Venus, Earth, Earth	Planets previously used for flybys
Aerocapture	Saves > 4 km/s	Enables orbiter science, relay
Aerocapture Geometry	54% of the event DSN observable	Critical event coverage, including minimum altitude

(J) TE has a robust mission design.

07-01121-15

Each day during the visibility period, the Orbiter passes overhead 4–5 times and is in view of the Lander for 5 to 61 min. during each overhead pass. The relay time available is ~731 min every 8 days. The Orbiter-to-Aerial Vehicle times are ~33% longer, as the Aerial Vehicle's view of the Orbiter is not constrained by terrain. In this case a 5° elevation constraint is used. The effect of Aerial Vehicle drift with the winds will cause changes in contact period timing.

4.3.6 Communications

The mission communications architecture uses the Orbiter as the primary path for science data return, with a UHF relay service providing links to both the Lander and Aerial Vehicle once the vehicles reach Titan. The Lander and Aerial Vehicle each have an additional direct-to-Earth (DTE) capability realized through X-band add-ons to the UHF relay transceivers, as described in Section 4.7.7.4 and 4.8.7.5, respectively.

All communications during cruise are achieved through the Orbiter using antennas mounted to the Cruise Stage structure. Umbilical connections between the Orbiter and the two other vehicles within their aeroshells enable telemetry and command links to the Lander and Aerial Vehicle during cruise.

At Titan, the Orbiter's 3-m gimbaled high gain antenna (HGA) provides the primary DTE communication path for the mission. It provides data rates exceeding 200 kbps at closest Earth–Titan range, as shown in Foldout 4-2C. The equivalent of a 70-m DSN ground station is assumed as the primary downlink receive capability at Ka-band. An X-band capability is utilized for lower-rate downlink, for emergency uplinks and downlinks during orbit operations, and to support communications throughout cruise. A monopulse system is used to precisely point the HGA for power-efficient, high-data-rate Ka-band downlink operation. With monopulse, the uplink signal is used to achieve HGA pointing accuracies better than the required 0.05°. To maximize data downlink during the 8-hour DSN track time, the Orbiter downlinks data open-loop in Ka-band while waiting for the uplink signal from ground to initiate monopulse. Open-loop data rates are half that of the monopulse Ka-band rates, as a result of the reduced HGA pointing accuracy of 0.1° and corresponding ~3-dB pointing loss. Given the mission average round trip light time of ~2.5 hours, open-loop Ka-band downlink comprises ~31% of the 8-hour DSN track. Further monopulse trades and design work are recommended for the next study phase.

The secondary DTE path from the Lander is available using a gimbaled 0.5-m HGA, albeit at a much reduced data rate capability (250 bps at maximum range). This path also serves as an enhanced data rate relay capability to the Orbiter (32 to 128 kbps). The Aerial Vehicle is capable of emergency rate commanding and beacon downlink for vehicle aliveness, status, and tracking at high Earth elevations only. Emergency rate downlink telemetry (7 bps) may also be possible at favorable Earth elevation and range, relative to the Aerial Vehicle. Further details of the communication capabilities are available in the Sections on the Orbiter (4.6.7.2), Lander (4.7.7.4), and Aerial Vehicle (4.8.7.5). Figures summarizing the various links for the mission are available in Foldouts 4-1 and 4-2. The total science data volume returned for the mission is shown in Fig. 4-10.

Vehicle	Total Science Data Return from Mission (CBE)*
Orbiter	3.4 Tbits
Lander	5.5 Gbits (UHF); 36 Gbits (X, HGA)
Aerial Vehicle	4.6 Gbits

Science data volumes are the current best estimates. Margin on downlink rate is 30%; margin on downlink time is ≥ 18% above shown volumes.

Figure 4-10. Total mission science data volume return allows all science objectives to be satisfied.

4.3.7 DSN Infrastructure Usage

DSN is utilized for 8 hours per day with 70-m equivalent Ka-band downlink, per the study guideline, during the 4-year Orbiter science mission. With the initial edge-on orbit to the Sun/Earth direction, some of the orbit is occulted from the DSN stations.

Foldout 4-2D shows typical DSN to Orbiter access times for Madrid, Goldstone and Canberra. As the mission progresses and the orbit plane precesses, the amount of total available tracking access improves until the entire orbit can be seen from the Earth ~431 days after the initial insertion at Titan, as shown in Foldout 4-2D. In Foldout 4-2D the peak at 250 days occurs between Earth–Titan quadrature (approximately day 200) and Sun-Earth-Titan opposition (approximately day 300).

The solar conjunctions, while not marked, can be seen in the SPE angle plot of Foldout 4-1B. At X-band, successful data return is achieved down to SPE angles of at least 2.3°, and down to 1.0° at Ka-band. During the 4-year Orbiter science phase, there are 4 X-band conjunctions, ranging in duration from 1.5 to 4.3 days; and no Ka-band conjunctions.

4.3.8 Critical Event Coverage

The Venus flybys of the baseline trajectory allow tracking of the spacecraft before, during, and after the flybys as described in Section 4.3.2. All TCMs and DSMs are required to have DSN coverage. The Lander and Aerial Vehicle insertion are visible from the Earth and take place on the sunlit side of Titan. The DSN sees 54% of the Orbiter aerocapture, including the minimum altitude passage and all of the active guidance phase (see Foldout 4-1F). As Foldout 4-1B shows, the SPE angle at arrival is about 6°, or about 3 months before solar conjunction. Further detailed analyses of coverage for each critical event are required in future work.

4.4 Flight System Design and Development

Discussion of the flight system design and development approach for each vehicle, including use of new versus existing hardware and software and fault tolerance, is included within the following sections describing each vehicle: Cruise Stage, Section 4.5; Orbiter, Section 4.6; Lander, Section 4.7; and Aerial Vehicle, Section 4.8.

The manufacturer and flight heritage information provided assumes that the vehicle is being built today. This information is representative but we expected that the project will leverage additional advancements and flight heritage that occur between now and the TE project start.

For any space flight component with TRL < 6, technology development required to bring the level to TRL 6 by project PDR is described in Section 4.13. The technology costs are included in the total project cost.

The radiation environment for TE, including solar proton flux and gamma rays and neutrons emitted as secondary particles by the RPS, is 40 krad, assuming 100 mils of shielding in a finite slab geometry. The analysis includes 100% margin above a conservative estimate. Single event upsets can result from galactic cosmic rays, solar protons, and neutrons from the RPS. However, TE poses no single event effects challenges beyond those met by standard interplanetary missions already flying.

The thermal environment and design are discussed in Sections 4.5.3.3 (Cruise Stage), 4.6.7.5 (Orbiter), 4.7.7.3 (Lander), 4.8.7.3 (Aerial Vehicle), and in Section 4.13 (Technology Needs).

4.5 Cruise Stage Flight System

4.5.1 Cruise Stage Key Driving Requirements and Key Characteristics

Key driving requirements for the Cruise Stage, flowed down from the requirements in Section 4.2.2, include:

- Provide structural load path from launch adapter to three vehicles,
- Provide separation capability for three vehicles.
- Provide a propulsion system that supplies all cruise ΔV and attitude control.
- Provide cruise communication antennas.
- Provide cruise star trackers.
- Utilize Orbiter for all control and power.
- Keep mass within Cruise Stage allocation.

Key features and benefits of the Cruise Stage flight system are listed in Fig. 4-11. The TE launch configuration is shown in Foldout 4-3A. The Vehicle Assembly (Orbiter, Lander, Aerial Vehicle, Cruise Stage) and Cruise Stage are shown with components labeled in Foldout 4-3B.

4.5.2 Cruise Stage Mass Allocations and Margin

Foldout 4-3C summarizes the Orbiter, Lander, Aerial Vehicle, Cruise Stage, and Adapter mass allocations and shows mass margin at the system level.

4.5.3 Cruise Stage Subsystems

4.5.3.1 Structures and Mechanisms

The Cruise Stage structural design is based on an APL heritage truss structure design first developed and flown successfully on the Department of Defense Midcourse Space Experiment (MSX). The structure is well adapted to the design requirements for this mission. It provides ample volumetric capability to interface with the three vehicles (electrically, mechanically, and thermally) and with the launch vehicle separation systems. Preliminary accommodations have been favorably assessed for propulsion and other subsystem accommodations. The truss structure design consists of a series of graphite epoxy "I" beam elements joined with titanium end fittings and sized to carry loads appropriate to their location on the structure. Stiffening rings are designed into the structure to distribute the loads to both the Lander and the Aerial Vehicle, thus minimizing local loading into these elements. The Orbiter interface to the truss structure is via a

Feature	Benefit
Cruise Stage configuration	Enables launch of three vehicles. Minimizes interfaces between three vehicles. No penetrations in aeroshell heatshields.
Independent bi-prop propulsion system in Cruise Stage	Reduces coupling between Orbiter and cruise/stack design. Reduces uncertainty in Orbiter center of gravity prior to aerocapture due to variability in cruise fuel use.
Orbiter provides power and control of Vehicle Assembly	Reduces number of required Cruise Stage subsystems.
Active cooling during cruise with design based on Mars Science Laboratory (MSL)	Maintains temperature inside aeroshells within requirements; uses heritage design.
System designed to point Orbiter heatshield to Sun inside of 2 AU.	Reduces heat load and variability on vehicle radiators
Propulsive control for first 8.5 years; Orbiter wheels used last year of cruise.	Enables use of finer pointing accuracy during approach maneuvers. Reduces use of wheels to 5 years, well below their 15-year lifetime qualification limits.
Orbiter/Cruise Stage provides command and telemetry path from ground to all three vehicles.	Enables health monitoring and data upload to all three vehicles during cruise.

Figure 4-11. Cruise Stage features provide multiple benefits.

4-point separating interface. The Cruise Stage structure interfaces via a 4-point separation nut and push-off spring interface with the Atlas Launch Vehicle truss adapter. The Adapter is designed for the heavy lift variant of the Atlas V vehicle to reduce mass and meet specific mission requirements. The first flight of the Atlas truss adapter is expected this year. The Adapter has been favorably evaluated by Atlas for the Titan mission. The Titan payload mass and mass properties are well within the capability of the Adapter, as confirmed by Atlas.

Separation mechanisms for the Orbiter, Lander, and Cruise Stage are baselined as push-off spring and heritage separation nut mechanisms. Several spinning separation system designs are under evaluation for the Lander and Aerial Vehicle and are the subject of a future trade study.

4.5.3.2 Cruise Stage Propulsion

The Titan Cruise Stage propulsion subsystem is a pressure-regulated bipropellant system that provides ΔV, attitude control, and momentum-dumping capability. Pressure-regulated bipropellant systems of this size and type are well characterized, well understood, and have significant flight history. All components but the custom propellant and pressurant tanks have extensive flight heritage. Custom tanks are required to optimize mass and volume, and interfaces with the primary structure.

There are four identical, custom titanium propellant tanks (two for fuel and two for oxidizer) and one custom composite-overwrapped pressure vessel (COPV). Different propellant management devices (PMDs) will be developed for inside the two MMH and the two NTO tanks. Several flight-proven options exist for each component of the propulsion system; therefore, only the tanks require qualification testing, though allocation has been made for delta-qualification testing of some components.

The launch propellant load for the Cruise Stage is 570 kg. The custom titanium propellant tanks are 132.0 L (8057 in^3) each and designed for a maximum expected operating pressure (MEOP) of 2.07 MPa (300 psia). The custom pressurant tank is 73.2 L (4465 in^3) and rated for MEOP of 20.7 MPa (3000 psia).

The ΔV thrusters are the robust 110 N (25 lbf) Aerojet R-1E, currently used as part of the Space Shuttle attitude control system (ACS). The specific impulse is ~280 s. There are several bipropellant options in the ~9 N (2 lbf) range; however the AMPAC-ISP Leros LTT is selected for its significant heritage. A modest optimization/delta-qualification effort is included to ensure that all engine types selected operate stably within the operating conditions and in the mounting configuration required for this spacecraft.

The remaining components used to monitor and control the flow of propellant – latch valves, filters, orifices, check valves, pyro valves, pressure regulators, and pressure and temperature transducers – are selected in Phase A from a large catalog of components with substantial flight heritage on APL and other spacecraft.

The propulsion system supplier is put on contract 30 months prior to the start of spacecraft integration and test (I&T) to ensure optimum communication between the propulsion team and the spacecraft mechanical design team. This schedule allows time for tank qualification, which typically requires 24 months. The primary spacecraft structure must ship to the propulsion system supplier 3 months before the start of I&T.

FOLDOUT 4-3: Cruise Stage

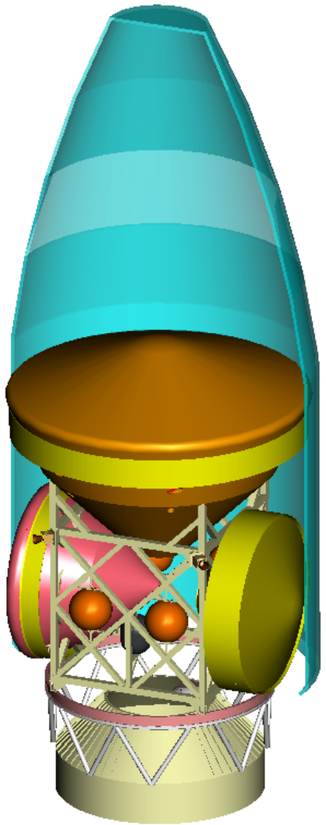

(A) Orbiter, Lander, Aerial Vehicle package in Atlas V 551 5-m fairing.

Vehicle Assembly

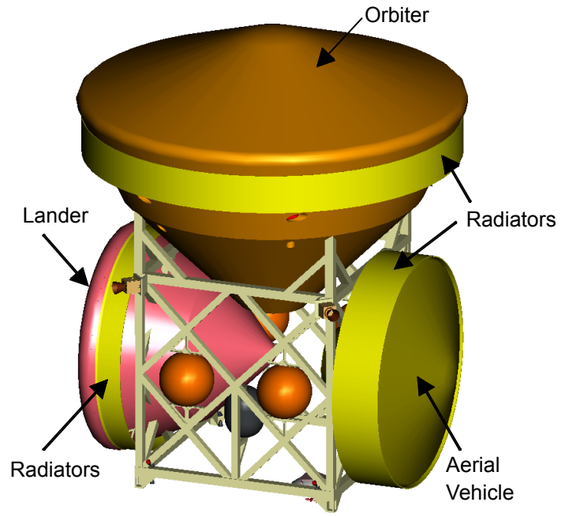

Cruise Stage

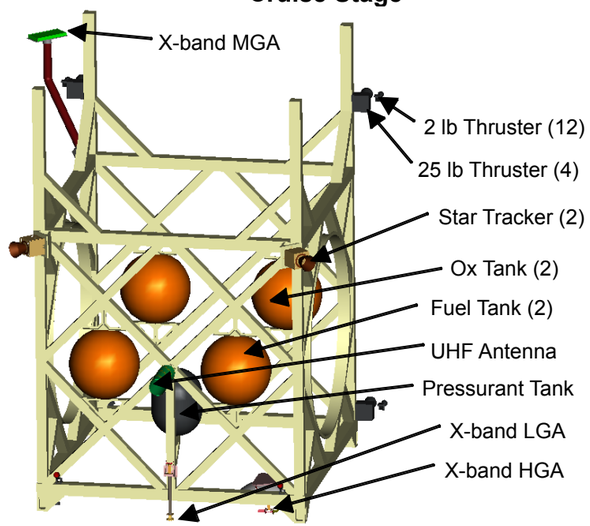

(B) Cruise Stage design enables delivery of three vehicles to Titan and minimizes design interfaces between the three vehicles.

Mass (kg)	CBE (kg)	CBE + Contin (kg)
Orbiter Dry Mass	1160	1349
Lander Mass	640	755
Aerial Vehicle Mass	418	499
Cruise Stage Dry Mass	593	698
Adapter	100	120
Launch Dry Mass	2911	(17.5%) 3421
Propellant		767
Launch Wet Mass		4188
System Margin	19.9%	682
S/C Dry Mass Alloc		4103
Launch Allocation		4870
Launch Capability*	Atlas V 551	4970

Mass (kg)	Dry Mass Allocation	Propellant	Allocation
Orbiter	1613	197	1810
Lander	897	0	897
Aerial Vehicle	588	0	588
Cruise Stage	849	570	1419
Launch Adapter	143	0	143
Unallocated	13	0	13
Total	4103	767	4870

*Adjusted from 5030kg, allocated 60kg to DLA; provides additional 100kg capability above system margin

(C) Total mass of the Orbiter, Lander, Aerial Vehicle and Cruise Stage is well within the minimum launch allocation mass with robust margins.

4.5.3.3 Cruise Stage Thermal

The thermal design for each vehicle: Orbiter, Lander, Aerial Vehicle, and Cruise Stage, is tailored for that vehicle's thermal requirements. Since all three primary vehicles use RPS power sources contained within aeroshells, the Mars Science Laboratory (MSL) heritage mechanical pump loop cooling systems connected to space-facing heat pipe radiator panels is leveraged. The cruise Sun attitude is constrained within 2 AU to keep all vehicle radiator panels in complete shadow relative to the Sun. The Orbiter's primary thermal protection system (TPS) is used as a sunshield, keeping all critical thermal control surfaces in complete shadow (see Foldout 4-3B). This allows for minimal mass and radiator area and reduces temperature sensitivity to solar constant variation as a function of solar distance. MESSENGER, which employs a similar concept with its sunshade, has shown almost no sensitivity to solar distance variations between 0.5 and 0.95 AU. Once the solar distance reaches about 2 AU, the Sun attitude constraint is relaxed to allow better positioning of the Cruise Stage antennas for communication with Earth.

Since each vehicle in the Vehicle Assembly maintains independent thermal control, and each thermal control design is unique to that vehicle. The Cruise Stage is designed to maintain the internal structure temperature between 15° and 25°C to accommodate the liquid bi-propellant propulsion system components. Cruise Stage thermal control is accomplished using multi-layer insulation (MLI) and heaters placed on critical propulsion and separation system components and Cruise Stage structure. Since the Vehicle Assembly thermal design is cold biased, the excess electrical output from the Orbiter is used to provide the heater power for the Cruise Stage. Any excess electrical power not used by the Orbiter and the Cruise Stage is shunted.

The thermal designs during cruise phase for the Orbiter, Lander, and Aerial Vehicles are similar in concept. When in their respective aeroshells, the Orbiter, Lander, and Aerial Vehicle critical temperatures are maintained by the Pacific Design Technologies Cruise Integrated Pump Assembly (CIPA), utilized by MSL, featuring internally redundant mechanical pumps. Liquid passing through RPS cooling tubes is warmed by the waste heat generated by the General Purpose Heat Sources (GPHSs) and passed via fluid loop to the vehicle specific radiators mounted external to the aeroshell, illustrated in Foldout 4-3B. The cold-biased radiators are sized for each vehicles RPS steady-state waste heat requirement. For the Orbiter, the pump radiator system is sized to accommodate the added heat to the system from solar effects inside of 2 AU. Attitude maintenance is critical for steady-state performance inside of 2 AU, but further studies will address the impact of worst-case transient deviations from this attitude for some specified period of time to ensure system robustness. The mechanical pump thermal control is needed only during the cruise phase of the mission. Thus the current packaging design has the CIPA components located on the outside of each vehicle's aeroshell behind the radiator assembly. This allows a clean separation from each RPS, in that only the fluid lines between the RPS and the CIPA need to be broken. The pumps and radiators for each vehicle are jettisoned together just prior to atmospheric entry for each vehicle. The solar constant and Sun attitude are not an issue when each vehicle separates from the Cruise Stage, and each vehicle's thermal design remains independent and unaffected by the departure of the other.

4.5.3.4 Cruise Stage Communication

Telecommunications during cruise are controlled by the Orbiter within its aeroshell using a series of antennas mounted to the Cruise Stage structure. Uplink and Downlink signals are routed between the Orbiter and Cruise Stage using umbilical RF connections, which are severed when the Orbiter separates from the Cruise Stage.

Before the Cruise Stage reaches a solar distance of 2 AU, the Orbiter aeroshell is directed toward the Sun for thermal control. During the same period, the Earth is at a wide range of SPE angles, as was shown in Foldout 4-1B. To facilitate communications during this period when the Earth is located in the same hemisphere of coverage as the Sun, an X-band fan beam (FB) medium gain antenna (MGA) is used along with the freedom to roll the Cruise Stage about the Sun-pointing vector. The FB is passively deployed to put the radiating area outside the obstruction of the Orbiter aeroshell and point 45° away from the Sun-pointing vector.

An X-band low gain antenna (LGA) is located on the opposite side of the Cruise Stage as the FB to accommodate links when the Earth is located in the opposite hemisphere of coverage. The LGA also accommodates, along with a UHF antenna, relay monitoring of the Lander and Aerial Vehicle at EDL and EDD, respectively. An X-band HGA on the Cruise Stage enables more substantial telemetry rates throughout cruise (outside 2 AU solar distance) and prior to separation of the three vehicles.

4.5.3.5 Cruise Stage Guidance and Control

The guidance and control (G&C) subsystem performs all spacecraft attitude determination, guidance, and attitude control functions during the cruise phase. The G&C system shares some hardware components with the Orbiter, augmented with Cruise-Stage only components. It utilizes the Orbiter integrated electronics module (IEM) main processor and interface cards, an internally redundant inertial measurement unit (IMU), and four reaction wheels (for the last year of Titan approach). On the Cruise Stage, and jettisoned with it, are mounted redundant star trackers and 12 small (10 N) and 4 large (110 N) bi-prop thrusters for attitude control, momentum dumping, and velocity control. The Orbiter interface card collects the sensor data and distributes commands to actuators, while the IEM main processor performs attitude determination, guidance, and control functions. The IMUs, like those successfully used on NEAR and in use on MESSENGER, provide high-bandwidth information needed for spacecraft control, and the star trackers provide absolute orientation in an inertial reference frame. All G&C areas have at least one level of redundancy.

Cruise Stage thrusters are arranged to provide trajectory correction velocity changes in any direction in inertial space. The design satisfies the pointing constraints, including the thermal constraint that requires the Orbiter heatshield to point toward the Sun when within 2 AU of the Sun. The star trackers enable attitude knowledge accurate to 25 μrad, and attitude is controlled to within 17 mrad in all 3 axes. Control is switched to the four Orbiter reaction wheels about 1 year from Titan orbit insertion to minimize thruster-induced trajectory perturbations during the Titan final approach. The G&C also orients the Cruise Stage for Lander, Aerial Vehicle, and Orbiter release and compensates for the Lander and Aerial Vehicle deployment perturbations. After separation, the Orbiter switches to Orbiter-mounted bi-prop thrusters and star trackers.

4.6 Orbiter Flight System

4.6.1 Orbiter Key Driving Requirements and Features

Key driving requirements for the Orbiter, flowed down from the requirements listed in Section 4.2.2, include:

- 4-year on-orbit mission
- Single-fault tolerant
- Accommodation requirements for 12 Orbiter instruments
- Successful aerocapture into Phase I aerosampling orbit

- 100 kbps mission-average science downlink data rate to meet science data downlink requirements
- Orbiter serves as a relay for the Lander and Aerial Vehicle during first year of Orbiter science mission
- Power to operate groups of instruments requiring simultaneous operation during a given science campaign
- Allocation mass within that defined for the Orbiter
- Package in aeroshell that fits volumetrically with cruise stack configuration and launch fairing
- Provide thermal control, including during cruise

Features of the Orbiter are summarized in Fig. 4-12.

4.6.2 Orbiter Key Characteristics

The Orbiter flight configurations, and instruments and components are shown in Foldout 4-4A, B, C. As shown in the block diagram, Foldout 4-4D, the Orbiter is single fault tolerant.

4.6.3 Orbiter Resources, Contingencies, and Margins

Contingencies and margins are shown in Fig. 4-13 for mass, power, data downlink and ΔV. Mass and power margins meet JPL requirements for allocations 43% above CBE. In this approach, the Advanced Stirling Radioisotope Generators (ASRGs) are assumed to be Government Furnished Equipment and no contingency or margin is allocated. System margins however are shown as percentages of total dry mass, not with the ASRG mass subtracted.

4.6.4 Orbiter Representative Payload Accommodation

The representative Orbiter science payload directly addresses the measurement objectives requiring an Orbiter at Titan. Fig. 4-14 lists the Orbiter instruments, their mass and average power allocations, and identified heritage proxies. Instrument details, including science objectives and measurement approaches, are provided in Section 2.

Feature	Benefit
12 science instruments plus radio science and engineering aeroshell instrumentation	Meets science requirements and provides engineering data for future missions.
Aerocapture	Maximizes mass to Titan orbit, saving ~4 km/s ΔV.
4-year on-orbit science	Meets science requirements, enables multiple science campaigns.
Near-polar, low initial beta angle, precessing circular science orbit	Meets global mapping, surface spectral mapping, and occultation requirements.
Aerosampling science orbit – two phases	Provides 23° latitude coverage near south pole and 40° latitude coverage near north pole over 240 days to meet science requirements.
3-m HGA dual axis	Meets downlink requirements; enables Orbiter orientation for simultaneous science and data downlink.
HGA used for communication and SAR/altimetry	Eliminates mass and packaging resources required for separate SAR/altimetry antenna; articulation feature also provides capability to stow HGA during aerosampling as needed.
Orbiter provides relay for Lander, Aerial Vehicle	Maximizes data downlink from in situ vehicles; provides critical event EDL, EDD coverage.
Five ASRGs	Meets instrument and communication power requirements.
Technology task and cost included for aerocapture flight demonstration at Earth	Enables TRL 7 prior to PDR; worked under Flagship Project

Figure 4-12. Orbiter features provide multiple benefits to the TE mission.

	Allocation	CBE	% Contingency	% Margin
Mass	1810 kg	1160 kg	16%	20%
Power (by operational mode)	637.5 W (5 ASRGs, 14 years end of life [EOL])	Aerosampling: 354 W Atmosphere: 447 W Ionosphere: 418 W Surface-day: 429 W Surface-night: 339 W	12%	60% 27% 36% 33% 67%
ΔV	408 m/s	344 m/s	CBE propellant mass calculated on Orbiter allocation mass	19%
Data Rate	159 kbps mission ave.	100 kbps science	CBE rate includes 3dB link margin	18% downlink time 30% data rate

Figure 4-13. Orbiter resource contingencies and margins meet or exceed APL and JPL practices.

The Orbiter science payload is grouped into focused campaigns, described in Section 4.10.1, which utilize a subset of instruments to optimize science return while minimizing power dissipation and telemetry bandwidth. During the Surface Campaign the Orbiter maintains nadir pointing, whereas during the Atmospheric, Ionospheric and Occultation Campaigns the Orbiter maneuvers about its roll axis acting as a scan platform.

Four areas on the Orbiter are available for instruments, as shown in Foldout 4-4A and 4-4C: the ram-facing bay, the anti-ram bay, the cold-side bay and the top-side deck. The Spectral Mapper and IR Spectrometer utilize passive cooling systems requiring large thermal radiators and are located in the Sun-protected cold-side bay. Careful interface definition of the flight instrument and Orbiter will result in a nearly 2 π steradian radiator field of view with area sufficient for cooling an instrument similar to Cassini/CIRS. The Ion/Neutral Mass Spectrometer, Langmuir Probe, and Plasma Package are provided direct access for local sampling in the Orbiter ram-facing bay.

Instrument Type	Representative Instrument	Mass CBE (kg)	Ave Power CBE (W)	Telemetry (kbps)
Spectral Mapper	MRO CRISM	25	37	High, Variable
Visible/1-Micron Imager	MESSENGER MDIS	3	7	High, Variable
IR Spectrometer	Cassini CIRS	35	20	4.0
UV Spectrometer	New Horizons Alice	5	4	400.0
Microwave Spectrometer	New instrument	30	80	9.0
Altimeter/SAR	New instrument	20	Ave < 40 Peak=170	Min 3.0 Max 85.0
Subsurface Radar/Ionosphere Sounder	Mars Express MARSIS	15	60	10.0
Ion/Neutral Mass Spectrometer	Rosetta ROSINA	25	38	10.0
Energetic Particles	JUNO JEDI	6	9	9.0
Plasma Package	New Horizons SWAP	6	10	0.3
Langmuir Probe		1	2	0.1
Magnetometer	MESSENGER MAG	1	2	1.0
Total		172		

Figure 4-14. Orbiter representative instruments meet science requirements and scope the Orbiter accommodation requirements.

FOLDOUT 4-4: Orbiter 1

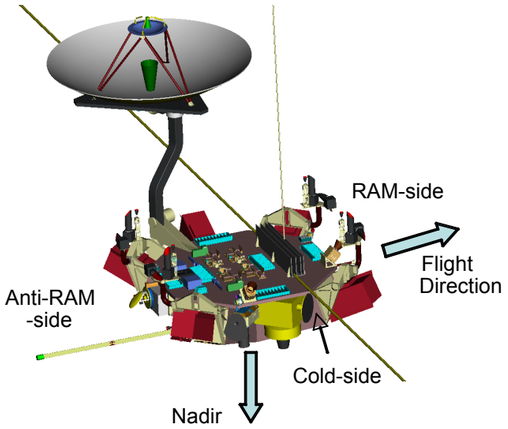

(A) Orbiter design provides simultaneous science measurements and Direct-to-Earth communication capability.

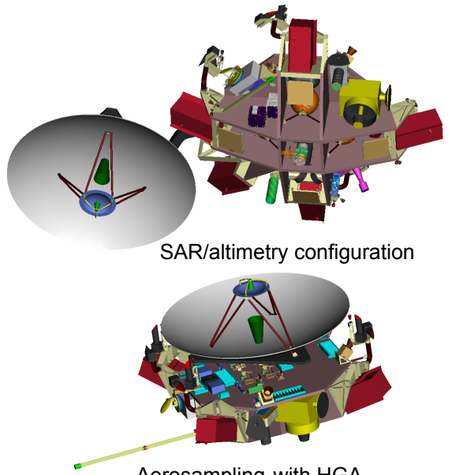

(B) The Orbiter HGA provides SAR/altimetry capability. The HGA can be stowed for aerosampling as needed.

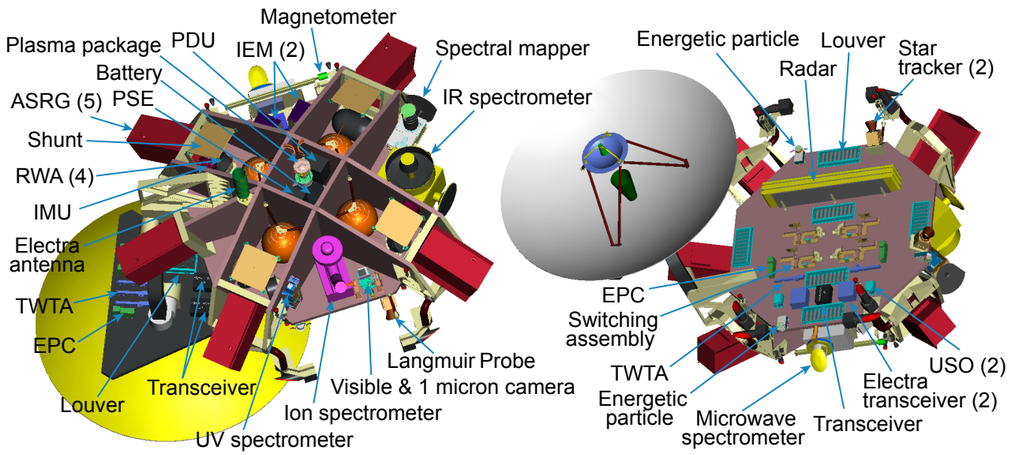

(C) Orbiter provides efficient structural and thermal design and meets all instrument accommodation requirements.

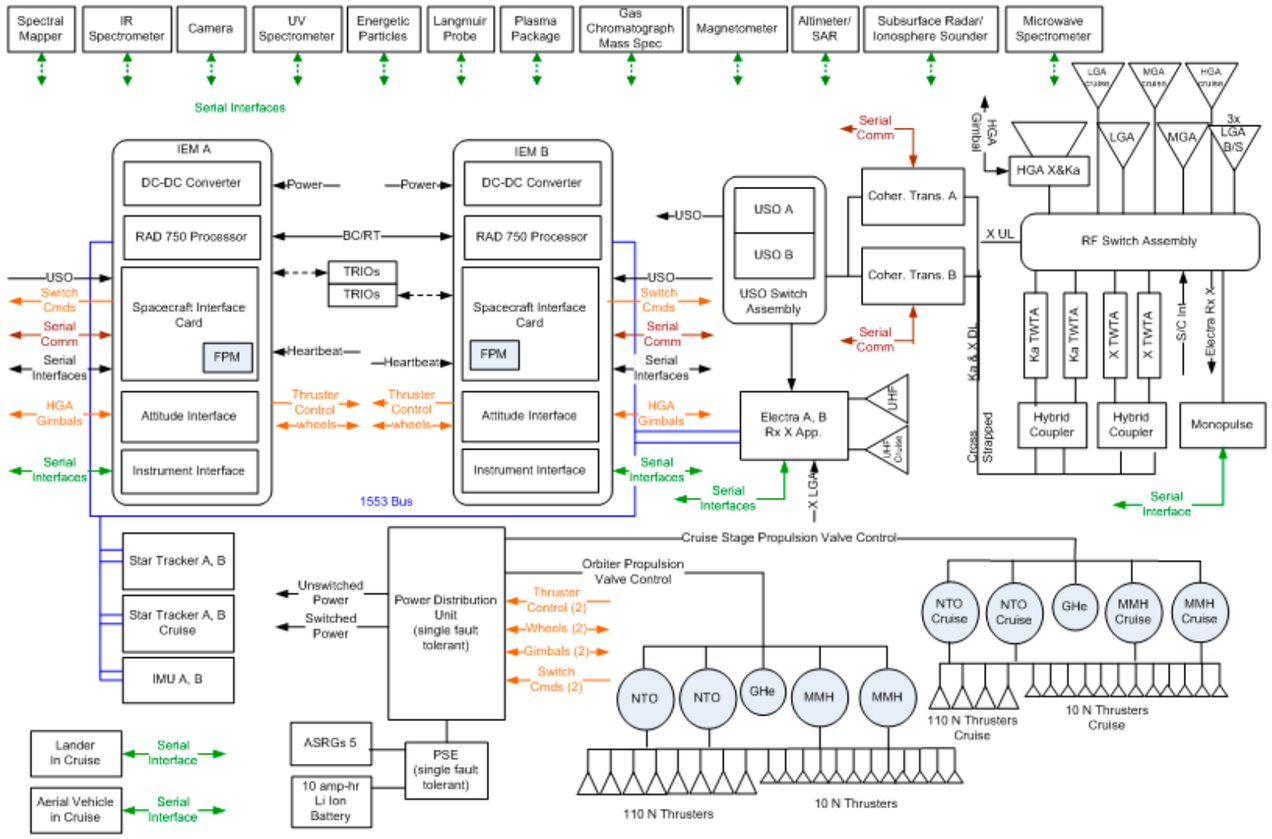

(D) Orbiter is single fault tolerant.

The Visible/1-Micron Imager and UV Spectrometer, while not requiring access to the ram direction, are small instruments and are also located in the ram-facing bay. The Microwave Spectrometer and the Magnetometer are located in the anti-ram bay with the Magnetometer Probe deployed on a boom along the anti-ram axis. The Subsurface Radar antenna is deployed from a stowed position on the top-side deck. Also on the top-side deck are a set of Energetic Particle instruments arrayed to achieve optimal field of view. The electronics for the Altimeter/SAR instrument, which utilizes the Orbiter HGA, are also installed on the top-side deck.

Most of the instruments generate modest (<10 kbps) science data rates and can be accommodated with typical low-speed telemetry interfaces. The Spectral Mapper, Visible/1-Micron Imager, UV Spectrometer and Altimeter/SAR, however, all can generate high science data rates and require high-speed telemetry interfaces. The actual telemetry rate produced by these instruments is highly configurable and can be adapted to meet onboard resource limitations.

4.6.5 Aerocapture

The Orbiter completes aerocapture at Titan using bank angle control of the vehicle's lift vector to modulate the energy removed by drag during the atmospheric flight. This guided approach allows uncertainties in navigated delivery states, Titan atmosphere uncertainty and variability, and aerodynamic uncertainty to be adjusted for autonomously. The aerocapture flight, and corresponding guidance approach, is similar to the human-rated skip reentry flight mode of Apollo. However, this option was never needed during Apollo mission operations, and therefore was never flown. It is also similar to the guided entry in development for MSL's guided precision landing. However, for TE risk reduction, an aerocapture flight demonstration, to validate the aerocapture guidance, is proposed. The aerocapture flight demonstration technology work is described in Section 4.13.

The TE aerocapture system leverages work completed in the peer-reviewed 2002 Titan ASAT Study (Lockwood et al., 2006) sponsored by NASA In-Space Propulsion Technology (ISPT) program (Munk and Moon, 2007); it also incorporates updates resulting from Cassini/Huygens data and technology advancements since the study sponsored by ISPT. The key updates include:

1. Improved knowledge of Titan's ephemeris, contributing in part to the improvement in navigated aerocapture entry states described in Section 4.3.4.
2. Reduction in the maximum percentage of methane (CH_4) expected in the Titan atmosphere at aerocapture altitudes, per the Titan Atmosphere Working Group, from 5% to 2.3%. This reduction significantly decreases the level of aeroheating resulting from radiation.
3. Advancements in the aeroheating analysis capability, supported by experimental work. This improvement also resulted in lower aeroheating rate and load estimates.
4. Characterization of TPS performance in a radiative environment, allowing TPS material such as SLA 561 and SRAM materials to be candidates (Laub et al., 2005).
5. Data further supporting the atmospheric density variability modeled in TitanGRAM.

The TE Orbiter entry mass is 1810 kg with a ~76 kg/m^2 ballistic coefficient. The 4.57-m-diameter aeroshell has a 0.25 lift-to-drag ratio (L/D). A lower L/D can likely be considered in future studies due largely to the lower navigated delivery dispersions described in Section 4.3.4. In addition, alternative aeroshell shapes can be considered; however, the current design is representative.

4.6.5.1 Atmospheric Flight Simulation and Performance

A 2000-case Monte Carlo aerocapture trajectory analysis of the TE Orbiter, completed by NASA LaRC, shows successful aerocapture at Titan in 100% of the trajectory cases. The guidance algorithm flown in the simulation is that described in Section 4.6.5.2. Dispersions modeled include entry state dispersions, aerodynamic uncertainties, and atmospheric variability and uncertainty. TitanGRAM (Justus and Duvall, 2003) was used to model the atmosphere variability and uncertainty. The density profiles at aerocapture altitudes are shown in Foldout 4-5B compared with the Cassini/Huygens data, showing that TitanGRAM encompasses the variability measured by Cassini. In addition, the TitanGRAM high-frequency perturbation model was included in the simulation, which significantly increases the variability beyond that shown in Foldout 4-5B. The nominal entry velocity and entry flight path angle at the 1000-km atmospheric interface are 6.55 km/s and –34.9°, respectively. Statistics on the aerocapture phase show accelerations less than 2.3 g's and apoapsis altitudes between 1650 km and 1750 km. Two propulsive maneuvers are planned after aerocapture to modify the orbit to a 1650-km apoapsis by 1170-km periapsis orbit in preparation for the first phase of aerosampling. These maneuvers require 113 m/s ΔV, with a 3-σ high value of ~120 m/s, as shown in Foldout 4-5A.

4.6.5.2 Guidance and Control

A Terminal Point Controller (TPC) guidance algorithm is used in the aerocapture simulation. The TPC uses bank control to guide the lifting vehicle to the desired apoapsis and inclination. TPC is a feedback guidance algorithm that uses exit condition sensitivities to changes in the state and control to determine the control at any point along the trajectory. The sensitivities are generated from a reference trajectory that is determined off-line prior to flight. TPC has an in-plane component that targets the velocity increment (ΔV) required to achieve a desired orbit after the atmospheric pass is complete and an out-of-plane component that targets inclination. TPC has been studied extensively for several proposed aerocapture missions. This algorithm is a derivative of the algorithm used in the Apollo program and that planned for MSL entry guidance.

4.6.6 Orbiter Flight Software

The Titan Orbiter flight software combines G&C and command and data handling (C&DH) functionality within a single redundant flight processor. G&C software tasks implement the spacecraft control functions described in Section 4.6.7.7, including support for cruise, aerocapture, and orbital operations with the 3-axis stabilized spacecraft. G&C attitude control and attitude estimation algorithms are developed as Matlab models, which are used with automated code generation tools to produce C code that is integrated into the flight software application. G&C tasks run in parallel with C&DH software tasks under a multitasking real-time operating system. The C&DH software is developed using the C language and is human-generated. Data handling functions in the C&DH software encapsulate the autocoded G&C algorithms and manage sensor and actuator inputs and outputs to and from those control algorithms.

C&DH features in the flight software include: real-time command processing and the ability to execute stored command sequences; time management and distribution; management of the uplink and downlink; distribution of commands to instruments and collection of telemetry from instruments; management of the solid-state recorder (SSR), and support for managing memory objects and uploads of new code applications. The software manages the Flash-based SSR using a file system with science and engineering data stored on the recorder in file format. Uploads to the Orbiter are managed in the form of files as well. File-based recording enables the flight software to make use of the CCSDS CFDP (Consultative Committee for Space Data Systems File

Delivery Protocol) for transmitting data to Earth. This protocol optimizes downlink bandwidth by allowing for retransmission of any file fragments previously lost to dropouts, without unnecessarily retransmitting an entire file. CFDP is used for data transmissions between the Orbiter and the Lander and Aerial Vehicle as well. Commands, memory and code loads that are destined for the Lander or Aerial Vehicle are transmitted from Earth as files that are stored on the Orbiter SSR. The Orbiter in turn transmits the files to the target vehicle when it next comes in view, via the relay radio link. CFDP ensures that intact files are received. This "store and forward" concept of operations is also the means by which science and engineering files are transferred from the Lander and Aerial Vehicle to the Orbiter, which then transmits them to Earth during future DSN contacts. The flight software uses serial interfaces to communicate with the Orbiter instruments and provides a service to compress images.

During the cruise phase, the Orbiter flight processor controls the Cruise Stage, and the flight software supports a communication interface to the flight computers in the Lander and the Aerial Vehicle. This interface provides a means of monitoring Lander and Aerial Vehicle telemetry and allows parameters or new code to be loaded. In a similar fashion, the primary flight processor communicates with the Orbiter's backup processor in all mission phases. Apart from the fault protection monitors (FPMs), which monitor processor health and can switch to the backup processor, the flight software includes a rule-based autonomy system that provides a means to monitor subsystem telemetry and execute corrective command sequences when faults are detected. The rules that define the fault protection monitors and responses can be uploaded without requiring any changes to the flight software application.

4.6.7 Orbiter Spacecraft Subsystems

4.6.7.1 Orbiter Propulsion Subsystem

The Orbiter propulsion subsystem is nearly identical to that of the Cruise Stage described in Section 4.5.3.2. The subsystem employs eight, rather than four, Space Shuttle-heritage Aerojet R-1E 110 N (25 lbf) thrusters for ΔV and attitude control during aerocapture and twelve ~9 N (2.0 lbf) AMPAC-ISP Leros LTT bipropellant thrusters for momentum dumps and fine attitude control.

The R-1E does not require radiative cooling of its thrust chamber or nozzle; consequently R1-Es with scarfed nozzles can be buried within the Orbiter aeroshell. Placement of the thrusters is based on experience from previous missions, including recent MSL experience. As mentioned in Section 4.5.3.2, a modest optimization/delta-qualification effort is included, both to ensure that the R-1E operates stably within the operating conditions and in the mounting configuration required and to characterize the impact on the performance of the scarfed nozzle.

As with the Cruise Stage, this propulsion system has four identical, custom titanium propellant tanks (two for fuel and two for oxidizer) and one custom COPV. Different PMDs are developed for inside the two hydrazine and two oxidizer tanks. All other components are identical to that of the Cruise Stage, allowing cost savings.

The Orbiter tanks are sized to a launch propellant load of 211.4 kg, providing ~7% volume margin above the maximum Orbiter propellant required. The custom titanium fuel and oxidizer tanks are 49.0 L (2990 in^3) each and designed for a 2.07 MPa (300 psi) MEOP. The custom COPV pressurant tank is 27.1 L (1656 in^3) and rated for a beginning or life (BOL) pressure of 20.7 MPa (3000 psia).

4.6.7.2 Orbiter Communications Subsystem

The Orbiter telecommunications subsystem is designed to provide up to 140 kbps raw DTE data rate at maximum Earth–Titan distance and greater than 200 kbps at Earth–Titan closest approach, as shown in Foldout 4-2C. Telecommunications operations (DTE) are designed for 3-dB telemetry margin using turbo coding to a frame error rate (FER) of 10^{-4} and 6-dB command margin to a bit error rate (BER) of 10^{-6} with simultaneous command, telemetry, and ranging capability considered nominal. Ka-band is utilized as the primary downlink band; X-band is used for lower-rate downlink, uplink, radio science, and backup downlink in case of in-flight anomaly and/or adverse weather. Downlink paths function at 35 W RF power, both at Ka-band and X-band, using redundant traveling wave tube amplifiers (TWTAs). When spacecraft power is available, both redundant Ka-band amplifiers can be activated, enabling twice the downlink data rate using polarization diversity–combining receivers on the ground.

The primary downlink path in Titan orbit is through a 3-m, 2-axis-gimbaled HGA that is shared with the Radar Altimeter/SAR instrument. By allowing the Orbiter to maintain a Titan nadir fixed attitude while accommodating a line of sight to Earth at all non-occulted parts of the spacecraft's orbit, the HGA gimbals facilitate simultaneous on-orbit science operations and data downlink at the rates listed in Foldout 4-2C. To achieve better than the required 0.05° HGA pointing accuracy, a monopulse feed design and associated receiver are used to drive the gimbals in conjunction with the ACS. The dual-frequency band (X/Ka) antenna uses the uplink signal to precisely point itself for power-efficient, high-data-rate downlink operation. An open-loop Ka-band mode can also be used, providing about half the data rate achievable through monopulse tracking. Open-loop HGA pointing accuracies are ~0.1° and result in a ~3-dB pointing loss. Further monopulse system and operations definition are included in future work in Section 4.12.1.

The Orbiter also carries an X-band MGA and LGA horn for backup, maneuver, and safe-mode DTE communications. The MGA gain pattern is matched to the range of SPE angles that occur over the course of the science mission, enabling a simple sun-pointing safe-mode communications configuration.

The Orbiter uses a series of coax and waveguide RF switches (transfer and/or SP3T), to be selected in Phase A. Redundant switches will also be considered. The team is aware of the MRO Waveguide Transfer Switch (WTS) anomaly and will consider each of the recommendations outlined in the MRO WTS anomaly report. Particular attention will be focused on plating and contamination control of all waveguide devices in the subsystem.

In addition to serving the command and telemetry needs of the Orbiter itself, the Orbiter telecommunications subsystem functions as a relay to both Lander and Aerial Vehicle. Ground commands are routed through the Orbiter using Electra UHF relay transceivers including 8.5-W solid state power amplifiers (SSPAs). Relay science and telemetry data are returned through the Electra to the Orbiter C&DH subsystem for insertion into the DTE downlink data stream. The relays also provide two-way Doppler information from each vehicle for location tracking. The relay transceivers monitor the Lander and Aerial Vehicle signals at EDL/EDD, either at UHF frequencies or at X-band using Electra X-band receive appliqués. The appliqué also enables enhanced data rate relay from the Lander to the Orbiter, augmenting the Lander's science return potential. Relay communications use a UHF antenna with pattern optimized for the relay geometry and an X-band LGA horn (possibly shared with the DTE communications path) for the enhanced data rate relay.

FOLDOUT 4-5: Orbiter 2

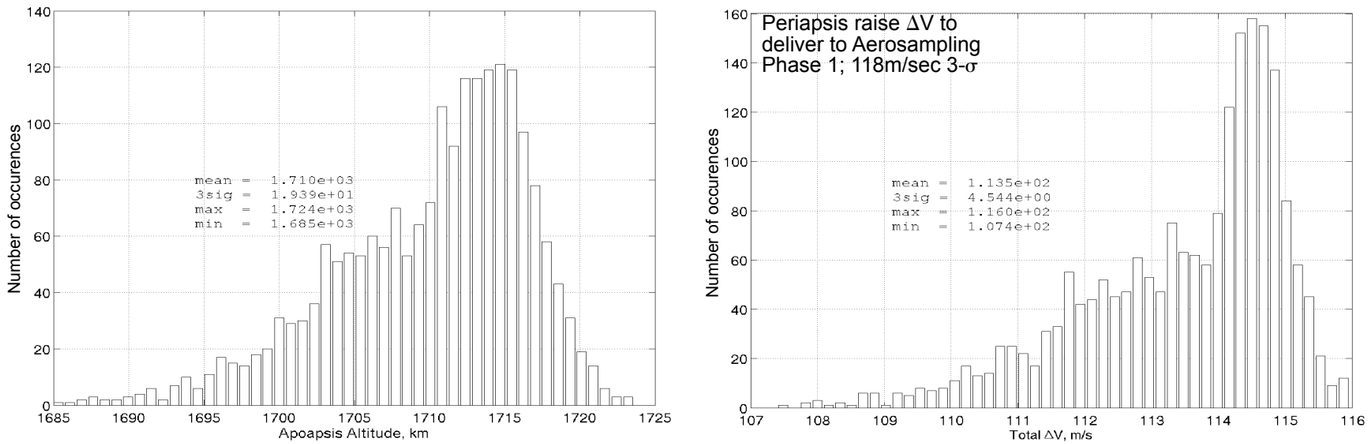

(A) 100% of Monte Carlo cases aerocapture successfully.

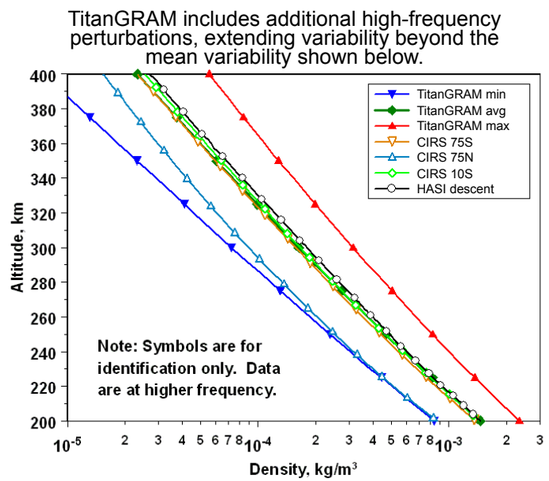

(B) TitanGRAM variability encompasses that measured by Cassini/Huygens.

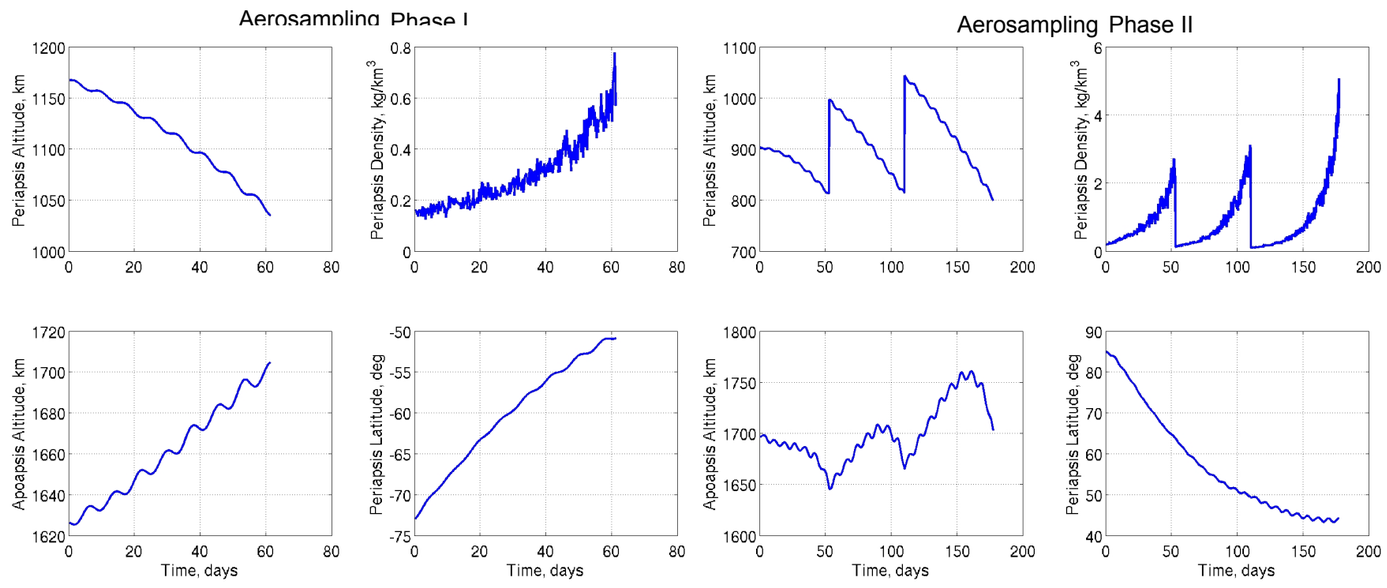

(C) Aerosampling provides ~23° of latitude coverage near the South Pole and ~40° of latitude coverage near the North Pole.

Two redundant ultra-stable oscillators (USOs) enable precise radio science measurements during Titan occultation and provide a tunable reference to the Electra radios carried for relay communications. The coherent transceivers include frequency synthesized uplink and downlink channels making flexible, phase-coherent turnaround ratios possible. This unique capability enables the Titan mission to take advantage of the DSN's Multi-Spacecraft Per Aperture (MSPA) capability to reduce DSN costs when simultaneous downlinks are desired from multiple Titan vehicles. The DSN can maintain two-way Doppler and ranging to both the Orbiter and Lander, for example, while providing a single X-band uplink.

The telecommunications architecture is dual-redundant and fully cross-strapped, enabling selectable paths between USOs, coherent transceivers, TWTAs, relay transceivers, and antennas. An RF switch assembly allows RF paths to be routed as required during cruise (to each of the Cruise Stage antennas), aerocapture (to a series of backshell X-band antennas, switched as a function of entry geometry), and science orbit. Similar to the Cruise Stage RF paths, the RF paths to the backshell antennas are severed upon backshell separation from the Orbiter.

4.6.7.3 Orbiter Power Subsystem

The Orbiter power system consists of five ASRGs, single-fault-tolerant power system electronics (PSE), shunt dissipater, and an eight-cell single-fault-tolerant lithium-ion battery. This system provides an unregulated 22- to 34-V bus.

4.6.7.4 Orbiter Structural/Mechanical Subsystems

The Orbiter mechanical structural design and vehicle layout are depicted in Foldout 4-4A, 4-4B, and 4-4C. Launch loads are transferred from the Cruise Stage separating interface (through the backshell) to the Orbiter primary structure (see Foldout 4-3A and 4-3B). The Orbiter structural design consists of a single aft aluminum honeycomb panel, equipment deck, and a frame design providing additional subsystem interfaces and stiffness to the equipment deck. Interfaces for all instruments and subsystems are uncomplicated and flat surfaces. All panels are aluminum honeycomb design with edge members buried inside the panels where local loads are high. The mechanical, thermal, and electrical interfaces of the RPS mounting plates to the primary aluminum structure are straightforward and can be designed to provide electrical and/or thermal isolation, both of which were done for New Horizons. Secondary structure required for instrument brackets and propulsion system thrusters is also standard.

The Orbiter aeroshell has heritage from the Mars Viking and MSL aeroshells in structure and TPS. Other TPS options are available, developed through ISPT, including the SRAM series TPS materials (SRAM 14, 17, 20) from ARA.

The apparent asymmetric layouts of the ASRGs achieves the required system center of gravity for aerocapture flight, via the coordinated placement of subsystems on the structure. The 3-m HGA is stowed for launch and deployed using a heritage pyrotechnic release. Post-deployment rotation for Earth communication, SAR/Altimetry, and aerosampling science is provided by heritage stepper motor antenna pointing gimbal systems. RF and telemetry are fed across the movable joints via slip rings and RF rotary joints. A mass study and a highly detailed volumetric study yield adequate growth potential within system constraints.

4.6.7.5 Orbiter Thermal Control Subsystem

During cruise, Orbiter thermal control is managed by the mechanical pump and heat pipe radiator system described in Section 4.5.3.3. On orbit, the Orbiter thermal control system provides a low-risk design approach, based on New Horizons heritage, using louvers and MLI. Waste heat from electronics is distributed throughout the MLI-covered structure, nearly eliminating the need

for spacecraft bus heater power. As with New Horizons, spacecraft and instrument electronics and all propulsion components are directly coupled to the structure. Heat dissipated by the electronics is spread throughout the structure by conduction and thermal radiation. Louvers, which are critical for bulk structure temperature regulation, are strategically placed on the Zenith-facing panels, allowing controlled heat leak to space. The Spectral Mapper and IR Spectrometer are designed to be passively cooled with radiator surfaces facing out of the cold-side of the Orbiter. As with New Horizons, the five externally mounted ASRGs are radiation cooled to space.

4.6.7.6 Orbiter Avionics Subsystem

The Orbiter Avionics, as shown in Foldout 4-4D, consists of the IEM, Remote Interface Units (RIUs), and the Power Distribution Unit (PDU). The IEM contains the main processor and interfaces to instruments and other subsystems. The off-the-shelf RAD750 processor supports commanding, data handling, data storage (using the SSR) and G&C. The IEM is an evolutionary design based on the Compact Peripheral Component Interface (cPCI) backplane bus that has flown on MESSENGER and STEREO and is planned for use on RBSP. The standard cPCI bus allows great flexibility in combining appropriate processor, memory, and interface cards.

The Titan Orbiter IEM contains five 6U cPCI cards: a RAD750 CPU, a spacecraft interface card, an attitude interface card, an instrument interface card, and a DC/DC converter card. These cards are designed for reuse in the Titan Lander and Aerial Vehicle. The IEMs are block redundant. Under most conditions, one IEM is unpowered.

The avionics subsystem also collects analog and digital telemetry via RIUs, which are based on the Remote Input-Output (RIO) Application Specific Integrated Circuits (ASICs) flown on several previous missions. These small, light-weight units collect and digitize telemetry points and transmit the data to the IEM using the industry standard I2C bus.

The PDU switches loads and controls thrusters via command from either IEM. The PDU is internally redundant with two field-effect transistors (FETs) in each solid-state switch to ensure that every load can be turned off. The slice-based design from RBSP contains redundant slices for power, command, and telemetry. Slices based on relays and FET switches are stacked as appropriate. FET switches incorporate resetable circuit breakers based on the power remote I/O (PRIO) ASIC.

The RAD750 CPU card is an existing design with 20 MB SRAM, 4 MB EEPROM, and 64-KB Fuse Link boot PROM. Various configurations are available, including SDRAM-based configurations that provide significantly more main memory and can be selected as needed.

The spacecraft interface card is the only IEM card that is not powered off. It contains the critical command decoder, which executes some commands directly in hardware and passes some directly to the PDU. It also contains the PDU, downlink, RIU interface circuitry, the backup oscillator, and clock/timing circuitry for the card. Also located on the board is the FPM, which monitors the health of the redundant IEM.

The attitude interface and instrument interface cards contain the interfaces to the engineering and science instruments. The Electra relay interfaces are treated as an instrument interface. Also located on the instrument interface card is 32 Gbits of triple-voted Flash memory for data storage (SSR). The circuitry has been allocated to these two boards to optimize reuse in the Lander and Aerial Vehicle. Communication with the science instruments is accomplished primarily with bidirectional asynchronous serial interfaces. Two instruments use dedicated, high-speed synchronous serial interfaces.

Each IEM contains an FPM. This module, on the spacecraft interface card, is powered by unswitched power. The FPM in the “off” IEM monitors health signals from the “on” IEM. When

the FPM detects a fault, it follows a decision tree and can command the PDU to switch IEMs. The FPM disables itself after use with a latching relay in the PDU. The FPMs can be enabled or disabled by critical command via either IEM (powered or unpowered) at any time.

4.6.7.7 Orbiter Guidance and Control Subsystem

The G&C subsystem performs all spacecraft attitude determination, guidance, and attitude control functions. Its architecture and hardware closely follow the successful NEAR, MESSENGER, and STEREO subsystems. The G&C system utilizes the IEM main processor and spacecraft interface cards; an internally redundant IMU containing four gyroscopes and accelerometers; four reaction wheels; two star trackers; 12 small thrusters (10 N) for slewing, momentum dumping, and fine velocity control; and 8 large thrusters (110 N) for control during aerocapture and the subsequent periapse raise maneuver. The spacecraft interface card collects data and distributes commands, while the IEM main processor performs attitude determination, guidance, and control functions. The IMU gyros, like those successfully in use on NEAR and MESSENGER, provide high-bandwidth information needed for spacecraft control, and the star trackers provide absolute orientation in an inertial reference frame. All G&C areas have at least one level of redundancy. The system uses flight-proven, off-the-shelf components available from multiple vendors, which provide high reliability and a very low hardware procurement risk.

During aerocapture, the G&C system controls the vehicle using the 110-N bi-prop thrusters based on the guidance bank angle commands, as described in Section 4.6.5.2. During science observations and fine velocity corrections, attitude knowledge is accurate to 25 μrad and is controlled to within 1.7 mrad in all 3 axes. The four reaction wheels are arranged in a tetrahedral configuration for redundant torque and momentum storage capability in all 3 axes while enabling minimization of control–structure interactions. The G&C system points the HGA toward Earth for data transmittal and to the Titan surface for the SAR/Altimetry measurement acquisition.

4.7 Lander Flight System

4.7.1 Lander Key Driving Requirements and Features

Key driving requirements for the Lander, flowed down from, or in addition to, the requirements listed in Section 4.2.2 include:

- 1 year Titan surface operations
- Single fault tolerance
- Accommodation requirements for nine Lander instruments
- Successful EDL, including 3-σ landing footprint within the Belet dune region
- 2.9 kbps science data rate, or 5.5 Gbits total science data return
- Primary science downlink via relay to the Orbiter with DTE backup
- Power adequate to operate required instruments simultaneously
- Allocation mass within that defined for the Lander
- Package in aeroshell that fits volumetrically within the cruise stack configuration
- Provide thermal control, including during cruise

Features of the Lander are summarized in Fig. 4-15.

4.7.2 Lander Key Characteristics

The Lander configurations and Lander instruments and components are shown in Foldout 4-6A and 4-6D. As shown in the block diagram, Foldout 4-6E, the Lander is single fault tolerant.

Feature	Benefit
9 science instruments plus a student experiment and aeroshell engineering instrumentation	Meets science requirements, provides E/PO opportunity, and provides engineering data for future missions.
1 year surface science Lander	Meets science requirements.
EDL heritage to Huygens and MPF/MER	Reduces EDL risk.
Self-righting petal design	Robust to tumble during landing on steep dune slope(up to 30°). Design can accommodate either a crushable structure (option) or an airbag (current baseline) landing system approach.
Airbag Lander design	Robust design accommodates steep (up to 30°) dune landing terrain; simple design, components high TRL.
0.5-m dual-axis HGA	Provides higher data rate to Orbiter plus backup DTE capability.
2 ASRGs	Meets science and communications power requirements.
Technology task and cost included for operation in a cryogenic environment and system-level validation of landing system	Enables TRL 6 prior to PDR, worked under Flagship Project.

Figure 4-15. Lander features provide multiple benefits.

4.7.3 Lander Resources, Contingencies, and Margins

Contingencies and margins are shown in Fig. 4-16 for mass, power, and data downlink. Mass and power margins meet JPL requirements for allocations 43% above CBE. In this approach, the ASRGs are assumed to be Government Furnished Equipment, and no contingency or margin is allocated. System margins however are shown as percentages of total dry mass, without subtracting the ASRG mass.

4.7.4 Lander Representative Payload Accommodation

The representative Lander science payload directly addresses the measurement objectives requiring a surface vehicle on Titan, and it contributes to achieving regional and global science goals by providing ground truth for measurements from the Orbiter and/or Aerial Vehicle. Fig. 4-17 lists the Lander instruments, mass and peak power allocations, and identified heritage proxies. Section 2 provides instrument details, including science objectives and measurement approaches.

The Lander science payload is grouped into investigations of three types: (1) imaging and spectroscopy, (2) in situ chemical analysis; and (3) environmental/geophysical analysis.

Type 1 investigations begin with the Descent Camera which operates only prior to landing. It requires a single-time deployment beyond the landing structure edge. The Lander Camera and Point Spectrometer use a scan platform on the single-time deployable mast, and the Microscopic Imager uses the arm to position itself at its 6-cm working distance using a contact stop. Of these

	Allocation	CBE	% Contingency	% System Margin
Mass	897 kg	640 kg	18%	19%
Power (by operational mode)	255 W (2 ASRGs, 14 years EOL)	Science, no chem, no comm: 90 W Science + chem, no comm: 169 W Science, no chem, comm: 177 W	14%	149% 32% 27%
Data rate	5 kbps (UHF); 32 kbps (X, HGA)	2.9 kbps (UHF) science; 18 kbps (X, HGA) science	CBE rate includes 3-dB link margin	25% relay time; 30% data rate

Figure 4-16. Lander resource contingencies and margin meet or exceed APL and JPL practices.

Instrument	Mass (kg)	Ave. Power (W)	Peak Power (W)	Heritage Proxy	
Lander Camera (Panoramic Imager)	4	2	5	MER	PanCam
Point Spectrometer	5	3	6	SMART-1, MER	SIR, Mini-TES
Microscopic Imager	1	2	2	MER	MI
Chemical Analyzer	30	40	100	MSL	SAM
Robotic Arm	10	10	20	Phoenix	RA
Seismometer	2.8	3	3	Netlander	SEIS
Magnetometer	2.5	4	4	MESSENGER	MAG
Met Package	2	2	2	MSL	MET
Descent Camera	2	10	10	MSL	MARDI
Student Experiment	2			(E/PO)	
Total	61.3	76			

Figure 4-17. Lander representative instruments meet science requirements and scope the Lander accommodation requirements.

instruments, the Lander Camera is expected to generate the greatest data volume through multispectral panoramas.

Type 2 analyses are conducted primarily by acquiring solid samples using the Robotic Arm with its sampling scoop. These are brought to the inlet of the Chemical Analyzer, where they are optionally crushed and/or size-sorted prior to loading into an analytical cell. The sample acquisition and delivery process is documented with the Lander Camera and/or the Microscopic Imager. The time from acquisition to analysis is minimized to avoid sublimation of volatiles while the sample is in contact with the scoop or inlet.

Type 3 analyses include magnetometry, seismometry, and meteorology. These do not stress the power or data rate levels of the Lander but do require quiet and/or long-term monitoring conditions, necessitating careful scripting of operations along with the Type 1 and 2 analyses, to assure that prime science is achieved early. The Magnetometer and Seismometer are deployed to the surface by the arm as self-contained sensor modules connected to the Lander via umbilical. As such they must be thermally insulated against the 94 K environment. Meteorology includes deployment of a dedicated mast.

4.7.5 Entry, Descent, and Landing

4.7.5.1 EDL Environment

As described in Section 4.3 above, the Lander is targeted to the Belet dune region. The dunes are characterized as sand-like terrain with slopes up to the angle of repose of ~30°. Based on Cassini radar data and on similarity to terrain on Earth, the terrain is estimated to have minimal hazards.

Titan surface atmospheric density is approximately four times that on Earth at sea level, with gravity ~1/7th of Earth gravity, resulting in EDL timelines of 2–3 hours, with no need for powered descent. Wind velocities near the surface are expected to be a maximum of ~2 m/s. As described previously, the temperature at Titan's surface is 94 K, with a minimum temperature of 70 K at ~44-km altitude.

4.7.5.2 EDL Event Sequence

The EDL sequence (shown in Foldout 4-7A) is based on heritage designs from Huygens and the Viking, Mars Pathfinder (MPF), and MER Mars missions. Huygens successfully landed on Titan in a ~3 hour EDL sequence from atmospheric interface (entry velocity = 6.0 km/s, nominal

entry flight path angle of −65° at 1000 km atmospheric interface) to touchdown with a ballistic spin-stabilized entry and a 3 disk-gap-band parachute system. The final Huygens parachute remained attached during and after touchdown. Although TE cannot utilize full heritage from Huygens, given that Huygens was developed by the European Space Agency (ESA) and its partners, the TE team's knowledge of the Huygens EDL system benefits the TE mission. TE interaction with the ESA team on Huygens includes work done through the NASA Engineering and Safety Center Independent Technical Assessment of Cassini/Huygens Probe Entry, Descent and Landing (NESC, 2005), and work with NASA ARC on the Huygens TPS. Examples of NASA's experience with the Huygens mission are included here for reference. AQ60, the Huygens heatshield material, has been tested by ARC; and the ESA TPS response model evaluated by ARC. NASA independently developed aerothermal environments and an aerodynamic database for Huygens. The NASA computational fluid dynamics (CFD) results were used by ESA for Day of Entry aerothermal environments assessments. NASA used the aerodynamic database in pre-flight Monte Carlo flight simulations, and reconstructed the database post-flight from onboard instruments to confirm the aerodatabase. Models of parachute performance and opening loads for Huygens were independently developed by NASA. Reconstructed data confirmed the performance model, but were of too low a frequency to evaluate opening loads. The NASA atmosphere model was used by NASA and ESA for flight mechanics simulations. Reconstruction of the atmospheric density profile shows good agreement with the model.

The TE Lander enters at 6.47 km/s with a nominal entry flight path angle of −60.2° at 1000 km atmospheric interface. The Lander entry is ballistic and spin stabilized. Entry g's are kept within the 18-g constraint (18 Earth g's) set by the ASRG.

The drogue parachute, the first of 3 disk-gap-band parachutes deployed, is mortar-deployed at approximately Mach 1.3 within the parachute Mach dynamic pressure constraints defined during the Viking program. Deployment is controlled by a timer based on an entry g-trigger.

The main parachute is deployed by the drogue parachute, also triggered by a timer, such that deployment occurs at subsonic speeds of < Mach 0.8 (Note that this Mach number can be lowered with minimal timeline penalty to further facilitate testing as necessary). The main parachute is sized to ensure successful heatshield separation.

Following pyrotechnic heatshield separation, the final landing chute is deployed by the main parachute. The landing chute is sized for a 4-m/s maximum vertical velocity at touchdown. (Huygens touchdown velocity was predicted to be 5–6 m/s.) The velocity is selected to minimize the landing loads on both the landing system and the ASRG. (The ASRG landing g constraint is 30 Earth g's.) Horizontal velocity is expected to be a maximum of ~2 m/s based on Titan winds. With a larger landing parachute, the landing velocity can be reduced further, but was kept at 4 m/s to reduce the possibility of updrafts at landing dragging the lander along the surface. Trades to assess sensitivities to winds and landing conditions are included in future work. Following landing parachute deployment, the Lander descends down a ~10-m bridle. The bridle length is sized to provide separation distance between the parachute and the Lander and allow time for the parachute to separate and drift relative to the Lander after touchdown.

A timer triggers the airbag release, and airbag inflation is completed. The airbags are vented to dissipate the impact energy at touchdown and remain inflated through the landing event. The parachute remains attached until the airbags sense ground contact, at which point the parachute is released. The current design results in landings that are significantly less than the 30-g ASRG constraint. The first bounce is estimated to be about 4–5 m above the ground. After the Lander comes to rest, the airbags deflate. The four Lander petals are opened, self-righting the Lander.

FOLDOUT 4-6: Lander 1

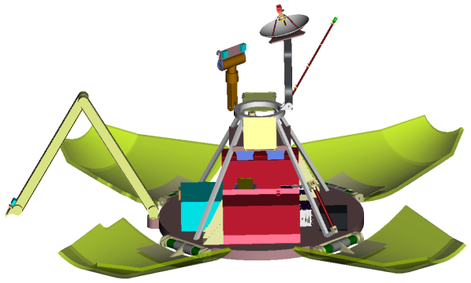

(A) Lander design provides access and fields of view for all instruments meeting Lander science requirements.

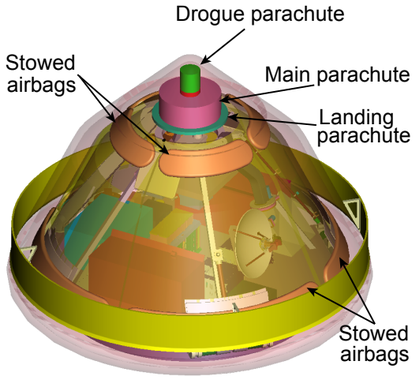

(B) Lander and entry, descent and landing system package with adequate volume inside entry aeroshell.

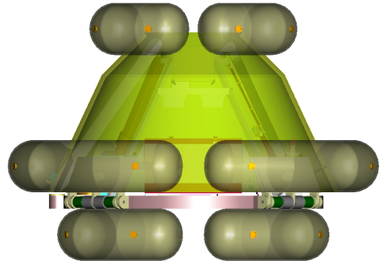

(C) Robust landing system design includes four self-righting petals and airbag landing system.

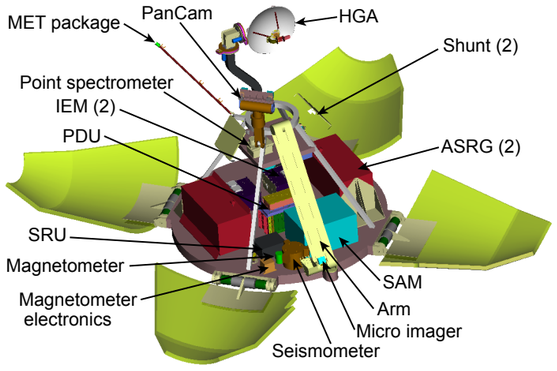

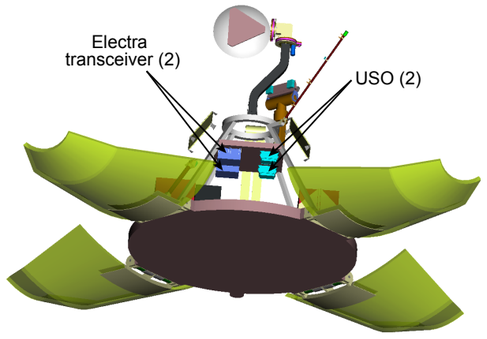

(D) Lander provides efficient structural and thermal design and meets all instrument accommodation requirements.

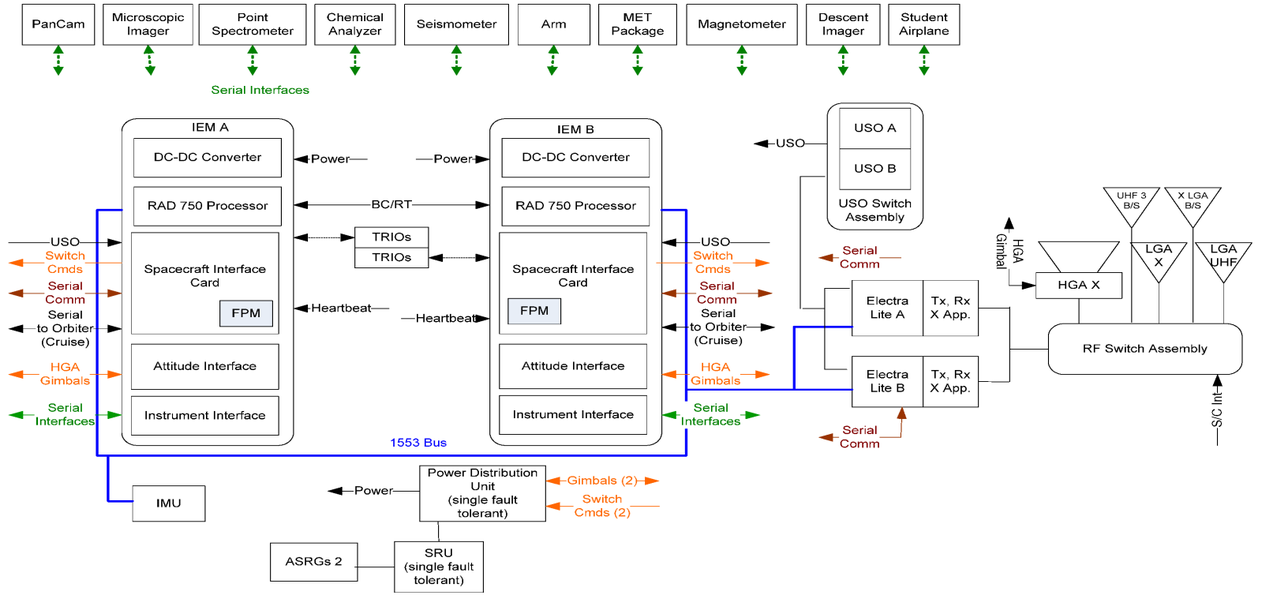

(E) Lander design is single fault tolerant.

FOLDOUT 4-7: Lander 2

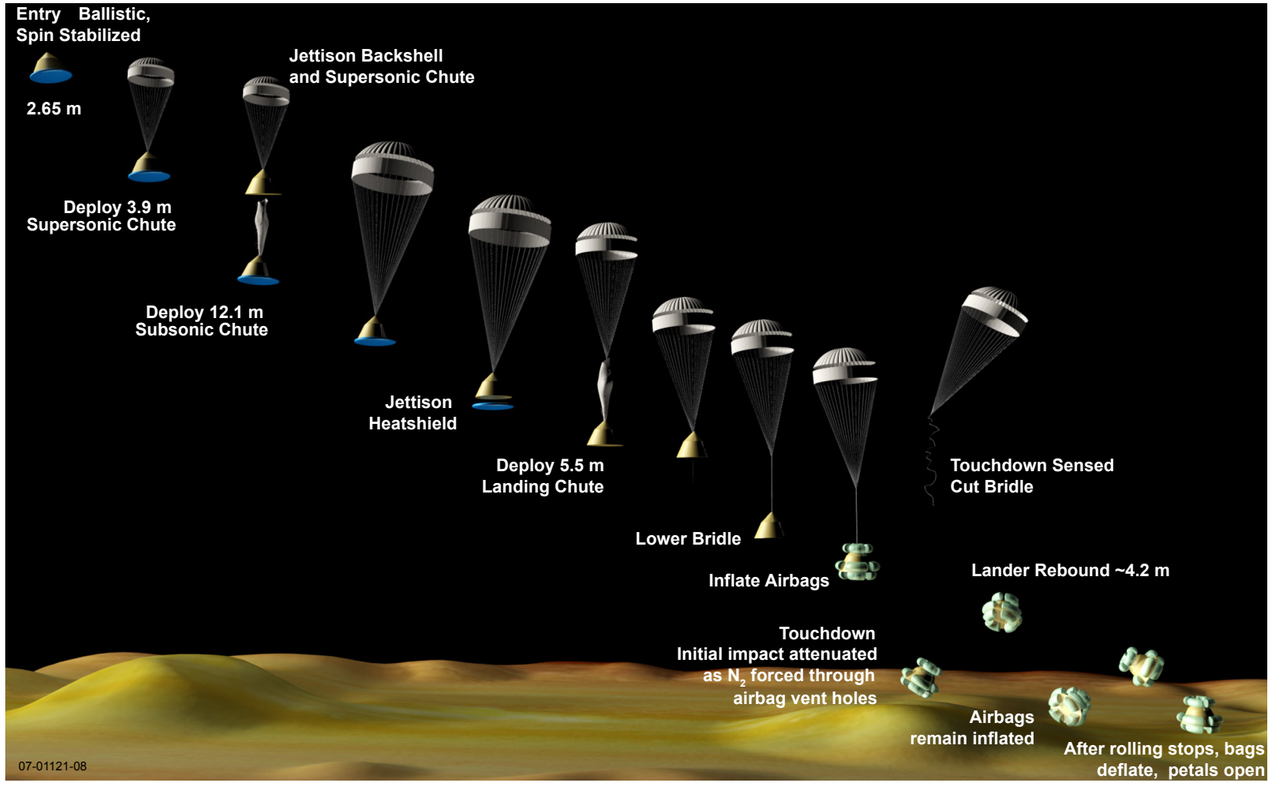

(A) Entry, Descent and Landing system has Huygens and MPF/MER heritage.

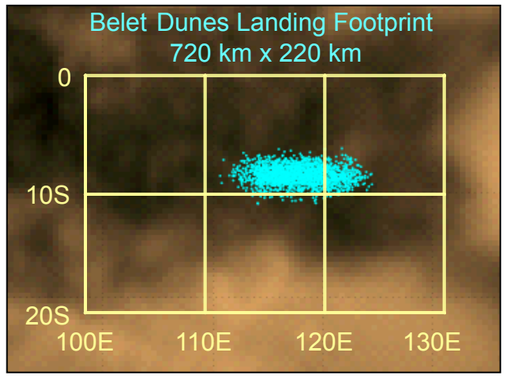

(B) Lander successfully lands well within ~1800 km x ~900 km Belet dune region.

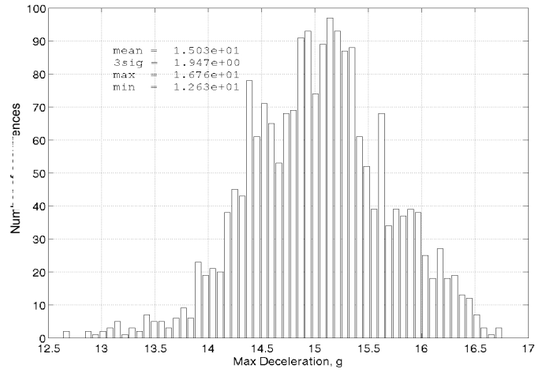

(C) Lander max entry g's < 18 g quasi-steady ASRG constraint.

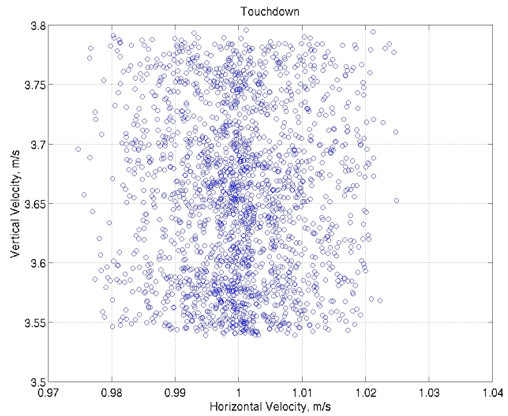

(D) Landing parachute is sized to provide touchdown vertical velocity <4 m/s, well within airbag landing capability.

4.7.5.3 EDL Flight Simulation Performance Results

A Monte Carlo trajectory analysis of the TE Lander, completed by NASA LaRC, shows that 100% of the trajectory cases touch down safely in the Belet dune region. Dispersions modeled include entry state dispersions, aerodynamic uncertainties, and atmospheric variability. The entry flight path angle dispersions are ±2.5º 3-σ based on the navigation analysis described in Section 4.3.4 above. TitanGRAM was used for modeling atmospheric variability and uncertainties. In addition, a Flasar mean wind profile was used with dispersions on wind azimuth and magnitude added. Uncertainties were also applied to the drag coefficients of the three parachutes.

Results of the Monte Carlo analysis show a landing footprint of 720 × 220 km within the Belet region, as shown in Foldout 4-7B. Performance indicators show the Lander system remains within all design requirements: The entry deceleration 3-σ high value is 17 g's (Foldout 4-7C); the dynamic pressures at the three parachute deploy points are less than 730 N/m^2, 290 N/m^2, and 15 N/m^2, respectively; and the velocities at touchdown are less than 4 m/s in the vertical direction and less than 2 m/s in the horizontal direction (Foldout 4-7D).

4.7.5.4 Landing System

As described in Section 4.7.5.2 and further described in Section 4.7.7.1, the baseline landing system includes an airbag system tailored to a Titan dune landing. Several approaches were considered for the landing system, and additional trades, described in Section 4.12.1, are recommended, including assessment of the crushable structure self-righting petal approach. The baseline design offers a robust landing design, and a cost and mass that are expected to encompass a range of candidate landing system designs. This range of options allows flexibility for further landing system trades outside the scope of the current study, without negative impact on the overall mission.

4.7.6 Lander Flight Software

The Lander flight processor is the same as that used in the Orbiter. As such, the Lander flight code shares many of the same C&DH functions found in the Orbiter software. The flight software supports command processing and distribution to instruments, collection of telemetry from instruments, the ability to execute stored time-tagged command sequences, and time management and distribution. Other standard flight software functions include managing memory objects, accepting uploads of objects or new software, compression of images, and SSR management.

As with the Orbiter, data on the recorder are managed in the form of files. CFDP is used for transmission of files to the Orbiter via relay radio, which in turn are transmitted to Earth during future DSN contacts with the Orbiter. Radio relay and CFDP are also used for receipt of files from the Orbiter, which can contain command sequences, uploaded memory objects, or software updates. The Lander flight software includes the autonomy evaluation engine described in the Orbiter software section. Stored autonomy rules define telemetry points to be monitored, the criteria for that data to indicate a fault, and the stored command sequence to be executed to perform corrective actions. The Lander G&C software provides g-triggers and timers for the EDL sequence. IMU data are recorded to permit after-the-fact trajectory reconstruction for science and engineering. Once landed, flight software controls the HGA to establish an RF link to the Orbiter when it is in view or to establish a DTE link for backup communication.

4.7.7 Lander Spacecraft Subsystems

4.7.7.1 Lander Structural/Mechanical Subsystem

The mechanical design and configuration of the Lander vehicle support entry, decent and landing in the dune terrain and science operations after landing. APL teamed with ILC Dover to develop an airbag landing concept appropriate for the TE requirements. The airbag design is shown inflated and to scale in Foldout 4-6C.

The airbag and parachute design have been successfully iterated to limit the landing forces to less than the ASRG requirement of 30 Earth g's. Once the Lander comes to rest, the airbags deflate, and the "petals" surrounding and protecting the internal Lander components open into the configuration depicted in Foldout 4-6A. Should the Lander's resting position be on its side, the petals right the design to the science operation configuration using the motor/spring hinge assemblies (calculated using geometry and center of gravity computations). Because they are small, the deflated airbags are trapped under the petals and do not impede science operations.

The Lander aeroshell has heritage from the Viking, MPF, MER, and MSL aeroshells in structure and TPS. Other TPS options are available, developed through ISPT, including the SRAM series TPS materials (SRAM 14, 17, 20) from ARA. The disk-gap-band parachutes have heritage from Viking, MPF, and MER.

Foldout 4-6A and 4-6D identify the science operations configuration, mechanical and structural design, and subsystem components. The lower deck provides simple, flat bolted mechanical and thermal interfaces for components. Access for ASRG installation is easily available with the petals open. Four struts that interface with the lower deck and terminate at a structural support ring provide petal support in the stowed condition. Deployment of the RF antenna and science robotic arms occurs after petal deployment. The Robotic Arm is based on the Mars Phoenix arm, but budget is allocated for the expected modifications to the existing design for seismometer and magnetometer deployment and to allow operation in the Titan cryogenic environment (see Section 4.13.3, Cryogenic Applications Technology). The RF system employs a space flight heritage antenna pointing gimbal stepper motor system. The stepper motor system requires heat for operation in the Titan cryogenic environment.

Packaging, mass, center of gravity, and volumetric studies have determined that this mechanical system can accommodate the required subsystems and science instruments in all configurations and within the volumetric constraints of the aeroshell.

4.7.7.2 Lander Power Subsystem

The Lander power system consists of two ASRGs, a single-fault-tolerant SRU, and a shunt radiator. The SRU is based on the New Horizons design and provides a regulated 28-V bus.

The ASRG is described in Section 4.6.7.3, Orbiter Power Subsystem.

The PSE is operational throughout the mission from launch. A single-fault tolerant design shunt regulator is selected to meet the long mission life. The SRU is based on the New Horizons SRU with modifications to accommodate the two ASRGs and is sized to process the BOL power of the two ASRGs. A more detailed description of the shunt regulator is provided in Section 4.6.7.3, Orbiter Power Subsystem.

Like the New Horizons power system, the Lander's power system has no battery. A large capacitor bank in the SRU supports switching inrush current transients and noise spikes. As on New Horizons, fast-acting semiconductor circuit breakers are incorporated in the PDU to detect and quickly isolate an overload condition. The Lander power bus is regulated.

4.7.7.3 Lander Thermal Control Subsystem

As with the Orbiter, the Lander's thermal control is managed during cruise by a redundant mechanical pump system connected to specifically designed space-facing radiator panels. Once on the Titan surface, thermal control is achieved using the waste heat from the ASRGs. Since the operating environment for the Lander is mainly cryogenic nitrogen at 1.5 atmospheres, low-thermal-conductivity open-cell foam-type insulation similar to that used for terrestrial insulation applications covers the external structure. Thermal design heritage and concept feasibility were demonstrated by an almost identical application when Huygens successfully used Basotect foam, manufactured by BASF, as the primary insulation. All gaps between insulating panels and other cutouts are closed using space-grade room-temperature-vulcanized (RTV) silicone. Natural convection transports the 1000 W of heat from the two ASRGs located on the Lander deck through the Lander. Appendages located outside of the vehicle core that must articulate are stowed in a "home" position, using heat from the vehicle core to maintain temperature control. Once the articulation is performed, the appendage returns to the home position. Radioisotope heater units (RHUs), in combination with foam insulation, are currently being evaluated as a means to augment the thermal designs of external components subject to the cryogenic atmosphere. This will be worked further in the Cryogenic Applications Technology effort described in Section 4.13.3.

4.7.7.4 Lander Communications Subsystem

The single-fault-tolerant Lander telecommunications subsystem is designed to communicate with the Orbiter via a UHF relay at rates between 2 and 8 kbps, depending on the slant range between the two vehicles. Each relay link is designed for 3-dB margin to a BER of 10^{-6} using rate ½ convolutional encoding. The UHF relay link utilizes an Electra-lite UHF transceiver with an SSPA transmit power of 8.5 W RF and, during the science phase, a hemispherical pattern UHF quadrifilar antenna.

The Lander also includes a 2-axis gimbaled 0.5-m HGA and LGA antenna pair with an X-band SSPA providing 15 W RF transmit power. The Electra-lite transceiver carries an X-band appliqué for both transmit and receive. This enables an enhanced relay link to the Orbiter using each vehicle's appliqué to achieve data rates between 32 and 128 kbps, depending on the slant range between the two. DTE telemetry data rates up to 250 bps are also available, either as a backup or an adjunct to the Orbiter relay link. If the Lander HGA experiences a failure and/or the Orbiter is free to point its 3-m HGA to the Lander, substantial relay links are still possible, even using the Lander's X-band LGA. A USO provides a stable reference for relay and DTE operations.

While the Lander is within its aeroshell during EDL, the relay signal is routed to a series of UHF patch antennas around the perimeter of the backshell using an RF transfer switch. The backshell antenna configuration is similar to that of the Orbiter, where the active antenna may be switched depending on the aeroshell entry attitude, except in this case the signal is monitored primarily by the Orbiter and not by an Earth ground station. Once the backshell separates from the Lander, the RF path to the backshell antennas is severed and the relay signal is routed to the quadrifilar antenna only.

4.7.7.5 Lander Attitude Control Subsystem

The Lander has no active attitude control system. It does, however, control the HGA to point towards the Earth or Orbiter. A small, low-cost, low-power MEMS IMU provides the data in conjunction with the Lander's science instruments, to determine the Lander's orientation on the surface of Titan. With a downloaded Orbiter and/or Earth ephemeris, the Lander can calculate the relative position of the Orbiter and command the HGA gimbal to point the HGA toward the Orbiter for data relay to Earth, or toward Earth for DTE communication, as necessary.

4.7.7.6 Lander Avionics Subsystem

The Lander IEM hardware is identical to the Orbiter IEM, configured by software. Since the power subsystem does not utilize a battery, fast-acting circuit breakers must be used to keep overloads from pulling the bus voltage too low. New Horizons design circuit breakers and switches are packaged in the RBSP form factor slices. These are used with the PDU power and control slices, as in the Orbiter.

4.8 Aerial Vehicle Flight System

4.8.1 Aerial Vehicle Key Driving Requirements and Features

Key driving requirements for the Aerial Vehicle, flowed down from the requirements listed in Section 4.2.2, include:

- 1-year Titan aerial flight
- Simple, low-cost, minimum-technology Pathfinder-type concept that meets science requirements
- Accommodation requirements for five Aerial Vehicle instruments
- Successful EDD
- Balloon buoyancy adequate to accommodate total float mass
- 1.7 kbps CBE science data rate for an Aerial Vehicle total science data return of 4.6 Gbits
- Power adequate to meet science requirements
- Allocation mass within that defined for Aerial Vehicle
- Package in aeroshell that fits volumetrically with cruise stack configuration
- Provide thermal control, including during cruise

Aerial Vehicle features are shown in Fig. 4-18.

4.8.2 Aerial Vehicle Key Characteristics

The Aerial Vehicle configuration, instruments, and components are shown in Foldout 4-8A and 4-8B, and the block diagram is shown in Foldout 4-8C.

4.8.3 Aerial Vehicle Resources, Contingencies, and Margins

Contingencies and margins are shown in Fig. 4-19 for mass, power and data downlink. Mass and power margins meet JPL requirements for allocations 43% above CBE. In this approach, the ASRGs are assumed to be Government Furnished Equipment, and no contingency or margin is allocated. System margins, however, are shown as percentages of total dry mass without subtracting the ASRG mass.

Feature	Benefit
5 science instruments plus aeroshell engineering instrumentation	Meets science requirements, provides engineering data for future flights
1 year aerial science	Meets science requirements
Montgolfiere balloon	Insensitive to small imperfections, damage to balloon
Aerial Vehicle altitude control	Robust to uncertainties in density, buoyancy; enables altitude change to locate desirable wind directions
Aerial Vehicle floats with zonal winds	Simple design, provides mobility over terrain
Balloon buoyancy (provided by MMRTG in balloon) is independent of gondola power and thermal sources (provided by ASRG in gondola)	Robust, decoupled design provides reliable power source and heat in gondola, plus dedicated thermal source to balloon.
Entry and descent heritage from Huygens	Reduces entry and descent risk
Technology task and cost included for balloon buoyancy, deployment and inflation, and system validation; includes cryogenic facility build	Enables TRL 6 prior to PDR, worked under Flagship Project

Figure 4-18. Aerial Vehicle features provide multiple benefits.

	Allocation	CBE	% Contingency	% System Margin
Mass	588 kg	418 kg	20%	18%
Power(by operating mode)	128 W (1 ASRG; 4 years EOL)	Met, Vis, Near-IR: 78 W Subsurface Radar: 54 W TDL: 89 W Comm: 81 W	13.4%	44% 109% 26% 39%
Data rate	3 kbps	1.7 kbps science	CBE rate includes 3-dB link margin	25% relay time; 30% data rate

Figure 4-19. Aerial Vehicle resource contingencies and margins meet or exceed APL and JPL practices.

4.8.4 Aerial Vehicle Representative Payload Accommodation

The representative Aerial Vehicle science payload directly addresses the measurement objectives requiring a mobile platform at several kilometers' altitude. It contributes to achieving global and surface science goals by providing measurements linking data at orbital and Lander scales. Fig. 4-20 lists the Aerial Vehicle instruments, mass and peak power allocations, and identified heritage proxies. Instrument details, including science objectives and measurement approaches, are provided in Section 2.

The Aerial Vehicle payload comprises a complementary set of five investigations with multiple capabilities for characterizing the atmosphere, surface, and subsurface of Titan. The Visible Imager system comprises a pair of wide FOV (60°) 1-Mpixel cameras pointed in nadir and off-nadir directions from the bottom of the gondola. At the low expected drift speeds (1–10 m/s), the maximum imaging rate is low (~0.01 Hz) at typical altitudes. Nevertheless the Visible Imager data volume (up to ~40 Mbits/h) is the largest of the Aerial Vehicle science payload. The Near-IR Spectrometer/Atmospheric Optics Monitor (NIRS/AOM) includes up- and down-looking spectrometers; a solar aureole camera, mounted near one edge of the gondola; and multiple Sun sensors arrayed on the gondola perimeter. The Subsurface Radar antenna is 3 m tip-to-tip and is deployed from a stowed position on one side of the gondola. The Subsurface Radar operates alternately as a science sounder (two channel) and an altimeter (high frequency only). During science operations the uncompressed data rate is relatively high (30 kbps), but the radar does not operate continuously as the imager does. The Tunable Laser Spectrometer (TLS) is also mounted to one side of the gondola, where it can directly sample the ambient atmosphere into a multi-pass absorption cell. The relatively high average (20 W) and peak (40 W) operational power is readily accommodated by the short integration time of 10 s per laser channel, permitting atmospheric

Instrument	Mass (kg)	Ave. Power (W)	Pk. Power (W)	Heritage Proxy	
Visible Imager	2	10	10	MSL	Visible Imager
Near-IR Spectrometer/Atmospheric Optics Monitor	7	10	15	Huygens	Near-IR Spec/Atmospheric Optics Monitor
Subsurface Radar Sounder	9	10	15	MRO	Subsurface Radar
Tunable Laser Spectrometer (incl. Nephelometer)	4	20	40	MSL Huygens	TDL Spectrometer (incl. Nephelometer)
Meteorology Package	3	2	4	Phoenix	Met Package
Totals	25	52			Totals

Figure 4-20. Aerial Vehicle instruments meet science requirements and scope the Aerial Vehicle accommodation requirements.

investigations to be duty cycled to manage the overall energy budget. The Aerial Vehicle Meteorology Package also provides point measurements, for both science and navigation. Temperature and pressure sensors are arrayed on the gondola perimeter to limit interference (no mast is required). Wind speed and direction changes are characterized with an acoustic anemometer and the IMU. The acoustic environment is recorded using a small microphone. Continuous meteorological measurements at a low rate yield ~200 kb per day. High-rate measurement modes (during density changes, cloud regions, etc.) are triggered selectively.

4.8.5 Aerial Vehicle Entry, Descent, and Deployment

4.8.5.1 Event Sequence

The EDD sequence is shown in Foldout 4-8D. Entry and descent are based on the heritage design from Huygens and the Viking, MPF, and MER Mars missions. The conceptual approach is defined here, and future work recommended in Section 4.12.3.

The TE Aerial Vehicle entry is ballistic and spin stabilized. The drogue parachute, the first of 2 disk-gap-band parachutes deployed, is mortar-deployed at approximately Mach 1.3 within the Mach dynamic pressure constraints defined during the Viking program. Deployment is controlled by a timer based on an entry g-trigger.

The main parachute is deployed by the drogue parachute, also triggered by a timer, such that deployment occurs at subsonic speeds of < Mach 0.8. The main parachute is sized to ensure successful separation of both the heatshield and the main parachute from the Aerial Vehicle.

Following pyrotechnic heatshield separation, the balloon is deployed by the main parachute. The gondola is released below the balloon to start the flow of ambient atmosphere (ram air) into the balloon. Shortly afterward, the main parachute is released. Parachute jettison timing is defined to ensure (1) that separation remains between the balloon/Multi-Mission Radioisotope Thermoelectric Generator (MMRTG) support structure and the gondola after the parachute is released; and (2) that the ballistic coefficient (with buoyancy included) mismatch between the Aerial Vehicle and the parachute provides a successful parachute separation.

As the air inflates the balloon and the heat from the MMRTG warms the balloon air, drag and buoyancy, respectively, slow the descent of the Aerial Vehicle. As the air in the balloon continues to be entrained and warmed, the balloon slowly descends to steady-state buoyancy at the design point of ~10 km to begin operations.

4.8.6 Aerial Vehicle Flight Software

The Aerial Vehicle flight processor is the same as that used in the Orbiter. The Aerial Vehicle flight code thus shares many of the same C&DH functions found in the Orbiter software. The flight software supports command processing and distribution to instruments, collection of telemetry from instruments, the ability to execute stored time-tagged command sequences, and time management and distribution. Other standard flight software functions include managing memory objects, accepting uploads of objects or new software, compression of images, and SSR management.

As with the Orbiter, data on the recorder are managed in the form of files. CFDP is used to transmit files to the Orbiter via relay radio, which in turn are transmitted to Earth during future DSN contacts with the Orbiter. Radio relay and CFDP are also used to receive files from the Orbiter, which can contain command sequences, uploaded memory objects, or software updates. The Aerial Vehicle flight software includes the autonomy evaluation engine described in the Orbiter software section. Stored autonomy rules define telemetry points to be monitored, the crite-

ria for data to indicate a fault, and the stored command sequence to be executed to perform corrective actions. The Aerial Vehicle flight software G&C control provides g-triggers and timers for the EDD sequence and to maintain vehicle altitude by controlling the balloon valve on the basis of altimeter data during the science mission phase.

4.8.7 Aerial Vehicle Spacecraft Subsystems

4.8.7.1 Montgolfiere Balloon

The Aerial Vehicle baselined for this mission incorporates a hot air, or Montgolfiere, type balloon (Fig. 4-21). Buoyancy is produced by heating atmospheric gas entrained in the balloon, thereby raising its temperature and lowering its density in comparison with the ambient environment. This method of buoyancy generation is relatively insensitive to small leaks in the balloon envelope. As Fig. 4-21 shows, the Montgolfiere balloon is vented to the atmosphere with a large opening at the top and bottom. A valve in the top opening, controlled by the flight computer with altimetry data from the subsurface sounder, provides buoyancy modulation through adjustable gas venting. The technique enables fine control of the Aerial Vehicle altitude.

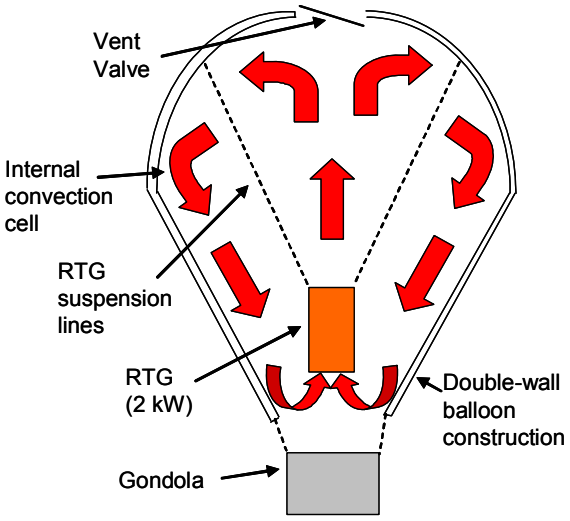

Figure 4-21. Titan Montgolfiere balloon utilizes MMRTG heat for buoyancy.

Hot air balloons are ubiquitous on Earth; heat is provided by propane burners located on top of the gondola near the throat of the balloon envelope. For the Titan application, the waste heat from an MMRTG provides the heat source. At Titan, significantly less heat is required than on Earth to provide the same buoyancy with the same size balloon (Jones et al., 2005). The cryogenic environment at Titan results in lower convective and radiative heat transfer coefficients, reducing heat loss from the balloon surface, and also greater buoyancy for a given temperature difference between the balloon internal temperature and the ambient temperature.

The MMRTG is located inside the balloon just above the bottom opening (Fig. 4-21 and Foldout 4-8A). The payload itself is in the gondola, which is suspended beneath the balloon and provides unobstructed views of Titan's surface and horizon for scientific observations. The balloon is fabricated from a cryogenic temperature compatible material developed by JPL and its industrial partners that consists of a polyester film and fabric laminate. Based on thermal analysis, a double-walled balloon design is used to insulate the warmer inside gas, thereby reducing the required heating power for the given float mass. Preliminary sizing characteristics of this design are presented in Fig. 4-22. As can be seen, the 12-m-diameter baseline balloon can float a 200-kg payload (beyond the mass of an MMRTG and the balloon envelope itself). Fur-

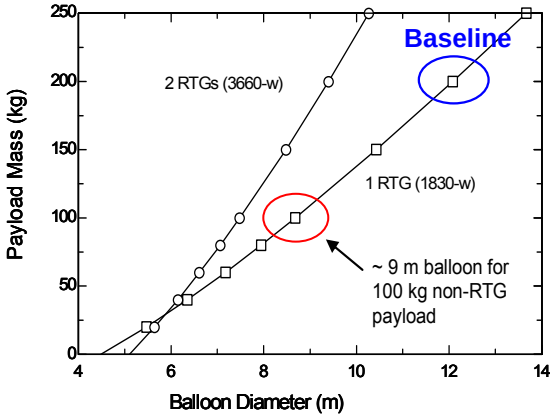

Figure 4-22. Balloon sizing curves.

FOLDOUT 4-8: Aerial Vehicle with Balloon

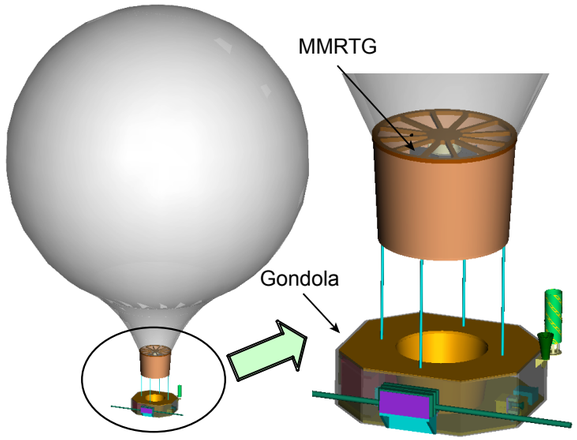

(A) Aerial Vehicle design provides capability to drift with winds for science measurements ~10km above Titan surface.

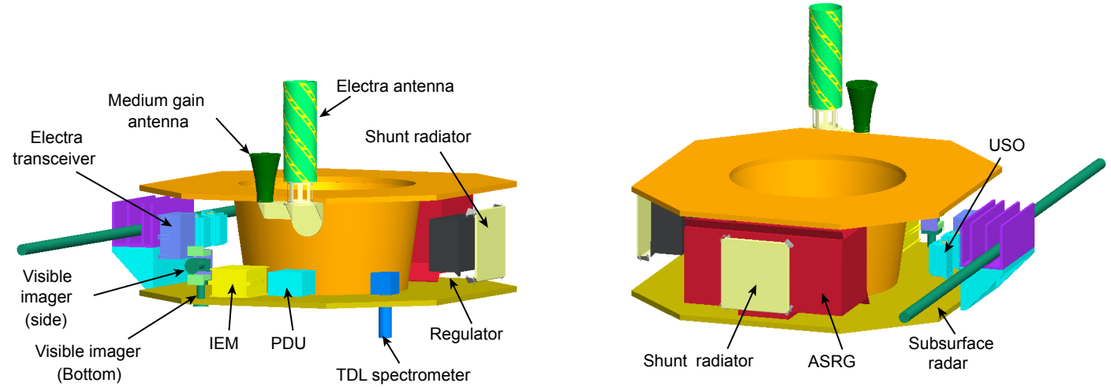

(B) Aerial Vehicle meets all instrument accommodation requirements.

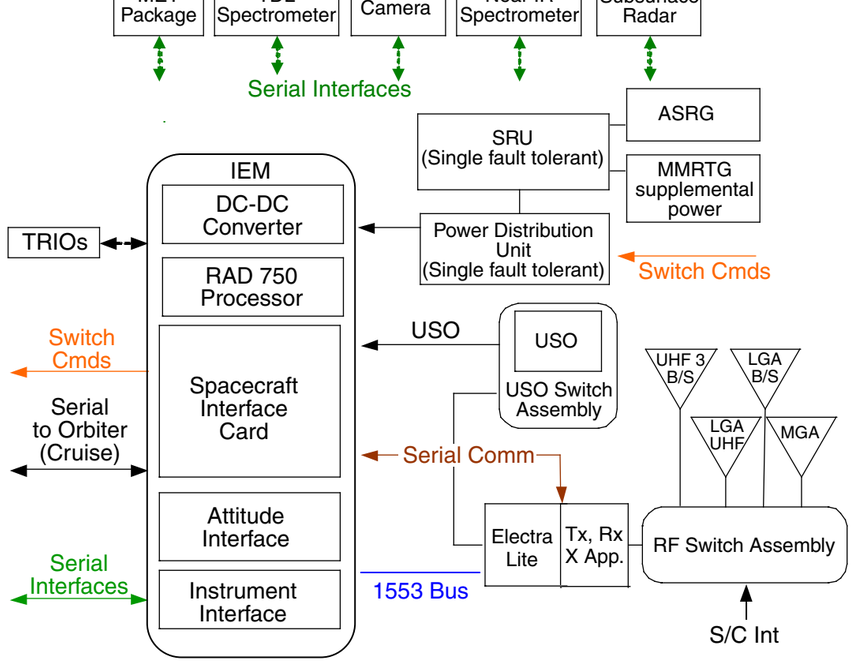

(C) Aerial Vehicle is a simple pathfinder-type design.

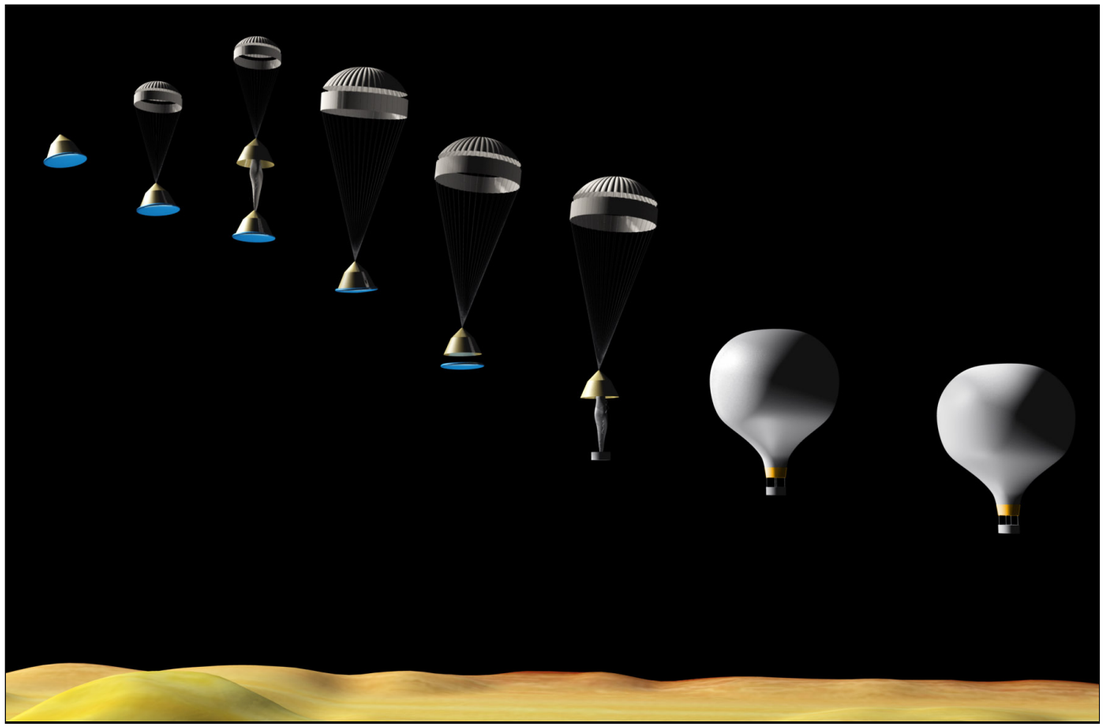

(D) Entry and descent system has Huygens, MPF, MER heritage.

07-05735-18

ther development of the balloon is recommended, as described in Section 4.12.4, Areal Vehicle Future Work, and Section 4.13.2, Titan Montgolfiere Balloon Technology.

4.8.7.2 Aerial Vehicle Power Subsystem

The Aerial Vehicle power subsystem consists of one ASRG, one MMRTG, a single-fault-tolerant SRU, and a dissipater shunt panel. The Aerial Vehicle and Lander SRUs are the same and are based on the New Horizons SRU design. The ASRG is described with the Orbiter power system, Section 4.6.7.3.

Although the Aerial Vehicle electrical power loads require power only from the ASRG, the potential for power augmentation from the MMRTG is provided. At MMRTG-qualified operating conditions, the electrical power for the MMRTG is 125 W at BOL and about 100 W after 14 years.

The PSE is operational throughout the mission from launch. A single-fault-tolerant design is selected to meet the long mission life. The SRU is based on the New Horizons SRU with small modifications to accommodate the ASRG and MMRTG.

The SRU and the shunt radiator are sized for maximum BOL power from the MMRTG and the ASRG. A more detailed description of the shunt regulator is provided in Section 4.6.7.3, where the Orbiter power subsystem is described.

As with the Lander, the Aerial Vehicle SRU includes a large capacitor bank to support switching inrush current transients and noise spikes, and the PDU incorporates fast-acting semiconductor circuit breakers to detect and quickly isolate an overload condition. The Aerial Vehicle power bus is regulated.

4.8.7.3 Aerial Vehicle Thermal Control Subsystem

Thermal control for the Aerial Vehicle gondola is similar in principle to that of the Lander. Basotect-type foam insulation wraps the external surfaces of the gondola. Natural convection transports the 500 W of heat removed from the single ASRG located on the lower deck of the gondola through the gondola. The MMRTG is used only for balloon operation and is not connected to the gondola for thermal management.

4.8.7.4 Aerial Vehicle Structural/Mechanical Subsystems

The Aerial Vehicle mechanical design and configuration are shown in Foldout 4-8A and 4-8B. The MMRTG, which provides heat for the required buoyancy during the science mission, is supported by a “wagon wheel” support ring located within the balloon. An electrical harness passes between the balloon and the gondola for valve control at the top of the balloon, and to bring supplementary power as available from the MMRTG to the gondola.

All of the Aerial Vehicle science instruments are packaged in the gondola, along with the bus components, as shown in Foldout 4-8B. The gondola mechanical design consists of an aluminum honeycomb aft deck, side panels, and top deck. A central cylinder connects the aft and top decks of the gondola and interfaces with the MMRTG/balloon interface ring and balloon deployment devices. The ASRG, which provides primary power to the Aerial Vehicle, is packaged in the gondola.

The Aerial Vehicle aeroshell has heritage from the Viking, MPF, MER, and MSL aeroshells in structure and TPS. Other TPS options are available, developed through ISPT, including the SRAM series TPS materials (SRAM 14, 17, 20) from ARA. The disk-gap-band parachutes have heritage from Viking, MPF, and MER.

Volumetric studies verify adequate internal volume for all subsystems in both the aeroshell/launch configuration and the flight operation configuration. Mass and center of gravity

estimates of the system (launch and deployed configurations) also confirm the validity of the packaging approach.

4.8.7.5 Aerial Vehicle Communications Subsystem

The Aerial Vehicle telecommunications subsystem is nearly identical to that of the Lander; the four distinct differences yield a simpler and lower mass and power design. (1) A medium gain horn antenna on the Aerial Vehicle replaces the 0.5-m HGA and LGA antenna pair on the Lander, which also eliminates the need for one RF transfer switch. (2) The UHF SSPA on the Aerial Vehicle provides 5.5 W RF transmit power, as opposed to the 8.5 W on the Lander, which reduces the Aerial Vehicle power load requirements. (3) The X-band SSPA provides 5.5 W RF transmit power on the Aerial Vehicle as opposed to the 15 W on the Lander, which reduces the Aerial Vehicle power load requirements. (4) The Aerial Vehicle telecommunication system is single string due to mass constraints, but selective redundancy may be inserted as the vehicle design is refined and accommodations become available.

The slightly lower UHF transmitter power results in a commensurate decrease in achievable relay data rate between the Aerial Vehicle and the Orbiter, ranging from 1 to 8 kbps, depending on the slant range between the two vehicles. The balloon material is RF transparent and it is assumed that the pattern of the quadrifilar antenna can tolerate the interference effects of the MMRTG and surrounding gondola structure, although further analysis is warranted to verify performance.

During the science mission, two-way Doppler information from the relay link between the Orbiter and Aerial Vehicle is downlinked to Earth to enable tracking of the Aerial Vehicle's position around Titan. The Electra-lite transceiver appliqués provide both transmit and receive capabilities at X-band, enabling a secondary path for obtaining tracking information directly from Earth. Direct tracking of the Aerial Vehicle from the ground is available over a limited range of Earth elevation angles using a zenith-facing medium gain horn antenna with a clear field of view of approximately ±20°. The X-band link also provides capability for transmitting very low data rate status tones as desired, and therefore an additional X-band LGA is carried on the backshell for potential Earth monitoring of the Aerial Vehicle signal during EDD. Emergency rate (7 bps) telemetry links may also be achieved over a further limited range of Earth elevations. A USO provides a stable reference for relay operations and for DTE status tone transmission.

4.8.7.6 Aerial Vehicle Avionics Subsystem

The Aerial Vehicle IEM shares the processor, spacecraft interface, instrument interface, and power supply card designs with the Orbiter and Lander. The attitude interface card is not needed. These cards are packaged in a shortened version of the chassis to reduce mass. Processor speed is adjusted to match the available power. Differences in the instrument suite are easily accommodated by minor changes to the field programmable gate arrays on the instrument interface card as necessary. Unused functions such as the FPM and unused interface circuitry are not populated.

The PDU uses the same slice-based design used on the other vehicles, but with significantly fewer slices required. The boards are selectively depopulated to reduce power and mass and to improve reliability.

4.8.7.7 Aerial Vehicle Attitude Control Subsystem

The Aerial Vehicle has an ACS to maintain the altitude above the Titan surface consistent with science requirements. The subsurface radar provides the necessary altitude measurements, and the balloon's thermal vent is controlled to raise or lower the altitude, as necessary. The alti-

tude and altitude tolerance can be set by uploadable parameters, enabling adjustments to optimize science data collection.

4.9 Assembly, Test, and Launch Operations

Assembly, Test, and Launch Operations (ATLO) for the Titan project are conducted in four phases: (1) Trailblazer verification, (2) vehicle integration and test, (3) vehicle environmental test, and (4) field operations at Kennedy Space Center/Cape Canaveral Air Force Station, culminating in the launch. Each phase is discussed separately below.

4.9.1 Trailblazer Verification

Because of the size and mass of the integrated Vehicle Assembly (Cruise Stage, Orbiter, Lander, and Aerial Vehicle); the complexity of the mechanical, thermal, and electrical interconnections; and the numerous RPSs a complete Trailblazer verification of the field operations at KSC/CCAFS is warranted. The Trailblazer is a flight-like mechanical build of the four vehicles and their electrical interconnects. Sufficient fidelity of the mechanical build is required to verify the flight design and integration operations for RPS installation, separation interfaces for vehicle mate, thermal subsystem interconnects, aeroshell integration, launch vehicle mate, and fairing installation. Sufficient fidelity of the electrical interconnects is required to verify umbilical interfaces between the vehicles and with the launch vehicle.

The Trailblazer verification simulates a full mechanical integration sequence in the facilities planned for the flight campaign. This approach is necessary to verify floor space requirements, crane requirements, access requirements, transportation, and pad operations. The electrical integration sequence verifies access of flight plugs, link connectivity throughout the processing sequence, and pad closeout activities. The RPS integration sequence verifies nuclear and personnel safety and transport system operations. The Trailblazer occurs early in the design flow to allow incorporation of lessons and modifications of the flight designs.

4.9.2 Vehicle Integration and Test

The four vehicles, Cruise Stage, Orbiter, Lander, and Aerial Vehicle, are processed in parallel. Each follows a methodical, hierarchal I&T approach designed to verify requirements and uncover potential problems early, reducing risk during both system-level integration and flight operations. This I&T approach has heritage on numerous planetary spacecraft.

Class A requirements are followed for all vehicles (separate prototype and flight hardware). Testing starts at the breadboard level where all designs undergo interface compatibility testing prior to release for flight fabrication. Piece parts, components, and boards are environmentally tested at stress levels higher than those the system encounters in test or operation. Instrument and spacecraft components are fully tested, both functionally and environmentally, before delivery for system integration. These practices are proven techniques to find problems early and minimize problems at system-level integration.

Integration of each vehicle occurs in facilities adequate for unique cleanliness requirements. The Cruise Stage and Orbiter are planned for Class 100,000 cleanliness, with localized higher cleanliness requirements met by special-purpose enclosures and continuous purges. The Lander and Aerial Vehicle are planned for Class 1,000 cleanliness, following Huygens mission practice.

Integration of a vehicle begins with delivery of the flight-qualified primary structure, which already includes the propulsion system, as appropriate to the specific vehicle. The spacecraft harness is then installed and tested to ensure that flight hardware can be integrated safely. Pre-Integration Reviews are held for each vehicle component and instrument. The integration team

reviews the results of the component or instrument testing program and plans for mechanical and electrical integration with the vehicle.

During the integration program, several special tests are conducted. These include RF compatibility tests, time system verification tests, special guidance and control tests, system self-compatibility tests, mission simulations including aerocapture, EDL, and EDD sequence tests, and jitter tests, as appropriate to the specific vehicle. Comprehensive performance tests (CPTs) are performed using a proven "test as you fly" approach and include a minimum set of mission operations tests. All command execution and telemetry evaluation is performed at the Mission Operations Center. System-level test equipment provides power and stimulates all sensors to test each vehicle throughout the I&T flow.

4.9.3 Space Vehicle Environmental Test

The environmental test program exercises the four vehicles in the launch and in-orbit environments. After a Pre-Environmental Review, the spacecraft vibration test is performed with each vehicle in its launch configuration, followed by acoustic test and shock/separation tests. Next are mass properties measurements (performed with the vehicle tanks filled with simulant, as appropriate to the design). Finally, the thermal balance and thermal vacuum cycling tests are conducted. During the thermal cycling tests, the Compatibility Test Trailers are used for RF compatibility tests and mission operations end-to-end simulations. CPTs are run prior to the thermal vacuum tests, during the thermal cycling test, and after the thermal cycling test. In addition, deployment tests and mechanical alignments are completed before and verified after completion of the environmental program. Electromagnetic compatibility testing is performed to verify vehicle-to-vehicle and vehicle-to-launch vehicle compatibility.

4.9.4 Field Operations

After Pre-Ship Review, field operations commence with the arrival of the vehicles, ground support equipment, and personnel at the launch site facilities that were used during the Trailblazer verification. Final vehicle preparation consists of a series of final inspections, deployment tests, vehicle final cleaning, thermal system closeouts, and subsystem checkouts. System-level vehicle testing, including a final CPT, occurs. The mission operations team completes mission simulations and DSN/ground station testing using MIL 71 at KSC. Vehicle fueling, ordnance installation, spin balance, and flight blanket installation are completed, as required.

Integration of the four vehicles occurs in the sequence demonstrated by the Trailblazer. RPS integration is discussed specifically in Section 4.9.4.1. Final electrical interconnects are performed prior to aeroshell encapsulation. Final thermal subsystem interconnects are performed, and the aeroshell is then closed. After aeroshell closure, vehicle commanding and monitoring are performed through the launch vehicle umbilical.

Launch vehicle integration occurs with a series of operations such as fairing encapsulation, vehicle mating, communication and ground system checkouts, launch vehicle and payload compatibility tests, and power monitoring. Vehicle purges are also monitored, maintained, and serviced from arrival through launch vehicle integration and up to launch vehicle main engine commit. The vehicle launch teams participate in mission dress rehearsals to thoroughly test the communication links and polling organizational structure required for success on launch day. Final steps prior to launch are a Launch Readiness Review and red-tag item removals. On launch day, proven countdown procedures are used to ensure configuration and readiness for launch.

4.9.4.1 RPS Integration

An evaluation was performed to address the concern that the TE mission does not lend itself to launch pad integration of nine RPS sources. Leveraging previous New Horizons RPS system integration experience and familiarity with the Atlas V launch campaign and associated ground processing operations, an alternative RPS integration is proposed.

We recommend that TE mission complete RPS integration into the vehicles at the Payload Processing Facility (PPF) prior to the start of launch vehicle fairing encapsulation operations, and then transport the integrated Vehicle Assembly encapsulated within the fairing to the pad for launch vehicle mate. The payload processing flow for Atlas V-class launch vehicle encapsulates the payload inside the fairing and transports the fairing/payload system to the pad under temperature and contamination control. TE uses those successful, existing redundant air conditioning and power source systems and, if needed, augments them with additional redundancy to ensure additional margins exist for transporting both the payload and RPS systems assembled as the integrated Vehicle Assembly to the pad for mating with the launch vehicle.

A preliminary study has found several significant advantages with this proposed process. An obvious advantage is that RPS integration is removed from the launch vehicle flow until the payload-to-launch vehicle mate occurs. This alleviates concern that issues found in RPS integration and corresponding vehicle checkout will surface on the pad, and it allows resolution prior to payload/fairing transport and launch vehicle integration. Personnel hazards from radiation are minimized when RPS units are installed at the PPF, where the space confinements of a fairing are not present. While further study is needed, hot-fit checks associated with heritage RPS integration may also be eliminated by going to a single flight mate occurring off the launch pad. Hazardous and security-related operations, previously applied to both payload and RPS transport-to-the-pad, are reduced to a single transport operation. Multiple hazardous operations required for pad crane operations (payload and RPS hoisting) are reduced to a single lift operation. The requirements to perform an end-to-end nuclear and personnel safety assessment, complete a Trailblazer operation, identify and apply risk reduction methodology, and secure the interagency approvals required for any RPS mission are recognized for this mission. However, these required processes are not likely to be more difficult than those employed for New Horizons.

4.10 Operational Scenario

The end-to-end operational data flow is shown in Fig. 4-23.

4.10.1 Orbiter Operational Scenario

Orbiter operating modes, shown in Fig. 4-24, are defined to support the science campaigns described in Section 2. The total Orbiter science data return is 3.4 Tbits for the 4-year mission. DTE communication can be accommodated simultaneously in all operating modes without duty cycling the instruments, except for the SAR and Altimeter Map Campaigns. During these campaigns, the HGA is used for SAR or Altimetry on the night side and DTE on the day side, facilitating power load management and SAR/Altimetry data downlink management.

4.10.2 Lander Operational Scenario

Conditions influencing the Lander science sequencing include:

- Continuous Seismometer, Magnetometer, and Meteorology Package operation
- Power duty cycling of the Chemical Analyzer with other science and with relay communications
- Lighting conditions for imaging
- Surface sampling/ground interaction timing

- Time from surface sample acquisition to Chemical Analyzer delivery
- Panoramic image data size
- Lander/Orbiter contact time
- 2.9 kbps CBE relay to Orbiter (UHF) for 5.5 Gbits returned in 1 year; 18 kbps CBE relay to Orbiter (X, HGA) is available as an option for 36 Gbits returned in 1 year

An initial estimate of the data set that can be obtained and downlinked during the 1 year of Lander operations, for the total Lander mission data return of 5.5 Gbits, is shown in Section 2.7.1.

4.10.3 Aerial Vehicle Operational Scenario

The Aerial Vehicle altitude is autonomously controlled using the Subsurface Radar Sounder, in altimeter mode, and the balloon valve. A combination of surface feature recognition, tracking data, and IMU data is used to locate the Aerial Vehicle relative to Titan's surface. Further development of this approach is included in the planned technology development and is described in Section 4.13.2.

The Aerial Vehicle science data relay rate of 1.7 kbps CBE results in a total science data return of 4.6 Gbits for the 1-year Aerial Vehicle mission. The science data set that can be obtained and downlinked is shown in Section 2.7.2. To optimize use of the Aerial Vehicle data rate relay to the Orbiter, data compression, downlink of thumbnail images for selection of higher-resolution image downlink, and stacked subsurface sounder profiles are planned. Further definition of the data flow is recommended for future work.

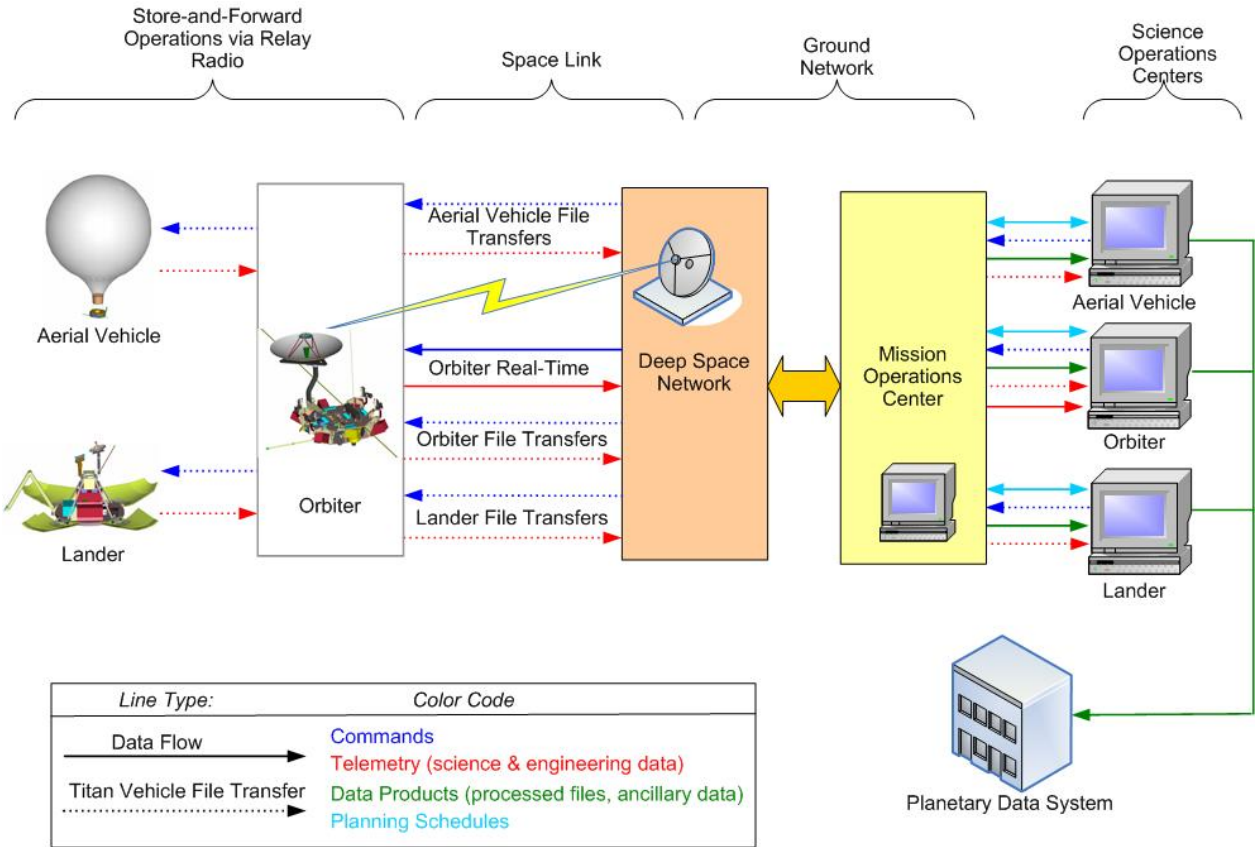

Figure 4-23. TE end-to-end operational data flow.

Science Campaigns:	Aerosampling	Atmosphere	Ionosphere	SAR Map, Altimeter Map		Instrument Articulation	S/C Roll Req'd	Instrument View	Radiator View
				Spectral Map					
Operating Modes:	**Aerosampling**	**Atmosphere**	**Ionosphere**	**Surface - Day**	**Surface - Night**				
Spectral Mapper	No	Yes	No	Yes**	No	Yes (Nadir to Limb)	Articulation and/or S/C Roll	0-10° off-Nadir /Limb	Cold Side
IR Spectrometer	No	Yes	No	No	No	No	Yes - Atmos, Ionos	Nadir/Limb	Cold Side
1 Micro, Vis Camera	Yes	Yes	Yes	Yes	Yes	Yes (Nadir to Limb)	Articulation and/or S/C Roll	Nadir/Limb	
UV Spectrometer	No	No	No	No	No	No	Yes - Occul	Limb	N/A
Energetic Particles	Yes	Yes	Yes	Yes	Yes	No	No	Omni	N/A
Langmuir Probe	Yes	Yes	Yes	Yes	Yes	No	No	Ram	N/A
Plasma Package	Yes	Yes	Yes	Yes	Yes	No	No	Ram	N/A
Ion/Neutral Mass Spec	Yes	No	Yes	Partial	Partial	No	No	Ram	N/A
Magnetometer	Yes	Yes	Yes	Yes	Yes	No	No	Omni	N/A
SAR/Altimeter	No	No	No	No	Yes	No	No	<10°off-Nadir /Nadir	N/A
Subsurface Radar /Ionosphere Sounder	No	No	Yes	Yes	Yes	No	No	Nadir	N/A
Microwave Spec	No	Yes	No	No	No	Yes: Nadir to Limb	Articulation and/or S/C Roll	Nadir/Limb	N/A
S/C Roll Required	No	Yes	Yes	No	No				
DTE Communication*	Yes	Yes	Yes	Yes	No				

* 8 hours per Earth day on Titan day-side ** Titan day-side only

Figure 4-24. Orbiter operational scenarios meet science requirements.

4.11 Planetary Protection

Following are the planetary protection guidelines provided for this study. All but the bold italic and "Future" Planetary Protection guidelines are met by the TE mission. The TE orbit cannot be maintained beyond the effective lifetime of the heat source. Because the planetary protection guidelines for Titan have not been finalized for this mission, NASA HQ recommended that the planetary protection guidelines be shelved for this study. The study followed that recommendation.

Current

- Category II, with additional requirements of Class 100,000 clean room assembly and organic material accounting (based on Cassini)
- Lander/Balloon: in addition, assemble using Class 1000 clean room procedures (based on Huygens)
- End-of-mission scenarios that account for the disposition of a radioisotope power source (RPS) may choose to
  - demonstrate orbital lifetime beyond the effective lifetime of the heat source,
  - burn-up/breakup analysis demonstrating that the RPS would not create a biological contamination concern, or
  - directed disposal of the spacecraft ***into an object that is not of concern for biological contamination.***

Future

- Additional requirements may be necessary:
  - For specific mission concepts, depending on mission objectives (e.g., subsurface access), and state-of-knowledge of Titan at that time.

- Subsequent to current Categorization (late 1980s), additional data regarding cryovolcanism have been gained, which may result in the identification of "special regions" on Titan that could permit the growth of Earth microbes.

4.12 Major Open Issues and Trades

Recommended future work is defined in general and by vehicle below. Priorities will depend on the objectives for the follow-on studies.

4.12.1 General – Future Work

- *ASRG vs. MMRTG:* The impact of changing from ASRGs to MMRTGs, if required, should be assessed in further detail. Thermal management during cruise will be affected by the higher thermal output. RPS and structural mass, and power available, are also affected.
- *Planetary protection:* The following work is recommended.
  - Planetary protection requirements definition
  - Assessment of localized heating from RPS on the Titan surface for the Lander, the Orbiter after end-of-life entry, and the Aerial Vehicle after end-of-mission landing
  - Assessment of mitigation approaches to meet requirements
- *ASRG-induced environments:* Assess ASRG effects on vehicle subsystems and instruments, including vibration, microphonics, thermal, and radiation (discussed in Section 4.4) effects. Develop mitigations.
- *Earth entry analysis:* Complete an initial probability of Earth entry analysis. Utilize results to guide definition of derived requirements on mission design and flight system, including Earth flyby distances and micrometeoroid protection, to meet the $<1 \times 10^{-6}$ probability of Earth entry requirement.
- *Thermal management system:* Complete an additional design iteration on the thermal design, particularly for cruise.
- *Backup launch date launch period analysis:* Complete higher-fidelity analysis of backup launch dates, including launch period analysis to ensure that any required modifications to the baseline flight system are accommodated.
- *Storage lifetimes:* Address storage lifetimes, in particular for deployables, rotary joints, etc. Assess design solutions for minimizing these components.
- *Navigation:* Complete navigation analysis sensitivities, including assessment of VLBI and optical navigation, Titan approach sequence margin, and flight system design.
- *Aeroheating and TPS:* Higher-fidelity aeroheating analyses of the Orbiter aerocapture and of the Lander and Aerial Vehicle entries is recommended. TPS selection and sizing based on higher-fidelity results is needed.
- *Aeroshell configuration:* Complete aeroshell configuration trade including 60° sphere cone, 70° sphere cones, and Apollo geometries.
- *Mission and science operations:* Refine definition of mission and science operations, data management, and ground data system requirements.
- *TitanGRAM:* Update TitanGRAM with Cassini/Huygens data for use in analyses of Orbiter aerocapture, aerosampling, circular orbit; Lander EDL; and Aerial Vehicle EDD and flight. Refine winds model for EDL, EDD, and Aerial Vehicle flight.

4.12.2 Orbiter – Future Work

- *Instrument accommodation:* Assess in greater detail the reference instrument accommodation requirements, including pointing accuracy and jitter/stability.

- *Aerosampling: Complete* Monte Carlo trajectory analyses and aero/aeroheating analyses of the aerosampling phases to refine the aerosampling concept of operations and ΔV requirements.
- *HGA for combined DTE and SAR/Altimetry vs. dedicated SAR/Altimetry antenna:* Assess alternative approaches to the baseline on the basis of performance, accommodation on the Orbiter, reliability, and risk.
- *Monopulse:* Trade monopulse with standard open-loop data downlink. Complete higher-fidelity definition of monopulse system and operations.
- *Lift-to-drag ratio:* Baseline navigation results indicate that aerocapture L/D can be reduced while maintaining significant margin. Revisit L/D requirements and reduce from L/D = 0.25 as appropriate.
- *Battery:* Further address battery performance for large number of cycles after a long-duration cruise.
- *Propulsion:* Trade bi-prop vs. mono-prop.
- *Technology plan:* Define launch approach for aerocapture flight demonstration.

4.12.3 Lander – Future Work

4.12.3.1 Landing System

As described in Section 4.7.5.2 and 4.7.7.1, the baseline landing system includes an airbag system tailored to a Titan dune landing. Several approaches were considered for the landing system as described below. Additional trades and higher-fidelity analyses outside the current study scope are recommended.

Landing Systems Considered

Crushable structure with self-righting petals: this design assumes minimal bounce at touchdown and uses a crushable structure to dissipate the energy. If the Lander slid and/or tumbled down the dune slope, the self-righting system would right the Lander. This design can be further assessed for dune landing. Technology work is required to develop the crushable structure, test and simulate landing dynamics, and verify the structure in a cryogenic environment. The crushable structure approach is recommended for further studies, and may be robust for the Titan dune terrain landing. If the performance results are positive, it is likely to be simpler and lower in cost than the baseline.

Baseline design: Vented airbags inflated with self-righting system: this design is more robust to uncertainties in the terrain (surface hardness, slope stability, small hazards, etc.) and encourages the Lander to roll down the dune slope to a "safer" terrain prior to self righting. Additional airbags can be added to completely cover the Lander if increased robustness to hazards is needed. Technology cost is included in the TE costs through the Cryogenic Applications Technology and Landing System Technology activities.

MPF/MER-type airbag design, either fully enclosed in airbags or not, including gas generator inflation. This design would require an altimeter like that on MPF/MER for timing of the gas generator inflation to accommodate the effects of cooling and contraction of the gas during landing. Technology verification of the airbag inflation and performance in the cryogenic environment would be required.

A design similar to Huygens[2] in concept was also considered – a crushable structure without self-righting. While this design is the simplest, it assumes that the Lander does not tumble on impact and therefore includes no self-righting system. It is not considered robust enough for the 30° sloping dune terrain.

4.12.3.2 Lander: Other Key Items for Future Work

- *Detailed technology plans:* Initial estimates of the scope and cost of the technology plans are provided as part of this study. More detailed technology plans can be developed and are recommended for the Cryogenic Applications and Landing System.
- *EDL:* Conduct further EDL design sensitivity studies, including analysis of sensitivity to winds for landing design and parachute release design; assess need for landing parachute separation augmentation for dune landing region; and conduct parachute trades including number of parachutes and deployment timing.
- *Science operations:* Complete further definition of Lander science operations sequencing and coordination with Orbiter relay communication schedule.
- *Alternative parachutes:* Consider ring-sail parachutes as an alternative subsonic parachute design for higher efficiency than the disk-gap-band parachutes. A ring-sail parachute has been tested through the Mars Technology Program.

4.12.4 Aerial Vehicle Design – Future Work

4.12.4.1 System Definition

The TE Aerial Vehicle design adopted the conservative approach of decoupling the balloon thermal source from the gondola power and thermal source. In addition, a complete MMRTG was assumed for the thermal source inside the balloon. Several variations on this approach can be traded, and such trades are recommended for future work. The balloon thermal source could be reduced to a set of GPHS units within a mission specific mounting/cooling system. Or the MMRTG within the balloon could be insulated to ensure that its temperature remained inside qualification limits in the Titan cryogenic balloon environment. The MMRTG could then serve as the power source for the Aerial Vehicle as well as the balloon thermal source, instead of carrying the ASRG in the gondola. In this scenario thermal augmentation in the gondola and/or more advanced insulative systems for the gondola may be needed.

The required location of the MMRTG (or alternate heat source) within the balloon is a topic included in the Technology Section below. Alternative mounting approaches can be considered that correspond to the location requirements.

4.12.4.2 Aerial Vehicle: Other Key Items for Future Work

- *Detailed Technology Plans:* Initial estimates of the scope and cost of the technology plans are provided as part of this study. More detailed technology plans can be developed and are recommended. Further development of the Aerial Vehicle technology plan is recommended to include an assessment at a detailed level of the testing that can be done in existing facilities and with field testing using possible similarity parameters for Titan cryogenic environment simulation. The objective is to determine if TRL 6 can be achieved without a new large-scale cryogenic facility. If the new facility is needed, a detailed test definition and facility requirements, and corresponding cost and schedule, should be developed.

[2] Post-impact operation was not a requirement on Huygens, beyond the provision of a data link and energy budget for 3 min.

- *Aerial Vehicle EDD:* Develop EDD simulation models, including inflation and buoyancy transient model. Complete EDD analyses and design sensitivity studies.
- *Science Operations*: Complete detailed definition of Aerial Vehicle science operations sequencing and coordination with Orbiter relay communication schedule.
- *Flight Software:* Onboard trending and decision making to determine which data are scientifically interesting, and thus give those data higher priority for downlink.

4.13 Technology Needs

The cost to bring each component of the Cruise Stage, Orbiter, Lander, and Aerial Vehicle to TRL 6 by PDR is included in the project development cost, except for the star trackers selected. If the star trackers do not reach TRL 6 by project start, alternate trackers will be selected from a wide variety of alternatives. Technology development plans for aerocapture, Titan Montgolfiere balloon, cryogenic applications, Lander definition, and RPS qualification are detailed below and costs itemized separately.

4.13.1 Aerocapture Technology

Objective: Achieve TRL 7 (space flight validation) for aerocapture technology using a low lift-to-drag aeroshell vehicle suitable for the TE mission.

Approach: The recommended approach is identical to that developed under the New Millennium Program ST9 Aerocapture Phase A study and flight test proposal. The premise of ST9 Aerocapture was that aerocapture is a mature technology that only requires an end-to-end flight test experiment to validate the aerocapture guidance system. The NASA HQ review of the ST9 proposal agreed with this assessment with the understanding that some advanced simulation work and hardware-in-the-loop guidance testing would be performed as part of the normal engineering development for the flight mission. TE includes the scope of the aerocapture demonstration as proposed in ST9 as the aerocapture technology demonstration under the TE project.

The aerocapture demonstration features a short-duration Earth orbit experiment as outlined in Fig. 4-25. The experiment uses aerocapture to precisely target a low-apogee orbit given a very high apogee starting trajectory. The guidance system is based on bank angle control of a low lift-to-drag (L/D ~ 0.2) blunt-body aeroshell, the same approach needed for aerocapture at Titan. The

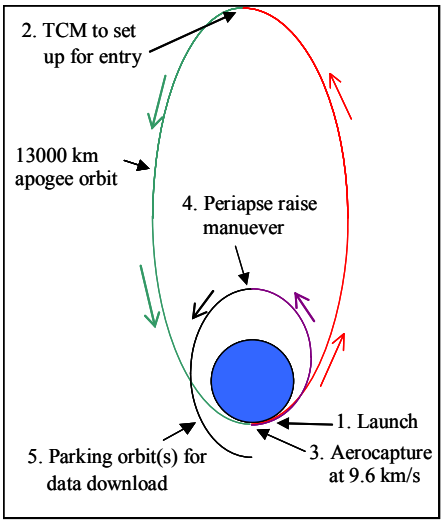

Figure 4-25. ST9 aerocapture mission profile.

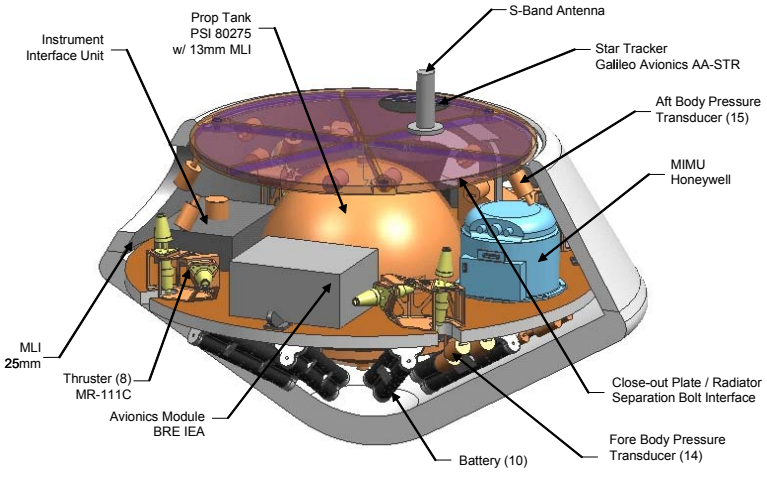

Figure 4-26. ST9 aerocapture vehicle.

test vehicle (Fig. 4-26) is a 1.2-m diameter, 3-axis controlled spacecraft with a CBE mass of 161 kg (wet). Primary batteries provide all electrical power for the 9.1-hour mission. The returned data volume is 10.8 Mbits, consisting of guidance and aerothermodynamic data.

Schedule: The ST9 Aerocapture flight project requires 42 months from start of Phase B through launch. Phase B is 14 months, Phase C is 28 months.

Cost: $107M (FY07) for the test vehicle, plus an amount to be determined for access to space (dedicated launch or secondary payload).

4.13.2 Titan Montgolfiere Balloon Technology

Objective: Achieve TRL 6 for the Montgolfiere balloon system through combined analysis and ground test program that culminates in cryogenic temperature testing of a full-scale prototype.
Approach: This technology development plan is structured as a risk mitigation program. A list of Montgolfiere balloon technical risks has been compiled and cross-indexed to analysis and test activities needed to address them and exit criteria for their retirement. Fig. 4-27 lists the top five risks as they are understood today. Risk levels for the Balloon Technology Development Plan are included in Section 4.14.10, Risk Management (see Foldout 4-11).

Much of the Montgolfiere balloon technology development can be done with analysis or room temperature experiments. However, achievement of TRL 6 requires relevant environment (80K) testing of full-scale (~10-m diameter) prototype balloons. A cryogenic test facility enough to accommodate this testing must be designed and constructed as part of the technology development activity. It is presumed that the prototype balloon will be constructed from the cryogenic balloon material already developed by JPL and its partners.

Cost: $30–$50M ($50M FY07 budgeted), including the cost of designing and building a new cryogenic test facility.

4.13.3 Cryogenic Applications Technology

Once in the Titan atmosphere, the Aerial Vehicle and Lander are subject to cryogenic environmental conditions. Hardware packaged inside either of the vehicle enclosures experiences somewhat benign environmental conditions. Hardware that is externally packaged must be thermally qualified to ~80 K to demonstrate survival and/or function in this environment. Three candidate areas, MMRTG, airbag system, and motor systems, have been identified as requiring cryogenic qualification testing as a result of this study.

The Aerial Vehicle uses the MMRTG primarily for balloon buoyancy and not for electrical power generation. Modifications to the MMRTG may be required to increase the case temperature. Independent of electrical output, the MMRTG will be temperature qualified in a simulated

48-month schedule:

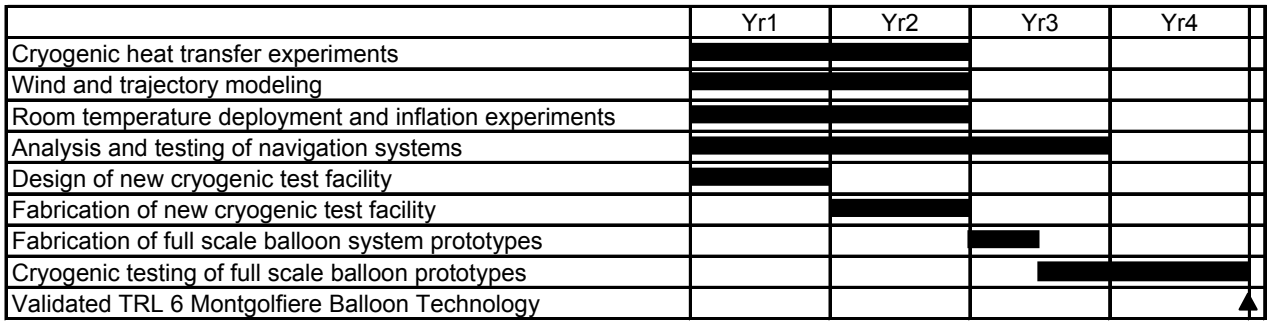

Titan environment to verify that the GPHS is unaffected by the cryogenic environments and that the expected heat is available for balloon operation.

The airbag system must be demonstrated in the cryogenic environment.

Motor systems are used to operate the sample drill and the HGA on the Lander. Because motors are typically qualified to –55°C, design, development, and qualification testing of a motor system to be used in cryogenic environments is needed.

36 months and $20M (FY07) are allocated for the cryogenic applications demonstration.

4.13.4 Lander Definition Technology

In addition to the cryogenic applications work described in the preceding section, development and testing of the landing configuration are needed for proof-of-concept, including tests to simulate landing conditions. 24 months and $5M (FY07) are allocated for the lander systems demonstration.

4.13.5 RPS Qualification

The ASRG must be qualified for the Titan environment. An extra ASRG purchase and $7M (FY07) for analysis are included as placeholders for the work per the study guidelines. A full MMRTG is included as the heat source for the balloon. Since no electrical power is required, there are no special qualification requirements for power. However, the MMRTG thermal and structural performance will be verified in the cryogenic conditions. During the next study phase, alternative approaches for the Aerial Vehicle thermal and power design as described in 4.12.2 are recommended. The results of those trades will influence this technology work.

4.14 Programmatics

The project organization draws from the successful design and implementation experience of long-life deep-space missions such as Voyager, Galileo, Cassini, and New Horizons. Galileo and Cassini are especially relevant to outer planets flagship mission development, as both involved major inter-center and international collaboration. The team members and organization will be

#	Risk Description	Consequence	Risk Retirement Exit Criteria
1	Heat loss to cryogenic environment exceeds design limits	RPS heat generates insufficient buoyancy, balloon does not float	Cryogenic heat transfer experiments correlated with CFD models on at least half scale balloon prototypes under steady-state and vertical maneuvering conditions
2	Balloon fails to fully inflate and heat up in time at start of mission	Immediate balloon failure, can only get “contingency” data during parachute descent for a couple of hours.	Successful deployment and inflation tests of a full scale balloon at correct dynamic pressure (enough to be statistically significant)
3	Aerial Vehicle system design issues result in additional technology development and validation requirements	Programmatic – cost and schedule to address technical issues	TRL 6 for Aerial Vehicle system, including RPS location and support in balloon, RPS thermal and power approach, and gondola separation through balloon inflation sequence. RPS modifications and qualification requirements.
4	Lack of large scale cryogenic test facilities to test full scale prototype balloons	Increased likelihood of system mechanical, thermal and operations problems during mission	Construction and use of new cryogenic test facilities.
5	Inability to adequately localize the Aerial Vehicle position on Titan.	Poor or incorrect science context for data.	Simulations with validated performance models that show adequate localization on Titan.

Figure 4-27. Top 5 Montgolfiere balloon technical risks.

addressed in a future study.

4.14.1 Management Approach

The complex, multi-element architecture that may be chosen for the flagship mission calls for a cohesive partnership between the entities making up the project. The management approach follows NPR 7120.5D and incorporates NASA lessons learned. The project approach includes a Work Breakdown Structure (WBS), technical management processes conducted by veteran systems engineers, and integrated schedule/cost/risk planning and management. The project takes advantage of existing infrastructure for planning, acquisition, compliance with the National Environmental Policy Act (NEPA), compliance with export control regulations including International Traffic in Arms Regulations (ITAR), independent technical authority (as called for in NPR 7120.5D), mission assurance, ISO 9001 compliance, and earned value management (EVM).

4.14.2 Organization and Decision Making

The project is led by a Project Manager (PM) who is responsible for all aspects of project development and operations. Deputy Project Managers are chosen from the external organizations delivering significant elements of the mission. A Project Scientist (PS) is appointed to represent science interests.

Decisions are made at the lowest level possible while ensuring that a decision made in one system does not adversely affect another system or the science data return. Pursuant to NPR 7120.5D, the project includes a project-level "Communications Plan" in its list of planning documents, which will include the dissenting opinion process. This detailed plan for communication and decision-making is due in Phase B, though a draft is completed in Phase A because of the anticipated project's complexity. The PM is the final project authority for all decisions that cannot be resolved at lower levels. If NASA selects individual principal investigator–led science investigations, the PS may also have a prominent role in arbitrating science priorities in support of science planning for the mission. PS concurrence is required for all decisions involving the quality and quantity of science data deliverables.

Replacement of key personnel, including the PM, PS, and Deputy PMs, is made only with NASA concurrence. Any change in mission objective or in a mission Level 1 requirement is made only with concurrence from the Program Director at NASA.

4.14.3 Teaming

Memoranda of understanding and agreement (MOUs and MOAs), as appropriate, are executed between the major partners of TE. TE complies with all export laws and regulations. Technical Assistance Agreements (TAA) governing technical interchange between the project and international partners are applied for early in the project development stages to facilitate required discussions.

4.14.4 Roles and Responsibilities

The PM is accountable to NASA for the formulation and implementation of the project and for its technical, cost, and schedule performance. The PM is responsible to the NASA Program Office. The PM prepares monthly reports to the Program Office and the NASA Management Office (NMO). All element-level management and financial reporting is through the PM. The PM is also responsible for the risk management activities of the project. The PM is supported by a Project Systems Engineer (PSE), Mission Manager, Mission Assurance Manager, Science Manager, Business Manager, and Risk Manager. Each flight element also has a PM. Individuals with

relevant experience and unique strengths will be appointed to these positions with the goal of building a strong team.

4.14.5 Work Breakdown Structure

The TE WBS is shown Foldout 4-9 and is compliant with Appendix G of NPR 7120.5D.

4.14.6 Schedule

The PM controls the project schedule, with support from a schedule analyst. An integrated project master schedule is used to plan and track key milestones, major reviews, and receivables/deliverables (Rec/Dels). Funded schedule reserves totaling 5.5 months, as shown in the project master schedule, Foldout 4-10, are funded at the peak burn rate, and exceed JPL and APL project practices. An additional month of reserve is included due to the complexity of multi-element integration. Further risk mitigation is realized by multiple launch opportunities (roughly one per year). The project utilizes an integrated cost/schedule system in Phase B to fully implement an EVM baseline in Phases C-E. Inputs will be supplied to NASA's Cost Analysis Data Requirements (CADRe) support contractor for reporting at major reviews. Schedule and cost estimates at completion (EACs) are prepared regularly as part of the EVM process.

The critical path begins with the pre-Phase A technology demonstrations (primarily the Balloon demonstration, since it takes the longest time) up to PDR. A 12-month pre-Phase A formulation period is included prior to a 12-month Phase A and a 14-month Phase B. Instrument solicitation is a parallel critical path up to PDR. Then the critical path shifts through instrument development and delivery up to system integration and initial comprehensive performance test (CPT). The critical path is shown in red in Foldout 4-10. Schedule reserves of 2.5 months are available through the 28-month Phase C and 3 additional months up to launch in the 25 month Phase D (5.5 months of reserve for the 4.5-year Phase C-D development period). The critical path is contingent on the release of the Announcement of Opportunity (AO) for the instruments. Basic schedule milestones on this path have been estimated by the study team, are based on previous flagship-class instrument AO schedules, and will be further assessed and modified by NASA management. This critical path indicates that any approaches toward making the instrument developments occur as planned has a significant positive impact on cost and schedule performance. Early identification of parts, materials, design guidelines, etc., for mitigating potential planetary protection challenges, would also be highly effective.

While planetary protection requirements for Titan are currently at Category II, part of the mission PDR is anticipated to include a review of the final planetary protection requirements and detailed implementation approach, including any major outstanding issues related to mission design, flight system design, or operations concepts.

4.14.7 Cost Estimating Methodology

The TE cost estimate was developed using two parametric methods – JPL's Outer Planet Mission Cost Model (OPMCM) and APL's model based on recent missions – plus a "grass-roots" estimate for improved fidelity. An independent cost estimate (ICE) was also performed as a final cross-check. The instrument costs were estimated using the NASA Instrument Cost Model (NICM) only, since detailed grass-roots estimates would be premature for this phase of study.

4.14.7.1 APL Parametric Cost Estimate

The APL parametric cost estimate was based on a simple model developed to support the Phase I architecture selection (although it has been updated with new data in Phase II). New Horizons, MESSENGER, and STEREO data were scaled as appropriate to determine a rough order-

of-magnitude (ROM) mission cost down to WBS level 3. The lower estimate in Phase I (when compared to the final estimate) was largely from an underestimate of the science team and project office functions for a flagship mission.

4.14.7.2 OPMCM Cost Estimate

JPL's OPMCM is a hybrid cost model for long-life outer planet missions. OPMCM provides an independent check for the APL cost estimates.

4.14.7.3 "Grass-Roots" Cost Estimate

A detailed estimate was performed by the study team incorporating industry ROMs where appropriate and estimating levels of effort by individual task.

4.14.7.4 Independent Cost Estimate

To help validate the TE cost estimates, independent cost estimates (ICEs) for major mission components were created by APL. The independent parametric estimates are based on a combination of widely used parametric cost estimating models for space systems as well as historically derived cost factors. The ICEs include a statistical "S-curve" component that captures the effects of risk and uncertainty on final cost. The ICE results provide a means for assessing the current best estimates (CBEs); an independent check on the reasonableness of the flagship cost cap; and associated cumulative probability functions, or "S curves", for judging the credibility and sufficiency of proposed reserves. The ICE results also highlight the technical, programmatic, and estimating elements that drive estimated costs. ICEs for TE spacecraft, instruments, operations, and "system of system" integration and engineering were prepared separately.

Recent historical research conducted by NASA for the Constellation Program indicates that the "system of system" costs associated with complex, multi-system programs is about 6% of system acquisition costs. Two-fifths of those costs are for program management; the remainder, for system-of-system engineering. For TE, with approximately $1.8 billion of hardware and software acquisition, program management is estimated to be approximately $43 million; system-of-system engineering, approximately $65 million.

Spacecraft Cost Estimates

Cost estimates for the Orbiter, Cruise Stage, Lander, and Aerial Vehicle are based on the 2006 version of the NASA/Air Force Cost Model (NAFCOM). NAFCOM is an automated parametric cost-estimating tool that uses cost, schedule, and technical data from dozens of previous space missions to predict the development and production costs of future space programs. NAFCOM includes parametric relationships for estimating subsystem- and component-level costs for a variety of aerospace configurations, including upper stages, buses, and smaller planetary spacecraft, which makes it applicable to estimating the costs of the proposed TE Orbiter.

NAFCOM cost estimating relationship (CER) equations are driven by mass, amount of new design, maturity of engineering and manufacturing processes, test requirements, and integration complexity, as well as subsystem-specific technical parameters such as power, design life, redundancy, and use of special materials.

NAFCOM includes a cost risk analysis capability based on the FRISK (Formal RISK Analysis) methodology software developed for the Air Force by the Aerospace Corporation. FRISK permits analysts to consider two sources of uncertainty associated with discrepancies between predicted and final cost: uncertainty in the value of the input variables to parametric cost estimating equations and prediction uncertainty in the cost estimating equations themselves, due to the fact that the CER equations do not perfectly fit historical data points. It is the combination of these two uncertainties that accounts for most of the divergence between estimated and final pro-

ject costs. FRISK enables cost analysts to sum WBS-element statistical costs represented by probability distributions to obtain a probability distribution of total cost. Analysts provide inputs for low (most optimistic), most likely, and high (worst-case) costs for each WBS element, along with pairwise correlations between those elements. Based on the inputs, the software calculates the mean and variance of total cost. Summation of WBS-element costs is done, not by Monte Carlo sampling, but by fitting a log-normal probability distribution to the mean and variance of total cost. The result is a cumulative probability distribution ("S-curve") that assigns every possible final cost outcome its probability of occurrence.

To account for input variable uncertainty – the first source of uncertainty – analysts varied subsystem mass inputs, reflecting evidence that mass growth is associated with cost growth. Current best estimate masses, which provided the best-case (low) masses; most likely, and high-case masses, were derived from historical cost growth trends, constrained by launch vehicle capacity. Maturity levels of design, engineering, and manufacturing processes were also varied. To account for CER equation uncertainty, the standard errors of estimates were used to adjust predicted cost.

Risk-adjusted ICEs for the TE Orbiter, Cruise Stage, Lander, and Aerial Vehicle are summarized in Section 4.1.9. The ICE value selected is from the 70th percentile and includes

- *Spacecraft subsystem level:* design, development, production, integration and test
- *Spacecraft level:* system engineering, project management, support equipment, Phase D launch operations, and orbital support

Instrument Cost Estimates

Cost estimates for TE instruments are based on the recently released NICM, which predicts a "starting point estimate with cost ranges" which represents the "average" cost for an instrument project. NICM improves on previous parametric tools for estimating instrument cost in several important ways: it is based on collection and analysis of a larger and more current data set than previously available data covering 100 instruments, its data set has been reviewed and normalized by a team of cost and technical experts, and it provides access to the underlying data set as well as system and subsystem CER equations.

NICM development began in 2004 under the sponsorship of NASA's IPAO. Initial training materials and models were released to the NASA cost community in April 2007. The system-level NICM model provides six CER equations covering the following types of instruments:

- Optical, planetary missions
- Optical, Earth-orbiting missions
- Particles
- Fields
- Active micro/sub-millimeter wave
- Passive micro/sub-millimeter wave

Instrument mass and power are inputs to all six equations. The full set of cost drivers by instrument type is shown in Fig. 4-28. Like NAFCOM, NICM includes the FRISK methodology for generating probability functions for the cost estimates.

4.14.8 Cost Reserves

A 10% reserve level is carried on Phase A activities. TE utilizes an established, consistent methodology for estimating required reserves based on previous history and specific attributes of the project implementation. This methodology is called the JPL Cost Risk Sub-factor Analysis (CRSA) and takes into account project complexities such as multiple flight elements, new soft-

	Mass	Peak Power	Data Rate	Development Time (Phases B, C/D)	Design Life	Launch Date	TRL Level
Optical (planetary)	X	X		X		X	
Optical (Earth-orbiting)	X	X	X				
Particles	X	X			X		
Fields	X	X			X		
Active microwave	X	X	X	X			X
Passive microwave	X	X	X	X			X

Figure 4-28. NICM cost drivers vary by instrument type.

ware teams, extreme environmental issues, etc. Specifically for TE, the multiple elements, operation in a harsh environment, technology developments required, and the development of a new architecture set reserves for Phases B through D at 54%. A 15% reserve is carried on Phase E. The TE CRSA details are included in Section 5.3 for the baseline and Orbiter-only missions. Reserves are not carried on launch services and radioisotope power systems. The technology demonstration estimates include reserves determined from previous efforts.

4.14.9 Estimated Mission Cost

The TE cost estimates at WBS level 2 are summarized in Fig. 4-29. All costs are reported in millions of fiscal year 2007 dollars ($FY2007M). TE provides flexibility in cost by facilitating international collaboration and/or incorporation of descopes down to an Orbiter-only mission. The Orbiter-only mission cost estimate is shown in Section 0.

4.14.10 Risk Management

As a Category 1, Class A mission, TE baselines a risk manager at the mission level and individual risk managers for each element reporting to the project office. Risk identification and as-

WBS	Area	APL Parametric Cost ($M, FY07)	JPL Parametric Cost ($M, FY07)	ICE Cost ($M, FY07)	"Grass-Roots Cost ($M, FY07)
01	**Project Management**	**103**	**163**	**107**	**119**
02	**Systems Engineering**	**74**	**148**	**81**	**129**
03	**Safety & Mission Assurance**	**63**	**110**	**82**	**82**
04	**Science Team**	**205**	**314**	**305**	**305**
05	**Payload**	**593**	**561**	**561**	**561**
	Payload Management	14	14	14	*Not Estimated*
	Payload Systems Engineering	9	9	9	
06	**Flight Elements**	**664**	**720**	**735**	**616**
07	**Mission Operations**	**420**	**345**	**341**	**341**
08	**Launch System w/ Nuclear Support**	**197**	**197**	**197**	**197**
09	**Ground Data System**	**45**	**83**	**55**	**55**
10	**I&T**	**61**	**78**	**90**	**90**
11	**E/PO (0.5% A-D CBE without 08 & 2% E CBE)**	**18**	**20**	**19**	**25**
12	**Mission Design**	**39**	**22**	**16**	**16**
13	**Tech Demo: Aerocapture**	**107**	**107**	**107**	**107**
	Tech Demo: Balloon	**50**	**50**	**50**	**50**
	Tech Demo: Cryo Apps	**20**	**20**	**20**	**20**
	Tech Demo: Landing System	**5**	**5**	**5**	**5**
	DSN Aperature	**116**	**116**	**116**	**116**
	RPS Development: 8 ASRGs, 1 MMRTG	**188**	**188**	**188**	**188**
	RPS Qual: ASRG + MMRTG Analysis	**33**	**33**	**33**	**33**
CBE Cost		**3000**	**3279**	**3108**	**3055**
Reserves[1]	**10% Phase A, 54% Phase B-D, 15% Phase E**	**991**	**1125**	**1040**	**998**
Total Mission Cost		**3990**	**4404**	**4148**	**4053**

1 – Reserve calculation does not include WBS 08, DSN, RPS, and Tech Demos.

Note: All yellow boxes were not estimated; most representative cost value used to provide Total Mission Cost.

Figure 4-29. The TE cost estimate provides for a robust flagship mission that facilitates all science objectives being met within cost and schedule constraints.

FOLDOUT 4-9: The Titan Explorer Work Breakdown Structure is structured to enable effective cost, schedule, and management integration and is fully compliant with Appendix G of NPR 7120.5D.

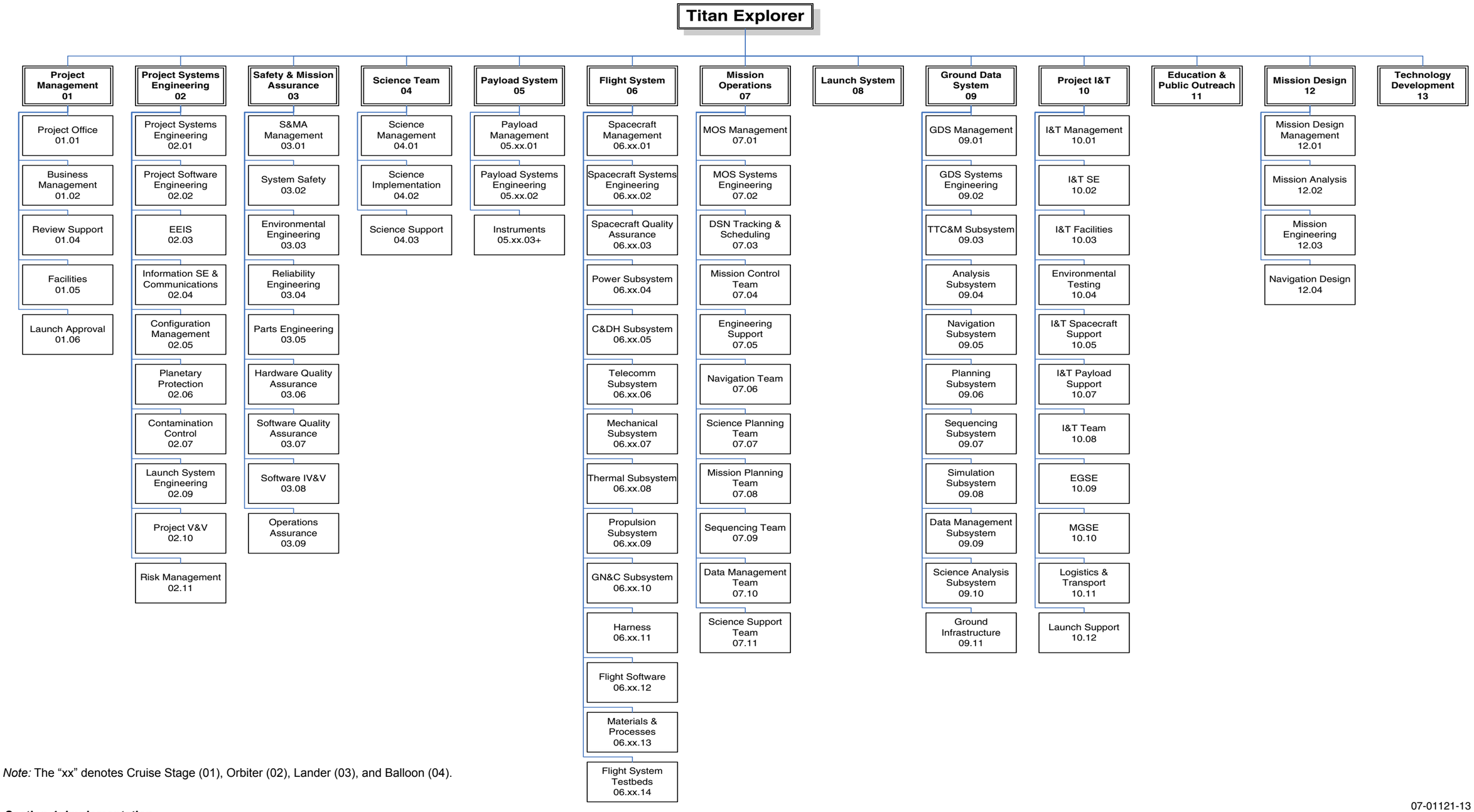

Note: The “xx” denotes Cruise Stage (01), Orbiter (02), Lander (03), and Balloon (04).

FOLDOUT 4-10: The TE Schedule Contains 5.5 Months of Reserve During the 4.5-Year Phase C-D and Allocations for Key Technology Demonstrations.

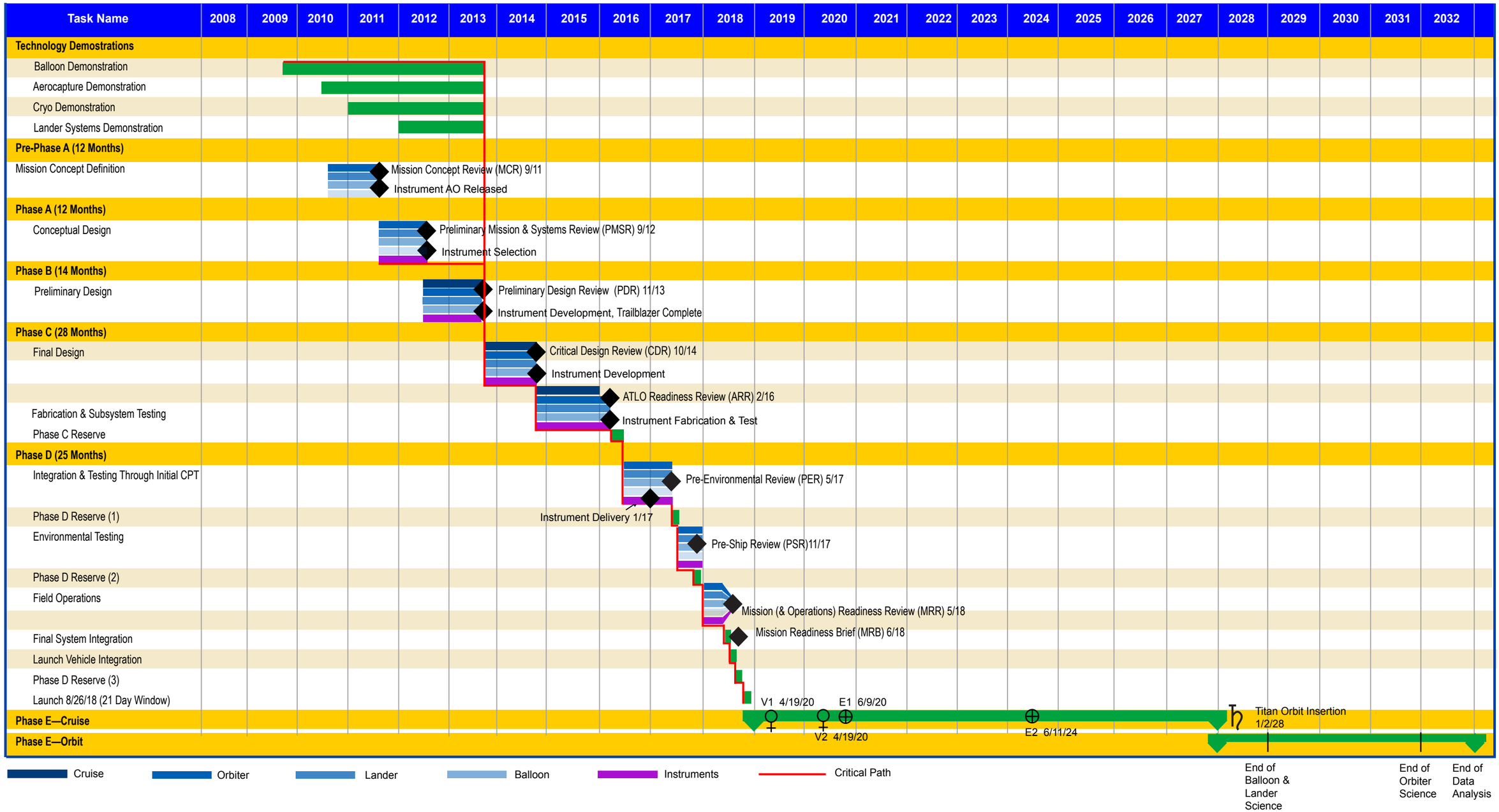

07-01121-10

sessment is part of the everyday management and systems engineering process, with all team members as active participants. All technical and programmatic margins carried on TE meet or exceed JPL and APL requirements and are prudent for a pre-Phase A study. In the event of unforeseen problems, a descope plan (outlined in the following section) has been developed for keeping the project within cost and schedule constraints without falling below the science floor. The TE risk assessment, including all moderate and high risks, is summarized in Foldout 4-11(A) and was performed using the criteria shown in Foldout 4-11(B).

The risk management process initiated for this study contains the key aspects that would be used during formal mission formulation and development. The Risk Manager monitors the common risks associated with staffing, technology, cost, schedule, and perception. Four primary activities are performed in the risk management process:

1. ***Risk identification:*** A continuous effort to identify and document risks as they are found and to provide an estimation of the risk attributes (i.e., the consequences of failing to achieve a desired result and the likelihood of failing to achieve that result)
2. ***Risk analysis:*** An evaluation of the submitted item to determine whether or not it qualifies as a project risk and a decision about what to do with the risks, which, for important risks, includes mitigation plans
3. ***Risk assessment:*** The process used to prioritize risks relative to each other (creation of the Risk Watch List)
4. ***Risk handling:*** Tracking and controlling risks – collecting and reporting status information about risks and their mitigation plans (where appropriate) and taking corrective action as needed (maintenance of the Risk Management Database)

The risk management activities are carried out during day-to-day activities of the team members, as well as during key meetings. At the project level, risks are tracked and reported through use of a database (excerpt shown in Foldout 4-11(A)) and all moderate and high risks are carried on the Risk Watch List to facilitate communication.

4.14.11 Descope Strategy

The TE mission implementation provides programmatic flexibility. Cost reduction options could be implemented through international collaboration and/or by mission descopes. The descope strategy was driven by science priorities. The first descope from the three-element architecture (Orbiter, Lander, and Aerial Vehicle) would be to remove the Aerial Vehicle and replace it with another identical Lander (savings of approximately $150M, since the Lander is of higher scientific priority). The next level of descope would be to eliminate the second Lander, resulting in an Orbiter and single Lander mission (save approximately $600M). Finally, the next descope would be to remove all in situ flight elements, resulting in an Orbiter-only mission, which is defined as the flagship mission science floor and approaches the $2B total mission cost level (see Fig. 4-30). The orbiter-only mission costs were determined using JPL's OPMCM and by modifying the baseline mission "Grass-Roots" estimate using engineering judgment. Instrumentation descopes and other options would be possible. For example, the duration of operations for each element could be reduced, depending on the science impact. All of the cost savings identified here are for descopes implemented prior to starting the mission and need to be re-evaluated for each major mission phase in a future activity.

The $2B mission should be examined in greater detail. Building the mission from the ground up (versus descoping down) should reduce cost while improving the science return. For example,

FOLDOUT 4-11: The Titan Explorer Risk Assessment.

Rank	Title	Statement	Consequence	Cf	Cf Rationale	Likelihood	Pf	Pf Rationale	RF	Mitigation Strategy	Rationale
1	Aerocapture Demo	(AERO) If the Apollo and CEV efforts are deemed insufficient mitigations, then an aerocapture demo may be required to be performed prior to PDR.	Mod	3	$30M, >3 Month CP Slip	High	4	75%	12	$107M aerocapture demo included in schedule and budget that is to be completed prior to PDR.	ST-9 proposal.
2	Balloon Technology	(BAL) If the required balloon technologies (e.g., inflation during descent, performance, materials, altitude control, autonomy) become too challenging, then the element may have to be descoped.	Mod	3	$15M, >3 Month CP Slip	High	4	75%	12	$50M balloon demo included in the schedule and budget that is completed prior to PDR.	TRL level.
3	ASRG Availability	(ASRG) If the system interactions with the ASRG (dynamics, control, thermal) cannot be adequately bounded for all elements or the technology does not mature in time, then the mission will have to switch to another RPS type.	Very High	5	Mission redesign, LV increase (>$200M)	Low	2	10%	10	ASRG qualification plan and demonstration of ASRG operation in Titan environment prior to PDR included in the budget and schedule. Monitor ASRG progress.	TRL level.
4	Planetary Protection	(PP) If the planetary protection requirements change, there will be cost and schedule impacts.	Mod	3	Mission redesign, $30M	Mod	3	25%	9	Determine cost impact of changing PP requirements and assign a cost risk lien within the reserves	Cassini continues to produce Titan science.
5	Plutonium Availability	(PA) If the supply of plutonium remains limited, then the number and type of RPS available may be reduced.	Mod	3	Mission redesign	Mod	3	25%	9	Minimize power requirements and develop plan to demonstrate compatibility with ASRG.	DOE status.
6	Cryogenic Materials & Applications	(CM) If the materials and applications necessary to operate in Titan's cryogenic environment cannot be adequately tested/demonstrated by PDR, then the in-situ portion of the project may be in jeopardy.	High	4	Lander descope	Low	2	10%	8	$20M cryogenic applications demo included in the schedule and the budget to be completed prior to PDR.	TRL level.
7	EDL Complexity	(EDL) If the EDL becomes too complex (e.g., landing system robustness to terrain uncertainty, landing ellipse, balloon inflation during descent), then an extended effort will have to be applied.	High	4	Mission redesign all elements	Low	2	10%	8	Leverage past work.	Past experience.
8	Launch Vehicle Logistics and Integration	(LV) If the launch vehicle logistics associated with NEPA and the integration of the RPS (with cooling), aeroshell, and fairing become too complex, then cost growth and potential schedule impacts may occur.	Low	2	1-3 Month CP Slip	High	4	50%	8	Develop plan for LV development and integration. Allocate $18M reserves as a lien.	New Horizons & Cassini experience; complex integration sequence.
9	Lander Sampling	(SMPL) If the sample handling and acquisition for the lander becomes too complex, then there will be cost and schedule impacts if the science is not descoped.	Mod	3	$25M	Low	2	15%	6	Leverage MSL work.	TRL level.
10	70-m Equivalent DSN Availability	(DSN) If the DSN capabilities are less than predicted then the mission science will be reduced.	Mod	3	Science loss	Low	2	10%	6	Design margins.	NASA budget.
11	Earth Flyby Requirements	(EF) If an Earth Flyby is required to maximize the mission potential and requirements are underestimated, there could be complications that will lead to cost and schedule issues.	Low	2	$10M	Mod	3	25%	6	Begin preparations early and leverage Cassini experience.	Cassini.

(A) Titan Explorer has an acceptable level of risk for a Flagship Mission pre-phase A study.

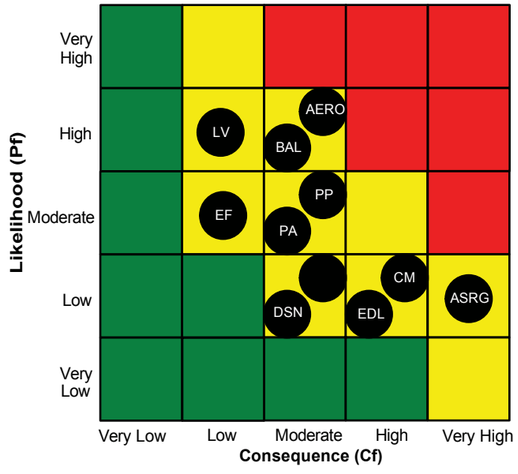

	Consequence	Cost	Schedule	Technical
1	Very Low	<$10M	<1 Month CP Slip	Loss of margin
2	Low	$10M-$25M	1-3 Month CP Slip	Reduced functionality, but minimum requirements still met
3	Moderate	$25M-$50M	3-6 Month CP Slip	Loss of redundancy or functionality that impacts ability to meet performance requirements
4	High	$100M	6-12 Month CP Slip	Loss of functionality, Inability to meet full science
5	Very High	>$200M	>1 Year CP Slip	Inability to meet minimum science
	Likelihood	**Programmatic**	**Technical**	
1	Very Low	<10% chance of occurrence	0.1-2% chance of occurrence	
2	Low	10-25% chance of occurrence	2-15% chance of occurrence	
3	Moderate	25-50% chance of occurrence	15-25% chance of occurrence	
4	High	50-75% chance of occurrence	25-50% chance of occurrence	
5	Very High	>75% chance of occurrence	>50% chance of occurrence	

(B) The TE risk assessment criteria allow issues to be quantified in terms of cost, schedule, and technical risk aspects.

WBS	Area	"Grass-Roots" Modified Cost ($M, FY07)	JPL Parametric Cost ($M, FY07)
01	**Project Management**	**94**	**91**
02	**Systems Engineering**	**91**	**69**
03	**Safety & Mission Assurance**	**82**	**61**
04	**Science Team**	**150**	**153**
05	**Payload (Orbiter)**[1]	**266**	**266**
06	**Flight Elements (Cruise Stage & Orbiter)**	**328**	**327**
07	**Mission Operations**	**219**	**262**
08	**Launch System w/ Nuclear Support**[2]	**156**	**156**
09	**Ground Data System**	**55**	**66**
10	**I&T**	**48**	**40**
11	**E/PO (0.5% A-D CBE without 08 & 2% E CBE)**	**16**	**11**
12	**Mission Design**	**12**	**12**
13	**Tech Demo:Aerocapture**	**107**	**107**
	DSN Aperature[3]	**116**	**116**
	RPS Systems:5 ASRGs + Qual	**121**	**121**
CBE Cost		**1860**	**1859**
Reserves[4]	**10% Phase A, 42% Phase B-D, 15% Phase E**	**455**	**460**
Total Mission Cost		**2314**	**2319**

1 – Instrument estimates from baseline mission cost estimate; further descopes may be possible (future study)
2 – Atlas V 511 based on preliminary analysis, detailed analysis required in a future study
3 – Science bandwidth assumed same as baseline mission; further descope may be possible (future study)
4 – Reserve calculation does not include WBS 08, DSN, RPS, and Tech Demos

Figure 4-30. The TE science floor may allow the Orbiter-only mission to fit within a $2B cost cap.

optimizing the trajectory for the smaller mass may result in a smaller launch vehicle and may eliminate the need for a separate cruise stage. The science of an orbiter-only mission can be improved in a number of areas to recover the lost in situ science. A key aspect of the baseline architecture is the allocation of high-resolution surface imaging to the Balloon, and to a lesser extent, to the Lander descent imaging. Lacking these contributions, investigation into enhancing the spatial resolution of the imaging radar and the spectral mapper should be pursued. Both of these have nominal pixel scales of 100 m, determined by the bandwidth available to make global maps of Titan at this resolution. However, neither instrument is fundamentally limited to this resolution; increased instantaneous power for the radar and a larger aperture for the spectral mapper could realistically attain ~20-m pixel scales in each case. The improved radar resolution should be attainable over most regions, although not the darkest lakes, and initial assessments (Young,, 2007) suggest that haze scattering still preserves a significant amount of surface contrast information at a 2-μm wavelength at the 20-m scale. Telemetry bandwidth will not be adequate for global maps at this resolution, but for specific targets of interest these enhanced capabilities go some way towards making up the lost science from the in situ vehicles. More speculatively, interferometric SAR may provide a window into surface deformations that improves knowledge of the interior, in part compensating for the loss of seismic monitoring capability on the Lander.

The balloon carries a subsurface sounder with a small footprint and good vertical resolution. The capabilities and limitations of the Orbiter subsurface radar/ionosphere sounder should be examined to establish if its wavelength range can be extended to shorter wavelengths to attain better resolution. Lacking a balloon, tracers of tropospheric air motions become more important. Consideration might be given to improving cloud monitoring with a wide-field-of-view instrument (perhaps by implementing automatic feature detection and tracking in the visible/1-micron imager.) One might even consider release of passive radar-cube-corner reflector balloons at arrival as tracers. Although no measurement can substitute for the surface chemistry capability of

the Lander, some thought toward chemistry measurements by a "sacrificial" mass spectrometer or similar instrument during aerocapture might be made, to observe how high-molecular-mass chemistry changes in the atmosphere down to ~400 km. The orbiter science operations plan might be re-thought, for example to include short, targeted radar imaging campaigns to re-observe known fiducial locations on Titan's surface to measure changes in its rotation state, since continuous precision Lander tracking is not available. More effort might be devoted also to observing specific surface sites with the spectral mapper at multiple phase and incidence angles, to allow better (although it will never be complete) subtraction of atmospheric effects from surface spectra, since Balloon and Lander spectra will not be available. Finally, all science on the orbiter can be enhanced by a longer mission duration.

4.14.12 NEPA Compliance and Launch Approval

Environmental review requirements are satisfied by the completion of a mission-specific Environmental Impact Statement (EIS) for TE. The Record of Decision (ROD) for this EIS is finalized prior to or concurrent with PDR.

The TE launch approval engineering (LAE) Plan is completed no later than the Preliminary Mission System Review (PMSR). This plan describes the approach for enabling satisfaction of NASA's NEPA requirements for TE, and includes the approach for obtaining nuclear safety Launch Approval as required by NPR 8715.3 and Presidential Directive/National Security Council Memorandum #25 (PD/NSC-25). The LAE Plan provides a description of responsibilities, data sources, schedule, and an overall summary plan for

- A mission-specific environmental review document and supporting nuclear safety risk assessment efforts
- Launch vehicle and spacecraft/mission design data requirements to support nuclear risk assessment and safety analyses in compliance with the requirements of NPR 8715.3 and the PD/NSC-25 nuclear safety launch approval process
- Support of launch site radiological contingency planning efforts
- Risk communication activities and products pertaining to the NEPA process, nuclear safety and planetary protection aspects of the project

NASA HQ initiates TE NEPA document development as soon as a clear definition of the baseline plan and option space is formulated. The Department of Energy (DOE) provides a risk assessment to support the mission-specific EIS development, based upon a representative set of environments and accident scenarios. This deliverable may be modeled after the approach used on the Mars Science Lander (MSL) EIS, and includes a preliminary inadvertent reentry analysis.

DOE provides a nuclear safety analysis report (SAR) based upon NASA-provided mission-specific launch system and spacecraft data to support the PD/NSC-25 compliance effort. The SAR is delivered to an ad hoc interagency nuclear safety review panel (INSRP) organized for TE. This INSRP reviews the SAR's methodology and conclusions and prepares a Safety Evaluation Report (SER). Both the SER and the SAR are provided by NASA to the Environmental Protection Agency, the Department of Defense, and DOE for agency review. Following agency review of the documents and resolution of any outstanding issues, NASA, as the sponsoring agency, submits a request for launch approval to the Director of the Office of Science and Technology Policy (OSTP). The Director of the OSTP reviews the request for nuclear safety launch approval and either approves the launch or defers the decision to the President. As part of broader nuclear safety considerations, TE will adopt ATLO, spacecraft, trajectory, and operations requirements that satisfy the nuclear safety requirements described by NPR 8715.3 based

on past missions carrying radioisotope power systems and using Earth gravity assists. The key requirement maintained by TE is the probability of less than one in a million of Earth impact.

Development of coordinated launch site radiological contingency response plans for NASA launches is the responsibility of the launch site radiation safety organization. Comprehensive radiological contingency response plans, compliant with the National Response Plan and appropriate annexes, are developed and put in place prior to launch as required by NPR 8715.2 and NPR 8715.3. TE supports the development of plans for on-orbit contingency actions to complement these ground-based response plans.

A project-specific Risk Communication Plan is completed no later than PDR. The Risk Communication Plan will detail the rationale, proactive strategy, process, and products of communicating risk aspects of the project, including nuclear safety and planetary protection. The communication strategy and process will comply with the approach and requirements outlined in the NASA Office of Space Science Risk Communication Plan for Deep Space Missions (1999) JPL D-16993 and the JPL Risk Communication Plan, 2002, JPL D-24012.

4.14.13 Education and Public Outreach

Education and Public Outreach (E/PO) was not investigated in depth during this study. A program similar to that of Cassini is envisioned. A mission to Titan offers many obvious exciting opportunities, especially with the in situ elements. One option is described in Section 2.6.3.12 is the Titan unmanned aerial vehicle (UAV). For this study, the E/PO allocation was defined as 0.5% of Phase A-D cost (less launch system and RPS) and 2% of Phase E as shown in the total mission cost.

5: Concept B Implementation

5. CONCEPT B IMPLEMENTATION

Because a single baseline architecture was selected in Phase 1 of the study, this section is not applicable.

6: Changes if Launched in Alternate Opportunity

6. CHANGES IF LAUNCHED IN ALTERNATE OPPORTUNITY

The 2018 Titan Explorer mission launch date is flexible and accommodating to programmatic schedule changes.

- Alternate launch opportunities exist every 1 to 2 years for the TE mission.
- Minimal modifications to the baseline TE flight system are needed to launch after 2018.

Alternate interplanetary trajectories are available every 1–2 years in the 2015–2022 timeframe for the Titan Explorer (TE) mission, as shown in Fig. 6-1. The worst-case trajectory from the TE baseline September 2018 launch period, described in Section 4.3.1, is shown in bold for comparison. All trajectories provide the same or more mass arriving at Saturn as compared with the baseline. The TE flight vehicle design is robust to programmatic changes in schedule.

Two Jupiter gravity assist trajectories are shown in Fig. 6-1, one having the highest mass capability and one having the shortest trip time for Jupiter gravity assist trajectories in the 2015–2022 timeframe. Note that both launch in 2015. For later launch dates within the 2015–2022 timeframe, Jupiter gravity assist trajectories provide no advantage over other gravity assist designs. Jupiter gravity assist trajectories are discussed further in Section 3.

As discussed in Section 4.12.1 on future work, analyses are required for backup trajectory selection and to determine if the backup trajectory drives flight system design requirements. Launch period analysis is needed to define deep space maneuver (DSM) requirements necessary to meet or exceed the arrival mass for the nominal trajectories shown in Fig. 6-1. If necessary, volume and mass are available to accommodate larger DSMs; propellant loading can be tailored for each launch opportunity. Navigation analyses, atmospheric flight Monte Carlo simulations, and a probability of Earth impact analysis for the backup trajectories are also recommended.

Trajectory*	Launch Date	Arrival Date	TOF (years)	DSM ΔV (m/s)	Saturn V-infinity (km/s)	Launch C_3 (km^2/s^2)	Launch Mass (kg)	Arrival Mass** (kg)
VEEJ	1 FEB 2015	19 OCT 2024	9.7	0	6.9	12.0	5120	5120
VVEE	25 JUN 2015	28 JAN 2024	8.6	0	8.3	14.9	4850	4850
VEEJ	20 JUL 2015	18 JUL 2023	8.0	0	6.9	16.2	4750	4750
VEE	15 SEP 2016	13 JAN 2026	9.3	30	8.4	13.8	4950	4895
VVEE	**30 SEP 2018**	**2 JAN 2028**	**9.3**	**100**	**8.5**	**14.7**	**4870**	**4695**
VEE	9 NOV 2019	2 JAN 2029	9.2	60	8.4	15.5	4800	4695
VEME	1 MAR 2020	28 JUL 2031	11.4	0	7.0	15.1	4835	4835
VEEE	8 NOV 2021	15 APR 2032	10.4	0	7.6	14.2	4915	4915

* V = Venus, E = Earth, J = Jupiter; M = Mars.

** "Arrival Mass" is the launch mass minus the propellant mass of the DSM for an Isp of 280 s.

Figure 6-1. Alternate interplanetary trajectories provide multiple launch opportunities.

7: Team Members and Roles

7. TEAM MEMBERS AND ROLES

Beyond scope of this study.

8: Summary

8. SUMMARY

Saturn's moon Titan is an exciting scientific object. Diverse and rich, Titan's similarities with Earth provide a familiarity and an ease of comparison, while thrilling and strange particulars expand our understanding. Study of the Titan system holds something for everyone. The Titan Explorer (TE) mission concept addresses all science objectives by utilizing multiple elements to examine Titan from multiple scales. TE benefits from synergy between the Orbiter, Balloon, and Lander, thus increasing science return and lowering programmatic risk. However, even a science floor Orbiter-only mission holds a robust science package at roughly half the cost of the $4B baseline science mission. The enormous scientific value and programmatic flexibility of the TE mission makes it a logical choice for the next flagship mission.

9: Appendices

9.1 References

9.1 References

Achterberg, R. K., B. J. Conrath, P. J. Gierasch, F. M. Flasar, and C. A. Nixon, Titan's middle-atmospheric temperatures and dynamics observed by the Cassini Composite Infrared Spectrometer, submitted to *Icarus*, 2007.

Atreya, S. K., E. Y. Adams, H. B Niemann,. J. E. Demick-Montelara, T. C. Owen, M. Fulchignoni, F. Ferri, and E. H. Wilson, Titan's methane cycle, *Planet. Space Sci., 54,* 1177–1187, 2006.

Barnes, J. W., J. Radebaugh, R. H. Brown, S. Wall, L. Soderblom, J. Lunine, D. Burr, C. Sotin, S. Le, Mouelic, B. J. Buratti, R. Clark, K. H. Baines, R. Jaumann, P. D. Nicholson, R. L. Kirk, R. Lopes, R. Lorenz, K. Mitchell, C. A. Wood, and the Cassini RADAR Team, Near-Infrared Spectral Mapping of Titan's Mountains and Channels, submitted to *J. Geophys. Res.*, 2007.

Barth, E., and S. C. Rafkin, TRAMS: A new dynamic cloud model for Titan's methane clouds, *Geophys. Res. Lett., 34,* L03203 doi:10.1029/2006GL028652, 2007.

Blamont, J., et al., Implications of the VEGA balloon results for Venus atmospheric dynamics, *Science, 231,* 1422–1426, 1986.

Cammarano, F., V. Lekic, M. Manga, M. Panning, and B. Romanowicz, Long-period seismology on Europa: 1. Physically consistent interior models, *J. Geophys. Res., 111,* E12009, doi:10.1029/2006JE002710, 2006.

Coustenis, A., and B. Bézard, Titan's atmosphere from Voyager infrared observations. IV. Latitudinal variations of temperature and composition, *Icarus, 115,* 126–140, 1995.

Coustenis, A. et al., The composition of Titan's stratosphere from Cassini/CIRS mid-infrared spectra, *Icarus, 189,* 35–62, 2007.

Cravens, T. E., I. P. Robertson, J. H. Waite, R. V. Yelle, W. T. Kasprzak, C. N. Keller, S. A. Ledvina, H. B. Niemann, J. G. Luhmann, R. L. McNutt, W.-H. Ip, V. De La Haye, I. Mueller-Wodarg, J.-E. Wahlund, V. G. Anicich, and V. Vuitton, Composition of Titan's ionosphere, Geophysical Research Letters, Volume 33, Issue 7, CiteID L07105, doi: 10.1029/2005GL025575, 2004.

Croft, T. A., Surface reflections of Pioneer Venus Probe radio signals, *Geophys. Rev. Lett., 7,* 521–524, 1980.

De La Haye, V., et al., Cassini Ion and Neutral Mass Spectrometer data in Titan's upper atmosphere and exosphere: Observation of a suprathermal corona, *J. Geophys. Res., 112,* A07309, doi:10.1029/2006JA012222. 2007.

Duron, J., P. Rosenblatt, M. Yseboodt, O. Karatekin, V. Dehant, T. VanHoolst and J.-P. Barriot, Joint estimation of Martian $\overline{C}_{20}$ and rotation variations from simultaneous geodetic measurements: Numerical simulations of a Network science experiment, *Geophys. Res. Lett., 30(18),* 1971, doi:10.1029/2003GL018353, 2003.

Dzierma, Y., M. K. Bird, R. Dutta-Roy, Miguel Pérez-Ayúcar, D. Plettemeier, and P. Edenhofer, Huygens Probe descent dynamics inferred from Channel B signal level measurements, *Planet. Space Sci.*, doi:10.1016/j.pss.2007.04.018, in press, 2007.

Elachi, C., S. Wall, M. Allison, Y. Anderson, R. Boehmer, P. Callahan, P. Encrenaz, E. Flamini, G. Francescetti, Y. Gim, G. Hamilton, S. Hensley, M. Janssen, W. Johnson, K. Kelleher, R. Kirk, R. Lopes, R. Lorenz, J. Lunine, D. Muhleman, S. Ostro, F. Paganelli, G. Picardi, F. Posa, L. Roth, R. Seu, S. Shaffer, L. Soderblom, B. Stiles, E. Stofan, S. Vetrella, R. West, C. Wood, L. Wye, and H. Zebker, Cassini Radar Views the Surface of Titan, *Science, 308,* 970–974, 2005.

Ferris, J. P. et al., . HCN: A plausible source of purines, pyrimidines and amino acids on the primitive Earth, *J. Molecular Evol., 11,* 293–311, 1978.

Flasar, F. M., et al., Titan's atmospheric temperatures, winds, and composition, *Science, 308,* 975–978, 2005.

Folkner, W. M., C. F. Yoder, D. N. Yuan, E. M. Standish, and R. A. Preston, Interior structure and seasonal mass redistribution of Mars from radio tracking of Mars Pathfinder, *Science, 278,* 1749, 1997.

Folkner, W. M., S. W. Asmar, J. S. Border, G. W. Franklin, S. G. Finley, J. Gorelik, D. V. Johnston, V. V. Kerzhanovich, S. T. Lowe, R. A. Preston, M. K. Bird, R. Dutta-Roy, M. Allison, D. H. Atkinson, P. Edenhofer, D. Plettemeier, and G. L. Tyler, Winds on Titan from ground-based tracking of the Huygens Probe, *J. Geophys. Res., 111,* E07S02, doi:10.1029/2005JE002649, 2006.

Fortes, A. D., Exobiological implications of a possible ammonia-water ocean inside Titan, *Icarus, 146,* 444–452, 2000.

Ganesan, A. L., W. B. Brinckerhoff, P. Coll, M.-J. Nguyen, F. Raulin, T. J. Cornish, and S. A. Ecelberger, Analysis of Titan tholins by laser desorption mass spectrometry, Abstract #1948 *38th Lunar and Planetary Science Conference,* (Lunar and Planetary Science XXXVIII), Houston, TX, 2007.

Golombek, M. P., et al., Overview of the Mars Pathfinder Mission: Launch through landing, surface operations, data sets, and science results, *J. Geophys. Res., 104,* 8523–8553, 1999.

Griffith, C. A., T. Owen, G. A. Miller, and T. Geballe, Transient clouds in Titan's lower atmosphere , *Nature, 395,* 575, 1998.

GSFC, *Titan Orbiter Aerorover Mission (TOAM),* http://www.lpi.usra.edu/opag/aerorover_mission_probes.pdf, 2005–2006.

Gurvits et al., in preparation.

Hall et al., An aerobot for global in situ exploration of Titan, *Adv. Space Res., 37,* 2108–2119, 2006.

Hodyss, R., G. McDonald, N. Sarker, M. A. Smith, P. M. Beauchamp, and J. L. Beauchamp, Fluorescence spectra of Titan tholins: In-situ detection of astrobiologically interesting areas on Titan's surface, *Icarus, 171,* 525–530, 2004.

Hueso, R., and A. Sánchez-Lavega, Methane storms on Saturn's moon Titan, *Nature, 442,* 428–431, 2006.

Imanaka, H., B. N. Khare, J. E. Elsila, E. L. O Bakes, C. P. McKay, D. P. Cruikshank, S. Sugita, T. Matsui, and R.N. Zare, Laboratory experiments of Titan tholin formed in cold plasma at

various pressures: implications for nitrogen-containing polycyclic aromatic compounds in Titan haze, *Icarus, 168,* 344–366, 2004.

Johnson, R. E., *Atmospheric Sputtering at Mars and Titan,* International Space Science Institute, Bern, Switzerland, June 2007.

Jones, J. A., J. A. Cutts, J. L. Hall, J.-J. Wu, D. A. Fairbrother, and T. Lachenmeier, Montgolfiere balloon missions for Mars and Titan, *IPPW,* Athens, Greece, June 2005.

Justus, C., and A. Duvall, *Engineering-level model atmospheres for Titan and Neptune,* paper AIAA-2003-4803, *39th AIAA/ASME/SAE/ASEE Joint Propulsion Conference and Exhibit*, Huntsville, AL, 20–23 July 2003.

JPL, *Titan Vision Study,* http://www.lpi.usra.edu/opag/oct_05_meeting/jpl_titan.pdf, 2005.

Khanna, R., Condensed species in Titan's stratosphere: Confirmation of crystalline cyanoacetylene (HC_3N) and evidence for crystalline acetylene (C_2H_2) on Titan, *Icarus, 178,* 165–170, 2005.

Khare, B., and C. Sagan, Red clouds in reducing atmospheres, *Icarus, 20,* 311, 1973.

Khare, B. N., C. Sagan, H. Ogino, B. Nagy, C. Er, K. H. Schram, and E. T. Arakawa,. Amino acids derived from Titan tholins, *Icarus, 68,* 176–184, 1986.

Kovach, R. L., and C. F. Chyba, Seismic detectability of a subsurface ocean on Europa, *Icarus, 150,* 279–287, 2001.

LaRC, *Titan Vision Study,* http://www.lpi.usra.edu/opag/oct_05_meeting/langley_titan.pdf, 2005.

Laub et al., *Updated TPS Requirements for Missions to Titan,* 2006.

Laub, B. and Chen, Y.-K. Updated TPS requirements for missions to Titan, *Proc., 3rd Int. Planet. Probe Workshop,* Attica, Greece, June 2005.

Ledvina, S., *Titan Hybrid Modeling,* International Space Science Institute, Bern, Switzerland, June 2007.

Lee, S. W., M. Zanolin, A. Thode, R. T. Pappalardo, and N. C. Makris, Probing Europa's interior with natural sound sources, *Icarus, 177,* 144–167, 2003.

Levine et al., *NASA LaRC Visions Missions Study,* http://www.lpi.usra.edu/opag/oct_05_ meeting/langley_titan.pdf, 2005

Levine, J. S., and H. S. Wright, *Titan Explorer: The Next Steps in the Exploration of a Mysterious World,* Final Report, 2005.

Liu, J. Y., Y. B. Tsai, S. W. Chen, C. P. Lee, Y. C. Chen, H. Y. Yen, W. Y. Chang, and C. Liu, Giant ionospheric disturbances excited by the M9.3 Sumatra earthquake of 26 December 2004, *Geophys. Res. Lett., 33,* L02103, doi:10.1029/2005GL023963, 2006.

Lockwood et al., *Aerocapture Systems Analysis for a Titan Mission,* NASA/TM-2006-214273, February 2006.

Lognonné, P., Planetary seismology, *Ann. Rev. Earth. Planet. Sci., 33,* 571–604, 2005.

Lognonné, P., et al., The NetLander very broad band seismometer, *Planet. Space Sci., 48*, 1289–1302, 2000.

Lopes, R., K. L. Mitchell, E. R. Stofan, J. I. Lunine, R. Lorenz, F. Paganelli, R. L. Kirk, C. A Wood, S. D. Wall, L. E. Robshaw, A. D. Fortes, C. D. Neish, J. Radebaugh, E. Reffet, S. J. Ostro, C. Elachi, M. D. Allison, Y. Anderson, R. Boehmer, G. Boubin, P. Callahan, P. Encrenaz, E. Flamini, G. Francescetti, Y. Gim, G. Hamilton, S. Hensley, M. A. Janssen, W. T. Johnson, K. Kelleher, D. O. Muhleman, G. Ori, R. Orosei, G. Picardi, F. Posa, L. E. Roth, R. Seu, S. Shaffer, L. A. Soderblom, B. Stiles, S. Vetrella, R.D. West, L. Wye, and H. A. Zebker, Cryovolcanic features on Titan's surface as revealed by the Cassini Titan Radar Mapper, *Icarus, 186*, 395–412, 2007.

Lorenz, R. D., The weather on Titan, *Science, 290*, 467-468, 2000a.

Lorenz, R. D., Post-Cassini exploration of Titan: Science rationale and mission concepts, *J. Brit. Interplanet. Soc., 53*, 218-234, 2000b.

Lorenz, R. D., and J. Mitton, *Lifting Titan's Veil*, Cambridge University Press, Cambridge, 2002.

Lorenz, R. D., J. R. Green, C. A. Wood, A. Coustenis, G. G. Ori, Ph. Paillou, R. Yelle, S. Bolton, K. Baines, R. Terrile, M. A. Gurwell, C. A. Griffith, A.-S. Wong, and K. Rages, Titan, *in* M. Sykes (ed) *The Future of Solar System Exploration 2003-2013*, pp. 253-262, ASP Conference Series 272, 2002a.

Lorenz, R. D., A. J. T .Jull, J. I. Lunine, and T. Swindle, Radiocarbon on Titan, *Meteorit. Planet. Sci., 37*, 867–874, 2002b.

Lorenz, R. D., R. D. West, and W. T. K. Johnson, Cassini RADAR constraint on Titan's winter polar precipitation, submitted to *Icarus*, 2007c.

Lorenz, R. D., C. A Griffith, J. I. Lunine, C. P. McKay, and N. O. Renno, Convective Plumes and the Scarcity of Clouds on Titan, *Geophysical Review Letters*, 32, L01201, 2005.

Lorenz, R. D., M. T. Lemmon, and P. H. Smith, Seasonal evolution of Titan's Dark polar hood: Midsummerearance observed by the Hubble Space Telescope, *Monthly Notices Roy. Astronom. Soc.*, 369, 1683–1687, 2006a.

Lorenz, R. D., S. Wall, J. Radebaugh, G. Boubin, E. Reffet, M. Janssen, E. Stofan, R. Lopes, R. Kirk, C. Elachi, J. Lunine, F. Paganelli, L. Soderblom, C. Wood, L. Wye, H. Zebker, Y. Anderson, S. Ostro, M. Allison, R. Boehmer, P. Callahan, P. Encrenaz, G. G. Ori, G. Francescetti, Y. Gim, G. Hamilton, S. Hensley, W. Johnson, K. Kelleher, K. Mitchell,D. Muhleman, G. Picardi, F. Posa, L. Roth, R. Seu, S. Shaffer, B. Stiles, S. Vetrella, E. Flamini, and R. West, The sand seas of Titan: Cassini radar observations of longitudinal dunes, *Science, 312*, 724–727, 2006b.

Lorenz, R. D, R. M. Lopes, F. Paganelli, J. I. Lunine, R L. Kirk, K. L. Mitchell, L. A. Soderblom, E R. Stofan, G. Ori, M. Myers, H. Miyamoto, J. Radbaugh, B. Stiles, S. D.Wall, C. A. Wood, and the Cassini RADAR Team, Fluvial Channels on Titan : Initial Cassini RADAR Observations, submitted to *Planet. Space Sci.*, 2007a.

Lorenz, R. D. C. A. Wood, J. I. Lunine, S. D. Wall, R. M. Lopes, K. Mitchell, F. Paganelli, Y. Z. Anderson, L. Wye, C. Tsai, H. Zebker, E. R. Stofan, and the Cassini RADAR Team, Titan's

young surface: Initial impact crater survey by Cassini RADAR and model comparison, *Geophys. Res. Lett., 34,* L07204, doi:10.1029/2006GL028971, 2007b.

Lorenz, R. D., R. D. West, and W. T. K. Johnson, Cassini RADAR constraint on Titan's winter polar precipitation, submitted to *Icarus,*, 2007c.

May, R. D., S. Forouhar, D. Crisp, W. S. Woodward, D. A. Paige, A. Pathare, and W. V. Boynton, The MVACS tunable diode laser spectrometers, *J. Geophys. Res., 106,* 17,673–17,682, 2001.

McDonald, G. D., W. R. Thompson, M. Heinrich, B. N. Khare, and C. Sagan, Chemical investigation of Titan and Triton tholins, *Icarus, 108(1),* 137–145, 1994.

McGuigan, M., J. H. Waite, H. Imanaka, and R. D. Sacks, Analysis of Titan tholin pyrolysis products by comprehensive two-dimensional gas chromatography-time-of-flight mass spectrometry, *J. Chromatogr. A, 1132,* 280–288, 2006.

McKay, C. P., and H. D. Smith, Possibilities for methanogenic life in liquid methane on the surface of Titan, *Icarus, 178(1),* 274–276, 2005.

McKay, C. P. , A. Coustenis, R. E. Samuelson, M. T. Lemmon, R. D. Lorenz, M. Cabane, P. Rannou, P. Drossart, Physical Properties of the Organic Aerosols and Clouds on Titan, *Planet. Space Sci., 49,* 79–99, 2001.

Mitchell, D., private communication, 2007

Mitchell, J. L., R. T. Pierrehumbert, D. M. W. Frierson, and R. Caballero, The Dynamics behind Titan's methane clouds, *Proc.,Nat. Acad. Sci., 103,*18421–18426, 2006.

Mitri, G., A. Showman, J. Lunine, and R. Lopes, Resurfacing of Titan by ammonia-water cryomagma, Abstract 1994, *Lunar and Planetary Science XXXVII,* 2006.

Munk, M. M., and S. A. Moon, Aerocapture technology developments from NASA's In-Space Propulsion Technology Program, *1st NASA Science Technology Conference,* Adelphi, MD, presented June 21, 2007.

National Research Council Space Studies Board, *New Frontiers in the Solar System: An Integrated Exploration Strategy* (the first Decadal Survey Report), National Academic Press,Washington, DC., 2003.

NASA, *Solar System Exploration,* Roadmap for the NASA Science Mission Directorate, http://www.lpi.usra.edu/opag/road_map_final.pdf, 2006.

NASA Engineering and Safety Center (NESC), *Independent Technical Assessment of Cassini/Huygens Probe Entry, Descent, and Landing (EDL) at Titan,* RP-05-67, May 26, 2005.

National Research Council, *The Limits of Organic Life in Planetary Systems,* National Academies Press, Washington, DC. 2007.

Neish, C. D., R. D. Lorenz, and D. P. O'Brien, The potential for prebiotic chemistry in the possible cryovolcanic dome Ganesa Macula on Titan, *Int. J. Astrobiol., 5,* 57–65, 2006.

Nelson, R. M., L. Kamp, D. L. Matson, P. G. J. Irwin, K. H. Baines, M. D. Boryta, F. E. Leader, R. Jaumann, W. D. Smythe, C. Sotin, R. N. Clark, D. P. Cruikshank, P. Drossart, J. C. Pearl, B. W. Hapke, J. Lunine, M. Combes, and G. B. Bellucci, Saturn's Titan: Cassini VIMS

reports regional reflectance change consistent with surface activity, Abstract #2158, *38th Lunar and Planetary Science Conference*, Houston, TX, 2007.

Niemann, H. B., S. K Atreya, S. J. Bauer, G. R. Carignan, J. E. Demick, R. L. Frost, D. Gautier, J. A. Haberman, D. N. Harpold, D. M. Hunten, G. Israel, J. I. Lunine, W. T. Kasprzak, T. C. Owen, M. Paulkovich, F. Raulin, E. Raaen, and S. H. Way, Huygens Probe gas chromatograph mass spectrometer: The atmosphere and surface of Titan, *Nature, 438,* 779–784, 2005.

O'Brien, D. P., R. D. Lorenz, and J. I. Lunine, Numerical calculations of the longevity of impact oases on Titan, *Icarus, 173(1), 2*43–253, 2005.

OPAG, *Scientific Goals and Pathways for Exploration of the Outer Solar System,* A report of the Outer Planets Assessment Group, http://www.lpi.usra.edu/opag/pathways.pdf, July 2006.

OPAG, *Titan Working Group Presentations,* http://www.lpi.usra.edu/opag/oct_05_meeting/titan_work_grp.pdf, 2005.

Panning, M, V. Lekic, M. Manga, F. Cammarano, and B. Romanowicz, Long-period seismology on Europa: 2. Predicted seismic response, *J. Geophys. Res., 111,* E12008, doi:10.1029/2006JE002712, 2006.

Pérez-Ayúcar M., R. D. Lorenz, N. Floury, R. Prieto, and J-.P. Lebreton, Surface properties of Titan from post-landing reflections of the Huygens radio signal, *J. Geopyhis Res.–Planets, 111,* E07001, doi:10.1029/2005JE002613, 2006.

Perron, J. T., M. P. Lamb, C. D. Koven, I. Y. Fung, E. Yager, and M. Adamkovics, Valley formation and methane precipitation rates on Titan, *J. Geophys. Res., 111,* E11001 doi:10.1029/2005JE002602, 2006.

Picardi, G., et al., Radar soundings of the subsurface of Mars, *Science, 310,* 1925–1928, 2005.

Plaut, J., et al., Subsurface radar sounding of the south polar layered deposits of Mars, *Science, 316,* 92–95, 2007.

Pogrebenko S. V., L. I. Gurvits, R. M. Campbell, I. M. Avruch, J.-P. Lebreton, and C. G. M. van't Klooster, *VLBI Tracking of the Huygens Probe in the Atmosphere of Titan,* ESA SP-544, 197–204, 2004.

Porco, C. C., E. Baker, J. Barbara, K. Beurle, A. Brahic, J. A. Burns, S. Charnoz, N. Cooper, D. D. Dawson, A. D. Del Genio, T. Denk, L. Dones, U. Dyudina, M. W. Evans, S. Fussner, B. Giese, K. Grazier, P. Helfenstein, A. P. Ingersoll, R. A. Jacobson, T. V. Johnson, A. McEwen, C.D. Murray, G. Neukum, W. M. Owen, J. Perry, T. Roatsch, J. Spitale, S. Squyres, P. Thomas, M. Tiscareno, E. P. Turtle, A. R. Vasavada, J. Veverka, R. Wagner, and R. West, Imaging of Titan from the Cassini spacecraft, *Nature, 434,* 159–168, 2005.

Preston, R. A., et al., Determination of Venus winds by ground-based radio tracking of the VEGA balloons, *Science, 231,* 1414–1416, 1986.

Radebaugh, J., R. Lorenz, R. Kirk, J. Lunine, E. Stofan, R. Lopes, S. Wall, and the Cassini RADAR Team, Mountains on Titan observed by the Cassini RADAR, *Icarus,* in press, 2007.

Rannou, P., F. Montmessin, F. Hourdin, and S. Lebonnois, The latitudinal distribution of clouds on Titan, *Science, 311,* 201–205, 2006.

Reh et al., *Titan and Enceladus $1B Mission Feasibility Study Report*, JPL D-37401, Jet Propulsion Laboratory, Pasadena, CA, 2007a.

Reh et al., *Titan Prebiotic Explorer (TiPEx) Mission Study Final Report,* Jet Propulsion Laboratory, Pasadena, CA, 2007b.

Richardson, J., A. McEwen, and R. D. Lorenz, Titan's surface and rotation – New insights from Voyager images, *Icarus, 170,* 113–124, 2004.

Safaeinilli, A., personal communication, 2007.

Sagdeev, R. Z., et al., Overview of VEGA Venus Balloon in situ meteorological measurements, *Science, 231,* 14410–1414, 1986.

Schofield, J. T., J. R. Barnes, D. Crisp, R. M. Haberle, S. Larsen, J. A. Magalhaes, J. R. Murphy, A. Seiff, and G. Wilson, The Mars Pathfinder Atmospheric Structure Investigation/ Meteorology (ASI/MET) experiment, *Science, 278,* 1752–1158, 1997.

Shemansky, D. E., A. I. F. Stewart, R. A. West, L. W. Esposito, J. T. Hallett, and X. Liu, The Cassini UVIS stellar probe of the Titan atmosphere, *Science, 308,* 978–982, 2005.

Simões, F., R. Grard, M. Hamelin, J. J. López-Moreno, K. Schwingenschuh, C. Béghin, J.-J. Berthelier, B. Besser, V. J. G. Brown, M. Chabassière, P. Falkner, F. Ferri, M. Fulchignoni, R. Hofe, I. Jernej, J. M. Jeronimo, G. J. Molina-Cuberos, R. Rodrigo, H. Svedhem, T. Tokano, and R. Trautner, A new numerical model for the simulation of ELF wave propagation and the computation of eigenmodes in the atmosphere of Titan: Did Huygens observe any Schumann resonance? *Planet. Space Sci.*, doi:10.1016/j.pss.2007.04.016, in press, 2007.

Skelley, A. M., H. J. Cleaves, C. N. Jayarajah, J. L. Bada, and R. A. Mathies, Application of the Mars Organic Analyzer to nucleobase and amine biomarker detection, *Astrobiology, 6(6),* 824–837, 2006.

Smith, P. H., M. T. Lemmon, R. D. Lorenz, L. A. Sromovsky, J. Caldwell, and M. D. Allison, Titan's surface, revealed by HST imaging, *Icarus, 119,* 336–349, 1996.

Soderblom, L. A., R. L. Kirk, J. A. Anderson, K. H. Baines, J. W. Barnes, J. M. Barrett, R. H. Brown, B. J. Buratti, R. N. Clark, D. P. Cruikshank, C. Elachi, M. A. Janssen, R. Jaumann, E. Karkoschka, S. Le Mouèlic, R. M. Lopes, R. D. Lorenz, J. I. Lunine, T. B. McCord, P. D. Nicholson, J. Radebaugh, B. Rizk, C. Sotin, E. R. Stofan, T. L. Sucharski, M. G. Tomasko, and S. D. Wall, Correlations between Cassini VIMS spectra and RADAR SAR images: Implications for Titan's surface composition and the character of the Huygens Probe landing site, *Planet. Space Sci.*, in press, 2007a.

Sotin, C. et al., Release of volatiles from a possible cryovolcano from near-infrared imaging of Titan, *Nature, 435,* 786–789, 2005.

Stofan, E. R., C. Elachi, J. I. Lunine, R. D. Lorenz, B. Stiles, K. Mitchell, S. Ostro, L. Soderblom, C. Wood, H. Zebker, S. Wall, M. Janssen, R. Kirk, R. Lopes, F. Paganelli, J. Radebaugh, L. Wye, Y. Anderson, M. Allison, R. Boehmer, P. Callahan, P. Encrenaz, E. Flamini, G. Francescetti, Y. Gim, G. Hamilton, S. Hensley, W. T. K. Johnson, K. Kelleher, D. Muhleman, P. Paillou, G. Picardi, F. Posa, L. Roth, R. Seu, S. Shaffer, S. Vetrella, and R. West, The lakes of Titan, *Nature, 441,* 61–64, 2007.

Stoker, C. R., P. J. Boston, R. L. Mancinelli, W. Segal, B. N. Khare, and C. Sagan, Microbial metabolism of tholin, *Icarus, 85(1),* 241–256, 1990.

Strobel, D., Gravitational tidal waves in Titan's upper atmosphere, *Icarus, 182,* 251–258, 2006.

Takenaka, N., A. Ueda, T. Daimon, H. Bandow, T. Dohmaru, and Y. Maeda, Acceleration mechanism of chemical reaction by freezing: The reaction of nitrous acid with dissolved oxygen, *J. Physical Chem., 100,* 13874–13884, 1996.

Tang C. H., T. I. S. Boak III, and M. D. Grossi, Bistatic radar measurements of electrical properties of the Martian Surface, *J. Geophys. Res., 82(28),* 4305–4315, 1977.

Thomas, C., O. Mousis, V. Ballenegger, and S. Picaud, Clathrate Hydrates as a sink of noble gases in Titan's Atmosphere, *Astron. Astrophys.,* in press, 2007.

Thompson, W. R., and C. Sagan, Organic chemistry on Titan: Surface interactions, *in: Symposium on Titan,* ESA SP, 338, pp. 167–176, 1992.

Tobie, G., O. Grasset, J. I. Lunine, A. Mocquet, and C. Sotin, Titan's Internal Structure inferred from a coupled thermal-orbital model, *Icarus, 175,* 496–502, 2005.

Tokano, T., and F. M. Neubauer, Tidal winds on Titan caused by Saturn, *Icarus, 158,* 499–515, 2002.

Tokano, T., and F. Neubauer, Wind-induced seasonal angular momentum exchange at Titan's surface and its influence on Titan's length-of-day, *Geophys. Res. Lett., 32,* L24203, doi:10.1029/2005GL024456, 2005.

Tokano, T., C. P. McKay, F. M. Neubauer, S. K. Atreya, F. Ferri, M. Fulchignoni, and H. B. Niemann, Methane drizzle on Titan, *Nature, 442,* 432–435, 2006.

Tomasko, M., B. Archinal, T. Becker, B. Bézard, M. Bushroe, M. Combes, D. Cook, A Coustenis., C. de Bergh, L. Dafoe, L. Doose, S. Douté, A. Eibl, S. Engel, F. Gliem, B. Grieger, K. Holso, E. Howington-Kraus, E. Karkoschka, H. Keller, R. Kirk, R. Kramm, M. Küppers, P. Lanagan, E. Lellouch, M. Lemmon, J. Lunine, , E. McFarlane, J. Moores, M. Prout, B. Rizk, M. Rosiek, P. Rueffer, S. Schröder, B. Schmitt, C. See, P. Smith, ,L. Soderblom, N. Thomas, and R. West, Rain, winds, and haze during the Huygens probe descent to Titan's surface. *Nature, 438,* 765–778, 2005.

Toon, Owen B.; McKay, Christopher P.; Courtin, Regis; Ackerman, Thomas P., Methane rain on Titan , Icarus, 75, 255–284, 1988.

Tortora, P., J. W. Armstrong, S. W Asmar, L. Iess, N. J. Rappaport, L. Somenzi, and F. Zingoni, Preliminary determination of Titan's gravity field with the spacecraft Cassini, American Astronomical Society, Div. Planet. Sci. meeting #38, #56.01, *Bull. Am. Astronomical Soc., 38,* 584, 2006.

Trainer, M. G., A. A. Pavlov, H. L. DeWitt, J. L. Jimenez, C. P. McKay, O. B. Toon, and M. A. Tolbert, Organic haze on Titan and the early Earth, *Proc., National Academy of Sciences, 103,* 18035–18042, 2006.

Waite, J. H., H. Niemann, R. V. Yelle, W. T. Kasprzak, T. E. Cravens, J. G. Luhmann, R. L. McNutt, W.-H. Ip, D. Gell, V. De La Haye, I. Müller-Wordag, B. Magee, N. Borggren, S. Ledvina, G. Fletcher, E. Walter, R. Miller, S. Scherer, R. Thorpe, J. Xu, B. Block, and K.

Arnett, Ion Neutral Mass Spectrometer results from the first flyby of Titan, *Science, 308,* 982–986, 2005.

Waite, J. H., D. T. Young, T. E. Cravens, A. J. Coates, F. J. Crary, B. Magee, and J. Westlake, The Process of tholin formation in Titan's upper atmosphere, *Science, 316,* 870–876, 2007.

Walterscheid, R. L., and G. Schubert, A tidal explanation for the Titan haze layers, *Icarus, 183,* 471–478, 2006.

Webster, C. R., S. P. Sander, R. Beer, R. D. May, R. G. Knollenberg, D. M. Hunten, and J. Ballard, Tunable diode laser IR spectrometer for *in situ* measurements of the gas phase composition and particle size distribution of Titan's atmosphere, *Appl. Optics, 29,* 907–917, 1990.

Wieczorek, M. A., et al., New views of the Moon, *Rev. Min. Geochem., 60,* 221–364, 2006.

Yelle, R. V., N. Borggren, V. De La Haye, W. T. Kasprzak, H. B. Niemann, I. Müller-Wodarg, and J. H. Waite, The vertical structure of Titan's upper atmosphere from Cassini Ion Neutral Mass Spectrometer measurements, *Icarus, 182,* 567–576, 2006.

Young, D., personal communication, 2005.

Young, E., personal communication, 2007.

Yseboodt, M., J-P Barriot, and V. Dehant, Analytical modeling of the Doppler tracking between a lander and a Mars orbiter in terms of rotational dynamics, *J. Geophys. Res., 108(E7),* 5076, doi:10.1029/2003JE002045, 2003.

9.2: Acronyms

9.2 Acronyms

Å	Angstrom
AA	Acoustic Anemometer
AA-STR	APS-based Autonomous Star Tracker
AC	Air Conditioning
ACS	Attitude Control System
AERO	Aerocapture
ALICE	Ultraviolet Imaging Spectrometer (New Horizons).
AO	Announcement of Opportunity
APL	The Johns Hopkins University Applied Physics Laboratory
Ar	Argon
ARC	NASA Ames Research Center
ARR	ATLO Readiness Review
ASAT	Aerocapture Systems Analysis Team
ASC	Advanced Stirling Converter
ASIC	Application-Specific Integrated Circuit
ASRG	Advanced Stirling Radioisotope Generator
ATLO	Assembly, Test, and Launch Operations
AU	Astronomical Unit
AV	Aerial Vehicle
AVTM	Aerial Vehicle Targeting Maneuver
AVTM-CU	Aerial Vehicle Targeting Maneuver Correction/Update
B	Billion
BAL	Balloon
BER	Bit Error Rate
BoE	Basis of Estimate
BoL	Beginning of Life
bps	Bits per Second
C&DH	Command and Data Handling
C22	Gravity Coefficient
CA	Chemical Analyzer Package
CADRe	Cost Analysis Data Requirements
CAPS	Cassini Plasm Spectrometer
CBE	Current Best Estimate
CC	Contamination Control
CCAFS	Cape Canaveral Air Force Station
CCD	Charge-Coupled Device
CCSDS	Consultative Committee for Space Data Systems
CDR	Critical Design Review
CER	Cost Estimating Relationship
CEV	Crew Exploration Vehicle
CFD	Computational Fluid Dynamics
CFDP	CCSCS File Delivery Protocol
CheMin	Chemistry and Mineralogy (MSL)
CIPA	Cruise Integrated Pump Assembly
CIRS	Composite Infrared Spectrometer (Cassini)
CIW	Caregie Institution of Washington
CM	Cryogenic Materials & Applications; also Configuration Management
CONTOUR	Comet Nucleus Tour
COPV	Composite-Overwrapped Pressure Vessel
cPCI	Compact Peripheral Component Interface
CPT	Comprehensive Performance Test;
CRISM	Compact Reconnaissance Imaging Spectrometer for Mars (MRO)
CRSA	Cost Risk Sub-factor Analysis
CTM	Contract Technical Manager
DA	Dalton
DC	Direct Current

DCO	Detailed Checkout
DIMES	Descent Image Motion Estimation System (MER)
DISR	Descent Imager/Spectral Radiometer (Cassini/Huygens)
DL	Downlink
DLA	Declination of Launch Asymptote
DoD	Department of Defense
DOE	Department of Energy
DSM	Deep Space Maneuver
DSMS	Deep Space Mission System
DSN	Deep Space Network
DTE	Direct-to-Earth
e	Eccenticity
E/PO	Education and Public Outreach
EAC	Estimate at Completion
EAR	Export Administration Regulations
EDD	Entry, Descent, and Deployment
EDL	Entry, Descent, and Landing
EDMG	Engineering Data Management Group
EEE	Electrical, Electronic, and Electromechanical
EEIS	End-to-End Information System
EEPROM	Electrically Erasable Programmable Read-Only Memory
EF	Earth Flyby
EGSE	Electrical Ground Support Equipment
EIS	Environmental Impact Statement
EL	Elevation
EMC	Electromagnetic Compatibility
EMI	Electromagnetic Interference
EOL	End of Life
EPA	Environmental Protection Agency
EPC	Electric Power Converter
ESA	European Space Agency
ESI	Electrospray Ionization
EVM	Earned Value Management
FB	Fan beam
FER	Frame Error Rate
FET	Field Effect Transistor
FOV	Field of View
FPGA	Field Programmable Gate Array
FPM	Fault Protection Module
FRISK	Formal Risk Analysis
FS	Flight System
FY	Fiscal Year
G&C	Guidance and Control
Gbits	Gigabits
GCM	Global Circulation Model
GCMS	Gas Chromatography Mass Spectrometry
GCR	Galactic Cosmic Rays
GDS	Ground Data System
GHz	Gigahertz
GN&C	Guidance, Navigation, and Control
GPHS	General Purpose Heat Sources
GPS	Global Positioning System
GSE	Ground System Equipment
GSFC	Goddard Space Flight Center
h2	Love Number.
HGA	High-Gain Antenna
HPLC	High Performance Liquid Chromatography
HQ	Headquarters
HST	Hubble Space Telescope o
HW	Hardware
I&T	Integration and Test
ICE	Independent Cost Estimate
IEM	Integrated Electronics Module

IIP	NASA Instrument Incubator Program
IMS	Ion Mass Spectrometer (Cassini)
IMU	Inertial Measurement Unit
INMS	Ion Neutral Mass Spectrometer
INSRP	Interagency Nuclear Safety Review Panel
IPAO	Independent Program Assessment Office
IR	Infrared
ISPT	In-Space Propulsion Technology
ISS	Imaging Science Subsystem (Cassini)
ISSI	International Society for Scientometrics and Infometrics
ITAR	International Traffic in Arms Regulations
IV&V	Independent Verification and Validation
J2	Gravity Coefficient
JACM	JPL Assembly, Test and Operations Cost Model
JEDI	Juno Energetic Particle Detector
JHU/APL	The Johns Hopkins University Applied Physics Laboratory
JPL	Jet Propulsion Laboratory
K	Kelvin
k2	Tidal Love Number
kb	Kilobits
kB	Kilobytes
kbps	Kilobits per second
KSC	Kennedy Space Center
L/D	Lift-to-Drag ratio
LAE	Launch Approval Engineering
LaRC	NASA Langley Research Center
LDI	Laser Desorption/Ionization
LE	Liquid-Based Chemical Extraction
LED	Light-Emitting Diode
LERMA	Laboratoire d'Etude du Rayonnement et de la Matière en Astrophysique
LGA	Low Gain Antenna
LIDAR	Light Detection and Ranging
LTM	Lander Targeting Maneuver
LV	Launch Vehicle
M	Million
M&P	Materials and Processes
m/z	Ion Mass-to-Charge Ratio
MAG	Magnetometer
MAHLI	Mars Hand Lens Imager (MSL)
MAMBO	Mars Atmosphere Microwave Brightness Observer
MARDI	Mars Descent Imager (Phoenix)
MARSIS	Multi-Frequency Synthetic Radar Altimeter with Around Penetration Capabilities (Mars Express)
MARVEL	Mars Volcanic Emission and Life (Mars Scout)
MCP	Microchannel Plate
MCR	Mission Concept Review
MDIS	Mercury Dual Imaging System (MESSENGER)
MEL	Master Equipment List
MEMS	Micro-Electro-Mechanical Systems
MEOP	Maximum Expected Operating Pressure
MER	Mars Exploration Rover
MeSH	Mechanized Sample Handler
MESSENGER	Mercury Surface, Space Environment, Geochemistry, and Ranging (Discovery mission)

MET	Metrology package; *also* Metoerological Instrument (Phoenix)
MGA	Medium Gain Antenna
MGS	Mars Global Surveyor
MGSE	Mechanical Ground Support Equipment
MI	Microscopic Imager
MIMI	Magnetospheric Imaging Instrument (Cassini)
MIMU	Miniature Inertial Measurement Unit
Mini-TES	Mini-Thermal Emission Spectrometer (MER)
MIRO	Microwave Instrument for Rosetta Orbiter
MLI	Multi-Layer Insulation
MMH	Monomethyl Hydrazine
MMR	Mission (& Operations) Readiness Review
MMRTG	Multi-Mission Radioisotope Thermoelectric Generator
MOA	Memorandum of Agreement
MOLA	Mars Orbiter Laser Altimeter (MGS)
MOS	Mission Operations System
MOSFET	Metal-Oxide-Semiconductor Field-Effect Transistor
MOU	Memorandum of Understanding
MPF	Mars Pathfinder
Mpix	Megapixel
MRB	Mission Readiness Brief
MRO	Mars Reconnaissance Orbiter
MS	Mass Spectrometry
MSAR	Microwave Spectrometer and Radiometer (proposed for Cassini)
MSL	Mars Science Laboratory
MSPA	Multiple Spacecraft Per Aperture
MSSS	Malin Space Science Systems
MSX	Midcourse Space Experiment
Myr	Million Years
NAC	Narrow Angle Camera (MESSENGER)
NAFCOM	NASA/Air Force Cost Model
NASA	National Aeronautics and Space Administration
NEAR	Near Earth Asteroid Rendezvous
NEPA	National Environmental Policy Act
NICM	NASA Instrument Cost Model
NIR	Near Infrared
NIRS/AOM	Near-IR Spectrometer/Atmospheric Optics Monitor
NMO	NASA Management Office
NPG	NASA Procedures and Guidelines
NPR	NASA Procedure Requirements
NRC	Nuclear Regulatory Commission
NTO	Nitrogen Tetroxide
NUV	Near Ultraviolte
OETM	Orbiter Entry Targeting Maneuver
OMEGA	Observatoire pour la Minéralogie, l'Eau, les Glaces, et l'Activité (Mars Express)
OPAG	Outer Plantes Assessment Group
OPMCM	Outer Planet Mission Cost Model
OSTP	Office of Science and Technology Policy
PA	Plutonium Availability
PDR	Preliminary Design Review
PEPE	Plasma Experiment for Planetary Exploration (Deep Space 1)
PER	Pre-Environmental Review

PIRLS	Probe Infrared Laser Spectrometer (Cassini/Huygens)
PM	Project Manager
PMCM	JPL Parametric Mission Cost Model
PMD	Propellant Management Device
PMSR	Preliminary Mission & Systems Review
PP	Planetary Protection
ppbv	Part Per Billion by Volume
PPF	Payload Processing Facility
ppm	Parts Per Million
ppt	Part Per Trillion
PRIO	Power Remote Input/Output
PROM	Programmable Read-Only Memory
PS	Project Scientist
PSC	Polar Stratospheric Cloud
PSE	Power System Electronics
PSE	Project Systems Engineer
PSR	Pre-Ship Review
QA	Quality Assurance
r	Radius
RA	Robotic Arm
RADAR	Radio Detection and Ranging (Cassini)
RAM	Random Access Memory
RARB	Resource Allocation Review Board
RBSP	Radiation Belt Storm Probe
Rec/Dels	Receivables/Deliverables
RF	Radio Frequency
RFA	Request for Action
RHU	Radioisotope Heater Unit
RIO	Remote Input/Output
RIU	Remote Interace Unit
ROD	Record of Decision
ROM	Rough Order-of-Magnitude
RPS	Radioisotope Power Source
RPWS	Radio and Plasma Wave Science (Cassini)
RSS	Radio Science Subsystem (Cassini)
RTG	Radioisotope Thermoelectric Generator
RTV	Room Temperature Vulcanized
RWA	Reaction Wheel Assembly
RY	Real Year
S/C, SC	Spacecraft
SAM	Sample Analysis at Mars (MSL)
SAR	Synthetic Aperture Radar
SDRAM	Synchronous Dynamic Random Access Memory
SDT	Science Definition Team
SE	Systems Engineering
SEIS	Seismic System (ExoMars)
SEP	Solar Electric Propulsion
SER	Safety Evaluation Report
SETI	Search for Extra-Terrestrial Intelligence
SHARAD	Shallow Subsurface Radar (MRO)
SIGNAL	Submillimeter Investigation of Geothermal Networks and Life
SIR	SMART-1 Infrared Spectrometer
SMA	Safety and Mission Assurance
SMPL	Lander Sampling
SPE	Sun-Probe-Earth
SPLD	South Polar Layered Deposit
SRAM	Static Random Access Memory
SRU	Shunt Regulator Unit
SS	Subsystem
SSE	Solar System Exploration
SSPA	Solid State Power Amplifier
SSR	Solid State Recorder

STEREO	Solar Terrestrial Relations Observatory (two satellites)
SV	Space Vehicle
SW	Software
SwRI	Southwest Research Institute
TAA	Technical Assistance Agreement
TBD	To Be Determined
Tbits	Terrabits
TCM	Trajectory Correction Maneuver
TDL	Tunable Diode Laser
TE	Titan Explorer
TiPEx	Titan Planetary Explorer
TLS	Tunable Laser Spectrometer
TOAM	Titan Orbiter with Aerorover Mission
TOF-MS	Time-of-Flight Mass Spectrometer
TPC	Terminal Point Controller
TPS	Thermal Protection System
TRIO	Temperature Remote Input/Oputput
TRL	Technology Readiness Level
TWTA	Traveling Wave Tube Amplifier
UAV	Unmanned Aerial Vehicle
UCLA	University of California Los Angeles
UHF	Ultrahigh Frequency
USGS	United States Geological Survey
USMC	United States Marine Corps
USO	Ultra-Stable Oscillator
UTC	Universal Time Coordinated
UV	Ultraviolet
UVIS	Ultraviolet Imaging Spectrograph (Cassini)
V&V	Verification and Validation
VIMS	Visual and Infrared Mapping Spectrometer (Cassini)
Vis	Visible
VLBI	Very Long Baseline Interferometry
VVEE	Venus-Venus-Earth-Earth
W	Watt
WAC	Wide Angle Camera (MESSENGER)
WBS	Work Breakdown Structure
WTS	Waveguide Transfer Switch
μCE	Micro Capillary Electrophoresis
σ°	Backscatter Sensitivity